UNIVERSITY OF THE WESTERN CAPE

A RE-ASSESSMENT OF THE GEOCHRONOLOGY AND GEOCHEMISTRY OF THE POSTBERG IGNIMBRITES, SALDANHA, WESTERN CAPE, SOUTH AFRICA

A thesis submitted in fulfilment of the requirements for the degree of Magister Scientiae in the Department of Earth Science, University of the Western Cape.

by

Matthew Misrole

Supervisor: Professor Dirk Frei

13 March 2020

To my mother Ingrid Africa and my father Hilton Misrole, I dedicate this body of work to the both of you. Thank you for EVERYTHING!

Science knows no country, because it belongs to humanity, and is the torch which illuminates the world.

~Louis Pasteur

DECLARATION

I declare that ***a re-assessment of the Geochemistry and Geochronology of the Postberg Ignimbrites, Saldanha, Western Cape, South Africa*** is my own work, that it has not been submitted for any degree or examination in any other university, and that all the sources I have used or quoted have been indicated and acknowledged by complete references.

Full name: Matthew Robin Misrole

Date: 13 March 2020

Signed: .....

KEY WORDS

Ignimbrite

Geotectonic development

Magmatism

Phenocrysts

Pyroclasic Flows

Rhyolite

Saldanha Bay

Saldania Belt

Saldanian Orogeny

S-type

SUMMARY / ABSTRACT

The Saldania Belt in southern Africa, a product of the Pan-African Saldanian Orogeny, forms part of a system of Neoproterozoic mobile belts that border and weld older cratons on the African continent. It is a low-grade orogenic belt situated along the southwestern margin of the Kalahari Craton and is composed of several inliers of greenschist facies metasedimentary and metavolcanic rocks (Malmesbury Group), unroofed in megaanticlinal hinges of the Permo-Triassic Cape Fold Belt. The Malmesbury Group rocks were syn- and post-tectonically intruded in a pervasive transpressive regime between 555 Ma and 515 Ma by Neoproterozoic to early Cambrian S-, I- and A-type granites, monzodiorites, gabbros and quartz syenites, which collectively constitute the rocks of the Cape Granite Suite (CGS). Along the south-western coastline of South Africa, the Saldanha Bay Volcanic Complex (which forms part of the CGS) is divided into two eruption centres both of which have been identified as “intra-caldera pyroclastic ignimbrites”. The Postberg eruption centre is situated to the south of the Saldanha Bay entrance and the Saldanha eruption centre is situated to the north of the entrance. Both eruption centres display distinct geochemical signatures, the most apparent being the greater TiO_2 concentrations (> 0.25 wt. %) of the Saldanha centre ignimbrites when compared to its Postberg centre counterparts.

The Postberg eruption centre consists of S-type rhyolitic ignimbrites which are subdivided into the two geochemically distinct Plankiesbaai and Tsaarsbank Ignimbrites. Small amounts of the Jacobs Bay and Saldanha Ignimbrites (less felsic tephra from the Saldanha eruption centre) are also present in the Postberg eruption centre. A robust geochemical analysis of both the Plankiesbaai and Tsaarsbank magma groups display high SiO_2 content (>76 wt. %), a lack of variation in TiO_2 and Zr, high Al_2O_3 and ASI (aluminium saturation index) values (> 1.0 and generally >1.1 which, on average, is higher than the Saldanha eruption centre ignimbrites), low CaO and Na_2O, and a highly ferroan character. The Plankiesbaai ignimbrite also display lower #Mg concentration compared to the Tsaarsbank ignimbrite. Typical geochemical trends in the Postberg eruption centre include the lack of variation in Zr content, higher Rb content and lower Sr, Ba, V and Zn concentrations when compared to the tephra of the Saldanha eruption centre found in the Postberg area.

The study's main aim is not only to assess the geochemistry of the ignimbrites relative to the previous phases of magmatism originally proposed by Scheepers (1995) for the magmatism of the Cape Granite Suite, but also their age distribution. Previously defined phases of magmatism include Phase I (S-type granites subdivided into Sb, Sa_1 and Sa_2 all of which are dated to 555 - 540 Ma), Phase II (I-type granites subdivided into Ia and Ib both dated to 540 – 520 Ma), Phase III (A-type granites subdivided into Aa and Ab dated to ~ 520 Ma) and Phase IV (S-type volcanic and subvolcanic rocks dated to 515 Ma).

Re-examination of the geochronology displays a U-Pb age for Postberg Centre Jacobs Bay Ignimbrite (tephra from the Saldanha eruption centre) of 538 ± 2.2 Ma: and for the Postberg Centre Tsaarsbank Ignimbrite between 536 ± 2 Ma – 540 ± 3.4 Ma. These new dates, in combination with the geochronological work done in the Saldanha Centre (particularly in light of the Clemens and Stevens (2016) and Clemens et al. (2017) studies that reclassify these rocks differing from the original and previous studies), place all the ignimbrites of the Saldanha Bay Volcanic Complex securely within the age bracket for the initial S-type magmatism of the CGS.

This thesis presents a revised order for the phases of magmatism of the Saldania Belt, and by extension, of the Cape Granite Suite. All S-type magmatism, including that of the Saldanha Bay Volcanic Complex (S_v), forms part of the Phase I magmatism of the Saldania Belt (Sa_1, Sa_2, and Sb) emplaced between 555 – 540 Ma.

ACKNOWLEDGEMENTS

This work is based on the research supported, in part by MerSeta (2017), and the National Research Foundation of South Africa (NRF, 2018), in the form of grant funding for a Master's Degree Scholarship to M. R. Misrole.

Professor D. Frei, H.O.D Earth Science, University of the Western Cape, is acknowledged for the continuous support in his capacity as the Primary Supervisor on this MSc. Applied Geology Thesis.

Professor D. Frei acknowledges support from the DST/NRF Centre of excellence for Integrated Mineral and Energy Resource Analysis (CIMERA).

Thank you to Professor G. Stevens and Professor J. D. Clemens, Stellenbosch University for providing various rock samples as well as consultation on the results of the research.

The West Coast Nation Park's board and personnel are acknowledged for allowing access to the conservation areas under their jurisdiction.

Kayla Friedman and Malcolm Morgan of the Centre for Sustainable Development, University of Cambridge, UK is acknowledged for producing the Microsoft Word thesis template used to produce this document.

A special thank you to my mother, Ingrid Africa and my father, Hilton Misrole as well as my sisters Cindy Jones, Loren Miller and Cherna' Misrole for their continuous motivation and support throughout my academic career.

CONTENTS

LIST OF TABLES

LIST OF FIGURES

LIST OF ABBREVIATIONS AND ACRONYMS

AEON	Africa Earth Observatory Network
ASI	Aluminium Saturation Index
Bt.	Biotite
Ca.	Circa - meaning “approximately”
CAF	Central Analytical Facility
CGS	Cape Granite Suite
Chl.	Chlorite
CICESE	Centro de Investigación Científica y de Educación Superior de Ensenada
CL	Cathodoluminescence
Crd.	Cordierite
CSZ	Colenso Shear Zone
EA	Electronic Appendix
Eds.	Editions
Et al.	Et alia - meaning “and others”
Fig.	Figure
Fs.	Feldspar
Ga	Giga annum
Grt.	Garnet
Hc.	Hercynite
ID- TIMS	Isotope Dilutions – Thermal Ionisation Mass Spectrometry
ICP-MS	Inductively Coupled Plasma Mass Spectrometry
LA-SF-ICP-MS	Laser-Ablation Sector-Field Inductively-Coupled-Plasma Mass-Spectrometry
Ma	Mega annum
MC-ICP-MS	Multi-collector Inductively Coupled Plasma Mass Spectrometer
MSWD	Mean Square Weighted Deviations
M.yrs.	Million years
NNW	North North West
NW	North West
Or.	Orthoclase

Pl.	Plagioclase
PPL	Plane Polarized Light
PWSZ	Piketberg - Wellington Shear Zone
PC	Postberg Centre
PC – JI	Postberg Centre - Jacobs Bay Ignimbrite
PC – PI	Postberg Centre - Plankiesbaai Ignimbrite
PC – TI	Postberg Centre - Tsaarsbank Ignimbrite
PC – SI	Postberg Centre - Saldanha Ignimbrite
Ppm	Parts per million
Px.	Pyroxene
QA – QC	Quality Assurance – Quality Control
Qtz.	Quartz
REE	Rare Earth Elements
SC	Saldanha Centre
SC – SI	Saldanha Centre - Saldanha Ignimbrite
SC – JI	Saldanha Centre – Jacobs Bay Ignimbrite
Sil.	Sillimanite
SSE	South South East
USGS	United States Geological Survey
UWC	University of the Western Cape
Vol. %	Volume percentage
Wt. %	Weight percentage
XPL	Cross Polarized Light
XRF	X-ray Fluorescence
Zn.	Zircon

1 INTRODUCTION

The Saldania Belt in southern Africa, a product of the Pan-African Saldanian Orogeny, forms part of a system of Neoproterozoic mobile belts that border and weld older cratons on the African continent. It is a low-grade orogenic belt situated along the southwestern margin of the Kalahari Craton and is composed of several inliers of greenschist facies metasedimentary and metavolcanic rocks (Malmesbury Group), unroofed in mega anticlinal hinges of the Permo-Triassic Cape Fold Belt (Gresse et al., 1992; Rozendaal et al., 1999). The Malmesbury Group rocks were syn- and post-tectonically intruded in a pervasive transpressive regime by Neoproterozoic to early Cambrian S-, I- and A-type granites, monzodiorites, gabbros, ignimbrites and quartz syenites; collectively known as the four "phases" of magmatism of the Cape Granite Suite (CGS, Gresse and Scheepers, 1993; Scheepers, 1995; Scheepers and Nortjé, 2000; Scheepers and Armstrong, 2002; Belcher and Kisters, 2003). Previously defined phases of magmatism (Scheepers, 1995) include Phase I (S-type granites subdivided into Sb, Sa_1 and Sa_2, all of which are dated to 555 - 540 Ma), Phase II (I-type granites subdivided into Ia and Ib dated to 540 – 520 Ma), Phase III (A-type granites subdivided into Aa and Ab dated to ~ 520 Ma) and Phase IV later added by Scheepers and Nortjé (2000) (S-type volcanic and subvolcanic rocks dated to 515 Ma).

Along the south-western coastline of South Africa, the Saldanha Bay Volcanic Complex (which forms part of the CGS) is divided into two eruption centres (Figure 1 and Figure 2), known as the Postberg and Saldanha eruption centres (Clemens and Stevens, 2016; Clemens et al., 2017). Two distinct suites of rock were identified for the "Phase IV" magmatism in the Saldania Belt. These rocks were described as the Postberg Ignimbrites (volcanics), found on the southern portion of the bay, and the previously proposed Saldanha "quartz porphyry"

(sub-volcanics) found at the opposite end (Scheepers and Nortjé, 2000; Scheepers and Poujol, 2002).

Figure 1: Vector image of South Africa indicating the geological position of the study area (Saldana Bay Volcanic Complex) indicated by the red rectangle.

The resultant linear depletion trends in the geochemistry were interpreted by Scheepers (1995) and Scheepers and Nortjé (2000) as the product of fractional crystallization. This distinguished the two rock types (the Postberg eruption centre ignimbrites and the Saldanha eruption centre "quartz porphyry") from one another and defined the ignimbrites as showing significantly lesser evidence of fractionation (prior to the eruption) when compared to the sub-volcanic "quartz porphyry". The U-Pb ID-TIMS (Isotope Dilutions – Thermal Ionisation Mass Spectrometry) age, in conjunction with the geochemistry and petrography for the "Phase IV" magmatism suggested that the volcanism, described as rhyolitic / rhyodacitic ignimbrite flows, took place on both the southern and northern portions of Saldanha Bay. Scheepers and Poujol (2002) presented a U-Pb age of 515 ± 3 Ma for the volcanic phase, marking the end of the magmatism for the CGS.

Figure 2: Google Earth™ image of the Saldanha Bay Volcanic Complex.

It is important to note, in terms of the re-assessment of the age distribution of the ignimbrites relative to previous works on the CGS, that there is approximately 35 ± 3.5 M.yrs between the first (Phase I; Hoedjiespunt granites at 552 ± 4 Ma) and the last phase of magmatism of the CGS (Phase IV; sub-volcanic and volcanic rocks – 515 ± 3 Ma). Both Phase I and Phase IV rocks are present and immediately adjacent to each other on the northern side of Saldanha Bay (Figure 3; Scheepers, 1995; Scheepers and Armstrong, 2002). Given that the 515 ± 3 Ma ID-TIMS age for the volcanic phase of the CGS was based on only two concordant zircons (which represented the entire Phase IV magmatism), recent zircon dating and reclassification of Saldanha Bay Volcanic Complex by Clemens and Stevens (2016) and Clemens et al. (2017), and the 35 ± 3.5 M.yrs between two immediately adjacent rocks in the Saldanha Bay Volcanic Complex (Figure 3, Phase I - Hoedjiespunt and Phase IV - "sub-volcanic" and volcanic rocks) brought into question the timing of the Phase IV volcanic and "sub-volcanic" rocks.

This initiated the re-examination of the field relations, thin section petrography, geochemistry and geochronology of the rocks of Saldanha Bay by Clemens and Stevens (2016) and Clemens et al. (2017). They redefined sequences on the northern section of the bay and described it as an "intra-caldera pyroclastic ignimbrite" previously referred to as "quartz porphyry" by Scheepers and Poujol (2002) and proposed that the entire Saldanha Bay area formed part of a single volcanic complex (Saldanha Bay Volcanic Complex) consisting of two eruption centres - the Postberg eruption centre and the Saldanha eruption centre. They further suggested that the incorrect interpretation of the rocks as "Saldanha quartz - porphyry" may be the result of viewing the rock body, as a whole, as intrusive; based on the cryptic nature of the mineralogy and the degree of partial melting.

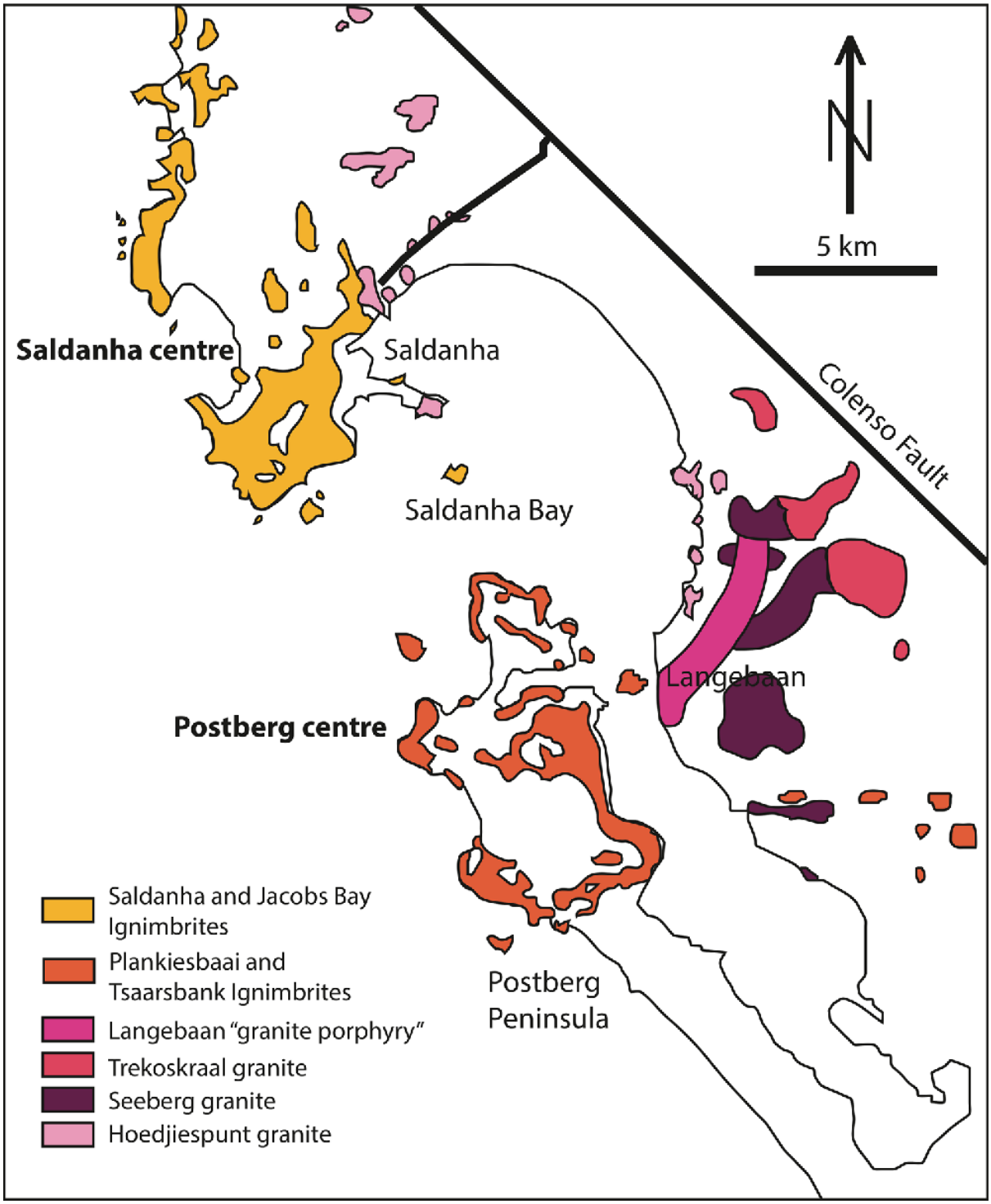

Figure 3: Map, based on Fig. 2 of Scheepers and Armstrong (2002), showing the areas of exposure of the Postberg and Saldanha volcanic rocks (intracaldera ignimbrites) and the outcrops of local granitic units. This figure is reproduced, with permission, from Prof. G. Stevens (2016) co-author of Clemens and Stevens (2016).

Such voluminous, caldera-forming ignimbrites are not uncommon (e.g., Gray and White, 2001; Cas et al., 2003; Bachman and Bergantz, 2004; Bachman and Bergantz, 2006, Bryan et al., 2006). The prevailing model showed that this type of ignimbrite represented erupted plutons that were almost fully crystallised before being partially re-melted as a result of the magma chamber being recharged by hotter mafic magma, which essentially triggered the eruption. Chemical variations of ignimbrites in such cases are commonly interpreted to represent zonation within the crystal mush of the magma chamber prior to eruption. Clemens et al. (2017) provides a revised model for such complexly zoned rhyolitic ignimbrites.

Upon review, Clemens and Stevens (2016) found four geochemically-distinct series of rocks in the Saldanha Bay Volcanic Complex; the Saldanha Ignimbrite and the Jacobs Bay Ignimbrite of the Saldanha eruption centre, dated to 542 ± 2 Ma by Clemens et al. (2017), and the Plankiesbaai Ignimbrite and the Tsaarsbank Ignimbrite which constitutes the bulk of the Postberg eruption centre. Minor portions of the Saldanha and Jacobs Bay Ignimbrites can be found in the Postberg centre as well. The available geochemical data for the two eruption centres, suggests that both centres may have been active around the same time, therefore, it is within reason to assume some close connections between the two eruption centres (Clemens and Stevens, 2016).

In light of the uncertainty around the exact timing of the ignimbrites and the new U-Pb age of 542 ± 2 Ma, presented by Clemens et al. (2017) for the Saldanha eruption centre, this thesis aims to re-examine and build a robust geochemical and geochronological dataset of the ignimbrites of the Postberg and Saldanha eruption centres. The new geochemical and geochronological data in conjunction with the re-examination work done by Clemens and Stevens (2016a) and Joseph (2012) and Clemens et al. (2017) will provide a new understanding of the timing and emplacement of the Postberg Centre Ignimbrites and by extension, the entire Saldanha Bay Volcanic Complex, and its place in the Cape Granite Suite. This thesis will present a Postberg centre petrographic review, various geochemical classification parameters, a robust U-Pb age determination on multiple magmatic zircons as well as Rb-Sr/ Sm-Nd isotope data on some of the ignimbrites to constrain the source of the magmatic events.

2 GEOLOGICAL SETTING

2.1 Introduction

The Saldania Belt, along the south-western coastline of South Africa, is considered one of the most inadequately understood Neoproterozoic to early Cambrian Pan-African fold belts. Notably, this lack of knowledge can be explained by the scantiness of the outcrop over large areas, the considerably weathered surfaces, its structural complexity, the low mineral exploration potential, and its burial beneath thick successions of siliclastic sedimentary rocks of the early Palaeozoic Cape Supergroup (Gresse et al., 2006). The prevailing confusion about the stratigraphy and tectonic makeup of the Saldania belt is highlighted by the common usage of the term “Malmesbury Group” for all the Neoproterozoic Lithostratigraphic units across the belt in spite of the differentiation between three separate terranes within the belt (Gresse et al., 2006; Frimmel et al., 2013).

Although a number of previous investigations have been undertaken, (Rozendaal et al., 1999; Belcher and Kisters, 2003; Buggisch et al., 2010; Rowe et al., 2010; Kisters et al., 2015) most of these investigations have focused on the petrology of the Cape Granite Suite along the coastal areas of the belt. Rozendaal et al. (1999) presented a regional study and established a model which considers the inter-relationships between the various volcanosedimentary sequences and the reconstruction of their palaeo-depositional environments. This model was discussed in relation to the late Proterozoic – early Cambrian plate tectonics.

Scheepers and Rozendaal (1992) and Gresse and Scheepers (1993) envisioned three major phases of magmatism of the Saldania Belt, with a volcanic fourth phase later added by Scheepers and Nortjé (2002). The model was later more accurately defined by Frimmel et al.

(2013) with a provenance study, involving U-Pb and Lu-Hf isotope analyses of detrital zircons, whole-rock geochemical analysis and Rb-Sr, Sm-Nd and Pb isotope analysis. This constrained the source domain and geodynamic models for the evolution of the Saldania Belt.

This chapter aims to describe the geological background of the Saldania belt, its formation during the Pan-African Saldanian Orogeny, its composition and structure, and syn- and post-tectonically intrusive Cape Granite Suite. The reader is referred to Scheepers and Rozendaal (1992), Gresse and Scheepers (1993) Scheepers (1995), Rozendaal et al. (1999), Scheepers and Nortjé (2000) and Frimmel et al. (2013) for further details. Nevertheless, a summary of the scope of events that led to the construction and evolution of the Saldania Belt will be presented.

A description and literature review of the local geology of Saldanha Bay has also been included to better understand the context of this study in relation to previous work done on the area of interest. A review of the Saldanha Bay Volcanic Complex has been inserted, with special focus on the rocks of the Postberg Eruption Centre. Clemens and Stevens (2016a) and Clemens et al. (2017) research on the Saldanha Centre suggest some close relationship between the two eruption centres, and although the Saldanha Centre is not the primary subject of this study, it has been included in a contextual and comparative capacity.

2.2 Regional Geology

2.2.1 The Saldanian Orogeny

The orogenic belts on either side of the Atlantic Ocean hold information about the initial fragmentation and rifting of an older supercontinent, Rodinia, around 780 - 750 Ma years ago. During the breakup of the supercontinent (see Figure 4), an interconnected complex of rift basins developed along the borders of the Paleo- to Meso-Proterozoic cratons. This exposed the seaboards around the craton margins resulting in the development of a wide oceanic basin, known as the Adamastor Ocean or proto-Atlantic (Frimmel et al., 2001). These semi-pull-apart rift basins became the depositional setting for the Pan-African 950-555 Ma greenschist facies, volcanosedimentary successions (Hartnady et al., 1985; Rozendaal et al., 1999; Gresse et al., 2006). The Gamtoos, Kaaimans, Kango and Malmesbury groups were deposited on the continental crust during the subduction of the ocean floor in Saldanian Orogeny which can be related to the increase in sea levels and the decrease of the 'freeboard' in geologic history (Dalziel et al., 1994; Rozendaal et al., 1999). These sedimentary and volcanic rocks are considered as the distal facies of the rift successions, overlying a mid-Proterozoic crystalline basement on the south-western edge of the Kalahari Craton (Rozendaal et al., 1999).

From ~600 Ma onward, the continental fragments of Africa and South America collided along subduction zones resulting in the closure of the Adamastor Ocean due to the subsequent docking of the Kalahari and Rio de le Plata cratons, and the subsequesnt orogenic mountain belts (Belcher and Kisters 2003; Kisters and Belcher 2018). The closure proceeded in a north to south zipper-like fashion during the continental construction of the southern supercontinent Gondwana, ca. 550 – 500 M.yrs ago in the late Neoproterozoic to early Cambrian (Rozendaal et al., 1999). Along the south-western portion of the Kalahari craton (Figure 5A), the product of this event is represented by the Damara, Gariep and Saldania belts. These mobile belts along the south-western coastline of southern Africa characterise the later stages of this evolution (Rozendaal et al., 1999).

2.2.2 The Saldania Belt

The Saldania Belt in southern Africa, a product of the Pan-African Saldanian Orogeny, forms part of a system of Neoproterozoic mobile belts that border and weld older cratons on the African continent (Figure 5A). It is a low-grade orogenic belt situated along the south-western margin of the Kalahari Craton and is composed of a number of inliers of greenschist facies metasedimentary and metavolcanic rocks (Malmesbury Group), unroofed in mega-anticlinal hinges of the Permo-Triassic Cape Fold Belt (Gresse et al., 1992; Rozendaal et al., 1999). The Malmesbury Group and its main exposure to the north of Cape Town constitute the oldest rocks in the belt. They are divided into three tectono-stratigraphic terranes (Figure 6) by predominant northwest trending sinstral/dextral strike-slip fault and shear zones (Hartnady et al., 1974). Towards the east of the belt, several smaller exposures of supposed ‘pre-Cape’ rocks form part of the Saldania Belt. As previously mentioned, these are the: Gamtoos Group in the Port Elizabeth area, the Kaaimans Group in the George area and the Kango Group in the Oudtshoorn area.

The folding and thrusting seen in the Saldania Belt was a result of the Permo-Triassic Cape Orogeny. This tectonism along with its weakly metamorphosed Neoproterozoic basement resulted in the overprinting of most of the earlier ‘pre-Cape’ structures and reset radiometric ages in the metamorphites (some granite as well) to 230-278 Ma (Halbich et al., 1983; Gresse and Scheepers, 1993). Structures indicating southeast-directed movement, common along the South African west coast, are notably absent along the south coast (Gresse and Scheepers, 1993). Within the Saldania belt ‘pre-Cape’ deformation, folding had a NNW-SSE trending fold axis. As indicated in Figure 5 B and Figure 6 along the western portions of the belt, this folding formed concentrated sinistral-transpressional deformation. This resulted in near vertical faults with the most prevalent being the Colenso Shear Zone (CSZ) and the Piketberg- Wellington Shear Zone (PWSZ).

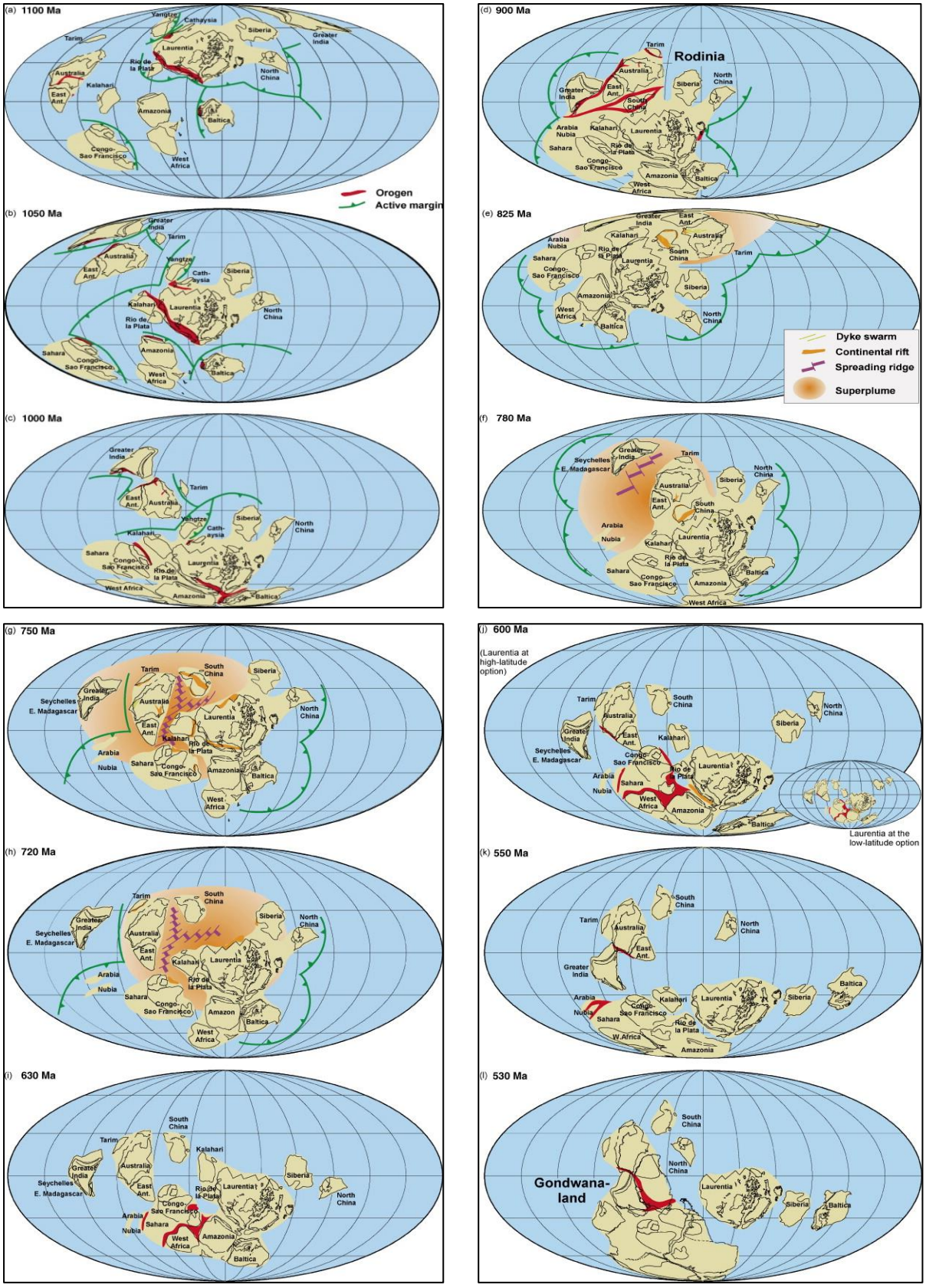

Figure 4: Diagram reproduced from Nance et al. (2014) showing the assembly and break-up of the supercontinent, Rodinia, and the construction of the supercontinent Gondwanaland. (a) 1100 Ma; (b) 1050 Ma; (c) 1000 Ma; (d) 900 Ma; (e) 825 Ma; (f) 780 Ma; (g) 750 Ma; (h) 720 Ma; (i) 630 Ma; (j) 600 Ma; (k) 550 Ma; (l) 530 Ma.

The Colenso (Saldanha-Stellenbosch) and Piketberg-Wellington fault zones are present on a regional scale (Figure 6). Stratigraphically, these large-scale NW-striking faults zones loosely separate the Malmesbury Group into three terranes known as the south-western Tygerberg terrane, the central Swartland terrane and the north-eastern Boland terrane (Hartnady et al., 1974). The CSZ separates the Swartland and Tygerberg terranes, and the PWSZ separates the Swartland and Boland terranes. The CSZ divides older S-type granites present in the Tygerberg terrane from the essentially younger I-type granites in the Swartland terrane (Rozendaal et al., 1994).

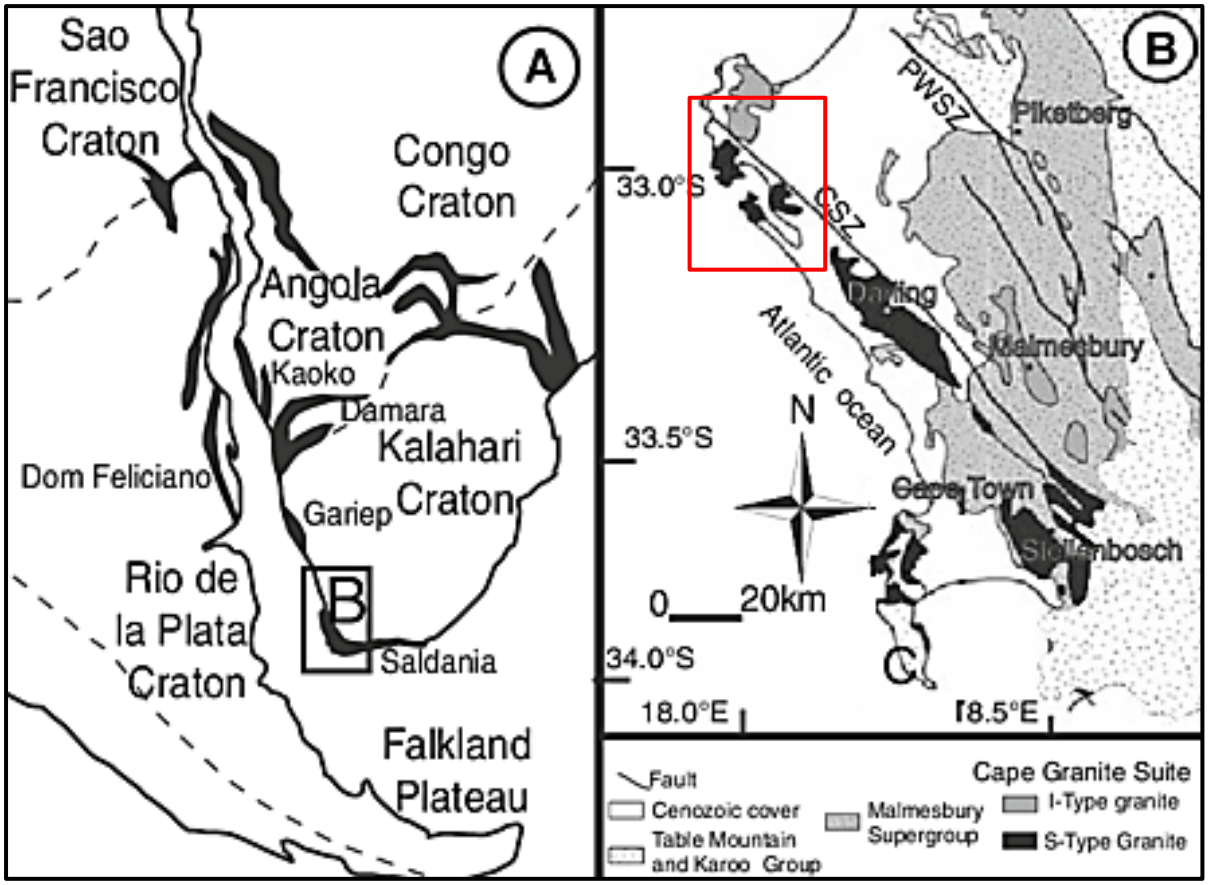

Figure 5: (A) Palaeographic reconstruction of the Saldania Orogeny at 550 Ma showing the distribution of the Pan-African orogenic belts in southern Africa and South America. (B) Geological map of the Saldania and Gariep Belts including the intrusive Cape Granite Suite (CGS) and the study area of this thesis indicated by the red rectangle (modified after Rozendaal et al., 1999).

However, this terrane model was challenged by Belcher and Kisters (2003) where they differentiated between an older redefined Swartland Group and a younger Malmesbury Group. This differentiation was seen across all three terranes where both groups were separated by an inferred unconformity. An alleged older deformation phase was recognised in the Swartland Group only and is described as a high-grade polydeformed paragneiss, which according to Frimmel et al. (2011) is likely to be part of the Mesoproterozoic basement of the Namaqua-Natal belt. This interpretation, however, becomes highly problematic. Frimmel et al. (2011) suggested that the Swartland "terrane" sediments must have been deposited on their basement rather than the Neoproterozoic one as previously mentioned. The same is likely for the basement of the Boland "terrane." Therefore, the Swartland and Boland tectono-stratigraphic units are no longer believed to be true terranes but rather represent para-autochthonous zones of the Kalahari Craton. Only the westernmost portion of the Tygerberg terrane might be a true autochthonous terrane.

Nevertheless, Rozendaal et al. (1999) suggested a possible Meso- to Paleo-Proterozoic crystalline basement on which the Malmesbury Group was deposited during the break-up of the supercontinent Rodinia (ca. 780 – 750 Ma). The existence of a Namaquan (1.0 - 1.2 Ga) and possibly an Eburnean (1.7 - 2.0 Ga) basement underlying the Malmesbury Group was confirmed by Da Silva et al. (2000), Scheepers and Armstrong (2002) and Villaros et al. (2012); with reported inherited zircon cores dated back to 1.1 - 1.9 Ga within the intruded granitoids of the Cape Granite Suite.

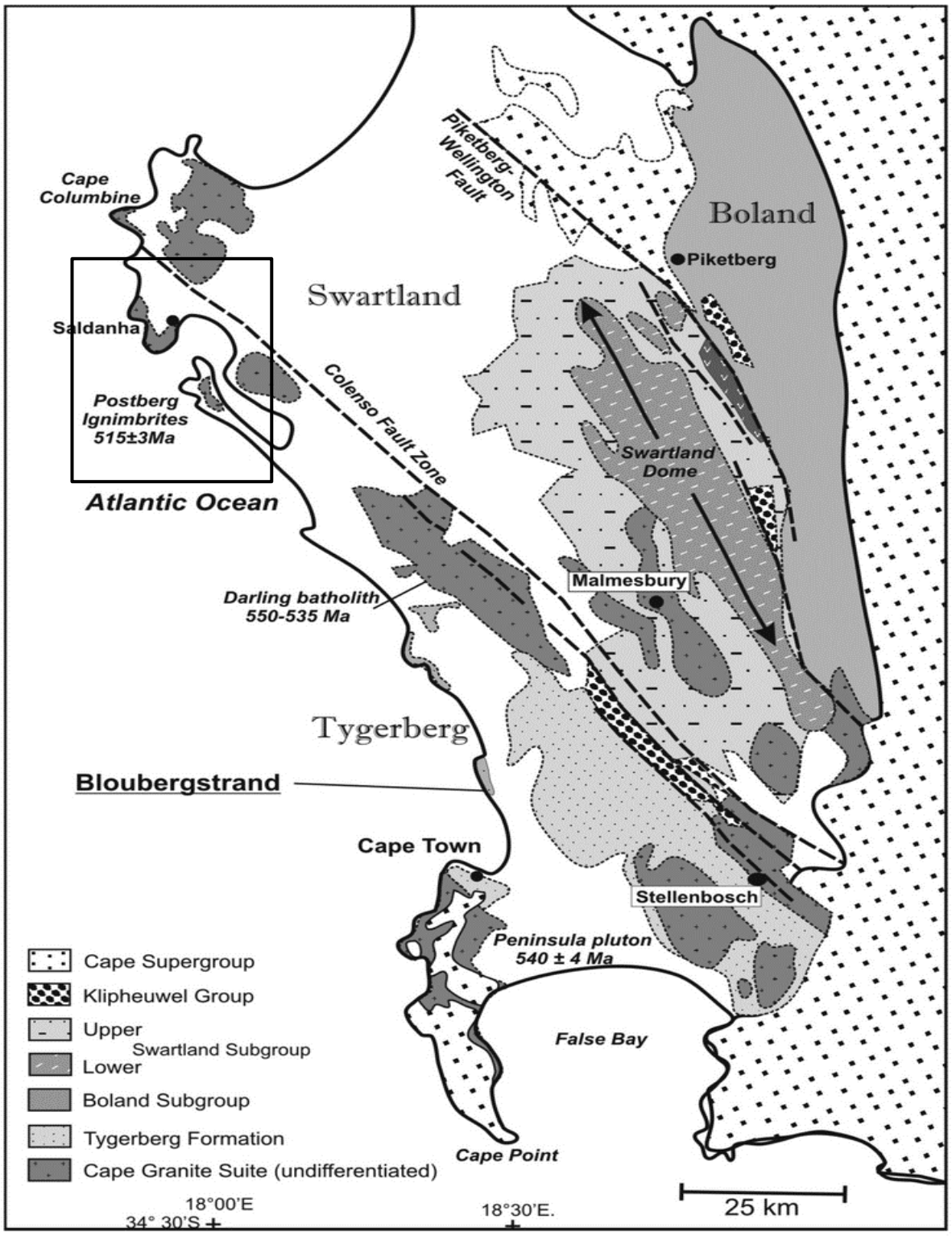

Figure 6: Geological map showing the southwestern coast of South Africa (the northern branch of the Saldanha belt) and the distribution of the various granitic plutons of the Cape Granite Suite (undifferentiated), major fault zones and the three terranes of the Malmesbury Group. The black square indicates the study area (after Hartnady et al, 1972; Theron et al.,1991).

2.2.3 The Cape Granite Suite

Subsequent to the closure of the Adamastor Ocean and continental collisions, the Malmesbury Group rocks were syn- and post-tectonically intruded in a pervasive transpressive regime between 555 Ma and 515 Ma by Neoproterozoic to early Cambrian S-, I- and A-type granites, monzodiorites, gabbros and quartz syenites. Collectively they constitute the Cape Granite Suite (CGS, Gresse and Scheepers, 1993; Scheepers, 1995; Scheepers and Armstrong, 2002; Belcher and Kisters, 2003). Scheepers (1995) subdivided these intrusive granitoids (S-, I- and A-type) primarily according to geological and petrological analysis as well as, to a lesser extent, on the field relations, multi-cationic interpretations, major and trace element geochemistry, rare earth element composition and age.

While the age of the Malmesbury Group is somewhat elusive, recent geochronological studies on the exposed upper portions of the Cape Granite Suite plutons points to a late-Neoproterozoic (~575 – 555 Ma) timing of deposition, sedimentation and volcanism making them the oldest rocks in the Saldania belt (Scheepers and Armstrong, 2002). The inliers of the Saldania belt are partly, unconformably overlain by successions of lower Phanerozoic (Ordovician to Silurian) sub-greenschist facies quartz-rich metasediments of the Cape Supergroup and were extensively affected during the Permo-Triassic Cape Orogeny (Gresse et al., 1992; Gresse et al., 1996; Barnett et al., 1997; Scheepers and Armstrong, 2002).

Based on internal structure, petrographic analysis, mineralogy, the nature of enclaves, geochemical features and relationships with enclosing rocks - Scheepers and Rozendaal (1992) and Gresse and Scheepers (1993) identified three major phases (I, II, III) of igneous magmatism for the Saldania belt. Scheepers and Nortjé (2000) later added an additional volcanic (rhyolitic) phase (IV). These four major phases of magmatism were further subdivided into seven distinct granitic associations (Table 1), each having one or more unique features: Sa1, Sa2, Sb, Ia, Ib, Aa and Ab (Scheepers, 1995).

Table 1: Summary of the major phases of the magmatism for the Saldania Belt, modified after Scheepers (1995).

Magmatism	Association	Rock Type	Examples
Phase IV 515 Ma	Volcanic	Ignimbrite, tuffisite, quartz porphyry	Postberg Ignimbrite, Saldanha "quartz porphyry"
Phase III 520 Ma	Aa	Alkali Fs granite, Quartz syenite	Klipberg granite
	Ab	Alkali Fs Granite	Cape Columbine granite
Phase II 540-520 Ma	Ib	Granite, alkali Fs granite	Paarl fine grained granite, Slippers Bay granite
	Ia	Monzogranite, granite, alkali Fs granite	Paarl coarse-and medium- grained granite, Vredenburg monzogranite, Greyton pluton
Phase I 555-540 Ma	Sb	Granite	Trekoskraal granite, Karnberg, Rondeberg granite, Coarse porphyritic, Darling granite
	Sa_2	Granite, alkali Fs granite	Stellenbosch fine grained granite, Contreberg granite, Olifantskop granite
	Sa_1	Granite	Hoedjiespunt granite, Seeberg granite, Peninsula granite

2.2.3.1 Phase I Magmatism

The first phase (555 – 540 Ma) of magmatism consists of collision-related syn- to late-tectonic granites with peraluminous to metaluminous S-type characteristics (Sb, Sa2, Sa1), intrusive mainly in the Tygerberg terrane (Scheepers, 1995). These granitoids were precursed by mafic and intermediate magmas of tholeiitic affinity and are characterised by low K_2O and granophile elements. The older and geochemically distinct Sa association (~560 Ma) is further subdivided into Sa_1 and Sa_2 where P_2O_5 and Th were used as the principle discriminating factors. For further differentiation Na_2O, K_2O, Zr, Nb, Y and REE discrimination was applied (Scheepers, 1995). The initial phase of magmatism of the Saldania Belt concluded with the intrusion of the Sb granititoids (540 Ma) along or in the vicinity of major fault zones. Scheepers (1995) describe the Sb association as "contaminated metaluminous melts with a high degree of fractionation" and inferred that the stability of amphiboles seen in some intrusions show the transition towards the I-type characteristics of the second magmatic phase.

2.2.3.2 Phase II Magmatism

The second phase (540 – 520 Ma) of magmatism is dominated by late-tectonic, metaluminous to slightly peraluminous I-type intrusions, currently exposed in the Boland and Swartland terranes. Two distinct associations are recognised: the first (Ia), showing high concentrations of Th and other radioelements, these rocks classify as high K calc-alkaline quartz-monzonites and granites with I-type features. The second (Ib) and slightly younger (~517 – 520 Ma) association, intrusive into the Ia quartz-monzonites, consists of alkali feldspar granites (Scheepers, 1995). Both associations can be found in the Swartland and the Boland terranes (Da Silva et al., 2000).

2.2.3.3 Phase III Magmatism

The third phase consists of a series of anorogenic A-type granites that intruded both the Tygerberg and Swartland terranes post-tectonically at ~520 Ma. The intrusion of a high-K calc-alkaline intermediate rock starts this phase of felsic magmatism and can be subdivided into two compositionally distinct A-type associations known as Aa and Ab (Scheepers, 1995). Scheepers and Poujol (2002) describes how the Aa associated granitic rocks, enriched in Nb, Zr and REE, vary in composition from Ab amphibole quartz- to biotitic quartz- syenite and alkali feldspar granite. This association lacks deformation and shows small-scale widely scattered xenoliths, whereas the Ab associated granitic rocks, enriched in Th, Y and REE, is primarily alkali feldspar granites, and show no such features (Scheepers 1995).

2.2.3.4 Phase IV Magmatism

The fourth and final phase of magmatism is assigned to the volcanic association of the felsic magmatic events that took place in the Saldania belt. Scheepers and Poujol (2002) described this phase as fractionated peraluminous S-type volcanic and subvolcanic rocks exposed in the Saldanha Bay area. There is a notable geochemical differentiation between the two, with the volcanics being enriched in SiO_2, having a higher ASI value and a higher Rb/Sr ratio than the subvolcanic counterpart. This phase was also described by Scheepers and Armstrong (2002) as extrusions of rhyolitic to rhyodacite peraluminous felsic rocks present as hypabyssal rhyolites, tuffisites, and ‘quartz porphyries’ on the northern side of Saldanha Bay. It was

concluded that the volcanism in Saldanha Bay, along the NW-SE orientated fracture zone, are primarily ignimbrite flows and tuffisite intrusions. Scheepers and Nortjé (2002) described the rocks of the Postberg peninsula, the southern portion of Saldanha Bay, as large ignimbrite flows which were dated at 515 ± 3 Ma by Scheepers and Poujol, (2002) using limited microprobe analysis on zircon.

Table 2: Summary table of the evolution of the Saldania Belt (after Rozendaal et al., 1999).

Event	Age (Ma)	Tectonic regime	Basin type	Sedimentation	Magmatism
Rifting Phase Break-up of supercontinent Rodinia and opening of proto-Atlantic Ocean	780 - 750	Transtensional, rifted margin	Stepped pull-apart basins	Rift related diamictite, arkosic quartzite, distal facies conglomerate quartzite and limestone (Goegamma Subgroup, Boland terrane, Gamtoos Group)	Rift volcanic/intrusive andesite, dolerite/diabase (Brewelskloof, Tulbag, Kango)
Ocean floor spreading	700 - 600	Transtentional	Evolving ocean/ continental margin basins	Deep water thick turbidite successions (Swartland terrane, Goegamma Subgroup, Kaaimans and Gamtoos groups)	Basaltic, WPB-MORM (Bridgetown Formation)
Reversal/ transpression and subduction phase Reversal of spreading and closure of proto-Atlantic Ocean Subduction/ oblique collision	600 - 570 570 - 545	Sinistral transpressional Poorly developed collision orogeny			Syn - and post-tectonic S-, I- and A-type granites (Cape Granite Suite)
(Cape Granite Suite) Foreland basin phase Development of syn- to post-orogenic basins	(550 - 510) 570 - 510	Syn- to post-orogenic	Foreland, intra-orogen and marginal pull-apart basins	Molassic and related deposits (Kansa subgroup, Franschhoek)	

2.3 Local Geology

2.3.1 Saldanha Bay, Saldanha, southwestern coastline of South Africa

Saldanha Bay's major lithological unit was initially mapped as a 250 km^2 high-level intrusive volcanic succession, known as "Saldanha quartz porphyry" (Scholtz, 1946). These rocks were originally dated by Schoch and Burger (1976) to have a U-Pb zircon age of 522 ± 12 Ma, and then later dated to 515 ± 3 Ma by Scheepers and Poujol (2002) using ion-microprobe analyses.

Scheepers and Poujol (2002) inferred that the "Saldanha quartz porphyry" was the younger magmatic phase when compared to the surrounding granites, due to the presence of older granitic enclaves (i.e. Hoedjiespunt Granite) inside the "quartz porphyry", thereby establishing what they interpreted as an intrusive relationship between the two rock types. These enclaves however, establishes an age relationship between the two rock types but does not provide evidence for an intrusive origin, as most explosive volcanism often produces large blocks of pre-existing rocks at the base of the deposits which was not the case in Saldanha Bay (Clemens and Stevens, 2016a; Branney and Kokelaar, 2002).

Scheepers and Nortjé (2000) identified the rocks on the southern side of Saldanha Bay, known as the Postberg peninsula, as ignimbrites. The rocks on the northern side, known as the Saldanha Peninsula, were described by Scheepers and Armstrong (2002) as hypabyssal rhyolites (sometimes known as 'quartz porphyries') and tuffisites (see Fig. 4A). Scheepers and Poujol (2002) proposed the term "Saldanha tuffisite" for those rocks with notable textural and mineral variations. These rocks exhibit flow banding, have a cryptocrystalline matrix and contain fragmented crystals, although, they become increasingly microcrystalline as one moves further away from the "intrusive" contacts. They proposed that the peraluminous rhyolitic phase of the Postberg peninsula and the "quartz porphyry/ tuffisite" of the Saldanha peninsula represented the volcanic to subvolcanic hypabyssal /near-surface end of the CGS (Scheepers and Armstrong, 2002; Scheepers and Poujol, 2002). The compositional variations seen between the Postberg Ignimbrites and the "quartz porphyry" indicated that the upper SiO_2 -rich portion of the magma chamber was tapped in the early stages of crystallisation. This described the formation of the basal rhyolitic phase and the crystallization of the upper

rhyodacitic phase, as the magma chamber became increasingly more depleted over time (Scheepers and Nortjé, 2000). Scheepers and Poujol (2002) concluded that the emplacement of the tuffisites and "quartz porphyry" was a direct result of the magma chamber undergoing a huge degassing event which caused a reduction in the magma flow, choking the vents, and creating rocks with subvolcanic features. Again, this interpretation may stem from the fact that they viewed the rock body, as a whole, as having an intrusive origin.

The presence of columnar jointing and recrystallized lapilli as well as evidence of recrystallized pumice fragments of feldspar and interlocking quartz, seen on both a macro and microscopic scale, raised the question of whether or not these rocks have been interpreted correctly as Saldanha "quartz porphyry." This initiated a re-examination of the Saldanha peninsula rocks. Clemens and Stevens (2016) established that the rocks are fragmented and show S-type volcanic characteristics and unconformably overlay an eroded surface of the Hoedjiespunt granite. They reinterpreted the geology of the Saldanha Bay area as having two separate bodies, both of which are S-type ignimbrites (Figure 7), on opposite ends of the Saldanha Bay entrance. One lies to the north, in the Saldanha peninsula, and the other to the south, mainly on the tip of the Postberg peninsula. They describe these S-type bodies as a massive welded ignimbrite succession and suggested that the area around Saldanha Bay represents a large composite caldera complex consisting of the Postberg and Saldanha eruption centres, together known as the Saldanha Bay Volcanic Complex (
Figure 7B). They concluded that the rocks of the Saldanha centre are not 'tuffisites' but predominantly ignimbrites and that the volcanic activity may have overlapped with that in the Postberg centre. Since the whole volcanic complex is roughly 30 km^2 in extent, it is reasonable to hypothesize a close relationship between the two eruption centres and their products (Clemens et al., 2017).

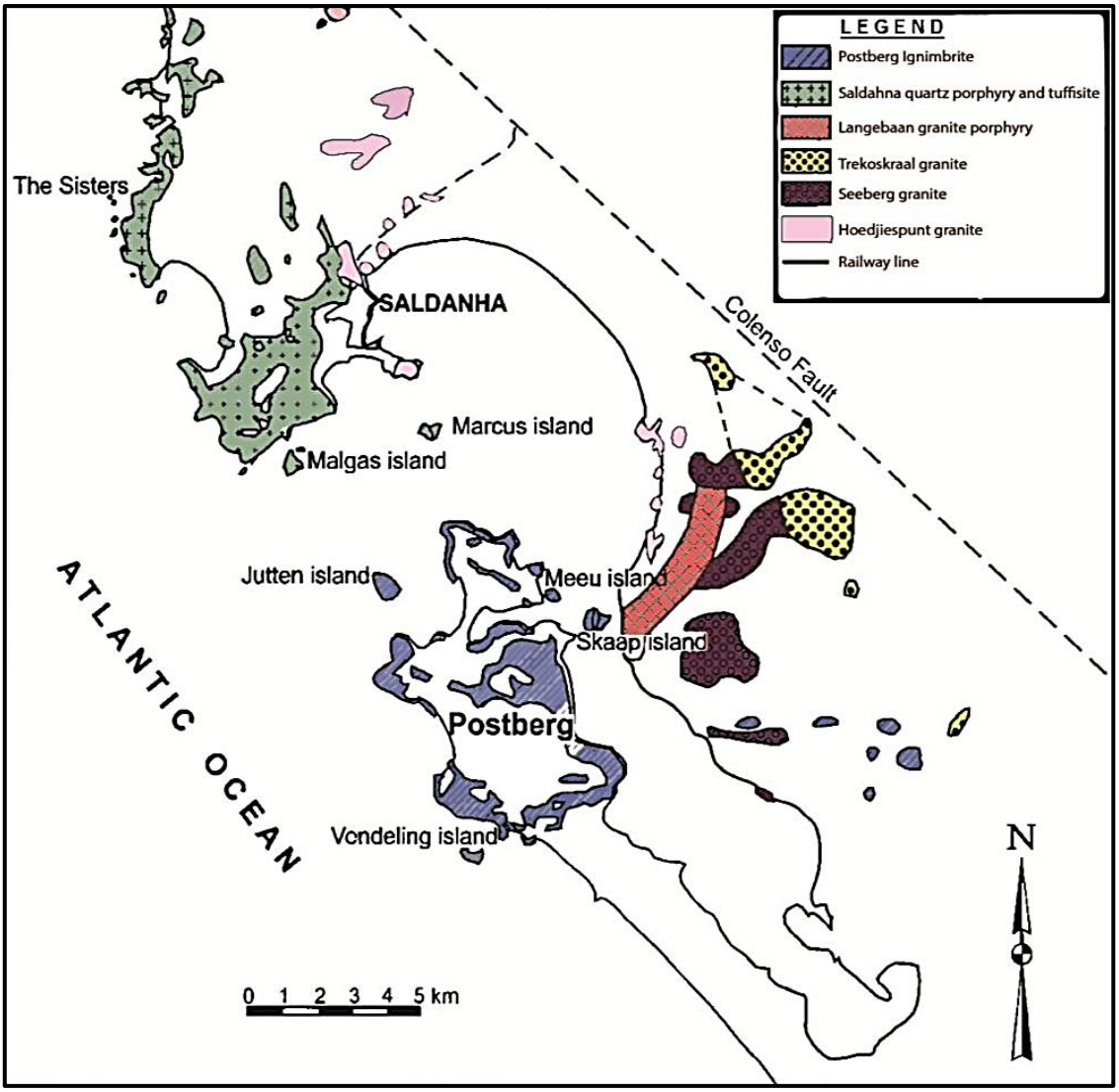

Figure 7: A simplified geological map illustrating the distribution of the granitic and volcanic phase, now considered to be an incorrect interpretation (after Scheepers and Armstrong, 2002).

Clemens and Stevens (2016a) found that in the Saldanha centre, two geochemically distinct ignimbrite magmas are present - the Saldanha and Jacob's Bay ignimbrites. They also recognised two geochemically distinct, more silicic magma groups in the Postberg centre - the Plankiesbaai and Tsaarsbank ignimbrites. The Plankiesbaai and the Tsaarsbank ignimbrites occurred exclusively in the Postberg centre while the other two members, the Saldanha and Jacobs Bay Ignimbrites, occur mainly in the Saldanha centre with minor volumes present in the Postberg centre.

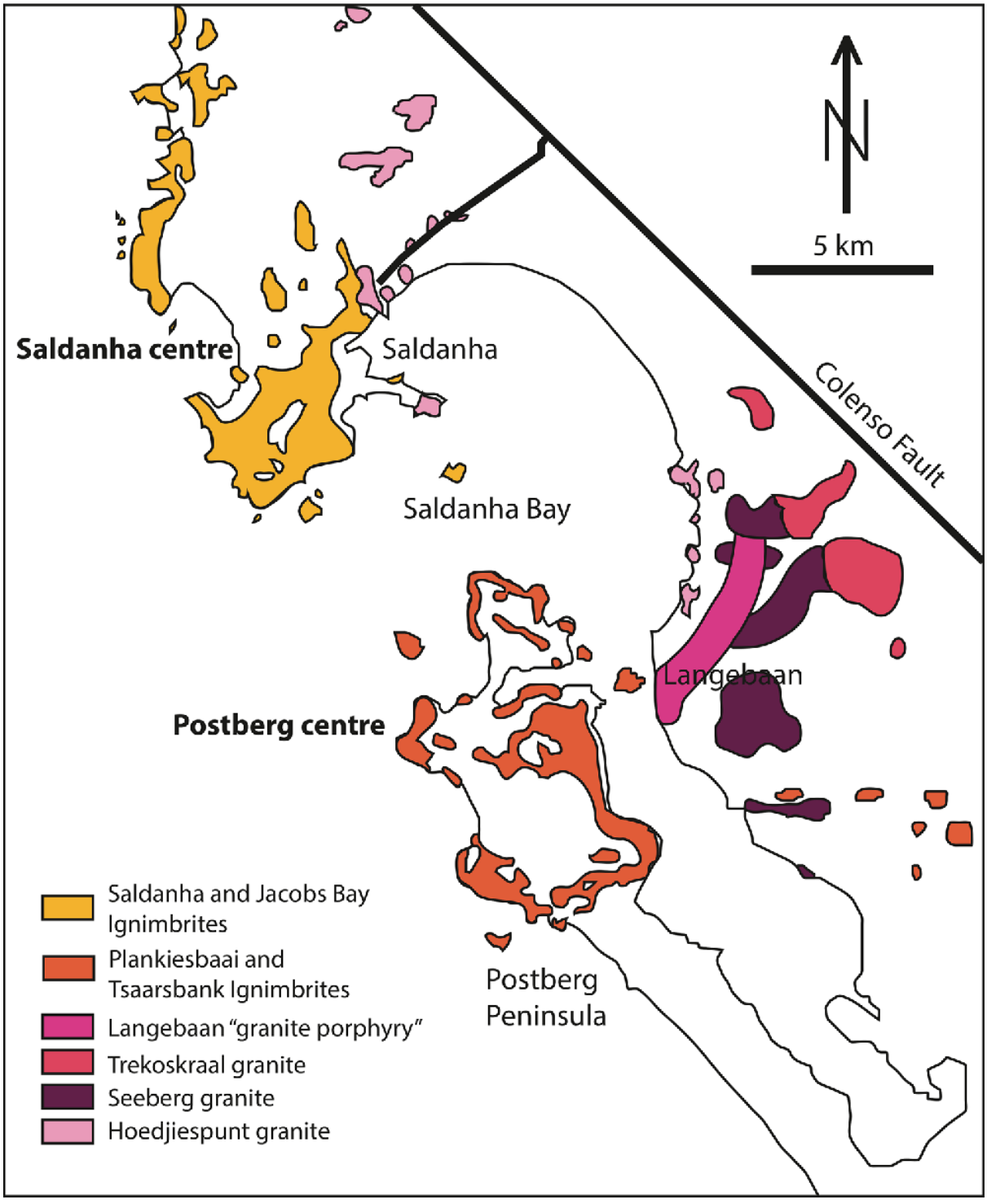

Figure 8: A geological map of the current interpretation of the Saldanha Bay Volcanic Complex showing the exposures of pre-volcanic granitic intrusions as well as the Postberg and Saldanha eruption centres (Note that both centres are now described as Ignimbrites). The white areas represent tertiary and quaternary sands and calcarenites. (after Clemens and Stevens, 2016).

Clemens et al. (2017) show that the rhyolitic magmas (Saldanha and Jacobs Bay Ignimbrites) erupted at 542 ± 3 Ma, which is considerably earlier than the published date for the Postberg ignimbrites at 515 ± 3 Ma by Scheepers and Poujol (2002). At least some volcanism (currently only confirmed for the Saldanha Centre rocks) was coeval with the main stages of magmatism in the CGS (550 – 530 Ma, Chemale et al. 2011).

The data presented here will show that the ignimbrites of the Postberg centre produces an almost identical U-Pb age to that of the Saldanha Centre ignimbrites (542 ± 2 Ma) at a date that is considerably earlier than the 515 ± 3 Ma age published by Scheepers and Poujol (2002). Clemens and Stevens (2016) suggested, based on the extent of the outcrop and revised mineralogy, that the volcanic activity of the eruption centres may have been co-synchronous but the volcanic activity of the Saldanha centre terminated slightly earlier than that of the Postberg centre. The new U-Pb ID- TIMS (Isotope Dilutions – Thermal Ionisation Mass Spectrometry) age of 542 ± 2 Ma for the Saldanha Centre presented by Clemens et al. (2017), in conjunction with the robust U-Pb age of 536 ± 3 – 542 ± 3 Ma presented in this thesis for the Postberg centre (see later), confirms this statement conclusively. It also confirms that the volcanism seen in the Saldanha Bay area was coeval with the main stages of magmatism of the CGS (550 – 530 Ma). A comprehensive and comparative geochemical data-set was built for the Postberg Ignimbrites by combining this studies' collected sample data with data from Scheepers and Poujol (2002), Scheepers and Nortjé (2000), Joseph (2012), Clemens and Stevens (2016), and Clemens et al. (2017). Rb-Sr/ Sm-Nd isotope correlations have also been included in order to constrain the source of the magmatic events of the Postberg Centre – Jacobs Bay Ignimbrite as well as to compare them to the Saldanha Centre- Jacobs Bay Ignimbrite's source.

3 Analytical Methods

3.1 Introduction

This chapter describes the criteria used in acquiring and developing the various datasets of this study. The outline of the entire analytical procedure as well as the quality control measures taken for each step is presented below. Sample sizes were chosen based on the prior knowledge of the study area and on aims for the analytical outputs. All data outputs were then processed and analysed accordingly.

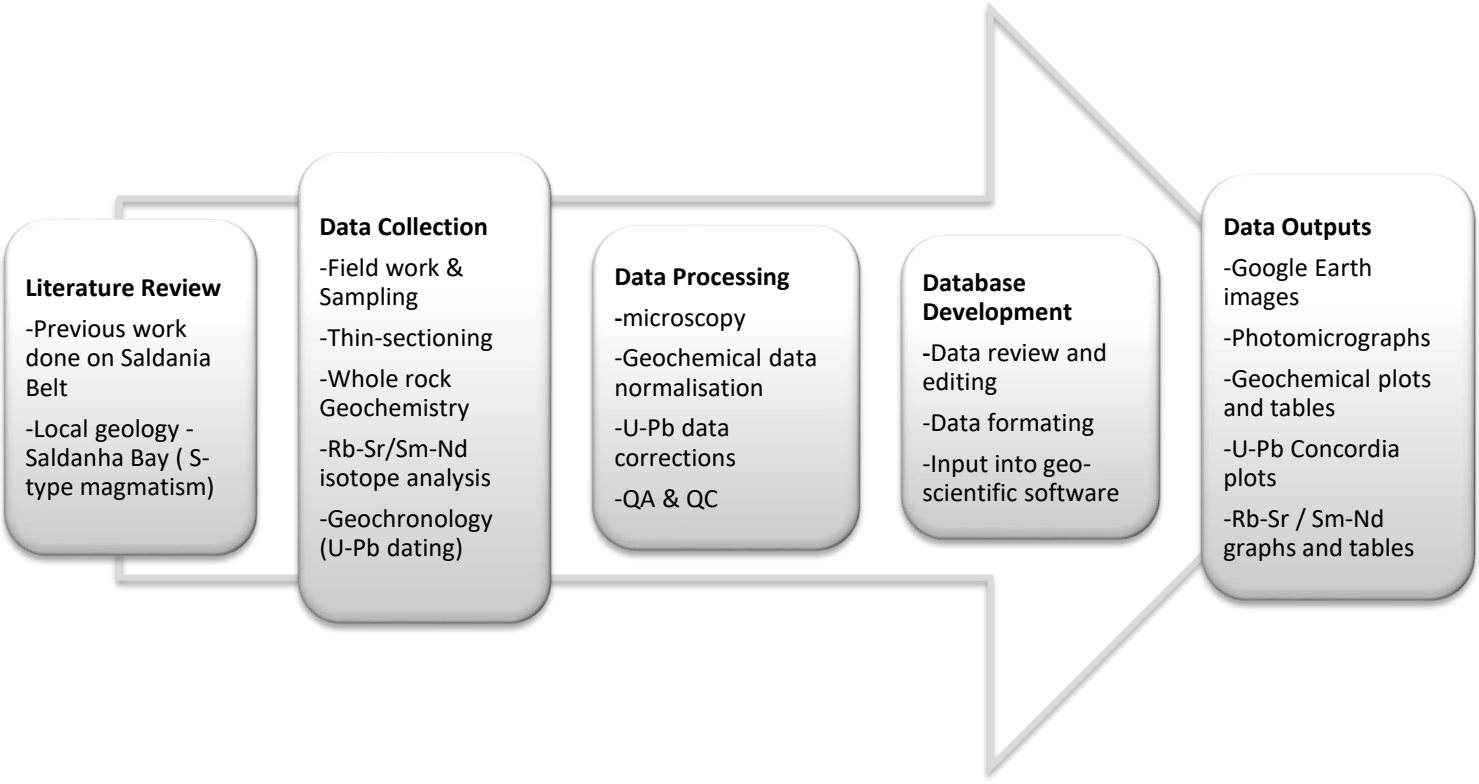

Figure 9: Flow chart outlining the research design, data collection, data processing and data outputs.

3.2 Research design and data collection

3.2.1 Fieldwork and sampling

The Postberg Ignimbrites of the Saldanha Bay Volcanic Complex are exposed exclusively in the West Coast National Park, South Africa. Permission from Cape Nature™ was obtained before the fieldwork commenced. A total of three representative samples weighing approximately 4-5 kg each of the Postberg Ignimbrites were collected in early August 2016, where standard sample-collection protocol was followed (see Figure 10 and Table 3). An additional two samples were received from Prof Gary Stevens at the University of Stellenbosch, from their extensive work done on the same area (see Clemens and Stevens, 2016). Altered or weathered segments of rock were removed with a diamond saw prior to thin sectioning and petrographic analysis at the University of the Western Cape, South Africa.

3.2.2 Petrographic analysis

Examination of the thin sections that were cut from various rock samples was performed at the University of the Western Cape's microscope laboratory using a Leica™ Microsystems DM300 Transmission microscope with Binocular 1000 x Transmitted light. Both normally transmitted plane-polarized and cross-polarized light was used for effective petrographic descriptions on the polished thin sections. Photomicrographs of the thin sections were taken on the same microscope with a Leica™ camera fitting.

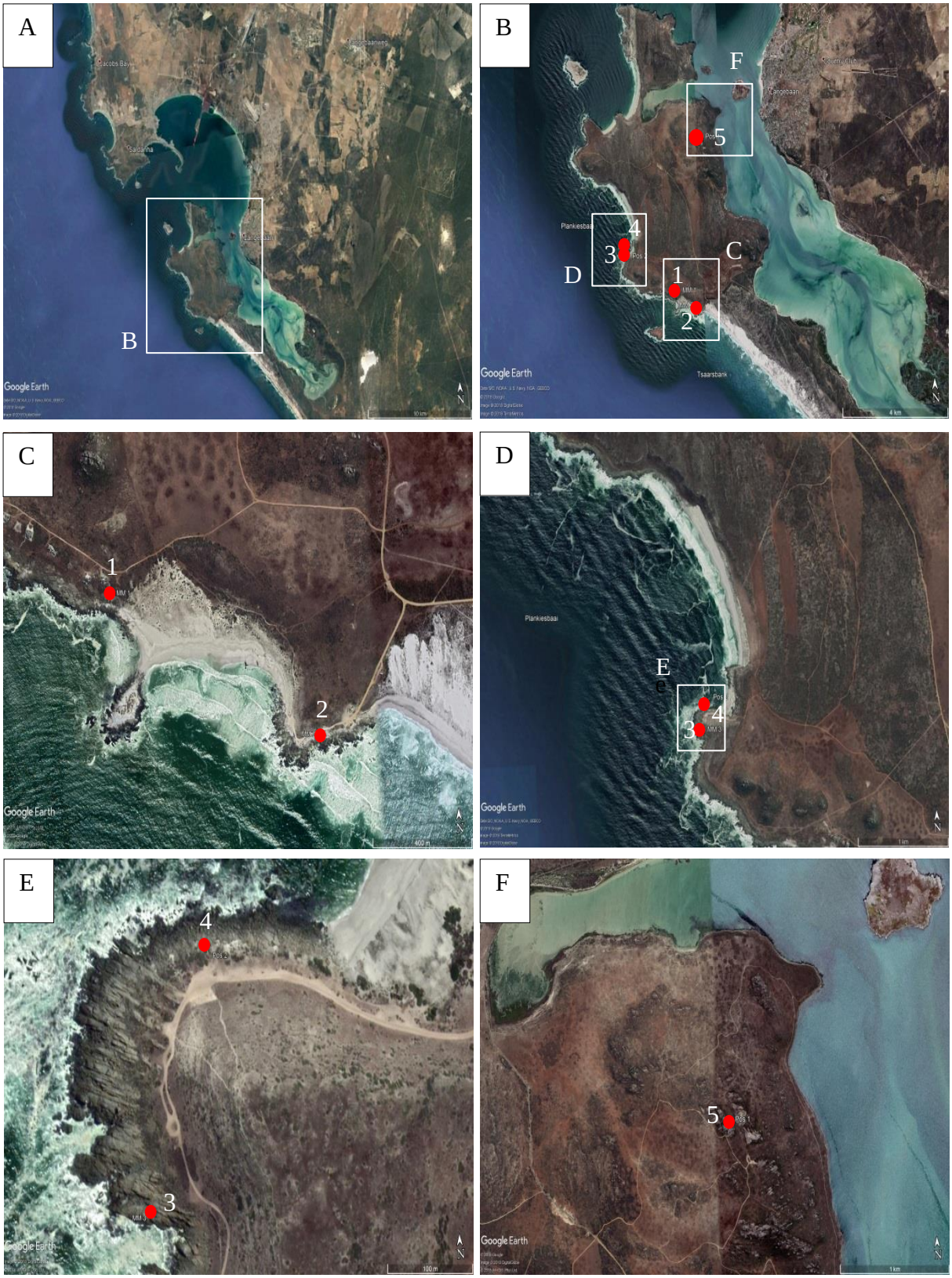

Figure 10: Google Earth™ images of the Saldanha Bay area showing the locations of all collected field samples: 1-MM1, 2-MM2, 3-MM3, 4-Pos1, and 5-Pos2. White boxes and corresponding letters represent zoomed in portions of the bay.

Table 3: Rock types and geographic location of all collected samples in the Postberg Centre, Saldanha Bay Volcanic Complex.

Sample Name	Rock Type	UTM	Longitude and Latitude	Elevation (m)
MM1	Ignimbrite	33H0779154 UTM-6328628	S 33° 08’42.7’’ E 17° 59’33.5’’	2
MM2	Ignimbrite	34H0220336 UTM-6328228	S 33° 08’54.1’’ E 18° 00’06.4’’	1
MM3	Ignimbrite	33H0777273 UTM-6329927	S 33° 08’02.3’’ E 17°58’19.6’’	5
Pos 1	Ignimbrite	-	S 33° 06’20.0’’ E 18°00’14.0’’	148
Pos 2	Ignimbrite	-	S 33° 07’53.0’’ E 17° 58’22.0’’	0

3.2.3 Whole rock chemistry

The bulk rock geochemical data is presented as electronic appendices EA1 and EA2 with a summary data table presented in EA3. Approximately 1-2 kg of rock sample were crushed to a fine powder (<1 mm) using a jaw crusher and tungsten swing mill prior to the preparation of a fused disc for whole rock analysis. The jaw crusher and swing mill were cleaned using pure quartz and acetone after processing each sample, to avoid cross contamination. Glass disks were prepared for XRF analysis at CAF, Stellenbosch University, South Africa, using 10g of high purity trace element and REE element free flux ($LiBO_2$ = 32.83%, $Li_2B_4O_7$ = 66.67%, LiI = 0.50%) mixed with 1g of the rock sample.

Whole rock major element compositions were determined by XRF spectrometry on a PANalytical Axios Wavelength Dispersive spectrometer. The instrument is fitted with a Rh tube, a gas–flow proportional counter, and a scintillation detector with the following

analysing crystals: LIF200, LIF220, LIF420, PE, and PX1. The gas–flow's proportional counter uses a 90% Argon and 10% methane gas mixture.

Major elements were analysed on a fused glass disk at 50 kV and 50 mA tube operating conditions. Matrix effects in the samples were corrected for by applying theoretical alpha factors and measured line overlap factors to the raw intensities measured with the SuperQ PANalytical software. The results are reported normalized to 100 wt% anhydrous, with total Fe expressed as FeO^T.

3.2.4 Trace element chemistry

The bulk rock geochemical data is presented as Electronic Appendices EA1 and EA2 with a summary data table presented in EA3. Fusion disks were prepared for XRF analysis by an automatic Claisse M4 Gas Fusion instrument and ultrapure Claisse Flux, using a ratio of 1:10 sample: flux, where the samples were coarsely crushed and a chip of sample mounted along with up to 12 other samples in a 2.4cm round resin disk. The mount was mapped and then polished for analysis.

An ASI 193 nm resolution Excimer laser connected to an Agilent 7500ce ICP–MS was used for the analysis of trace elements in bulk rock samples and single mineral grains. Ablation was performed in He gas at a flow rate of 0.35L/min, and then mixed with argon (0.9L/min) and Nitrogen (0.004L/min) just before introduction into the ICP. For traces in fusions, 2 spots of 100µm were ablated on each sample using a frequency of 10Hz and 3.6J/cm^2 energy (See Table 4 for further details).

Trace elements were quantified using NIST 612 for calibration and the wt.% SiO_2 from XRF measurement as internal standard, using standard - sample bracketing. Two replicate measurements were made on each sample, with the average reported as the measured concentration. The calibration standard was run every 12 samples. A quality control standard was run in the beginning of the sequence as well as with the calibration standards throughout. Further queries regarding the analytical procedures and methods should be addressed to the Central Analytical Facility (CAF) at Stellenbosch University, South Africa.

3.2.5 Rb-Sr & Sm-Nd isotope analysis

Tracer-isotope data collected for the Postberg Centre – Jacobs Bay Ignimbrites are presented as Electronic Appendix EA7. Chemical preparation of whole-rock Sr and Nd isotope analysis (Table 1) was performed in PicoTrace® clean lab facilities and isotope ratios were measured with a Nu Instruments thermal ionization mass spectrometer (Nu-TIMS) at Departamento de Geología, Centro de Investigación Científica y de Educación Superior de Ensenada (CICESE) in the state of Baja California (Mexico), equipped with twelve fixed Faraday cups and the Nu-instruments zoom optics for perfect alignment of all masses of interest into the Faraday cups. Element separation was achieved in two steps, first with quartz-glass columns filled with DOWEX AG 50W-X8 resin to separate Sr and REE and then with Ln-Spec® resin to separate Nd. Samples were loaded on Re filaments in double filament technique with H_3PO_4 for Nd and with single filament technique together with a TaF4 activator for Sr. Both Sr and Nd isotope ratios were measured in static mode (8 blocks of 10×16 s integrations). Correction for mass bias for Sr and Nd was achieved by normalizing to $^{86}Sr/^{88}Sr = 0.1194$ and $^{146}Nd/^{144}Nd = 0.7219$, respectively.

3.2.6 Zircon U-Pb geochronology

All U-Pb data for the samples collected from the Postberg Centre, Saldanha Bay Volcanic Complex, is presented as an Electronic Appendix EA6. Prior to U-Pb dating, the following sample preparation procedures were followed: Crushing and milling of approximately 2-5 kg rock sample, panning and magnetic separation by Frantz Isodynamic Separator, and heavy liquid separation (tetrabromoethane – $Br_2CHCHBr_2$) to further separate the non-magnetic fractions. From the processed sample, zircons were handpicked using a Wild M3Z microscope. A mixed SpeciFix Resin and Curing Agent along with the EpoFix Resin and hardener were poured into the mould and allowed to cure (1-inch resin mount). The mount was then polished (1µm) and prepared for cathodoluminescence (CL) imaging with a Zeiss MERLIN Field Emission Scanning Electron Microscope (FE-SEM) at CAF, Stellenbosch University.

In-situ U-Pb age dating of zircons was performed at the Central Analytical Facility (CAF) at Stellenbosch University. All U–Pb age data obtained at the CAF were acquired by laser ablation - single collector - magnetic sectorfield - inductively coupled plasma - mass spectrometry (LA-SF-ICP-MS) employing a Thermo Finnegan Element2 mass spectrometer coupled to an ASI Resolution SE S155 Excimer laser ablation system. Prior to age dating, the internal textures of the zircons were studied by CL imaging obtained at Central Analytical Facility (CAF) at Stellenbosch University (see Table 4).

All U-Pb age data presented here was obtained by single spot analyses with a spot diameter of 30 µm and a crater depth of approximately 10-15 µm. The methods employed for analysis and data processing are described in detail by Frei and Gerdes (2009) and Cornell et al. (2016). The calculation of Concordia ages and plotting of Concordia diagrams were performed using Isoplot/Ex 3.0 (Ludwig, 2003). For detailed method descriptions see Table 4 as well as Frei and Gerdes (2009).

Table 4: LA-SF-ICP-MS U-Th-Pb dating methodology provided by CAF, Stellenbosch University.

Laboratory & Sample Preparation	
Laboratory name	Central Analytical Facility, Stellenbosch University
Sample type / mineral	Magmatic zircons
Sample preparation	Conventional mineral separation, 1-inch resin mount, 1 µm polish to finish
Imaging	CL, LEO 1430 VP, 10 nA, 15 mm working distance
Laser ablation system	
Make, Model & type	ASI Resolution SE S155, ArF Excimer Atlex ATL
Ablation cell & volume	Laurin Technology S155 double Helix large volume cell
Laser wavelength	193 nm
Pulse width	4 ns
Fluence	1.4 J/cm^{-2} (measured with external energy meter above sample funnel)
Repetition rate	9 Hz
Spot size	30 µm
Sampling mode / pattern	30 µm single spot analyses
Cell carrier gas	100% He, Ar and N_2 make-up gases combined using injectors into double Helix sampling funnel
Pre-ablation laser warm-up (background collection)	3 cleaning shots followed by 20 seconds background collection
Ablation duration	15 seconds
Wash-out delay	15 seconds
Cell carrier gas flows	330 ml/min He
ICP-MS Instrument	
Make, Model & type	Thermo Finnigan Element2 single collector HR-SF-ICP-MS
Sample introduction	Via Nylon 10 tubing
RF power	1350 W
Make-up gas flow	910 ml/min Ar & 0.03 ml/min N_2
Detection system	Single collector secondary electron multiplier
Masses measured	202, 204, 206, 207, 208, 232, 233, 235, 238
Integration time per peak	4 ms
Total integration time per reading	1 sec *(represents the time resolution of the data)*
Sensitivity	30000 cps/ppm Pb
Dead time	6 ns
Data Processing	
Gas blank	20 second on-peak
Calibration strategy	GJ-1 used as primary reference material, Plešovice & M127 used as secondary reference material (Quality Control)
Reference Material info	GJ-1 (Jackson et al. 2004), Plešovice (Slama et al. 2008), M127 (Nasdala et al. 2008; Mattinson 2010)
Data processing package used / Correction for LIEF	In-house spreadsheet data processing using intercept method for LIEF correction
Mass discrimination	Standard-sample bracketing with $^{207}Pb/^{206}Pb$ and $^{206}Pb/^{238}U$ normalized to reference material GJ-1
Common-Pb correction, composition and uncertainty	204-method, Stacey & Kramers (1975) composition at the projected age of the mineral, 5% uncertainty assigned
Uncertainty level & propagation	Ages are quoted at 2 sigma absolute, propagation is by quadratic addition. Reproducibility and age uncertainty of reference material and common-Pb composition uncertainty are propagated.
Quality control / Validation	M127: Concordia age = 529±4 Ma (2s, MSWD = 0.27) Plešovice: Concordia age = 340±2 Ma (2s, MSWD = 0.47)

3.3 Data quality control

3.3.1 Whole rock chemistry

The control standards used in the calibration procedures for major element analyses were NIM-G (granite from the Council for Mineral Technology, South Africa) and BHVO-1 (basalt from the United States Geological Survey, Reston). For quality control, GJ-1 was used as the primary reference material and Plešovice & M127 as the secondary reference material. In-house spread-sheet data processing using intercept method was used for LIEF correction. Standard-sample bracketing with $^{207}Pb/^{206}Pb$ and $^{206}Pb/^{238}U$ was normalized to reference material GJ-1, see Electronic Appendix EA4.

3.3.2 Trace element chemistry

BCR-2 or BHVO 2G, both basaltic glass certified reference standards produced by USGS (Dr Steve Wilson, Denver, CO 80225), were run at the beginning of the sequence. A fusion control standard from certified basaltic reference material (BCR-2, also from USGS) was also analysed in the beginning of a sequence to verify the effective ablation of fused material. The reference material is from published BHVO glass in Jochum et al. (2005) and BHVO powder form Jochum et al. (2016). Data tables are presented as Electronic Appendix EA4.

3.3.3 Rb-Sr & Sm-Nd isotope analysis

The neodymium standard JNdi-1 (Tanaka et al., 2000), analysed in the same run as the unknowns, yielded $^{143}Nd/^{144}Nd = 0.512103 \pm 3$ (2σ); the average of six analyses within the same month was 0.512099 ± 4 (1 s.d.). NIST 987 standard yielded $^{87}Sr/^{86}Sr = 0.710236 \pm 10$ (2σ) when measured with the unknowns, and an average of 0.710236 ± 8 (1 s.d.) for six analyses carried out in the same month as the analysis of the unknowns.

3.3.4 Zircon U-Pb geochronology

For quality control, the Plesovice (Sláma et al., 2008) and M127 (Nasdala et al., 2008; Mattinson, 2010) zircon reference materials were analysed, and the results were consistently in excellent agreement with the published ID-TIMS ages. Full analytical details and the results for all quality control materials analysed are presented as Electronic Appendix EA5 (Figure 37Figure 40). Table 4: LA-SF-ICP-MS U-Th-Pb describes the dating methodology of CAF, Stellenbosch University.

4 RESULTS

4.1 Introduction

This chapter aims to embody all the data outputs of the Postberg Ignimbrite - Saldanha Bay research. An array of figures, graphs and tables are presented beginning with a petrolographical display of the Postberg Ignimbrite samples. Various photos of rock cuttings are displayed along with their corresponding thin-section photomicrographs.

The geochemical outputs are displayed as a variety of chemical variation diagrams. It is important to note, as this thesis aims to re-asses both geochemistry and the age distribution of these ignimbrites relative to previous studies, that the geochemical data for the Postberg eruption centre is a collection of various studies, including Scheepers and Poujol (2002), Scheepers and Nortjé (2000), Joseph (2012), Clemens and Stevens (2016), and Clemens et al. (2017) with additional field samples collected for this report. Furthermore, a variety of geochemical plots from Clemens et al. (2017) have been included for the Saldanha Centre Ignimbrites. Although they are not part of the primary study, they have been inserted for contextual, comparative and classification purposes.

Rb/Sr and Sm/Nd tracer isotope data for Postberg Centre – Jacobs Bay ignimbrites is displayed as a variety of correlation plots and tables, which includes those of the Saldanha Centre – Jacobs Bay ignimbrites in order to compare their magmatic source to that of the Postberg eruption centre. All the modified data tables are displayed as Electronic Appendices.

The U-Pb isotope data results are presented as cathodoluminescence (CL) images, Concordia data plots and probability-density distribution plots for selected samples of the Postberg

Centre. A description of the form, colour, and internal structure of the extracted zircon grains are presented with the U-Pb age for the various samples, referenced to their corresponding figures and their respective data tables, are displayed in the Electronic Appendices along with quality control diagrams for selected reference material.

In this chapter, several abbreviations are used for the various types of ignimbrites found in the Postberg and Saldanha eruption centre. When referring to the eruption centres themselves, the abbreviations “PC” is used for the Postberg Centre and “SC” for the Saldanha Centre. As mentioned before the Saldanha Bay Volcanic Complex has four geochemically distinct magma series. The abbreviations for the different magma series were done as follows: the Plankiesbaai Ignimbrites “PI” and Tsaarsbank Ignimbrites “TI” (both found exclusively in the Postberg Centre) and the Saldanha Ignimbrite “SI” and Jacobs Bay Ignimbrite “JI” (found in both eruption centres). Therefore, when describing a specific magma series (PI, TI, SI or JI) within an eruption centre (PC or SC) the abbreviation was made as follows: “eruption centre” – “magma series”. For example, the Postberg Centre - Saldanha Ignimbrite is abbreviated to (PC-SI) and Saldanha Centre - Saldanha Ignimbrite to (SC-SI) etc.

4.2 Petrography

The three representative “MM” samples of this study collected from the Postberg Centre are fine-grained pyroclastic rocks that chemically classify as Jacobs Bay Ignimbrites (PC-JI). They are light/medium grey to pale brown in colour (Figure 11) and contain small magma clasts.

Phenocrysts constitute around 50-65 vol. % of the Postberg Ignimbrites with varied phenocrystic assemblages of (note these are expressed as a percentage of the phenocrysts vol. %) alkali feldspar (35%), quartz (25%), plagioclase (20%), biotite (15%) and orthopyroxene (5%). The crystal grain size varies between microcrysts of ~ 0.1 mm to 0.6 mm and phenocrysts from ~ 0.8 mm to ~6mm. Several textures and alterations can also be seen in the photomicrographs and will be discussed later. The diagrams display a variety of photo-macrographs (**Error! Reference source not found.**) and photomicrographs (**Error! Reference source not found.**,**Error! Reference source not found.** and**Error! Reference source not found.**) with some areas of interest displayed at 10x/0.25 magnification (displayed in both cross and plane polarised light).

Alkali feldspar (usually light to medium-grey/pale brown to tan in colour) and quartz (pale to medium grey in colour) make up the greatest proportion of phenocrysts in the Postberg Ignimbrites (~60% of the total phenocrystic vol. %). Approximately 35 vol. % of the Postberg Ignimbrites is groundmass - primarily recrystallized polygonal quartz and feldspar (plagioclase and alkali feldspar) granules with some recrystallized biotite ingrowths.

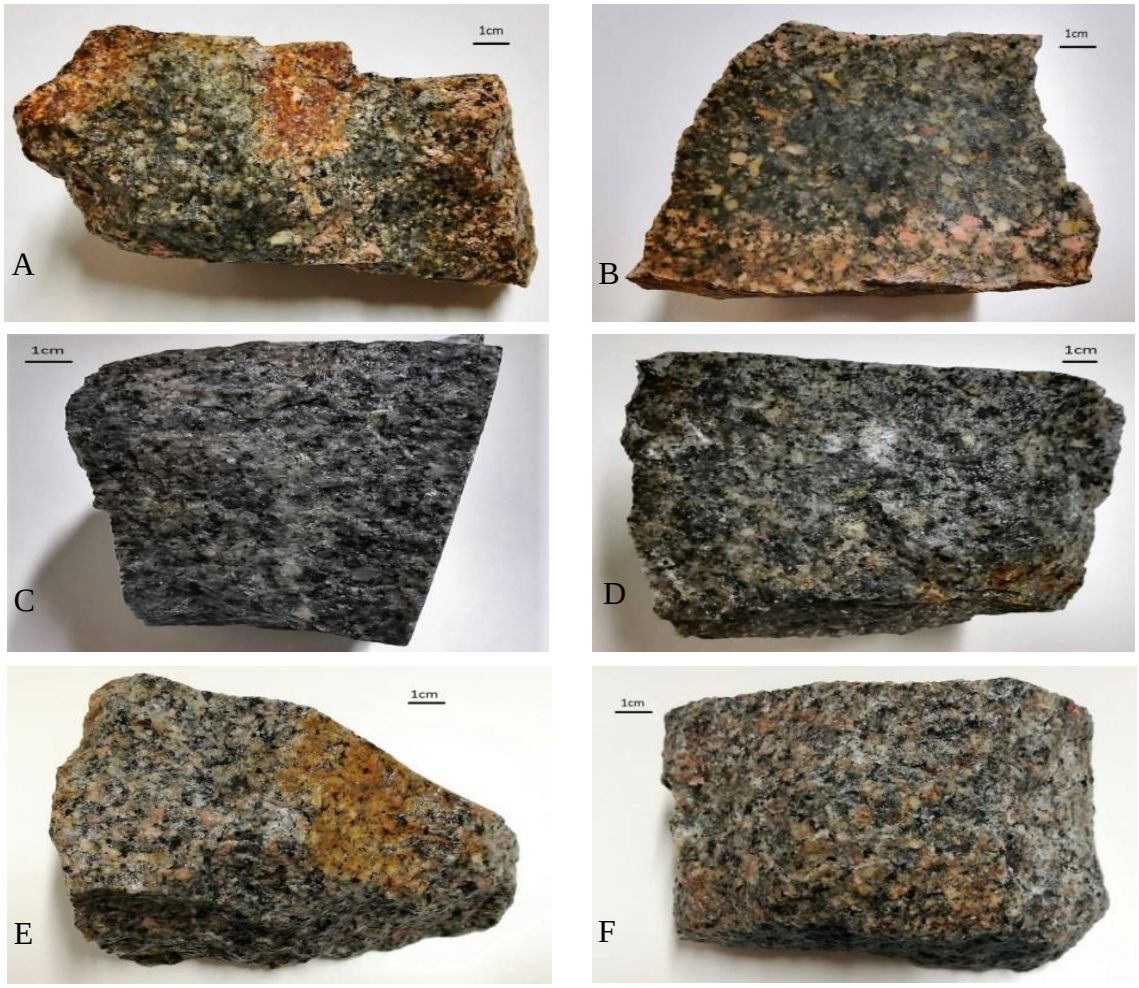

Figure 11: Macrophotographs of the rock samples collected in the Postberg Centre. A & B) - Sample MM1; C & D) -Sample MM2; E & F) -Sample MM3.

Alkali feldspar phenocrysts (~1-6 mm grain size) form subhedral to anhedral grain shapes. They are often fractured/broken (Figure 12 A, C, & F and Figure 13 A, C & A) and exhibit some rounding at the edges of the crystal (Figure 12 A, C & F and Figure 13 A, C & F). Exsolution of albite lamellae (Figure 13 A & E) as well as sericite and chlorite alteration (Figure 12 E, Figure 13 C & D and Figure 14 C & D), although highly variable, are not uncommon. The perthitic texture seen in these crystals, caused by subsolidus unmixing of two minerals, resulted in an intergrowth of both sodic and potassic feldspar during recrystallization (Figure 13 E). Under higher magnification, displays of both simple and multiple twinning are observed in most alkali feldspar phenocrysts, where multiple inclusions of biotite, orthopyroxene and zircons (Figure 12 A & B, Figure 13 B, C & D and Figure 14 B, C & D) are a regular occurrence.

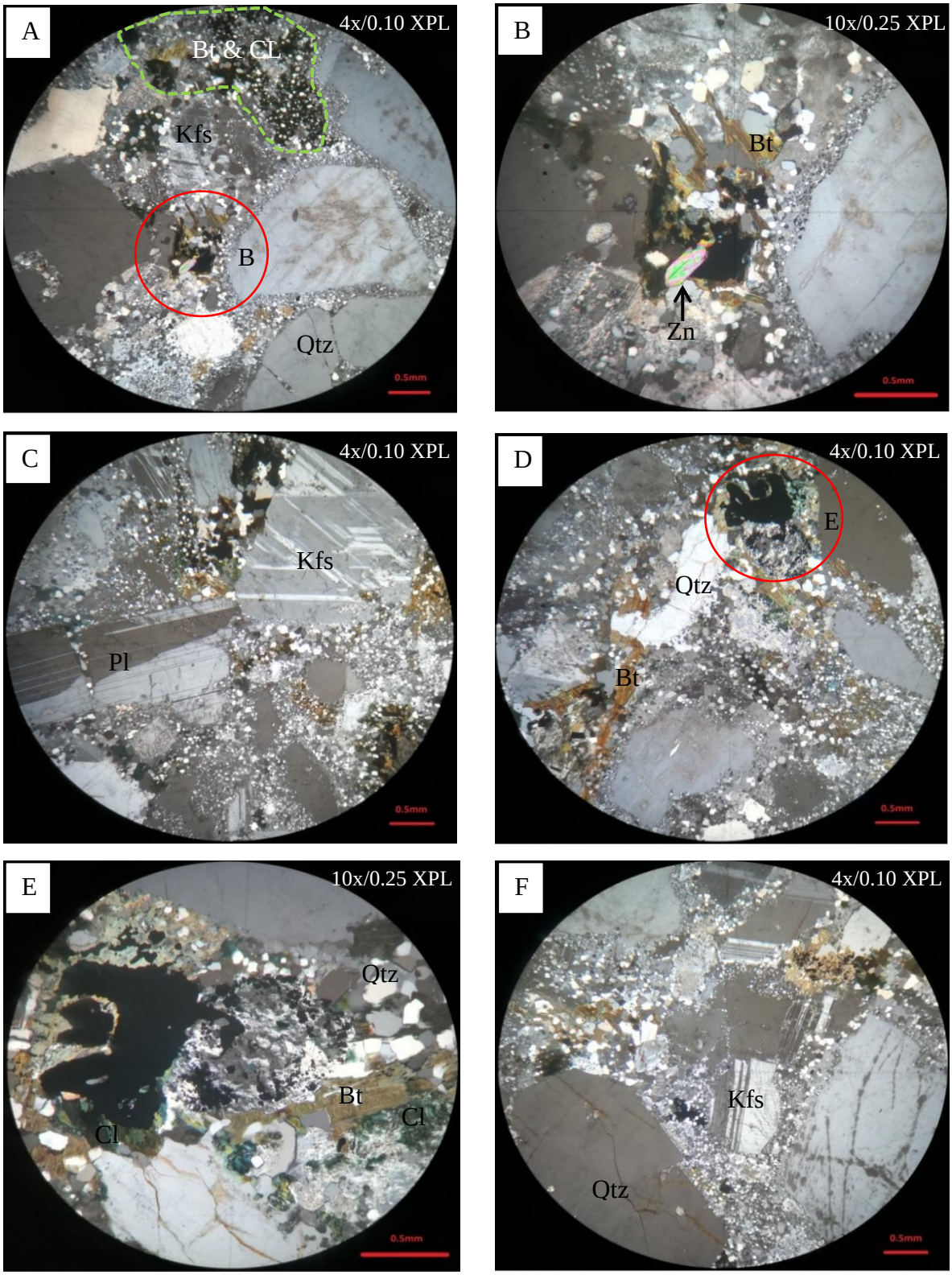

Figure 12: Photomicrographs of representative sample MM1 for the Postberg Centre in the Saldanha Bay Volcanic Complex showing the mineralogy and textures. All images were taken under cross polarized light. Please note plate B) and E) are taken at a higher magnification (10x0.25) and are represented by the red circles in plate A) and D) respectively. Please note that the polarisation on the microscope is not quite right (the two polarising lenses are slightly offset from exactly perpendicular to each other).

Quartz phenocrysts are euhedral to subhedral and have a grain size range of around ~1-6 mm (Figure 12 A and Figure 13 A & F) and microcrysts ranging from 0.1-1 mm (Figure 12 E). Both sub grain and monocrystalline varieties (exhibiting characteristic undulose extinction, seen in Figure 13 A and E. The red box indicating the original position of the stage and the blue box indicating the rotated position) are observed across all three of the samples' thin sections. Both types display slight fracturing around the edges of the crystal and are typically filled with fine-grained matrix materials (polygonal feldspar, quartz and biotite) or quartz microlites (Figure 12 E & F and Figure 13 A, E & F).

Plagioclase phenocrysts (grain size range of ~0.5-6 mm) have euhedral forms (Figure 12 C and Figure 13 A, C & F). These crystals display well- to poorly-defined fracturing and display characteristic oscillatory zoning sometimes obscured due to sericite or chlorite alteration, which is more predominant here than in the alkali feldspar phenocrysts (Figure 12 A and Figure 13 C).

Biotite phenocrysts, the main ferromagnesian mineral in the rock samples, forms reddish-brown tabular/plate shaped crystals (Figure 12 B & D, Figure 13 E and Figure 14 C & D). They have varied grain sizes ranging from ~0.1 mm (microcrysts) to 4 mm (phenocrysts). Interstitial and lamellar laths can be observed within larger crystals of biotite as well as within other minerals that had pre-existing fractures (Figure 12 B and Figure 13 E). On occasion, biotite overgrows the matrix and become partly altered in the process (Figure 12 A-indicated by green dashed line, B, D & E, Figure 13 C & D and Figure 14 C). They contain inclusions of alkali feldspar, quartz and zircons (Figure 12 B, Figure 13 B, C & D and Figure 14 B, C & D). Sericite, iron oxide and chlorite alterations are often associated with these phenocrysts. In PPL biotite is typically light brown to a reddish brown in colour with circular spots known as "pleochroic halos."

Phenocrystic pyroxene ranges between 0.1-0.5 mm in length and display a pinkish blue to yellowish brown colour. The crystal maintains strong angular edges (slightly fractured) while biotite reaction coronas can be seen around fractured sections of the phenocryst (Figure 13 F).

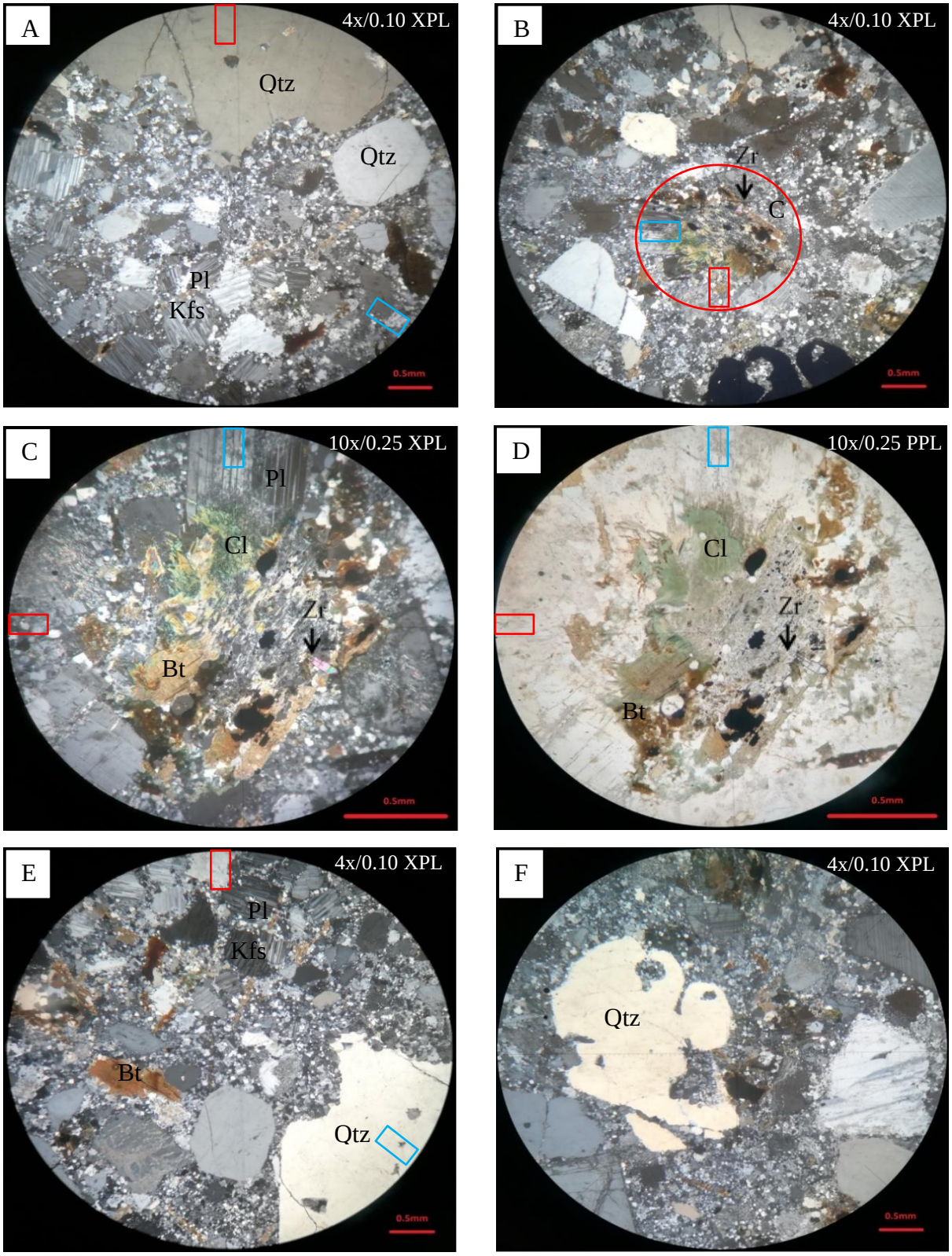

Figure 13: Photomicrographs of representative sample MM2 for the Postberg Centre in the Saldanha Bay Volcanic Complex showing mineralogy and textures. These images were taken under cross-polarized light except for plate D) which was taken under plane polarised light. Please note plate C) and D) are taken at a higher magnification (10x0.25) and is represented by the red circle in plate B) (red box indicates the original orientation; the blue box indicated the rotated position). Please note that the polarisation on the microscope is not quite right (the two polarising lenses are slightly offset from exactly perpendicular to each other).

The groundmass has undergone substantial recrystallization where most of its original textures, which would generally classify them as pyroclastic, were removed in the process. The microcrystalline groundmass shows considerable compositional variation between individual samples, as well as within a single samples' thin section. It is primarily made up of equigranular, recrystallized polygonal -quartz and -feldspar granules with some recrystallized biotite ingrowths (Note, the groundmass grain size are much smaller around some of the quartz and feldspar phenocrysts as seen in Figure 12 A, C & F, Figure 13 A & E and Figure 14 A). In some areas of the thin sections', between adjacent or broken phenocrysts, the matrix grains vary in size form ~20 µm to ~1 mm and contain similarly sized crystals quartz or slightly coarser glomerocrysts of feldspar, quartz and biotite; or in some cases, quartz and biotite only (Figure 12, Figure 13 and Figure 14). There are also some chlorite alterations, displaying a dark green to olive colour and constitutes the main alteration assemblage for the ignimbrites of the Postberg and Saldanha eruption centres (Figure 12 E, Figure 13 C & D and Figure 14 C & D).

One or two zircon grains (Figure 12 B, Figure 13 A & E and Figure 14 A) displaying cloudy/patchy colours of light-pink and green are also seen in some photomicrographs (high order interference colours). They are generally tetragonal-prismatic shaped with dipyrimidal gain-tip terminations, commonly found within, or surrounded by biotite and pyroxene (brown/light brown/green).

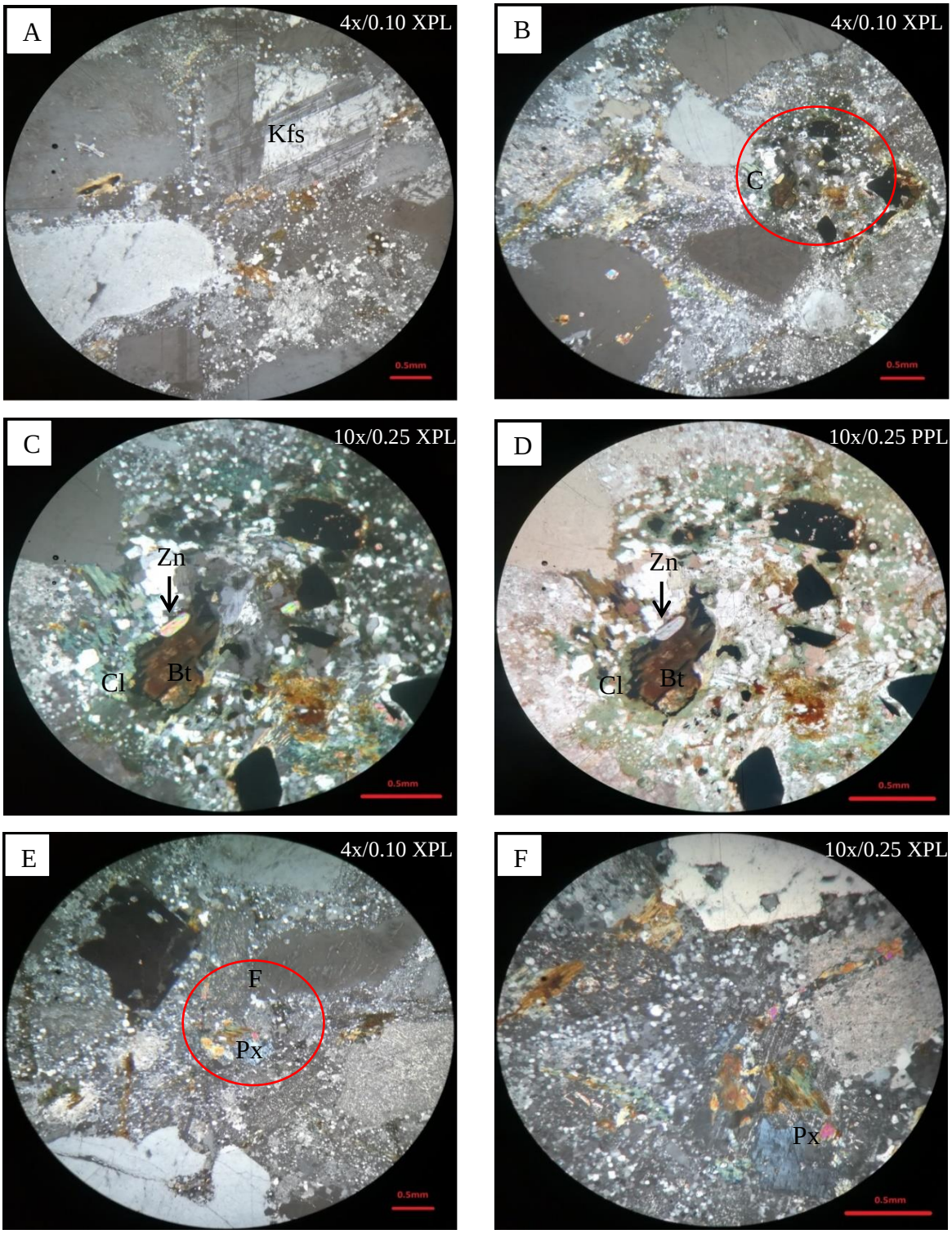

Figure 14: Photomicrographs of representative sample MM3 for the Postberg Centre in the Saldanha Bay Volcanic Complex showing mineralogy and textures. These images were taken under cross-polarized light except for plate D) which was taken under plane polarised light. Please note plate C), D) and F) are taken at a higher magnification (10x0.25) and is represented by the red circle in plate B) and E) respectively. Please note that the polarisation on the microscope is not quite right (the two polarising lenses are slightly offset from exactly perpendicular to each other).

4.3 Bulk rock chemistry

4.3.1 Ignimbrite of the Saldanha Bay Volcanic Complex

The bulk-rock chemical data for the Saldanha Bay Volcanic Complex is presented in Electronic Appendix EA1 and EA2. Since the Postberg Ignimbrites form the primary focus of this study, the Saldanha Ignimbrites have only been added for contextual and comparative purposes. A summary table of the geochemical data for both eruption centres are presented as Electronic Appendix EA3.

Both geochemical datasets include samples A1-A40 and B1-B32 from Scheepers and Poujol (2002), some of which were tabulated by Scheepers and Nortje (2000), with alternative sample numbers with QP prefixes added by Scheepers and Poujol (2002). For those selected samples, both sample numbers are given, separated by commas (e.g. EA2 – B10, QP4). Samples CJA1-CJA7, CJB9-CJB30, MB1-MB26, WIG and WP8-WP31B are from Joseph (2012). Samples Pos1 & Pos2 in EA1 and Sal1-Sal8 in EA2 are from Clemens et al. (2017). Note, this dataset was originally used by Clemens et al. (2017) and modified by the addition of samples LQP1-LQP6 form Scheepers and Nortje (2002) as well as three additional samples form present work (MM1, MM2 and MM3). Both Scheepers and Poujol (2002) and Joseph (2012) had samples with ‘A’ and ‘B’ prefixes; thus, to clearly differentiate the two sets, ‘CJ’ has been added to the prefixes of the relevant Joseph (2012) samples.

As previously stated, Clemens and Stevens (2016) showed that Saldanha Bay Volcanic Complex has two bodies of S-type ignimbrites at opposite ends of the Saldanha Bay entrance, with the Saldanha eruption centre to the north and the Postberg eruption centre to the south. In the Saldanha Centre (SC), two chemically distinct ignimbrite magmas are present - the Saldanha Ignimbrite (SI) and Jacob’s Bay ignimbrites (JI). The initial recognition and chemical characterisation of these ignimbrites are best illustrated on the TiO_2 vs. K_2O (Figure 17 B) plot after Clemens and Stevens (2016).

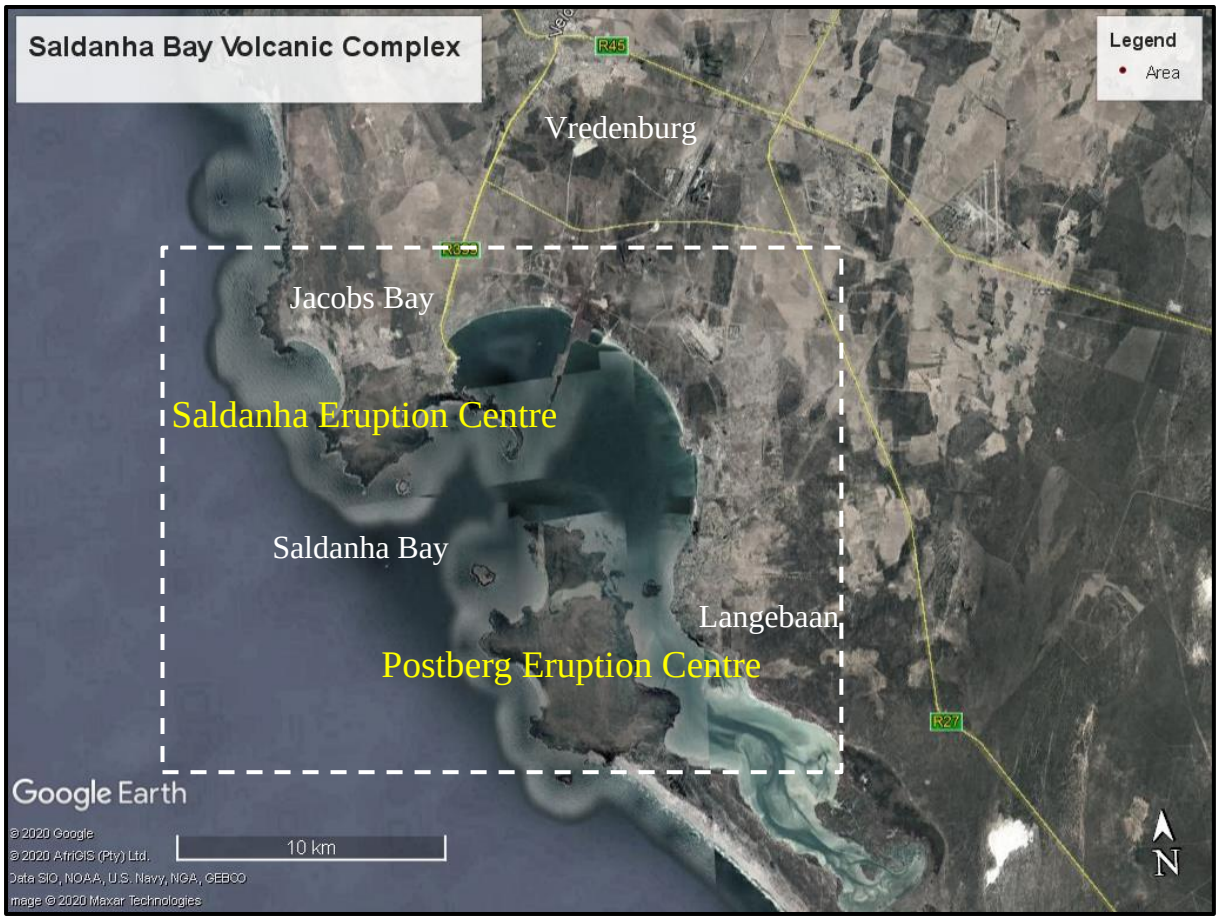

Figure 15: Google Earth™ image of the Saldanha Bay Volcanic Complex (indicated by the white dashed-line box) displaying the Postberg eruption centre and the Saldanha eruption centre.

They also recognised two chemically distinct, more silicic magma groups in the Postberg centre (PC) - the Plankiesbaai Ignimbrites (PI) and Tsaarsbank Ignimbrites (TI). The chemical differences between these two ignimbrites are best illustrated on plots with K_2O as the abscissa. The Mg# (mol. 100 Mg/ [Mg + Fe]) vs. K_2O plot (Figure 16) shows a clear gap in Mg# between the Tsaarsbank and the Plankiesbaai ignimbrites, with the latter being more ferroan in composition (Mg# < 13).

Since the Plankiesbaai and the Tsaarsbank Ignimbrites occurred exclusively in the Postberg centre and the other two members, the Saldanha and Jacobs Bay Ignimbrites, occur mainly in the Saldanha Centre, with minor volumes present in the Postberg Centre (two pink triangles and one blue triangle in Figure 16 a & b), Clemens and Stevens (2016) surmised that the volcanic activity in the two eruption centres may have occurred simultaneously, but the

activity in the Saldanha centre may have terminated earlier than that of the Postberg centre (discussed later with the new geochronology data).

It is for this reason that the samples collected from the Postberg Centre (MM samples, red circles) as well as the volcanic (LQP, yellow circles) samples from Scheepers and Nortje (2002) in Figure 16 a) & b) had to be classified accordingly. Figure 16 displays all the samples from both the Postberg Centre and the Saldanha Centre with the R^2 as correlation coefficients for each ignimbrite.

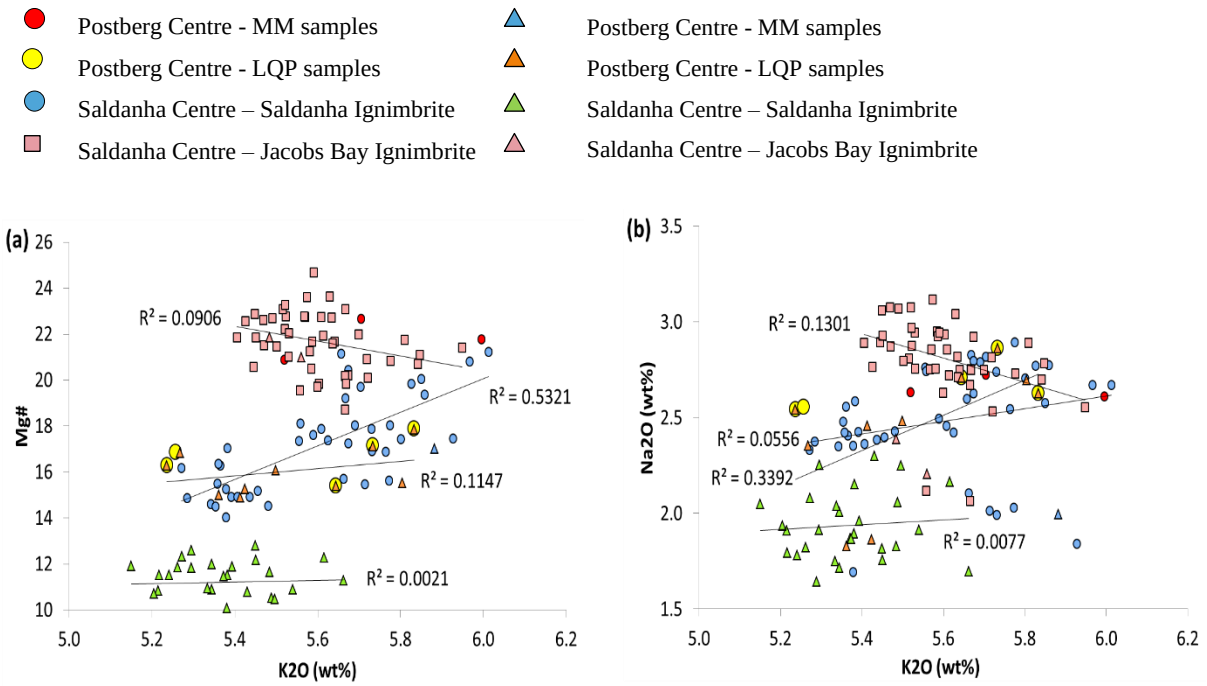

Figure 16: Diagram showing the chemical variation between the Ignimbrites of the Saldanha Centre (represented by various coloured squares and circles) and Postberg Centre (represented by various coloured triangles). MM samples from present work and LQP samples from Scheepers and Nortje (2002) have also been included as red and yellow circles respectively. Plot (a) Mg# (mol. 100 Mg/ [Mg + Fe]) is modified after Fig. 20a from Clemens and Stevens (2016). Plot (b) is modified after Fig. 10d from Clemens et al. (2017).

4.3.2 Sample classification

When all the geochemical data is viewed on a single chemical variation plot, as seen in Figure 16, it is unclear or challenging to identify which of the four known magma groups the collected Postberg Ignimbrites samples relate to. For example in Figure 16 (a), the Postberg Ignimbrite LQP samples (PC-LQP, yellow circles) lie within the same general area as both the Saldanha Centre, Saldanha Ignimbrites (SC-SI, blue circles) and the Postberg Centre Tsaarsbank Ignimbrites (PC-TI, orange triangles). Likewise, the PC-MM samples (red circles) could belong to either Saldanha Centre, Jacobs Bay Ignimbrite (SC-JI, pink squares) or the Saldanha Centre, Saldanha Ignimbrites (SC-SI, blue circles).

Figure 17 presents a number of chemical variation diagrams; Figure 17 a & c (Zr, K_2O vs. SiO_2), b & d (TiO_2, FM vs. K_2O) and e & f (TiO_2, Al_2O_3 vs. FM) which classify the MM samples collected in the Postberg Centre as Jacobs Bay Ignimbrites (PC-JI).

Figure 18 a & b displays two chemical variation plots (TiO_2, CaO vs. K_2O) and classifies the volcanic LQP samples collected in the Postberg Centre by Scheepers and Nortje (2002) as Tsaarsbank Ignimbrites (PC-TI).

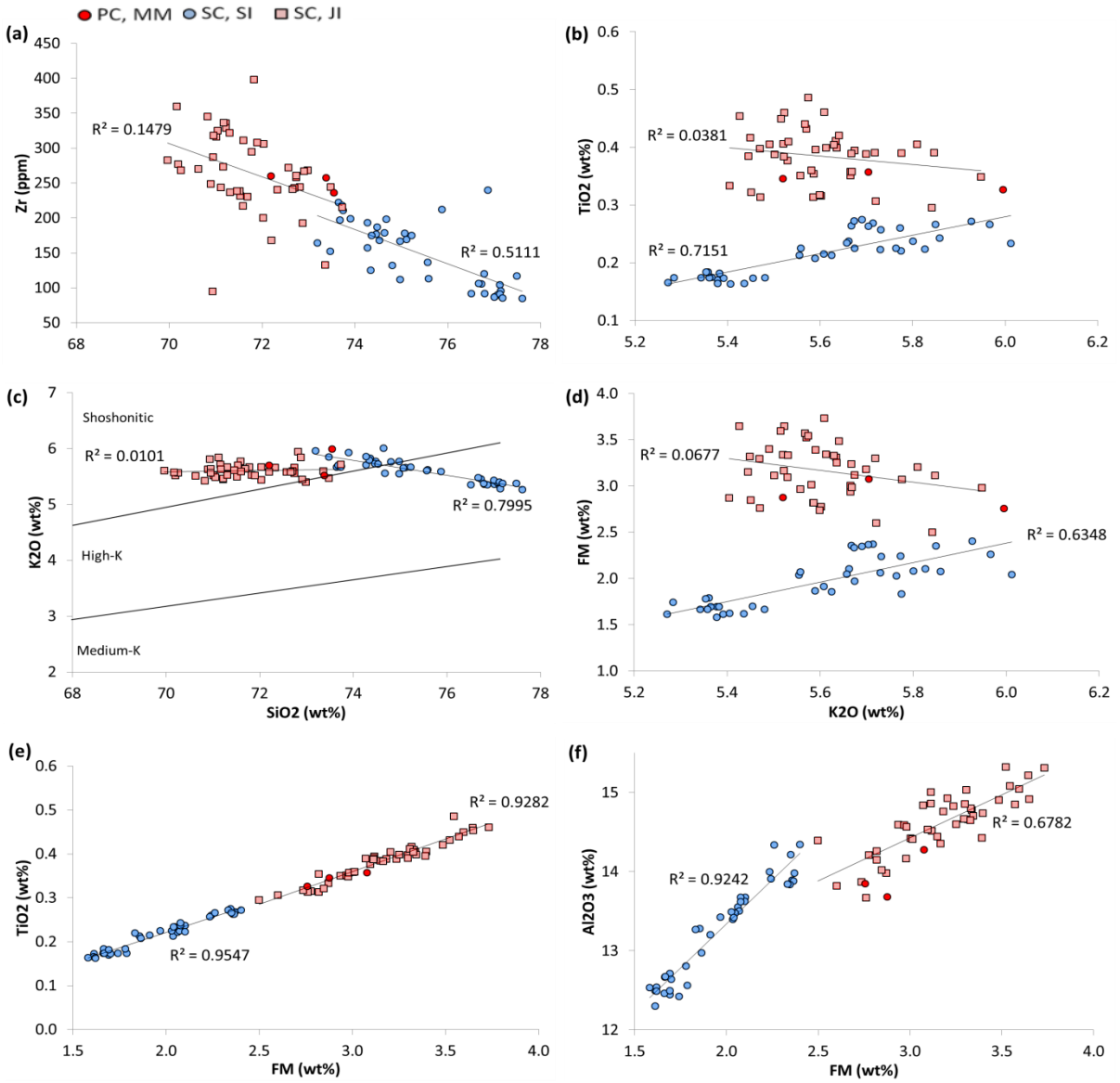

Figure 17: Selection of chemical variation plots showing rocks of the Saldanha Centre-Jacob's Bay Ignimbrite (SC-JI, pink squares), the Saldanha Centre-Saldanha Ignimbrite (SC-SI, blue circles) as well as the Postberg Centre-MM samples (PC-MM, red circles) collected for the present work. Plots Zr and K_2O vs. SiO_2 are modified versions of the Harker plots Fig. 6b and Fig. 4e from Clemens et al. (2017) respectively. Plots TiO_2 and FM [FeO^T + MnO + MgO] vs. K_2O are modified after Fig. 7a, b from Clemens et al. (2017). Note the geochemical difference (TiO_2 & FM vs K_2O and TiO_2 Al_2O_3 vs FM) in the of the magmas that formed the Saldanha Ignimbrite and the Jacob's Bay Ignimbrite of the Saldanha eruption centre. The PC-MM samples can therefore be classified as Jacob's Bay Ignimbrites.

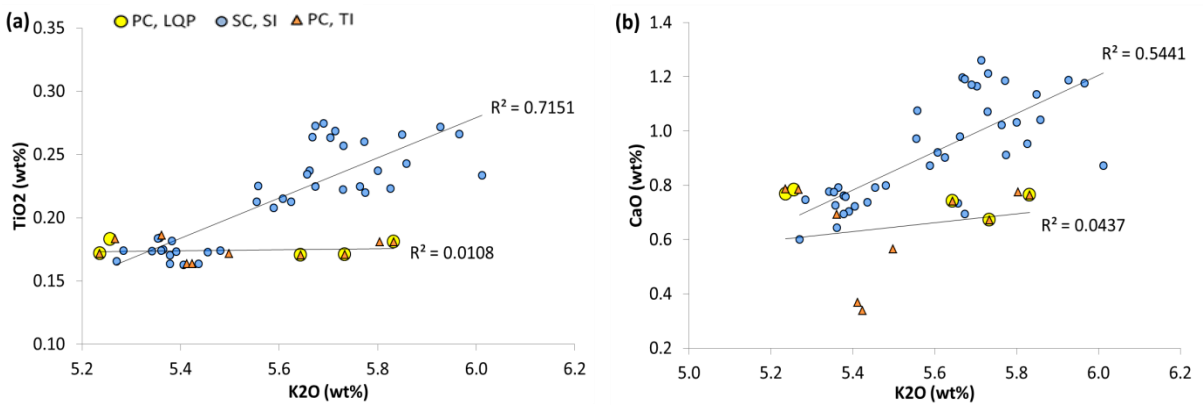

Figure 18: Diagram showing chemical variation plots between the Saldanha Centre-Saldanha Ignimbrite (SC-SI, blue circle) and the Postberg Centre-Tsaarsbank Ignimbrite (PC-TI, orange triangle) as well as the Postberg Centre Volcanic rock samples from Scheepers and Nortje (2002) (PC-LQP, yellow circles). These plots clearly display the chemical differences between the Saldanha and Tsaarsbank ignimbrites which may not be apparent in Figure 16 (a) and (b) and certainly classifies the PC-LQP samples as Postberg Centre- Tsaarsbank Ignimbrites (PC-TI).

4.3.3 Ignimbrites of the Postberg Centre

Using the TAS diagram (Figure 19; after Bas et al., 1986) and the molar Na_2O – Al_2O_3 – K_2O plot (Figure 20), all the analysed samples from both the Postberg Centre and the Saldanha Centre are peraluminous, form part of the subalkaline/tholeiitic series and are classified as rhyolites. As previously stated, the initial chemical characterisation of two distinct magma groups within the Postberg Centre was recognised by Clemens and Stevens (2016) – Plankiesbaai and Tsaarsbank Ignimbrites. Both magma groups are characterised by high SiO_2 contents (>76 wt.%), a lack of variation in TiO_2, and Zr, high Al_2O_3 and ASI values (aluminium saturation index), low CaO and Na_2O, and a highly ferroan character, with Mg# values of < 18.

The results of the geochemical analysis for samples of the Postberg Ignimbrites (Figure 21Figure 24) are in excellent agreement with the work done by Clemens and Stevens (2016) and Clemens et al. (2017). Figure 21 displays a variety of Harker diagrams for selected major oxides (TiO_2, Al_2O_3, CaO, P_2O_5, Mg# (mol. 100 Mg/[Mg + Fe]), Na_2O, K_2O and ASI (mol. Al_2O_3/ [CaO - 3.33 P_2O_5 + Na_2O + K_2O]) showing the fields for various magma series and plotted with SiO_2 as the abscissa. Figure 22 displays Harker diagrams for selected trace elements (Rb, Sr, Zr, Ba, V, Zn) verses SiO_2 content. The same plots are displayed in Figure 23 and Figure 24 this time plotted against the K_2O content.

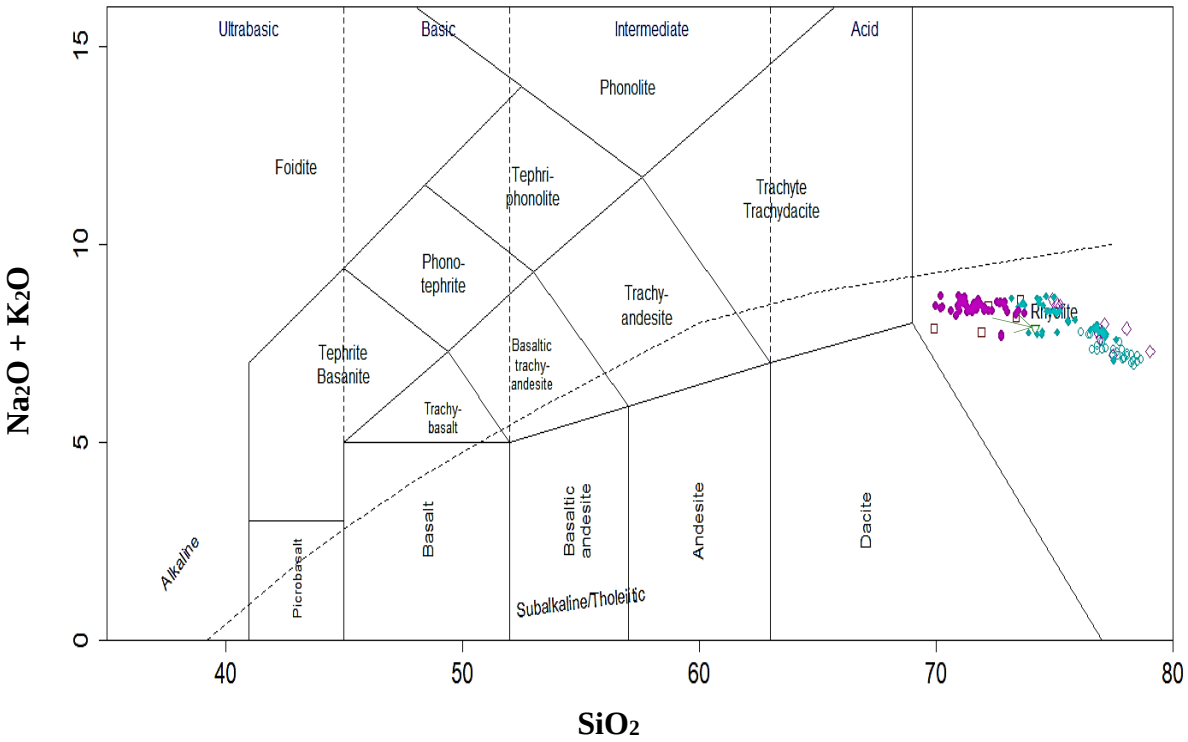

Figure 19: TAS diagram (after Bas et al., 1986) for all the samples of the Saldanha Bay Volcanic Complex, classifying them as subalkaline/tholeiitic rhyolites. Postberg Centre Saldanha Ignimbrites (green triangles indicated by green arrow), Postberg Centre Jacobs Bay Ignimbrite (red squares) Postberg Centre Plankiesbaai Ignimbrites (closed blue diamond), Postberg Centre Tsaarsbank Ignimbrites (open purple diamonds), Saldanha Centre Saldanha Ignimbrites (closed blue diamonds), Saldanha Centre Jacobs Bay Ignimbrites (closed purple diamonds). Alkali/sub - alkali boundary line after Irvine and Baragar (1971).

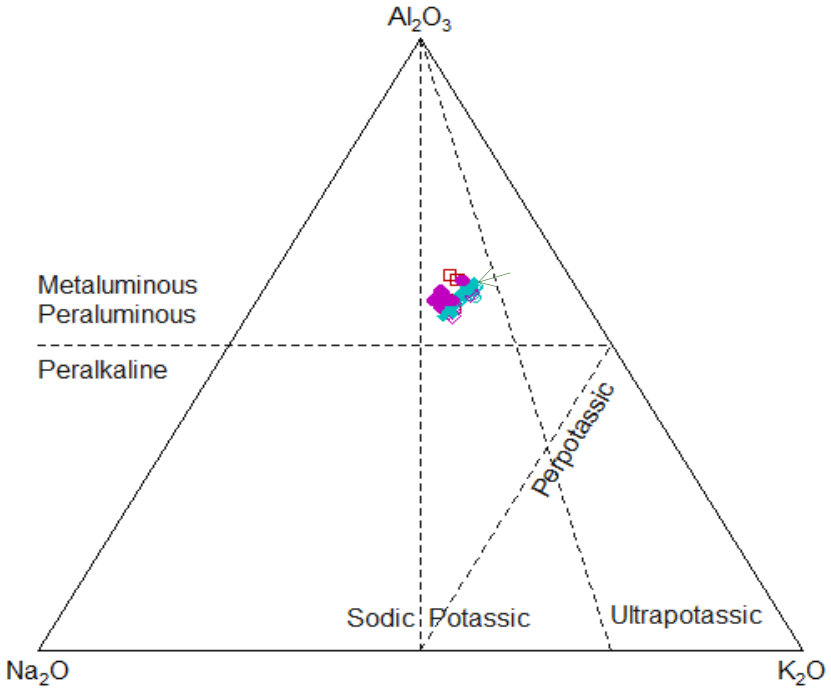

Figure 20: Molar Na_2O – Al_2O_3 – K_2O plot displaying all samples of the Saldanha Bay Volcanic Complex, classifying them as peraluminous. Postberg Centre Saldanha Ignimbrites (green triangles, hidden behind sample points but indicated by green arrow), Postberg Centre Jacobs Bay Ignimbrite (red squares), Postberg Centre Plankiesbaai Ignimbrites (open blue diamond), Postberg Centre Tsaarsbank Ignimbrites (open purple diamonds), Saldanha Centre Saldanha Ignimbrites (closed blue diamonds), Saldanha Centre Jacobs Bay Ignimbrites (closed purple diamonds).

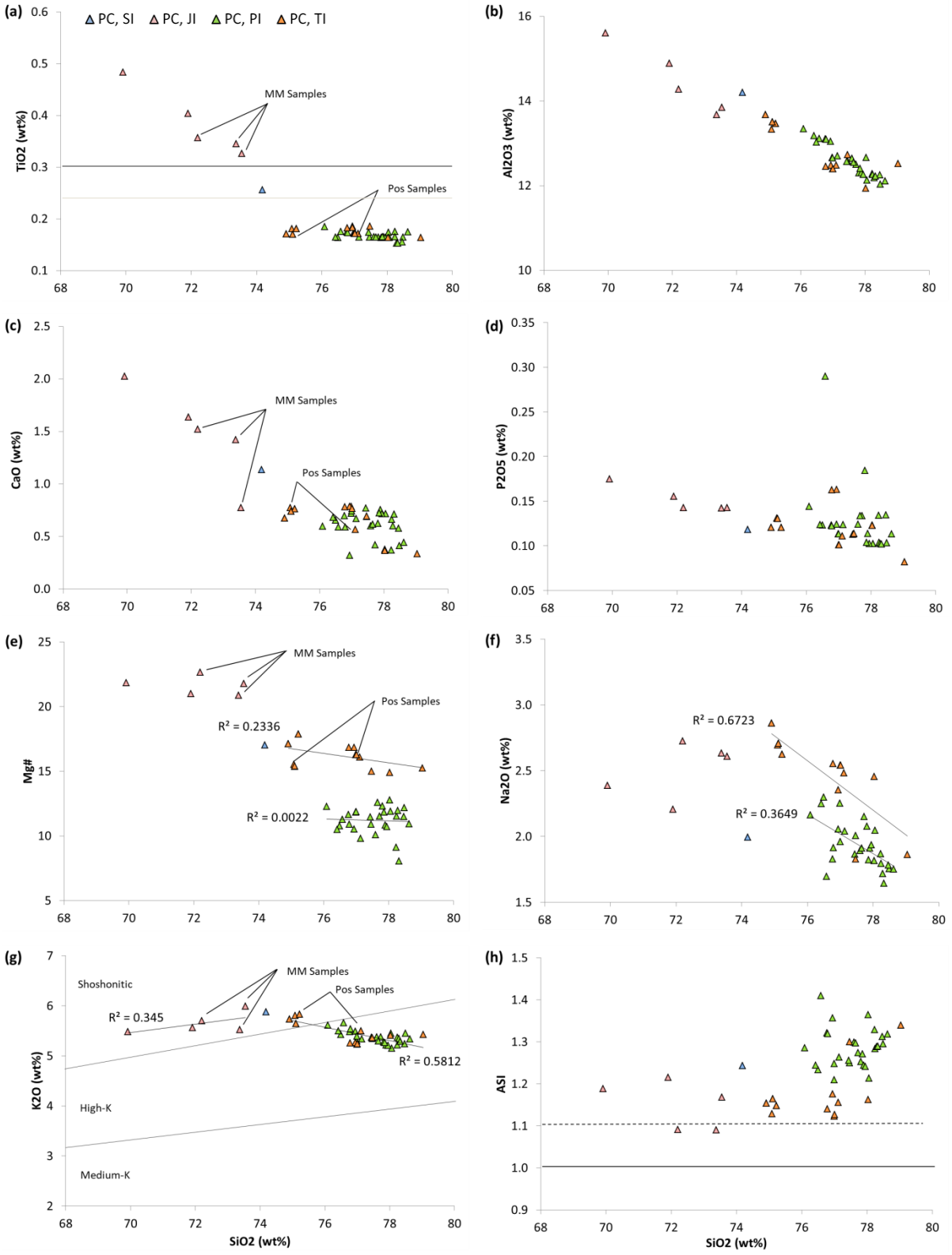

Figure 21: Harker plots of selected major oxides and derived parameters for rocks of the Postberg Centre in the Saldanha Bay Volcanic Complex; (a) TiO_2, (b) Al_2O_3, (c) CaO, (d) P_2O_5, (e) Mg# (mol. 100 Mg/[Mg + Fe]), (f) Na_2O, (g) K_2O showing the fields for various magma series, (h) ASI (mol. Al_2O_3/ [CaO - 3.33 P_2O_5 + Na_2O + K_2O]). Plankiesbaai Ignimbrite (PC-PI, green triangle), Tsaarsbank Ignimbrite (PC-TI, orange triangle), Saldanha Ignimbrite (PC-SI, blue triangle) and Jacob's Bay Ignimbrite (PC-JI, pink triangle).

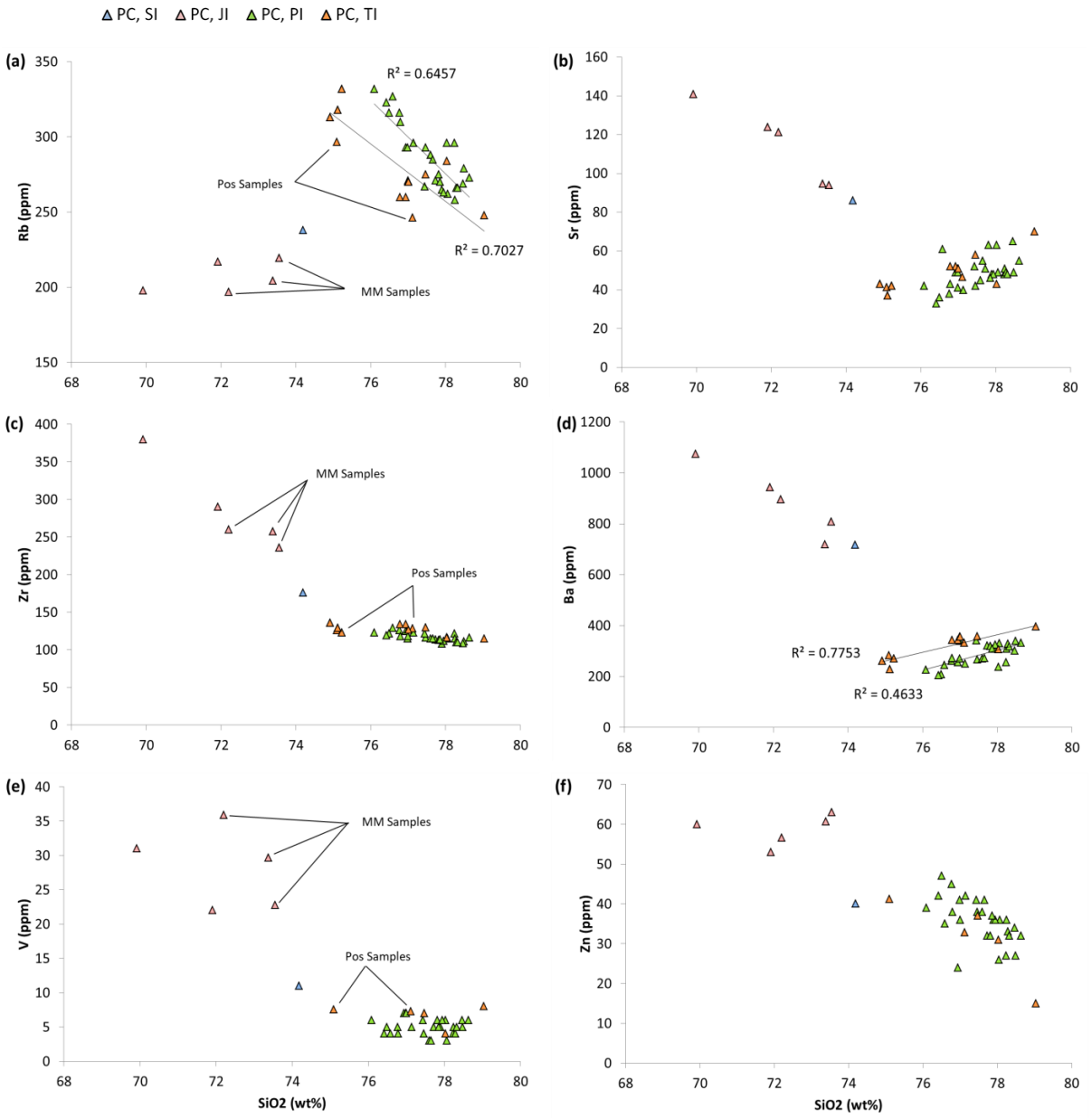

Figure 22: Harker plots of selected trace elements for rocks of the Postberg Centre in the Saldanha Bay Volcanic Complex; (a) Rb, (b) Sr, (c) Zr, (d) Ba, (e) V, (f) Zn. Plankiesbaai Ignimbrite (PC-PI, green triangle), Tsaarsbank Ignimbrite (PC-TI, orange triangle), Saldanha Ignimbrite (PC-SI, blue triangle) and Jacob's Bay Ignimbrite (PC-JI, pink triangle).

All the PC samples have ASI values (mol. Al_2O/ [$CaO - 3.33P_2O_5 + Na_2O + K_2O$]) that are > 1.0 and generally >1.1, with only two samples of the PC-JI having ASI values of 1.09 (Figure 21 H). They have high Al_2O_3 content (avg. 13.58 wt.%), a low CaO content (avg. 1.06 wt.%) and Na_2O (avg. 2.48 wt.%). They have fairly high SiO_2 contents (69.92 wt.% - 79.04 wt.%) with an average SiO_2 for the PC-PI and PC-TI between 77.55 wt.% and 76.33 wt.% respectively. The ignimbrites found exclusively in the Postberg Centre (PC-PI & PC-TI) is more silicic than its PC-SI (SiO_2 = 74.18 wt.%) & PC-JI (SiO_2 = 72.19 wt.%) counterparts.

These ASI and SiO_2 values are characteristic of S- type magmas as described by Cheppell and White (1974).

Figure 21 a (TiO_2 vs. SiO_2) shows a clear distinction between the TiO_2 content of PC-JI and PC-SI as well as the PC-PI and PC-TI. The TiO_2 ranges are as follows: PC-JI (0.33-0.48 wt.%), PC-SI (0.26 wt.%), PC-TI (0.16-0.19 wt.%), PC-PI (0.15-0.19 wt.%). The dividing TiO_2 content between PC-SI & PC-JI and PC-TI &PC-PI is set at < 0.2 wt.% (represented by the solid grey line in Figure 21 a). The dividing TiO_2 content set at 0.28 wt% by Clemens et al. (2017) for the SC- SI and SC-JI (represented by the solid black line in Figure 21 a) also hold true for the SI and JI found in the Postberg Centre, although a slightly lower limit of 0.25 wt.% is suggested.

The Mg# (mol. 100 Mg/ [Mg + Fe]) in Figure 21 e and Figure 23 e, is the only clear geochemical parameter that shows a distinct separation between the Plankiesbaai and Tsaarsbank Ignimbrites, with Mg# values ranging PI: 8.07-12.79 and TI: 14.90-17.87. Based on the 43 samples from the PC (28 samples for PC-PI and 15 samples for PC-TI) the dividing Mg# content is set at Mg# = 14, with PC-PI $\leq$ 14 and PC-TI $\geq$ 14 (Figure 21 e & Figure 23 e). PC-PI and PC-TI are characterised by a lack of variation in Zr content, higher Rb content and lower Sr, Ba, V and Zn content when compared to its PC-SI and PC-JI counterparts (Figure 22 a-f). These observations become even clearer with the selected trace elements plotted with K_2O as the abscissa (Figure 24 a-f) although, without the R^2 values (correlation coefficient lines) for each particular ignimbrite, it is quite difficult to distinguish between the PI and TI using trace element data alone. Nevertheless, they do show that these magmas are distinctly different from the magmas of the Saldanha Eruption Centre.

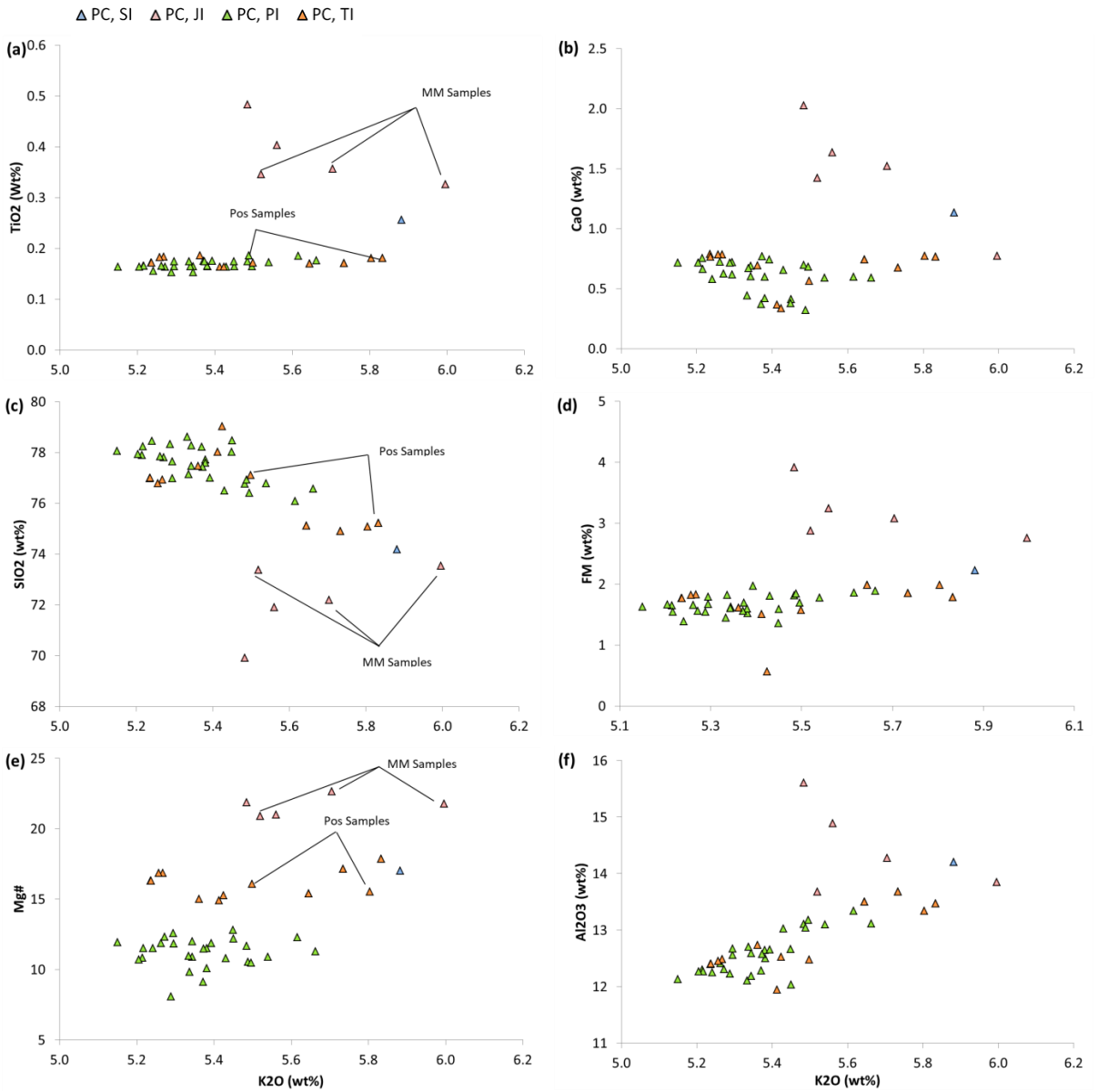

Figure 23: Variety of major oxides and derived parameters for the rocks of the Postberg Centre in the Saldanha Bay Volcanic Complex, plotted against K_2O content. (a) TiO_2, (b) CaO, (c) SiO_2, (d) FM [FeO^T + MnO + MgO], (e) Mg# (mol. 100 Mg/[Mg + Fe]), (f) Al_2O_3. Plankiesbaai Ignimbrite (PC-PI, green triangle), Tsaarsbank Ignimbrite (PC-TI, orange triangle), Saldanha Ignimbrite (PC-SI, blue triangle) and Jacob's Bay Ignimbrite (PC-JI, pink triangle).

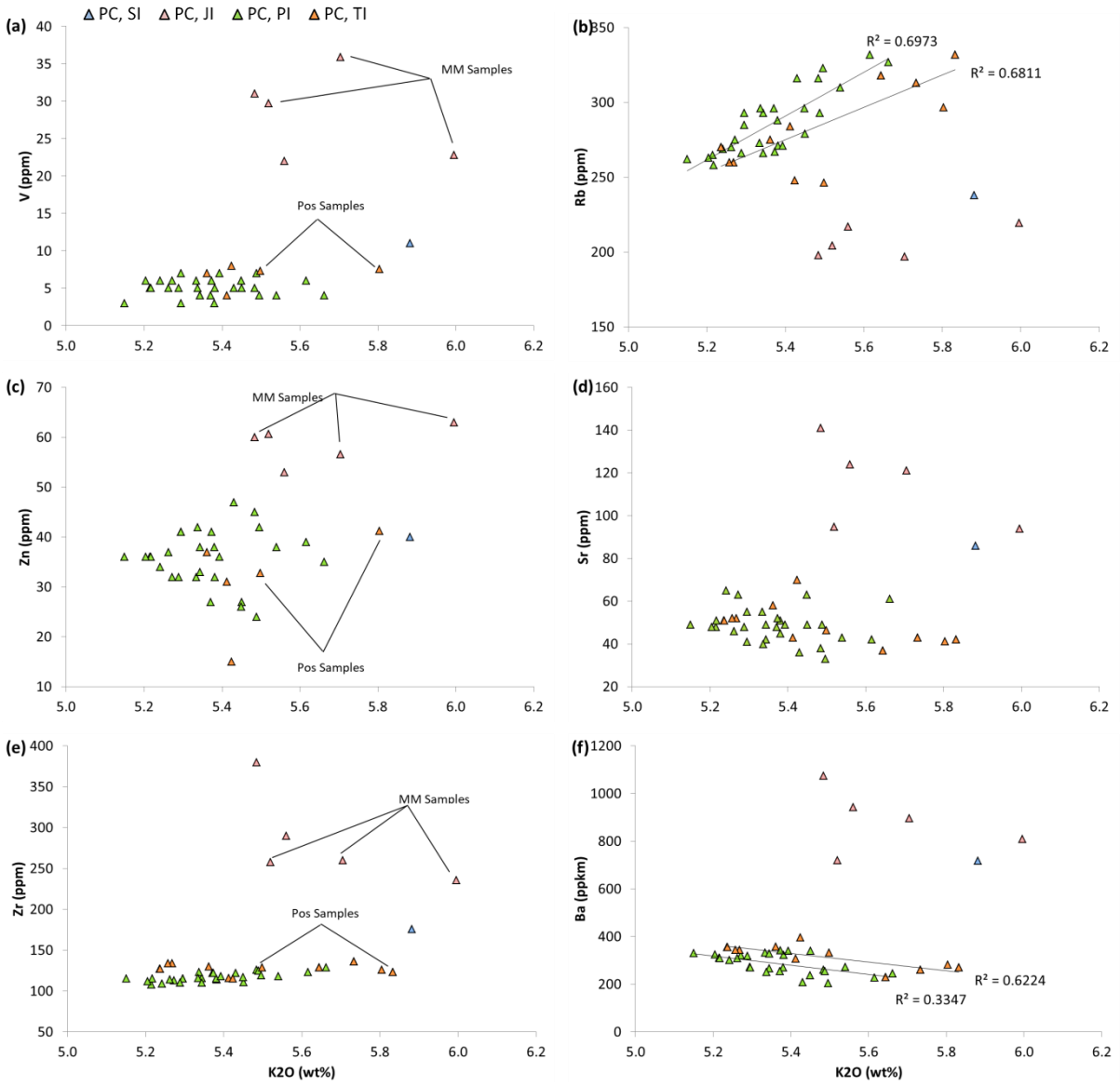

Figure 24: Variety of trace element concentrations for the rocks of the Postberg Centre in the Saldanha Bay Volcanic Complex, plotted against K_2O content. (a) V, (b) Rb, (c) Zn, (d) Sr, (e) Zr, (f) Ba. Plankiesbaai Ignimbrite (PC-PI, green triangle), Tsaarsbank Ignimbrite (PC-TI, orange triangle), Saldanha Ignimbrite (PC-SI, blue triangle) and Jacob's Bay Ignimbrite (PC-JI, pink triangle).

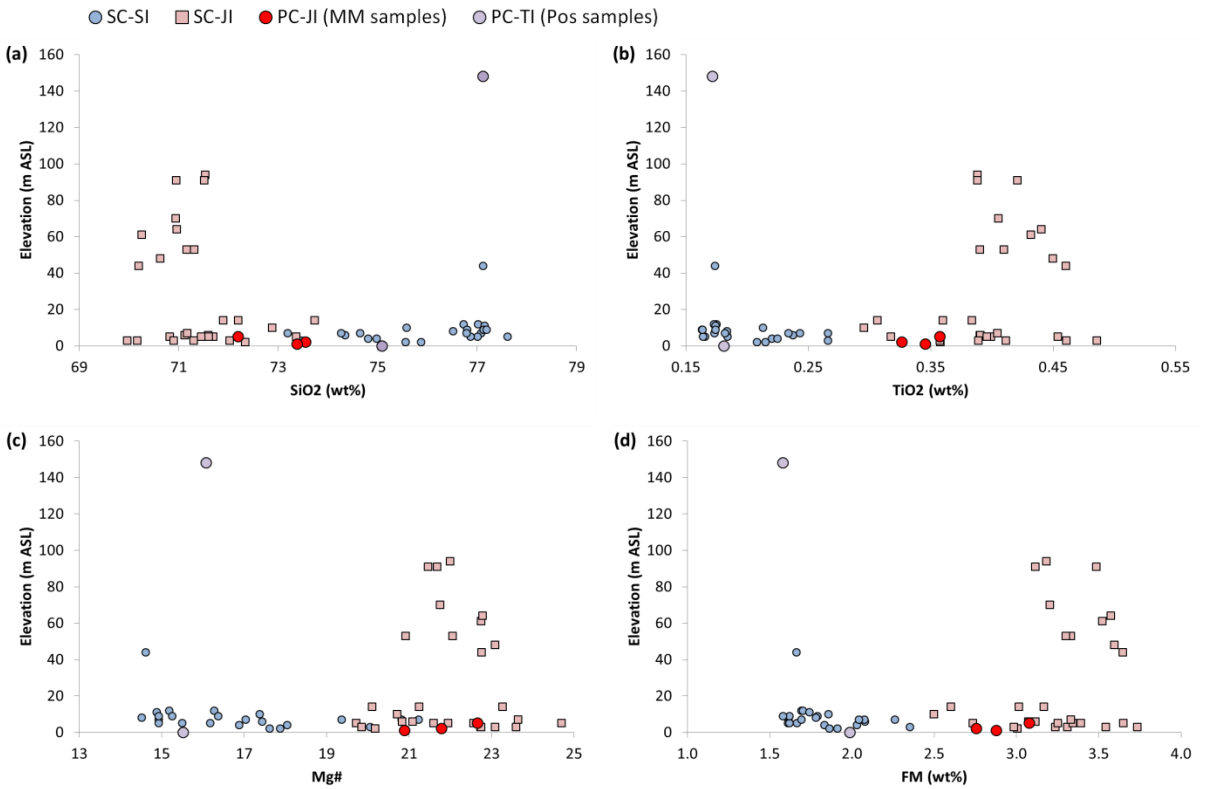

Figure 25: Selected major oxides and derived parameters of the rocks of the Saldanha Centre and the Postberg Centre in the Saldanha Bay Volcanic Complex, plotted against height (in meters above sea level) - an alternative for stratigraphic position. (a) SiO_2, (b) TiO_2, (c) Mg# (mol. 100 Mg/ [Mg + Fe]), (d) FM [FeO^T + MnO + MgO]. The rocks of the Saldanha Centre-Saldanha Ignimbrite (SC-SI) are plotted as blue circles, the Saldanha Centre- Jacob's Bay Ignimbrite (SC-JI) plotted as pink squares, the Postberg Centre-Jacob's Bay Ignimbrite (PC-JI; MM samples only) plotted as red circles and the Postberg Centre-Tsaarsbank Ignimbrite (PC-TI; Pos 1&2 only) plotted as purple circles.

4.3.4 Rb-Sr & Sm-Nd tracer-isotopes for the Postberg Centre

Whole-rock Sr and Nd tracer-isotope analysis (Table 5) was performed in PicoTrace® clean lab facilities. The isotope ratios were measured with a Nu Instruments thermal ionization mass spectrometer (Nu-TIMS) at Departamento de Geología, Centro de Investigación Científica y de Educación Superior de Ensenada (CICESE) in the state of Baja California (Mexico). Full analytical details as well as QA/QC procedures can be found in the Chapter 3 (Analytical Methods) of this thesis.

Table 5: Tracer-isotope data, calculated at 538 Ma, for the rocks of the Postberg Centre – Jacobs Bay Ignimbrites in the Saldanha Bay Volcanic Complex.

Sample	$^{87}Sr/^{86}Sr_0$	Rb (ppm)	Sr (ppm)	$^{87}Rb/^{86}Sr$ (calc.)	$^{87}Sr/^{86}Sr_t$	εNd_t	t_{DM} (Ga)
MM1	0.704132	225.67	89.38	7.474	0.761449	-7.60	1.430
MM2	0.697057	241.75	94.94	7.533	0.754826	-7.92	1.405
MM3	0.701667	227.84	102.06	6.603	0.752304	-7.73	1.409

Sample	$^{143}Nd/^{144}Nd_0$	Sm (ppm)	Nd (ppm)	$^{147}Sm/^{144}Nd$ (calc.)	$^{143}Nd/^{144}Nd_t$	εNd_i	t_{2DM} (Ga)
MM1	0.511810	10.04	49.69	0.122	0.512240	-2.63	1.411
MM2	0.511806	10.21	52.03	0.119	0.512224	-2.71	1.417
MM3	0.511811	10.57	53.29	0.120	0.512234	-2.61	1.409

The analysed samples for the PC-JI have $\varepsilon Nd_{538\ Ma}$ values of -7.60 (MM1), -7.92 (MM2) and -7.73 (MM3) with calculated, two stage, depleted mantle model (t_{2DM}) of 1.411 Ga, 1.417 Ga, 1.409 Ga respectively (Table 5, Figure 26 and Figure 27). The $^{143}Nd/^{144}Nd_i$ values show little variation across the three MM samples at ~0.5118. The $^{87}Sr/^{86}Sr_i$ values, however, vary significantly 0.697057 - 0.704132, which is consistent with the inference of partial melting of a heterogeneous source. The $^{87}Sr/^{86}Sr_{538\ Ma}$ values are significantly higher than the $^{87}Sr/^{86}Sr_i$ of the PC-JI samples with values of 0.761449 (MM1), 0.754826 (MM2) and 0.752304 (MM3).

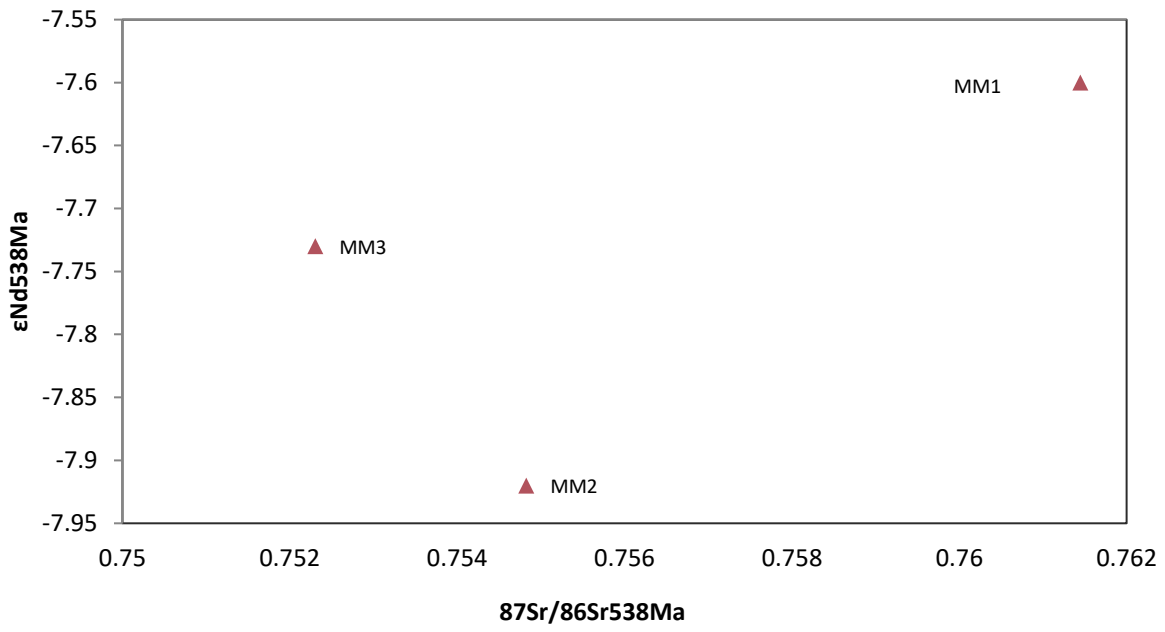

Figure 26: Isotope-correlation plot for the analysed samples of the Postberg Centre - Jacobs Bay Ignimbrite, represented as red triangles.

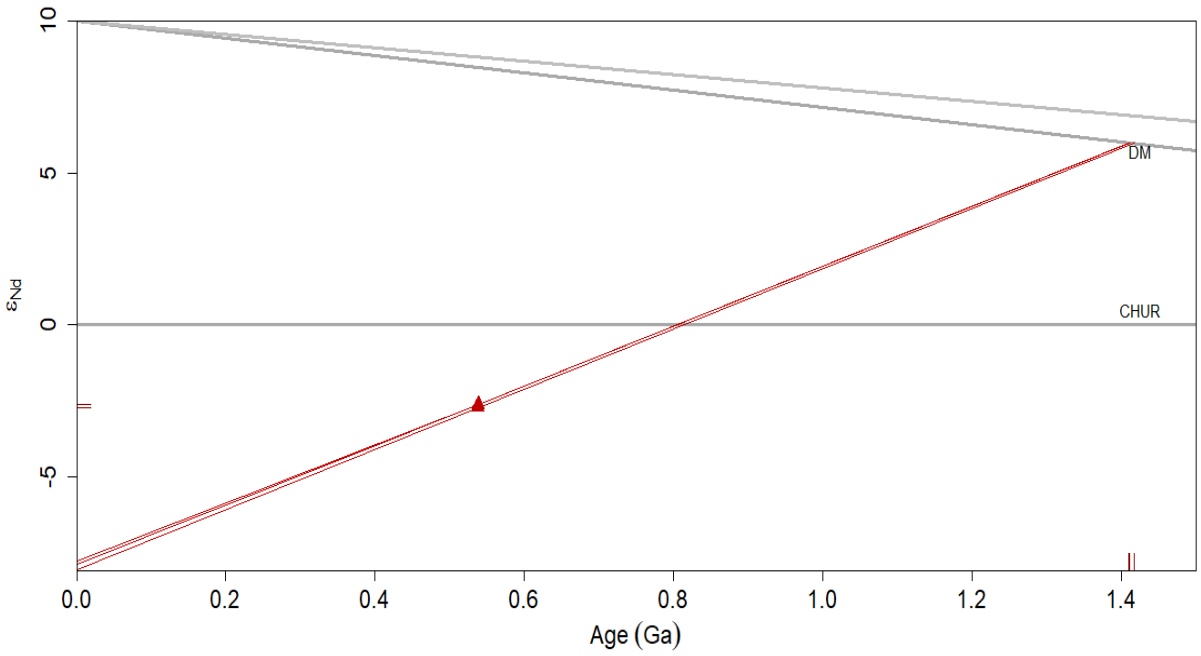

Figure 27: Nd isotopic growth diagram (two stage) for analysed Postberg Centre - Saldanha Ignimbrite samples, represented as red triangles. The $t_{2DM\ GA}$ values for MM1 (1.411 Ga), MM2 (1.417 Ga) and MM3 (1.409 Ga).

4.3.5 Ignimbrites of the Saldanha Centre

Displayed below is a selection of geochemical diagrams from the Saldanha Centre as a contextual and comparative dataset (Clemens and Stevens, 2016; Clemens et al., 2017). Figure 28Figure 30 shows that the Saldanha Ignimbrite (SI) and Jacobs Bay Ignimbrite (JI) are geochemically distinct from one another. They occur mainly in the Saldanha Centre with minor proportions in the Postberg Centre. The uppermost sections of the Saldanha Centre are made up exclusively by the Jacobs Bay Ignimbrites (see Figure 25), while the Saldanha and Jacobs Bay Ignimbrites are adjacent to each other at stratigraphically lower sections of the Saldanha peninsula (Clemens and Stevens, 2016).

The Saldanha and Jacobs Bay Ignimbrites show contrasting and roughly linear trends when plotted on Harker diagrams (Figure 28). Clemens et al. (2017) explained that it may simply be due to variation within a series derived from a single parent magma, however, when viewed on variation diagrams with K_2O as the abscissa, the differences between the two become apparent- this rules out the simple differentiation of one series from the other (Figure 30). It is also important to note that the Saldanha and Jacobs Bay Ignimbrites have virtually identical phenocrystic make-ups. Since they can only be distinguished geochemically, it is

sensible to assume that the compositional contrasts between the two must be due to the variation in the composition of the liquid portions of the magma. The reader is referred to Clemens and Stevens (2016a) and Clemens et al. (2017) for further details.

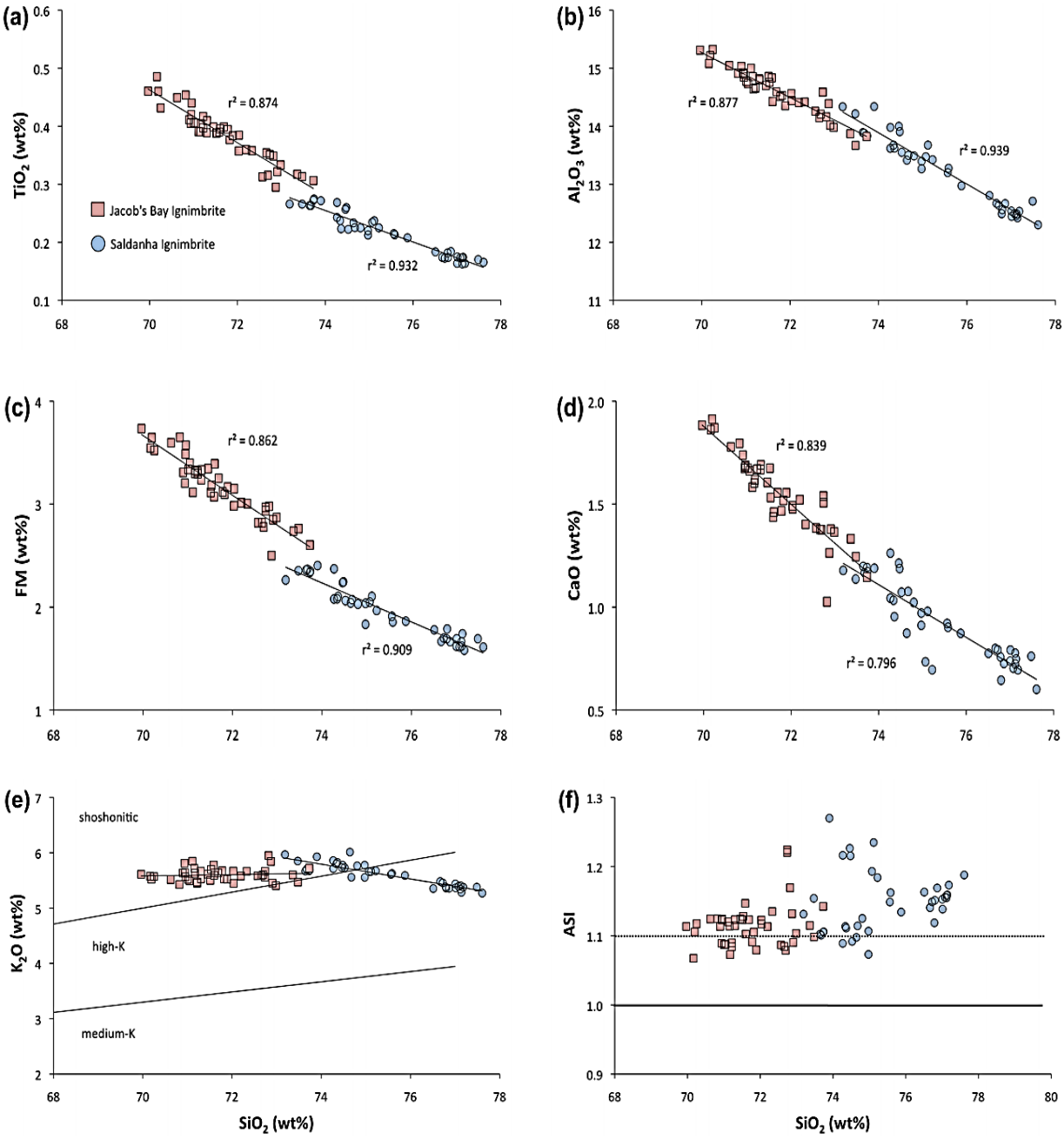

Figure 28: Harker plots of selected major oxides and derived parameters for rocks of the Saldanha Centre in the Saldanha Bay Volcanic Complex; (a) TiO_2, (b) Al_2O_3, (c) FM, (d) CaO, (e) K_2O showing the fields for various magma series, (f) ASI (mol. Al_2O_3/ [CaO - 3.33 P_2O_5 + Na_2O + K_2O]). Saldanha Ignimbrite (blue circles) and Jacobs Bay Ignimbrite (pink squares). These plots are reproduced with permission from Clemens et al. (2017), and are only presented here for contextual and comparative purposes.

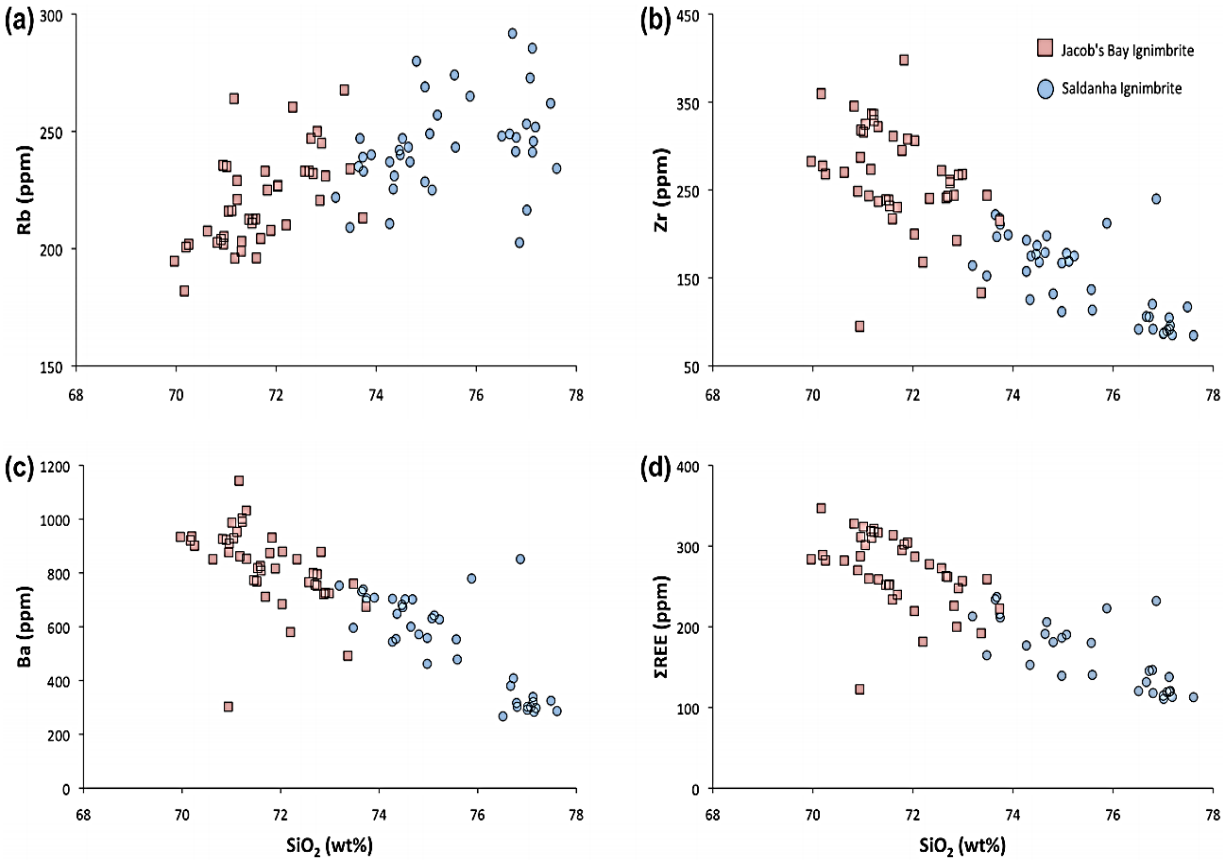

Figure 29: A selection of Harker plots for the rocks of the Saldanha Centre in the Saldanha Bay Volcanic Complex; (a) Rb, (b) Zr, (c) Ba and (d) ∑REE (total rare-earth element content). Saldanha Ignimbrite is plotted as blue circles and the Jacobs Bay Ignimbrite is plotted as pink squares. These plots are reproduced with permission from Clemens et al. (2017), and are only presented here for contextual and comparative purposes.

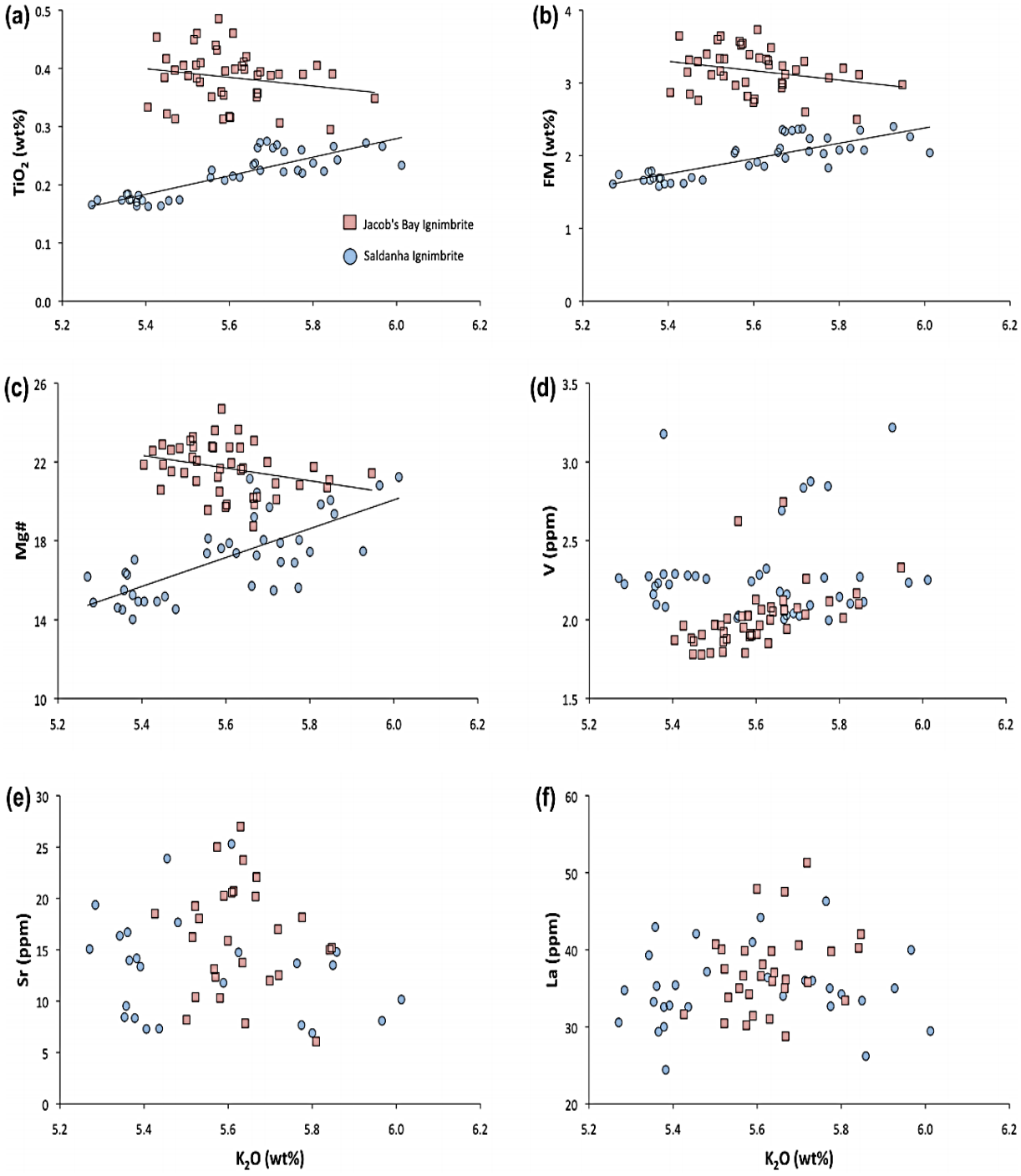

Figure 30: Variety of chemical parameters for rocks of the Saldanha Centre in the Saldanha Bay Volcanic Complex, plotted against K_2O content; (a) TiO_2, (b) FM (FeO^T + MnO + MgO), (c) Mg# (mol. 100 Mg/[Mg + Fe]), (d) V, (e) Sr, and (f) La. Note the mostly clear differences between the magmas that formed the Saldanha and Jacobs Bay Ignimbrites (blue dots and pink squares, respectively). These plots are reproduced with permission from Clemens et al. (2017), and are only presented here for contextual and comparative purposes.

4.3.6 Rb-Sr & Sm-Nd tracer-isotopes for the Saldanha Centre

Table 6, tracer-isotope data for the Saldanha Centre rocks by Clemens et al. (2017), have been added as a comparative data set. The analysis was carried out at the University of Cape Town AEON labs, using a solution of quadrupole ICP-MS for the element solution MC-ICP-MS for the present-day isotope ratios. For more information about the methodology used to obtain these results the reader is referred to Electronic Appendix EA2 of Clemens et al. (2017). Samples Sal1, Sal3 and Sal3b represent the Saldanha Centre – Saldanha Ignimbrites. Samples Sal6, Sal7 and Sal8 represent the Saldanha Centre – Jacobs Bay Ignimbrites.

Table 6: Tracer-isotope data, calculated at 542 Ma, for rocks of the Saldanha Centre in the Saldanha Bay Volcanic Complex (after Clemens et al., 2017)

Sample	$^{87}Sr/^{86}Sr_0$	± 2σ internal	Rb (ppm)	± 1σ	Sr (ppm)	± 1σ	$^{87}Rb/^{86}Sr$ (calc.)	$^{87}Sr/^{86}Sr_t$	± 2σ
Sal3	0.779979	15	248.2	2.0	73.5	0.8	9.84	0.70518	70
Sal3b	0.781806	11	259.6	1.0	79.6	0.23	9.50	0.70959	35
Sal6	0.751618	10	219.3	1.8	114.9	1.29	5.50	0.70944	42
Sal7	0.756319	10	246.6	2.0	110.4	0.36	6.49	0.70696	31
Sal8	0.745440	14	293.9	0.6	181.3	0.69	4.71	0.70967	16

Sample	$^{143}Nd/^{144}Nd_0$	± 2σ internal	Sm (ppm)	Nd (ppm)	$^{147}Sm/^{144}Nd$ (calc.)	εNd_t	± 2σ (assumed)	t2DM (Ga)
Sal1	0.512332	12	5.7	22.9	0.1507	− 2.8	0.2	1.48
Sal3	0.512270	12	7.7	33.9	0.1377	− 3.1	0.2	1.53
Sal 3b	0.512284	19	7.8	36.4	0.1300	− 2.3	0.2	1.55
Sal6	0.512250	12	11.3	55.7	0.1226	− 2.4	0.2	1.48
Sal7	0.512248	9	11.0	58.1	0.1144	− 1.9	0.2	1.46
Sal8	0.512226	13	16.3	89.7	0.1100	− 2.0	0.2	1.49

The Saldanha Centre - Jacobs Bay Ignimbrites (Sal6, Sal7 and Sal8) from Clemens et al. (2017), inserted here as for contextual and comparative dataset, have $\varepsilon Nd_{542\ Ma}$ values of -2.4 (Sal6), -1.9 (Sal7), -2.0 (Sal8) and calculated, two stage, depleted mantle model (t_{2DM}) of 1.48 Ga, 1.46 Ga, 1.49 Ga respectively (Table 6). The $^{143}Nd/^{144}Nd_i$ shows very little variation across the three "Sal" samples at ~0.5122. The $^{87}Sr/^{86}Sr_i$ values vary significantly 0.751618 (Sal6), 0.756319 (Sal7) and 0.745440 (Sal8) with $^{87}Sr/^{86}Sr_{542\ Ma}$ values of 0.70944 (Sal6), 0.70696 (Sal7) and 0.70967 (Sal8).

4.4 Geochronology

4.4.1 Zircon U-Pb Geochronology for the Postberg Centre, Jacobs Bay Ignimbrites

The three samples from the Postberg Centre (samples MM 1, 2 and 3) are chemically classified as Jacobs Bay Ignimbrites. A combination of 74 single spots were analysed, nine of which are discordant with the remaining 65 showing a ≥ 95-105% concordance. A number of cathodoluminescence (CL) images are displayed in Figure 31 A & C (MM1); B & D (MM2) and Figure 32 A, B & C (MM3), each with their corresponding Concordia diagrams (Figure 31 E - MM1; F - MM2 and Figure 32 D - MM3).

A histogram and probability-density distribution plot, which displays all three samples, is shown in Figure 33. Full analytical details are described in the analytical methodology section of this thesis. The U-Pb age summary tables (Table 23Table 29), of all the analysed samples, are presented as Electronic Appendix EA6.

The Concordia QC diagrams for the Plešovice and M127 zircon reference material, displayed in the Appendix (Figure 37 and Figure 38), shows a combined Concordia age of 340 ± 2 Ma and 529 ± 4 Ma respectively, which is in excellent agreement with the published ID-TIMS ages (Sláma et al., 2008; Nasdala et al., 2008 and Mattinson, 2010). The quality control U-Pb age summaries are displayed as Electronic Appendix EA5.

The volcanic zircons extracted from the three PC-JI samples (MM 1, 2 & 3) are generally translucent and in some cases exhibited a slightly pale brown, light grey or pinkish tint. A variety of forms and grain sizes were identified ranging from ~200 – 300 µm and having a slightly elongated euhedral to subhedral grain form with a prismatic grain tip termination. Prior to analysis, cathodoluminescence (CL) imaging (Figure 31 A, B, C & D ; Figure 32 A, B & C) was conducted in order to view the internal structure of the zircon grains as well as select suitable sections for single-spot analysis, described in the analytical methodology. Approximately 20-30% of the zircons displayed oscillatory zonation while the rest had homogeneous internal structures.

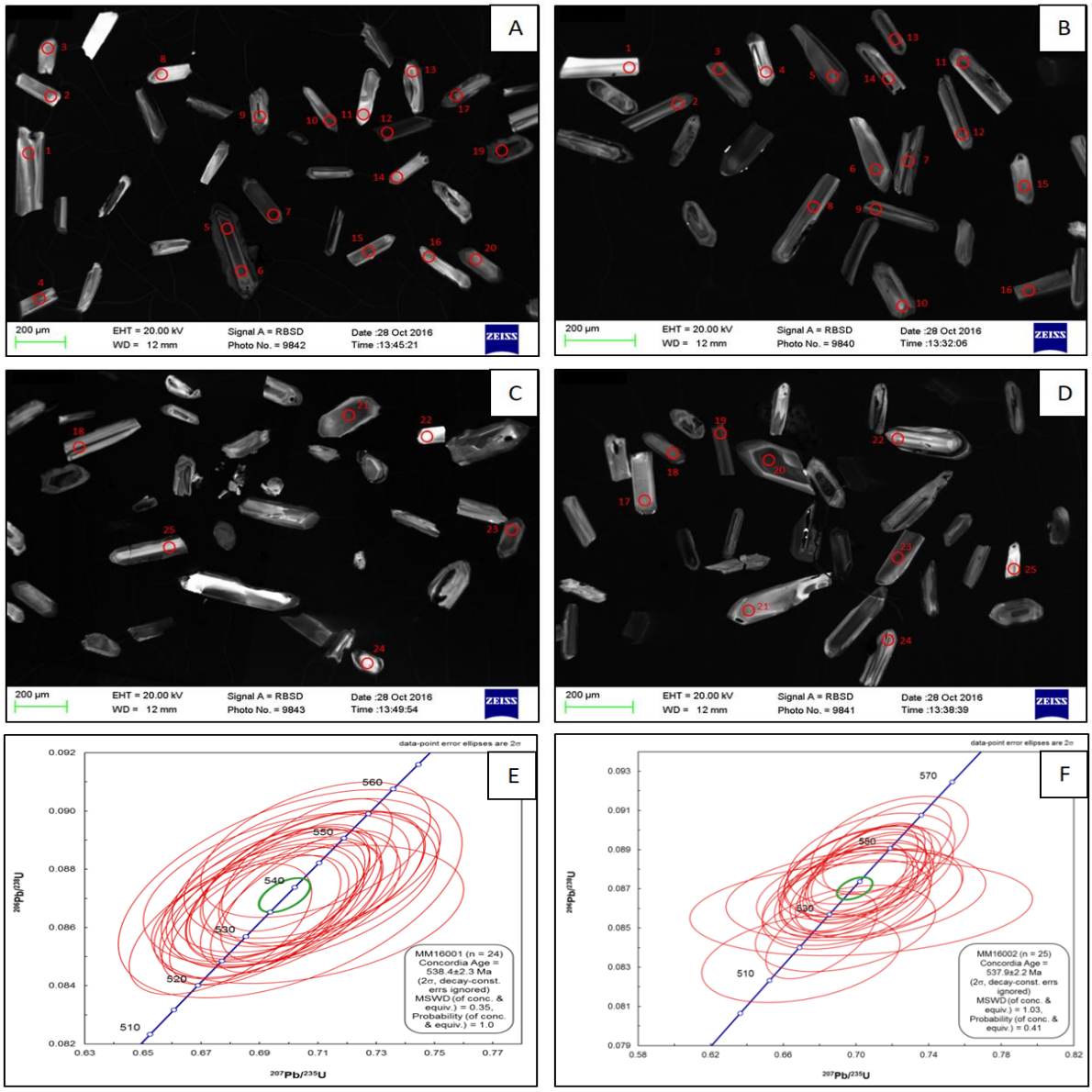

Figure 31: U-Pb Concordia diagrams (E, F) and representative annotated cathodoluminescence (CL) images of zircons from Postberg Centre Jacobs Bay Ignimbrite sample MM1 (A, C) and MM2 (B, D). Error ellipses are plotted at 2σ. E) Concordia diagram of sample MM1 showing 24 analysed spots and a $^{206}Pb/^{238}U$ age of 538.4±2.3 Ma. F) Concordia diagram of sample MM2 showing 25 analysed spots and a $^{206}Pb/^{238}U$ age of 537.9±2.2 Ma.

Twenty-four spot-analyses were made on sample MM1, all of which are ≥ 95-105% concordant and define a combined U-Pb Concordia age of **538 ± 2.3 Ma** (Table 23, Figure 31 E, n=24; MSWD = 0.35). A single zircon (A_301) has been omitted from the analysis due to residual Pb. A further twenty-five spot-analyses were made on sample MM2, all of which are ≥ 95-105% concordant and define a combined U-Pb Concordia age **537.9 ± 2.2 Ma** (Table 24, Figure 31 F, n=25; MSWD = 1.03). A single zircon grain yielded an apparent $^{206}Pb/^{238}U$ age of 517 Ma as a result of Pb loss (A_069). Twenty-five spot-analyses were made on MM3

all of which are ≥ 95-105% concordant and define a combined U-Pb Concordia age **538.2 ± 2.2 Ma** (Table 25, Figure 32 D, n=25; MSWD = 0.82). There is one inherited grain (A_091) that yielded an apparent $^{206}Pb/^{238}U$ age of 558 Ma. Since zircons are thermally strong, this inherited grain may have come from the older surrounding country rock or from the volcanic shaft the magma passed through during the crystallization of the Postberg Ignimbrites and thus did not contribute to the calculation of the 538.2 Ma Concordia age.

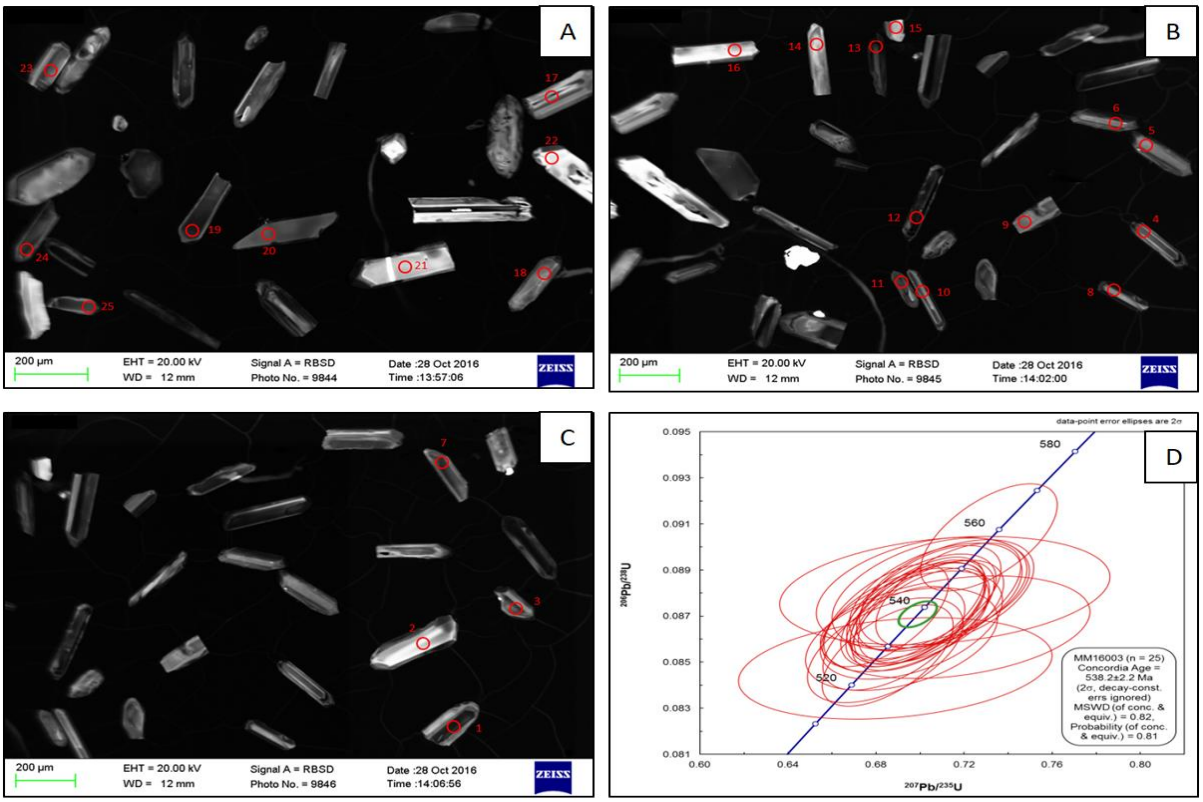

Figure 32: U-Pb Concordia diagram (D) and representative annotated cathodoluminescence (CL) images of zircons from Postberg Centre Jacobs Bay Ignimbrite sample MM3 (A, B & C). Error ellipses are plotted at 2σ. D) Concordia diagram of sample MM3 showing 25 analysed spots and a $^{206}Pb/^{238}U$ age of 538.2±2.2 Ma.

The probability density diagram (a combination of all three PC-JI samples) shows a fairly normal distribution curve for the PC-JI, with the ages peaking at **538 ± 2.2 Ma** (Figure 33). Of the combined seventy-four analyses, nine are discordant with the remaining 65 showing a ≥ 95-105% concordance and define an average **U-Pb Concordia age for the Postberg Centre -Jacobs Bay Ignimbrites (PC-JI) of 538.3 ± 2.2 Ma**. Full analytical data is provided in Electronic Appendix EA6. This is considered the best U-Pb age estimate for the Phase IV Postberg Centre – Jacobs Bay Ignimbrites of the CGS.

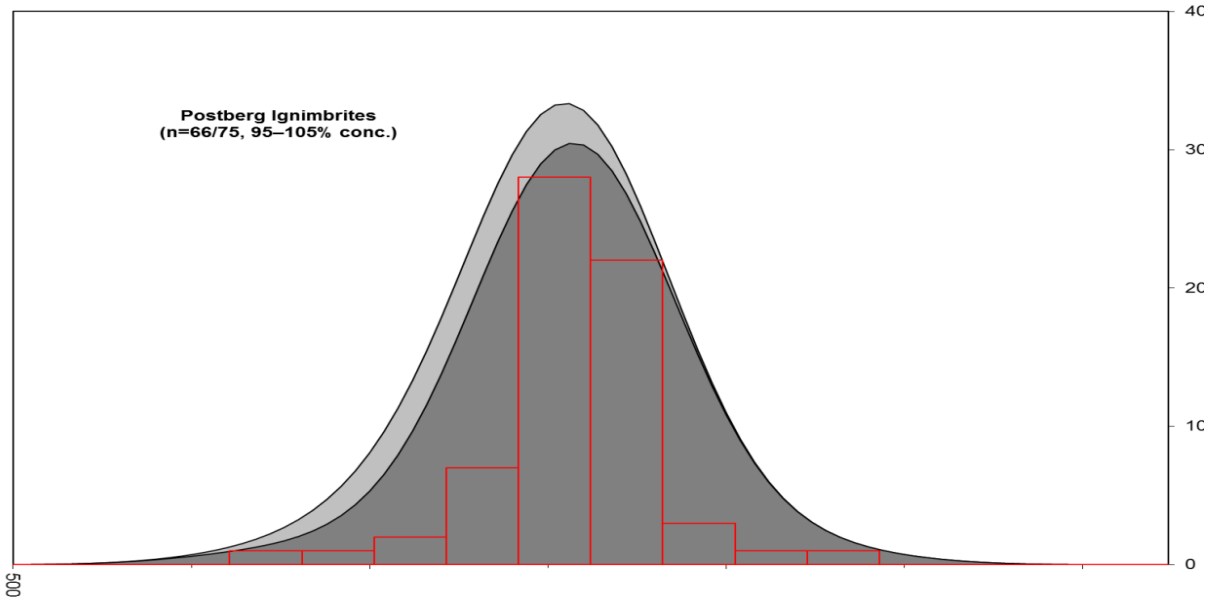

Figure 33: Combined histogram and probability density distribution of all 3 Postberg Centre Jacob's Bay Ignimbrite samples (MM1, MM2 and MM3) showing that the $^{206}Pb/^{238}U$ ages obtained are normally distributed. From the 75 analysed spots 66 spots have a 95-105% concordance. Dark grey area = concordance, light grey area = discordance. Zircon U-Pb Geochronology for the Postberg Centre, Tsaarsbank Ignimbrites

4.4.2 Zircon U-Pb Geochronology for the Postberg Centre, Tsaarsbank Ignimbrites

Two samples collected from the Postberg Centre, chemically classified as Tsaarsbank Ignimbrites were selected for analysis (samples Pos1 and Pos2). A combined 109 single spots were analysed. Only 23 displayed useful data points for accurate Concordia ages. For the two samples, a number of cathodoluminescence (CL) images are displayed in Figure 34 A, B, C & D and Figure 35 A, B, C, D, E, & F each with their own corresponding Concordia diagrams (Figure 34 E and Figure 35 G). A histogram and probability density distribution plot for Pos1 and Pos2 is shown in Figure 34 F and Figure 35 H respectively. Full analytical details are described in the analytical methodology. The U-Pb age summary tables (Table 26Table 27) of all the analysed samples are presented as Electronic Appendix EA5

For quality control, the Plešovice (Sláma et al., 2008) and M127 (Nasdala et al., 2008; Mattinson, 2010) zircon reference materials were analysed. U-Pb result summaries are displayed in Electronic Appendix EA6. The Concordia QC diagrams display U-Pb age of 338 ± 1.3 Ma and 528 ± 1.9 Ma respectively. These ages are in excellent agreement with the published ID-TIMS ages (Figure 39 and Figure 40).

The Pos 1 and Pos 2 samples, geochemically classified as Postberg Centre - Tsaarsbank Ignimbrites, have euhedrally-shaped prismatic zircon grains ranging from ~50 -400 µm in size. They are translucent, with some having a slight brown/grey tint. Most of the zircons show simple magmatic zonation in CL imaging but roughly 20-30% of the zircons contain what are interpreted as inherited, xenocrystic cores (see Figure 34 A, B, C & D and Figure 35 A, B, C, D, E & F). Of the 109 single-spots, 3 data points were omitted from Pos1 (inherited zircons), displaying $^{206}Pb/^{238}U$ ages of 758 Ma, 616 Ma and 621 Ma. A further 15 data points were omitted as a result of Pb loss, displaying $^{206}Pb/^{238}U$ ages ranging between 401 – 521 Ma. For Pos 2, 8 data points were omitted (inherited zircons), displaying $^{206}Pb/^{238}U$ ages of between 566 – 1157 Ma. A further 4 data points were omitted as a result of Pb loss, displaying ages $^{206}Pb/^{238}U$ ranging between 363 - 512 Ma. Of the combined 109 single-spots that were analysed, 27 of 44 spots (Pos 1) and 49 of 61 spots (Pos2) were considered, after the omission of data points as described above.

For Pos 1, concordance ranges from 20 - 106%. Only those with 95-105% concordance was considered. Of the 44 spots, 14 fall within this range and define a coherent cluster of data from zircon grains for the PC-TI, with a combined U-Pb Concordia age of **536.6 ± 2.1 Ma** (Figure 34 E, n = 44, 14/44 = 95-105 Conc. % wtd. by data- pt. errors only, 0 of 14 rejected, MSWD = 1.7). The probability density diagram displayed in Figure 34 E shows a fairly normal distribution with ages peaking at 536 ± 2 Ma.

For Pos 2, concordance ranges between 18 – 110%. Only those whose concordance is between 95-105% were considered. Of the 61 spots, only 10 fell within this range with one being omitted due to residual Pb. The resultant 9 spots define a coherent cluster for of data from the zircons grains for the PC-TI, with a combined U-Pb Concordia age **540.2 ± 3.4Ma** (Figure 35 G, n = 61, 10/61 = 95-105 Conc. % wtd. by data-pt. errors only, 1 of 10 rejected, MSWD = 1.6). The probability density diagram displayed in Figure 35 H shows a fairly normal distribution skewed slightly to the right.

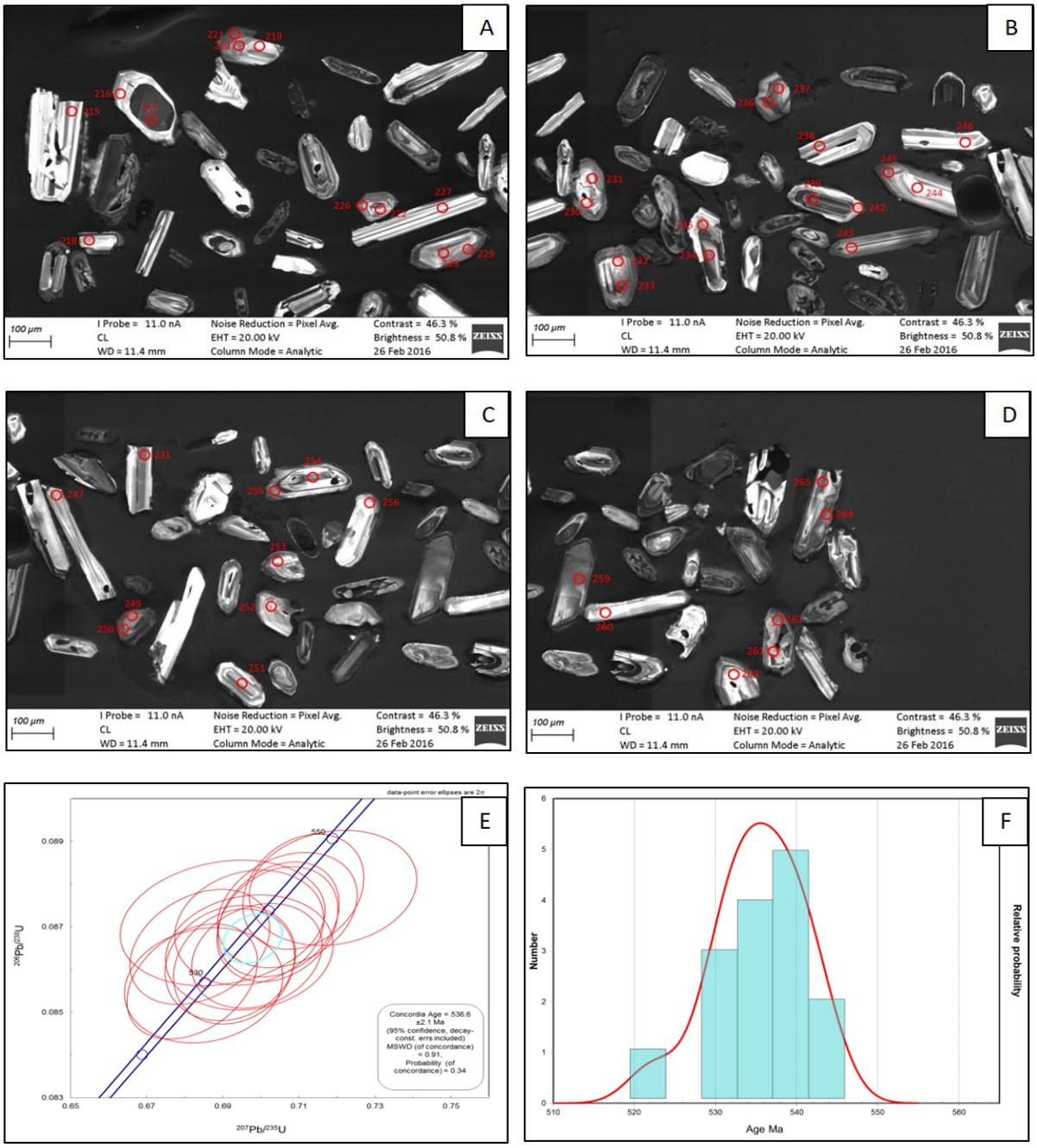

Figure 34: U-Pb Concordia diagram (E) and representative annotated cathodoluminescence (CL) images of zircons from Postberg Centre Tsaarsbank Ignimbrite sample Pos 1 (A, B, C & D). Error ellipses are plotted at 2σ. E) Concordia diagram of sample Pos1 showing 14/44 analysed spots and a $^{206}Pb/^{238}U$ age of 536.6±2.1 Ma with quoted errors at 95% confidence level. F) Probability density distribution of Pos1 $^{206}Pb/^{238}U$ ages obtained showing a normal distribution.

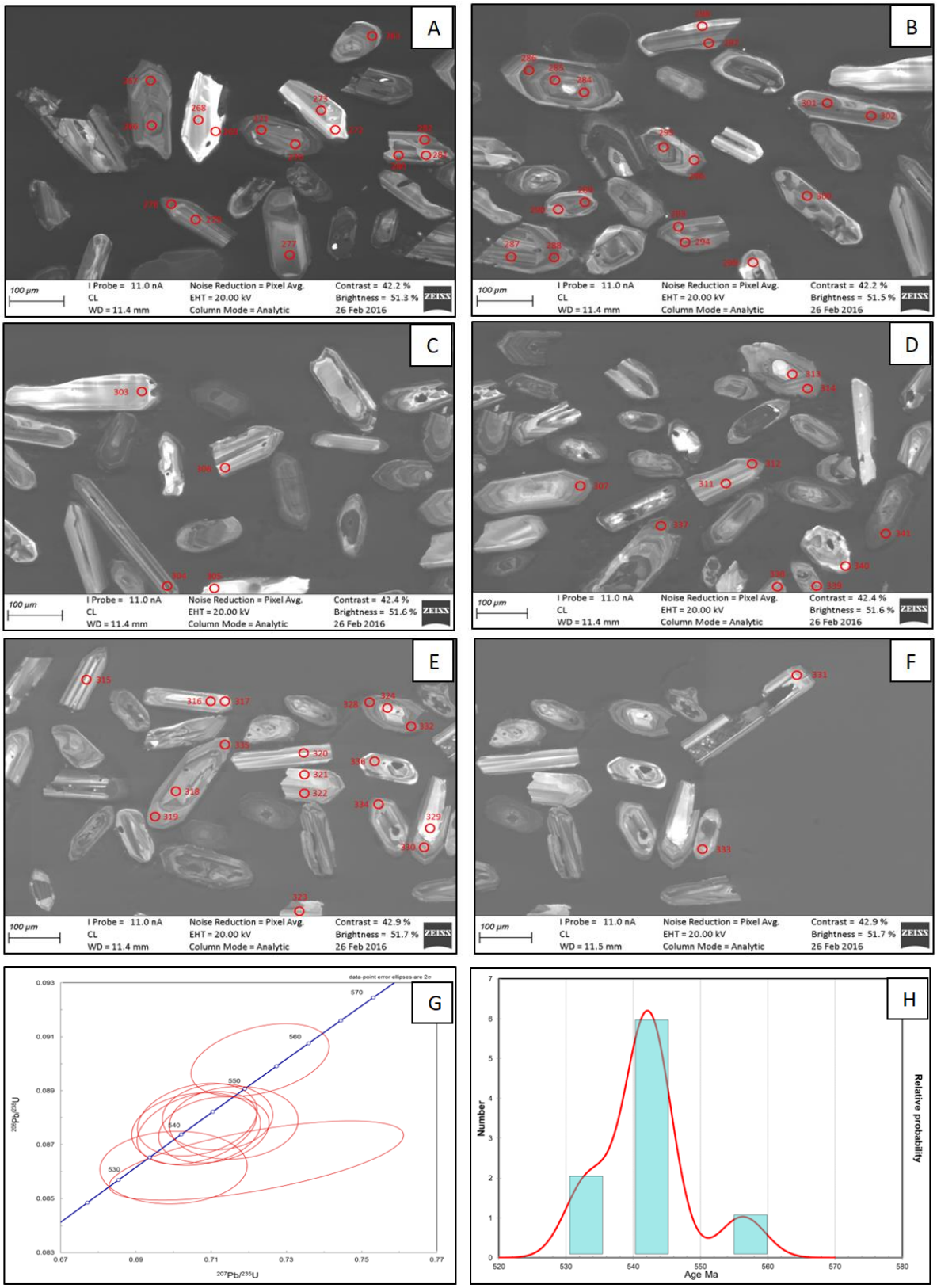

Figure 35: U-Pb Concordia diagram (G) and representative annotated cathodoluminescence (CL) images of zircons from Postberg Centre Tsaarsbank Ignimbrite sample Pos 2 (A, B, C, D, E & F). Error ellipses are plotted at 2σ. G) Concordia diagram of sample Pos2 showing 9/61 analysed spots and a $^{206}Pb/^{238}U$ age of 540.2 ± 3.4 Ma with quoted errors at 95% confidence level. H) Probability density distribution of Pos2 $^{206}Pb/^{238}U$ ages showing a fairly normal distribution skewed slightly to the right.

5 Discussion

5.1 Introduction

This chapter aims to review and describe all the data outputs of this study. The Petrography section describes the samples' mineral assemblages, alterations, textures as seen in the photomicrographs presented in the results section (4.2, Figure 12, Figure 13 and Figure 14). The Bulk-rock chemistry section (5.3) describes the distinct geochemical make-up of the various magma series found in the Postberg and Saldanha eruption centres. The differences between the magma series are described and various geochemical "limits" are presented in order to differentiate between them. Tracer Rb-Sr/Sm-Nd isotope data (section 5.3.1) is discussed using isotope correlation plots and Nd isotopic growth diagrams to compare two stage, depleted mantle, model ages of the PC-JI and SC-JI rock samples. A description of the form, colour, and internal structure of the extracted zircon grains are presented in the Results chapter of this thesis with the U-Pb age for the various samples referenced to their corresponding figures and their respective data tables in the Electronic Appendices. The results are discussed here in section 5.4.

In this chapter, as well as in the previous, several abbreviations are used for the various types of Ignimbrites found in the Postberg and Saldanha Centre. When referring to the eruption centres themselves the abbreviations "PC" is used for the Postberg Centre and "SC" for the Saldanha Centre. As mentioned before the Saldanha Bay Volcanic Complex has four geochemically distinct magma series. The abbreviations for the different magma series were done as follows: the Plankiesbaai Ignimbrites "PI" and Tsaarsbank Ignimbrites "TI" (both found exclusively in the Postberg Centre) and the Saldanha Ignimbrite "SI" and Jacobs Bay Ignimbrite "JI" (found in both eruption centres). Therefore, when describing a certain magma series (PI, TI, SI or JI) within an

eruption centre (PC or SC) the abbreviation is “eruption centre” – “ magma series” For example, the Postberg Centre - Saldanha Ignimbrite is abbreviated to (PC-SI) and Saldanha Centre Saldanha Ignimbrite to (SC-SI) etc.

5.2 Petrography of the Postberg Centre Ignimbrites

The groundmass has undergone substantial recrystallization where most of its original textures, which would generally classify them as pyroclastic, were removed in the process. The only evidence of their pyroclastic origin is the large broken/fractured phenocrysts in the fine-grained groundmass of polygonal quartz and feldspar, seen in the Postberg eruption centre ignimbrites (Figure 12, Figure 13 and Figure 14) as well as in the ignimbrites of Saldanha eruption centre described by Clemens and Stevens (2016a) and Clemens et al. (2017). The absence of these original textures was likely the reason why the ignimbrites were incorrectly interpreted as “intrusive” tuffisites by Scheepers and Poujol (2002).

Clemens et al. (2017) show that the earlier date (542 ± 2Ma) for the Saldanha Centre magmatism, compared to the 515 ± 3 Ma by Scheepers and Poujol (2002), suggested that the products of the eruption may have spread to the Postberg Centre and was likely that small amounts of Saldanha Centre “tephra” underlie the “tephra” of the Postberg peninsula. Their observations show that the groundmass grain-size increases upwards in the succession of Saldanha Centre. Only the shattered phenocrysts in the most coarse-grained ignimbrites identify them as fragmental-volcanic rocks. This interpretation, inferred to be from the rapid eruption of intracaldera ignimbrites and thermal blanketing, suggests that a significant portion of the succession was removed by erosion because the most coarsely-grained sections are presently exposed at the top of the sequence in the Saldanha eruption centre. Since shattered phenocrysts are a common occurrence in the PC–JI and the groundmass is generally more coarse-grained than its SC-JI counterparts, it is reasonable to conclude that the samples collected at the base of the Postberg peninsula (PC- JI, dated to 538 ± 2 Ma) is the current uppermost portion of the Saldana Centre ignimbrite sequence. Therefore, the magmatism associated with the Saldanha Centre – Jacobs Bay Ignimbrite continued for at least 4 Ma after the calculated date by Clemens et al. (2017) of 542 Ma as it extended to the Postberg Centre, as the Postberg Centre – Jacobs Bay Ignimbrites.

Since the samples collect for this study in the Postberg Centre bears such a close textural resemblance to the Saldanha Centre ignimbrites (note the samples displayed as thin sections is tephra from the SC-JI) and display the same shattered phenocrysts that mark them as volcanic rather than an igneous body, suggests that the Postberg Centre rocks are in fact ignimbrites.

5.3 Bulk-rock chemistry for the Postberg Centre Ignimbrites

All the rocks of the Saldanha Bay Volcanic Complex have S-type characteristics and are strongly peraluminous (Figure 20 and Figure 19). Chappell and White (1974) were the first to describe the geochemical and mineral characteristics of S-type rocks as having low Na_2O/K_2O, high Al_2O_3 and SiO_2, contain alkali feldspar, quartz, orthopyroxene, biotite, phenocrysts and lack hornblende.

Although Clemens and Stevens (2016) noticed two geochemically distinct ignimbrites in the PC, they could not be certain that the sampled rocks fairly represented the entire Postberg Centre. Clemens et al. (2017) described both magma groups (the PC-PI and PC-TI) as having high SiO_2 contents (>76 wt.%), a lack of variation in TiO_2 and Zr, High Al_2O_3 and ASI values (on average higher than the SC Ignimbrites), low CaO and Na_2O, and a highly ferroan character (Mg# values of < 18). This description, however, only establishes that the PC ignimbrites were not derived from the magmas of the SC and could not have been derived from each other by crystal-liquid differentiation but does not differentiate between compositions of the Plankiesbaai and Tsaarsbank Ignimbrites themselves. With this in mind, the geochemical results presented here for the PC ignimbrites (Figure 21 Figure 24, Table 9Table 12) is in excellent agreement with the geochemical work done by Clemens and Stevens (2016a) and Clemens et al. (2017), although no dividing geochemical parameters were set.

PC-PI and PC-TI are characterised by a lack of variation in Zr content, higher Rb content and lower Sr, Ba, V and Zn content when compared to its PC-SI and PC-JI counterparts (Figure 21 and Figure 22). These observations become even clearer with the selected trace elements plotted with K_2O as the abscissa (Figure 23 and Figure 24) although, without the R^2 values

(correlation coefficient lines) for each particular ignimbrite, it is quite difficult to distinguish between the PI and TI using trace element data alone. Nevertheless, they do show that these magmas are distinctly different from the magmas of the Saldanha Centre.

5.3.1 Rb/Sr & Sm/Nd isotope analysis for the Postberg Centre – Jacobs Bay Ignimbrites

From the petrography and geochemistry, the Postberg Centre – Jacobs Bay Ignimbrites are S-type and peraluminous; which suggests that the source rock from which they were produced were dominated by metasediments (the reader is referred the description of S-type characteristics by Chappell and White (1974). A suitable starting point for interpretation and discussion of this data would be an in-depth look at the isotope analysis of the Saldanha Centre – Jacobs Bay Ignimbrite by Clemens et al. (2017) presented as Table 6. They suggest that the source rock of the Saldana Centre Ignimbrites is inferred to have formed through partial melting of a heterogeneous source, most likely Malmesbury Group or Swartland complex metamorphosed volcaniclastic rocks and greywackes.

For the Postberg eruption centre $^{87}Sr/^{86}Sr_i$ values of the PC-JI's (avg. 0.713348) are significantly lower when compared to SC-JI's $^{87}Sr/^{86}Sr_i$ values (avg. 0.75112) while the PC-JI's $^{87}Sr/^{86}Sr_{538\ Ma}$ values (avg. 0.756193) much higher than the SC-SI's $^{87}Sr/^{86}Sr_{542\ Ma}$ values (avg. 0.70869). Rapidly emplaced ignimbrite sheets (thermal blanketing) contain considerable heat that can cause grain coarsening of the groundmass and overgrowths on phenocrysts. Since the initial εNd_i of the PC-JI (-2.61, -2.63, -2.71) is only slightly higher than εNd_{542Ma} values of the SC-JI (-2.4, -1.9, -2.0) and the εNd_{538Ma} of the PC-JI is significantly higher (-7.60, -7.73, -7.92) compared to the εNd_{542Ma} SC-JI values; suggests that grain coarsening continued in the Postberg Centre. This is consistent with the observations made in the petrography description section 4.2 (Petrography), which indicates that the PC-JI has a more coarsely recrystallized groundmass and a larger proportion of phenocrystic overgrowths. Therefore, the source rock of the PC-JI's are inferred to have formed through partial melting of a heterogeneous source, most likely Malmesbury Group or Swartland complex metamorphosed volcaniclastic rocks and greywackes.

5.4 Geochronology of the Postberg Centre, Saldanha Bay Volcanic Complex

5.4.1 The place of the Saldanha Bay Volcanic Complex in the CGS

The above zircon U-Pb dates clarify the position of at least some of the S-type volcanism within the CGS magmatic cycle. With the new age data for the Saldanha Centre Ignimbrites (**SC-SI at 542 ± 2 Ma** and **SC-JI at 541 ± 2 Ma**) by Clemens et al. (2017) as well as the Postberg Centre Ignimbrite dates (**PC-JI at 538 ± 2.2 Ma** and **PC-TI at 536 ± 2 Ma & 540 ± 3.4 Ma**) from this study, we are now able to firmly place the Saldanha Bay Volcanic Complex in the S type magmatic cycle of the CGS (Figure 36 and Table 8). Other S-type members of the CGS have also been dated using the U-Pb zircon technique. These include the **Hoedjiespunt Granite at 552 ± 4 Ma**, the **Seeberg Granite at 540 ± 4 Ma** and the **Trekoskraal Granite at 539 ± 4 Ma** all dated by Scheepers and Armstrong (2002); the **Darling Pluton at 547 ± 6 Ma** by da Silva et al. (2000) and **538.13 ± 1.5 Ma** by Villaros et al. (2012); and the two samples of the **Peninsula Pluton at 538.2 ± 1.5 Ma and 532.7 ± 1.9 Ma** by Villaros et al. (2012).

Magmatism in the Postberg Centre started around 540 ± 3.4 Ma, which was around the same age, within uncertainty, as the Saldanha Centre Ignimbrites at 542 ± 2 Ma as well as the Trekoskraal and Seeberg Granites. This place's the rocks of the Saldanha Bay Volcanic Complex in the age bracket for the initial S-type magmatism of the Cape Granite Suite, which lasted for approximately 20 M. yr. from 552 ± 4 Ma to 532.7 ± 1.9 Ma. The geochronology of this thesis and U-Pb dates by Clemens et al (2017) for the Saldanha eruption centre, suggests that the activity in the Saldanha Centre and Postberg Centre did overlap, and their magmas co-erupted. Although the implication of this for the tectonic evolution of this area is still unclear, Clemens et al. (2017) suggested that in order to provide the required flux of mantle-heat to the crust for high partial melting of the deep crust, some sort of "ridge subduction or slab break off" was needed – possibly from the collision between the Rio de la Plata and Kalahari cratons during its waning phase.

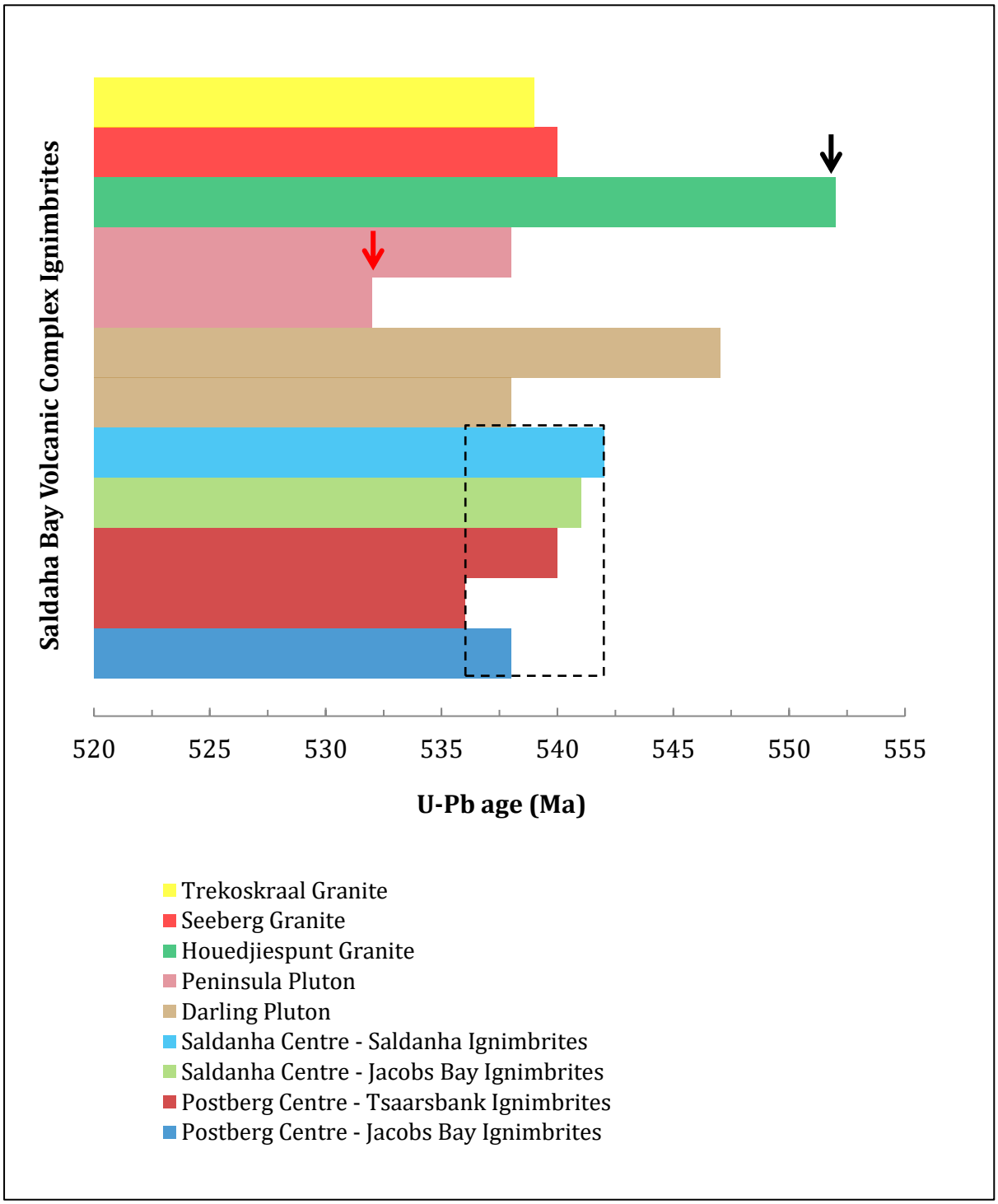

Figure 36: Bar graph displaying the age (Ma) of the S-type members of the Cape Granite Suite, dated using the U-Pb technique on magmatic zircon grains (da Silva et al., 2000; Scheepers and Armstrong, 2002; Villaros et al., 2012 and Clemens et al., 2017). The black arrow indicates the start of the CGS magmatic cycle and the red arrow indicates when the S-type magmatism of the CGS ended.

CONCLUSION

This study supplements the earlier studies and findings of Clemens and Stevens (2016) and Clemens et al. (2017) adding extra data points in terms of both geochemistry and geochronology, particularly those of the Postberg eruption centre to the south as opposed to the Saldanha eruption centre which was examined by Clemens and Stevens (2016) and Clemens et al. (2017). The study's main aim is to assess the geochemistry and age distribution of these ignimbrites relative to the previous phases of magmatism originally proposed by Scheepers (1995) for the magmatism of the Cape Granite Suite. Recent zircon dating has called this classification into question and this study aims to examine the volcanic rocks around Saldanha, particularly in light of the Clemens and Stevens (2016) and Clemens et al. (2017) studies that reclassify these rocks differing from the original and previous studies.

Based on internal structure, petrographic analysis, mineralogy, the nature of enclaves, geochemical features and relationships with enclosing rocks - Scheepers and Rozendaal (1992) and Gresse and Scheepers (1993) identified three major phases (I, II, III) of igneous magmatism for the Saldania belt. Scheepers and Nortjé (2000) later added an additional rhyolitic volcanic phase (IV) dated to 515 ± 3Ma by Scheepers and Poujol (2002). These four major phases of magmatism are further subdivided into seven distinct granitic groups (**Error! Reference source not found.**), each having one or more unique features: Sa1, Sa2, Sb, Ia, Ib, Aa and Ab (Scheepers, 1995).

Table 7: Summary of the major phases of the magmatism for the Saldania Belt modified after Scheepers (1995), highlighting the "quartz porphyry" classification Phase IV dated to 515 Ma.

Magmatism	Association	Rock Type	Examples
Phase IV 515 Ma	Volcanic	Ignimbrite, tuffisite, quartz porphyry	Postberg Ignimbrite, Saldanha "quartz porphyry"
Phase III 520 Ma	Aa	Alkali Fs granite, Quartz syenite	Klipberg granite
	Ab	Alkali Fs Granite	Cape Columbine granite
Phase II 540-520 Ma	Ib	Granite, alkali Fs granite	Paarl fine-grained granite, Slippers Bay granite
	Ia	Monzogranite, granite, alkali Fs granite	Paarl coarse- and medium-grained granite, Vredenburg monzogranite, Greyton pluton
Phase I 555-540 Ma	Sb	Granite	Trekoskraal granite, Karnberg, Rondeberg granite, Coarse porphyritic, Darling granite
	Sa_2	Granite, alkali Fs granite	Stellenbosch fine-grained granite, Contreberg granite, Olifantskop granite
	Sa_1	Granite	Hoedjiespunt granite, Seeberg granite, Peninsula granite

This initial observation, as described above, places the rhyolitic volcanism as a separate phase of magmatism (Phase IV). This interpretation and its position in the model for magmatism of the Saldania belt may have stemmed from Scheepers and Poujol (2002) viewing the rock body, as a whole, as intrusive. This interpretation, however, is considered here to be incorrect or at least confims the possibility of a younger zircon forming episode 25 M.yrs after the Saldanha Bay Volcanic Complexs' formation. Clemens and Stevens (2016a) re-interpreted the rocks in the Saldanha Centre as S-type Ignimbrites, rather than "quartz porphyry."

Table 8: New summary table of the phases of magmatism for the Saldania Belt (modified after Scheepers, 1995; Scheepers and Nortjé, 2000 and Scheepers and Poujol, 2002) displaying the new sequence of the magmatic events as well as the newly interpreted volcanic phase of 542 - 538±2 Ma.

Magmatism		Association	Rock Type	Examples
Phase III 520 Ma		Aa	Alkali Fs granite, Quartz syenite	Klipberg granite
		Ab	Alkali Fs Granite	Cape Columbine granite
Phase II 540 - 520 Ma		Ib	Granite, alkali Fs granite	Paarl fine grained granite, Slippers Bay granite
		Ia	Monzogranite, granite, alkali Fs granite	Paarl coarse-and medium- grained granite, Vredenburg monzogranite, Greyton pluton
Phase I 555 - 533 Ma	Sv Ignimbrite (536 – 540 Ma)	Sb	Granite	Trekoskraal granite, Karnberg, Rondeberg granite, Coarse porphyritic, Darling granite
	Saldanha Bay Volcanic Complex Postberg Centre ignimbrites (Plankiesbaai and Tsaarsbank Ignimbrites)	Sa_2	Granite, alkali Fs granite	Stellenbosch fine grained granite, Contreberg granite, Olifantskop granite
	Saldanha Centre ignimbrites (Saldanha and Jacobs Bay Ignimbrite	Sa_1	Granite	Hoedjiespunt granite, Seeberg granite, Peninsula granite

Upon closer observation and a more holistic view of all the S-type members of the CGS (Figure 36), the new age data places all the ignimbrites of the Saldanha Bay Volcanic Complex securely within the age bracket for the initial burst of **S-type magmatism** of the Cape Granite Suite (Figure 36). Therefore, based on the geochronological results of this study, a revised order for phases of magmatism for the Saldania belt is proposed (Table 8). The S-type intrusive granites (Sa1, Sa2 and Sb) as well as the Saldanha Bay Volcanic Complex ignimbrites were emplaced ca. 555 – 533 Ma (Phase I) leaving the

crustal magma source slightly depleted. The addition of residual heat from the initial intrusion to the same, already volatile magma source, resulted in a volcanic event that rapidly emplaced an ignimbrite sheet (542 – 536 ± 2 Ma) in the vicinity of the S-type granites. The rapid emplacement and high temperatures of the ignimbrite sheets stimulated the partial melting, grain coarsening and phenocrystic overgrowth seen in both centres of the ignimbrites of the Saldanha Bay Volcanic Complex.

6 REFERENCES

Bachmann, O. and Bergantz, G. W., 2004. On the origin of crystal-poor rhyolites extracted from batholithic crystal mushes. Journal of Petrology, 45 (8), 1565–1582.

Bachmann, O. and Bergantz, G. W., 2006. Gas percolation in upper-crustal silicic crystal mushes as a mechanism for upward heat advection and rejuvenation of near-solidus magma bodies. Journal of Volcanology and Geothermal Research, 149 (1–2), 85–102.

Barnett, W., Armstrong, R. A. and De Wit, M. J., 1997. Stratigraphy of the upper Neoproterozoic Kango and lower Palaeozoic Table Mountain Groups of at the Cape Fold Belt revisited. South African Journal of Geology, 100, 237-250.

Belcher, R. W. and Kisters, A., 2003. Lithostratigraphic correlations in the western branch of the Pan-African Saldania belt, South Africa: the Malmesbury Group revisited. South African Journal of Geology, 106 (4), 327-342.

Branney, M. J. and Kokelaar, B. P., 2002. Pyroclastic Density Currents and the Sedimentation of Ignimbrites. Geological Society Memoir, 27. The Geological Society Publishing House, Bath, 152pp.

Bryan, S. E., Ferrari, L., Reiners, P. W., Allen, C. M., Petrone, C. M., RamosRosique, A. and Campbell, I. H., 2006. New insights into crustal contributions to large-volume rhyolite generation in the Mid-Tertiary Sierra Madre Occidental Province, Mexico, revealed by U-Pb geochronology. Journal of Petrology, 49 (1), 47–77.

Buggisch, W., Kleinschmidt, G. and Krumm, S., 2010. Sedimentology, geochemistry and tectonic setting of the Neoproterozoic Malmesbury Group (Tygerberg Terrane) and its relation to neighbouring terranes, Saldania Fold Belt, South Africa. Neues Jahrbuch für Geologie und Paläontologie, 257, 85–114.

Cas, R. A. F., O'Halloran, G., Long, J. A. and VandenBerg, A. H. M., 2003. Middle Devonian to Carboniferous: late to post-tectonic sedimentation and magmatism in an arid continental setting. In: Birch, W. D. (Ed.) Geology of Victoria. Geological Society of Australia, Victorian Division, Melbourne, pp. 157–193.

Chappell, B. W. and White, A. J. R., 1974. Two contrasting granite types. Pacific geology, 8 (2), 173-174.

Chemale, E. J., Scheepers, R., Gresse, P. G. and van Schmus, W. R., 2011. Geochronology and sources of late Neoproterozoic to Cambrian granites of the Saldania Belt. International Journal of Earth Sciences, 100, 431–444.

Clemens, J. D. and Stevens, G., 2016. The Saldanha Bay Volcanic Complex: Clarifying the Cambrian geology of the Postberg – Saldanha Area, West Coast, South Africa. South African Journal of Geology, 119, 347-358.

Clemens, J. D., Stevens, G., Frei, D., Joseph, C. S. A., 2017. Origins of cryptic variations in the Ediacaran – Fortunian rhyolitic ignimbrites of the Saldanha Bay Volcanic Complex, Western Cape, South Africa. Contribution Mineral Petrol, 172, 99pp.

Cornell, D. H., Zack, T., Andersen, T., Corfu, F., Frei, D. and Van Schijndel, V., 2016. Th-U-Pb zircon geochronology of the Paleoproterozoic Hartley Formation porphyry by six methods, with age uncertainty approaching 1 Ma. South African Journal of Geology, 119, 473-494.

Dalziel, I. W. D., Dalla Salda, L. H., Gahagan, L. M., 1994. Palaeozoic Laurentia–Gondwana interaction and the origin of the Appalachian–Andean mountain system. Geological Society of America Bulletin, 106, 243–252.

Da Silva, L. A., Gresse, P. G., Scheepers, R., McNaughton, N. J., Hartmann, L. A. and Fletcher, I., 2000. U-Pb SHRIMP and Sm-Nd age constraints on the timing and sources of the Pan-African Cape Granite Suite, South Africa. Journal of African Earth Sciences, 30, 795-815.

Frei, D. and Gerdes, A., 2009. Precise and accurate in situ U–Pb dating of zircon with high sample throughput by automated LA-SF-ICP-MS. Chemical Geology, 261, 261-270.

Frimmel, H. E., Zartmann, R. E. and Spaeth, A., 2001. The Richtersveld Igneous Complex, South Africa. U-Pb Zircon and Geochemical evidence for the beginning of Neoproterozoic Continental Breakup. The Journal of Geology, 109, 493-508.

Frimmel, H. E., Basei, M. S. and Gaucher, C., 2011. Neoproterozoic geodynamic evolution of SW - Gondwana: a southern African perspective. International Journal of Earth Sciences, 100, 323–354.

Frimmel, H. E., Basei, M. A. S., Correa, V. X. and Mbangula, N., 2013. A new lithostratigraphic subdivision and geodynamic model for the western Pan-African Saldania Belt, South Africa. Precambrian Research, 231, 218-235.

Gray, C. M. and White, A. J. R., 2001. Reduced granites and volcanics of the Central Victorian Magmatic Province. AGSO Record 2001/3

Gresse, P. G., Chemale, F., Da Silva, L. C., Walraven, F. and Hartmann, L. A., 1996. Late-to post-orogenic basins of the Pan-African–Brasiliano collision orogen in southern Africa and southern Brazil. Basin Research, 8 (2), 157-171.

Gresse, P. G. and Scheepers, R., 1993. Neoproterozoic to Cambrian (Namibian) rocks of South Africa: a geochronological and geotectonic review. Journal of African Earth Sciences, 16 (4), 375-393.

Gresse, P. G., Theron, J. N., Fitch, F. J. and Miller, J. A., 1992. Tectonic inversion and radiometric resetting of the basement in the Cape Fold Belt. In: De Wit, M. J. and Ransome, I. G. D (Eds.), Inversion tectonics in the Cape Fold Belt, Karoo and Cretaceous basins of southern Africa. Balkema Rotterdam, The Netherlands, pp.217-228.

Gresse, P. G., Von Veh, M. W. and Frimmel, H. E., 2006. Namibian (Neoproterozoic) to early Cambrian successions. In: Johnson, M. R., Anhaeusser, C. R. and Thomas, R. J. (Eds.), The geology of South Africa. Geological Society of South Africa. Council for Geoscience, South Africa, 395-420.

Hälbich, I. W., Fitch, F. J., Miller, J. A., 1983. Dating the Cape Orogeny Geodynamics of the Cape Fold Belt. In: Sohnge, A. P. G., Hälbich, I. W. (Eds.), Spec. Publ. Geological Society of South Africa, 12, 149 -164.

Hartnady, C. H., Joubert, P. and Stowe, C., 1985. Proterozoic crustal evolution in south-western Africa. Episodes 8, 236-243.

Hartnady, C. J. H., Newton, A. R. and Theron, J. N., 1974. The stratigraphy and structure of the Malmesbury Group in the south-western Cape. Bulletin of the Precambrian Research Unit, University of Cape Town, South Africa, 15, 193-214.

Irvine, T. N. and Baragar, W. R. A., 1971. A guide to the chemical classification of the common volcanic rocks. Canadian Journal of Earth Sciences, 8, 523-548.

Jackson, S., Pearson, N. J., Griffin, W, L. and Belousova, E. A., 2004. The application of laser ablation – inductively coupled plasma – mass spectrometry to in situ U–Pb zircon geochronology. Chemical Geology, 211, 47–69.

Jochum, K. P., Nohl, U., Herwig, K., Lammel, E., Stoll, B. and Hofmann, A. W., 2005. GeoReM: A New Geochemical Database for Reference Materials and Isotopic Standards. Geostandards and Geoanalytical Research, 29, 333-338.

Jochum, K. P., Weis, U., Schwager, B., Stoll, B., Wilson, S. A., Haug, G. H., Andreae, M. O. and Enzweiler, J., 2016. Reference Values Following ISO Guidelines for Frequently Requested Rock Reference Materials. Geostandards and Geoanalytical Research.

Joseph, C. S. A., 2012. The petrogenesis of the ignimbrites and quartz porphyritic granites exposed along the coast at Saldanha, South Africa. MSc Thesis, University of Stellenbosch, 79pp.

Kisters, A. F. M., Agenbach, C. and Frei, D., 2015. Age and tectonic significance of the volcanic Bloubergstrand Member in the Pan-African Saldania Belt, South Africa. South African Journal of Geology, 118, 213-224.

Kisters, A. F. M. and Belcher, R. W., 2018. The stratigraphy and structure of the western Saldania Belt, South Africa. In: Geology of SW Gondwana, Regional Springer Book Series, Chapter 14, pp. 387-410.

Ludwig, K., 2003. Isoplot/Ex version 3: A Geochronological toolkit for Microsoft Excel. Geochronology Centre, Berkeley.

Mattinson, J. M., 2010. Analysis of the relative decay constants of ^{235}U and ^{238}U by multi-step CA-TIMS measurements of closed-system natural zircon samples. Chemical Geology, 275, 186-198.

Nance, R., Murphy, J. and Santosh, M., 2014. The supercontinent cycle: A retrospective essay. Gondwana Research, 25, 4-29.

Nasdala, L., Hofmeister, W., Norberg, N., Mattinson, J. M., Corfu, F., Dörr, W., Kamo, S. L., Kennedy, A. K., Kronz, A., Reiners, P. W., Frei, D., Košler, J., Wan, Y., Götze, J., Häger, T., Kröner, A. and Valley, J. W., 2008. Zircon M257 – a homogeneous natural reference material for the ion microprobe U-Pb analysis of zircon. Geostandards and Geoanalytical Research, 32, 247–265.

Rowe, C. D., Backeberg, N. R., Van Rensburg, T., MacLennan, S. A., Faber, C., Curtis, C. and Viglietti, P. A., 2010. Structural geology of Robben Island: implications for the tectonic environment of Saldanian deformation. South African Journal of Geology 113, 57–72.

Rozendaal, A., Gresse, P. G., Scheepers, R., De Beer, C. H., 1994. Structural setting of the Riviera W–Mo deposit, Western Cape, South Africa. South African Journal of Geology, 97, 184–195.

Rozendaal, A., Gresse, P. G., Scheepers, R. and Le Roux, J.P., 1999. Neoproterozoic to Early Cambrian Crustal Evolution of the Pan-African Saldania Belt, South Africa. Precambrian Research, 97, 303-323.

Scheepers, R., 1995. Geology, Geochemistry and petrogenesis of late Precambrian S, I and A-type granitoids in the Saldania Mobile Belt, South-western Cape Province. Journal of African Earth Science, 21, 35-58.

Scheepers, R. and Armstrong, R., 2002. New U-Pb SHRIMP zircon ages of the Cape Granite Suite: implications for the magmatic evolution of the Saldania Belt. South African Journal of Geology, 105 (3), 241-256.

Scheepers, R. and Nortjé, A. N., 2000. Rhyolitic Ignimbrites of the Cape Granite Suite, south-western Cape Province, South Africa. Journal of African Earth Sciences, 31, 647-656.

Scheepers, R. and Poujol, M., 2002. U-Pb zircon age of Cape Granite Suite ignimbrites: characteristics of the last phases of the Saldanian magmatism. South African Journal of Geology, 105 (2), 163-178.

Scheepers, R. and Rozendaal, A., 1992. Relationship of the Riviera W (Mo Cu) deposit to magmatism in the south-western Cape Province, South Africa. Geocongress 1992 Abstracts, 339-341.

Schoch, A. E. and Burger, A. J., 1976. U-Pb ages of the Saldanha Quartz Porphyry. Transactions of the Geological Society of South Africa, 79, 239-241.

Scholtz, D. L., 1946. On the younger pre-Cambrian granite plutons of the Cape Province. Geological Society of South Africa Transactions and Proceedings, 49, 35-82.

Sláma, J., Košler, J., Condon, D. J., Crowley, J. L., Gerdes, A., Hanchar, J. M., Horstwood, M. S. A., Morris, G. A., Nasdala, L., Norberg, N., Schaltegger, U., Schoene, B., Tubrett, M. N. and Whitehouse, M. J., 2008. Plešovice zircon - a new natural reference material for U–Pb and Hf isotopic microanalysis. Chemical Geology, 249, 1-35.

Stacey, J. S. and Kramers, J. D., 1975. Approximation of Terrestrial Lead Isotope Evolution by a 2-Stage Model. Earth and Planetary Science Letters, 26 (2), 207-221.

Tanaka, T., Togashi, S., Kamioka, H., Amakawa, H., Kagami, H., Hamamoto, T., Yuhara, M., Orihashi, Y., Yoneda, S., Shimizu, H., Kunimaru, T., Takahashi, K., Yanagi, T., Nakano, T., Fujimaki, H., Shinjo, R., Asahara, Y., Tanimizu, M., Dragusanu, C., 2000. JNdi-1: a neodymium isotopic reference in consistency with LaJolla neodymium. Chemical Geology, 168, 279-281.

Villaros, A., Buick, I. S. and Stevens, G., 2012. Isotopic variations in S-type granites: an inheritance from a hetrogeneous source? Contribution Mineral Petrol, 163, 243-257.

7 APPENDICES

7.1 Electronic Appendix EA1- Geochemical data of the Ignimbrites from the Postberg Centre in the Saldanha Bay Volcanic Complex.

Table 9: EA1.1 - Bulk-rock analytical data for the Saldanha Ignimbrite form the Postberg eruption centre

Sample	Abbr.	latitude S	longitude E	ht ASL	SiO_2	TiO_2	Al_2O_3	FeO	MnO	MgO	CaO	Na_2O	K_2O	P_2O_5	FM	Mg#	ASI	V	Cr	Ni	Cu	Zn	Rb	Sr	Y	Zr	Nb	Mo	Cs	Ba	Hf	Ta	Pb	Th	U	La	Ce	Pr	Nd	Sm	Eu	Gd	Tb	Dy	Ho	Er	Tm	Yb	Lu
		(deg min sec)	(deg min sec)	(m)																																													
A35	PC-SI				74.18	0.26	14.20	1.97	0.03	0.23	1.13	1.99	5.88	0.12	2.23	17.03	1.24	11	7	2		40	238	86	41	176	15			717			33	19	3.0																
* major and minor oxides normalised to 100 wt% volatile-free and with all Fe expressed as FeO^T; trace elements in ppm by wt																																																	
Mg# =100 × mol. Mg / (Mg + Fe)																																																	
ASI = mol. Al_2O_3 / (CaO - 3.33P_2O_5 + Na_2O + K_2O)																																																	

Table 10: EA1.2 - Bulk-rock analytical data for the Jacob's Bay Ignimbrite from the Postberg eruption centre

Sample	Abbr.	latitude S	longitude E	ht ASL	SiO_2	TiO_2	Al_2O_3	FeO	MnO	MgO	CaO	Na_2O	K_2O	P_2O_5	FM	Mg#	ASI	V	Cr	Ni	Cu	Zn	Rb	Sr	Y	Zr	Nb	Mo	Cs	Ba	Hf	Ta	Pb	Th	U	La	Ce	Pr	Nd	Sm	Eu	Gd	Tb	Dy	Ho	Er	Tm	Yb	Lu
		(deg min sec)	(deg min sec)	(m)																																														
A33	PC-JI				71.91	0.40	14.89	2.78	0.05	0.41	1.64	2.21	5.56	0.16	3.24	21.00	1.22	22	9	2.0		53	217	124	48	290	19			943			36	26	3.0																	
A34	PC-JI				69.92	0.48	15.61	3.34	0.05	0.52	2.03	2.39	5.48	0.17	3.92	21.86	1.19	31	11	7.0		60	198	141	52	380	21			1074			34	31	4.0																	
MM01	PC-JI	33 08 43	17 59 34	2	73.55	0.33	13.85	2.35	0.04	0.37	0.77	2.61	6.00	0.14	2.76	21.79	1.17	22.80	87.00	15.05	13.50	63.00	219.65	93.90	39.65	235.90	21.95	5.46	6.35	808.50	6.86	1.37	34.75	19.39	3.72	48.15	101.65	11.77	44.90	8.95	1.36	7.91	1.23	7.14	1.43	4.23	0.65	3.59	0.59
MM02	PC-JI	33 08 54	18 00 06	1	73.38	0.35	13.68	2.47	0.04	0.37	1.42	2.63	5.52	0.14	2.88	20.90	1.09	29.70	144.15	15.10	14.90	60.65	204.55	94.80	39.70	257.45	21.25	10.25	8.63	719.00	7.41	1.29	32.25	19.05	5.43	48.40	103.30	11.59	42.60	8.30	1.51	7.51	1.28	7.56	1.55	4.11	0.55	4.23	0.52
MM03	PC-JI	33 08 02	17 58 20	5	72.20	0.36	14.28	2.61	0.04	0.43	1.52	2.72	5.70	0.14	3.08	22.66	1.09	35.90	213.20	11.85	16.05	56.60	196.95	121.25	41.65	260.00	20.40	13.90	6.44	896.50	7.24	1.41	32.50	22.23	3.93	56.65	117.85	13.68	50.80	9.85	1.76	8.80	1.46	8.10	1.62	4.77	0.53	3.92	0.55
* major and minor oxides normalised to 100 wt% volatile-free and with all Fe expressed as FeO^T; trace elements in ppm by wt																																																
Mg# =100 × mol. Mg / (Mg + Fe)																																																
ASI = mol. Al_2O_3 / (CaO - 3.33P_2O_5 + Na_2O + K_2O)																																															

Table 11: EA1.3 - Bulk-rock analytical data for the Plankiesbaai Ignimbrite from the Postberg eruption centre

Sample	Abbr.	latitude S	longitude E	ht ASL	SiO_2	TiO_2	Al_2O_3	FeO	MnO	MgO	CaO	Na_2O	K_2O	P_2O_5	FM	Mg#	ASI	V	Cr	Ni	Cu	Zn	Rb	Sr	Y	Zr	Nb	Mo	Cs	Ba	Hf	Ta	Pb	Th	U	La	Ce	Pr	Nd	Sm	Eu	Gd	Tb	Dy	Ho	Er	Tm	Yb	Lu
		(deg min sec)	(deg min sec)	(m)																																														
A7	PC-Pl				77.73	0.16	12.50	1.41	0.01	0.10	0.42	2.15	5.38	0.13	1.52	11.53	1.27	5	3	2		32	271	51	43	114	13			322			29	17	5																	
A8	PC-Pl				78.48	0.17	12.04	1.46	0.02	0.11	0.41	1.75	5.45	0.10	1.59	12.19	1.30	5	3	2		27	279	49	39	111	13			340			30	15	4																	
A9	PC-Pl				77.81	0.16	12.30	1.43	0.02	0.11	0.62	2.08	5.27	0.18	1.56	12.32	1.25	6	3	2		32	275	63	45	113	14			320			31	17	4																	
A10	PC-Pl				78.03	0.17	12.66	1.25	0.01	0.10	0.38	1.82	5.45	0.12	1.36	12.79	1.36	6	4	2		26	296	63	42	117	15			238			29	13	1																	
A11	PC-Pl				77.46	0.16	12.59	1.50	0.02	0.10	0.69	2.01	5.34	0.11	1.62	10.89	1.25	4	7	2		38	293	42	49	116	15			266			30	18	6																	
A12	PC-Pl				77.60	0.17	12.64	1.48	0.02	0.09	0.60	1.89	5.38	0.12	1.59	10.08	1.30	3	6	2		38	288	45	48	115	15			270			29	17	5																	
A13	PC-Pl				78.23	0.18	12.28	1.47	0.01	0.08	0.37	1.87	5.37	0.13	1.56	9.11	1.33	4	3	2		27	296	48	46	122	16			255			29	17	6																	
A14	PC-Pl				77.65	0.16	12.55	1.53	0.02	0.12	0.62	1.91	5.29	0.13	1.67	12.59	1.30	3	3	2		41	285	55	50	115	15			272			29	16	6																	
A15	PC-Pl				76.58	0.18	13.12	1.74	0.02	0.12	0.59	1.70	5.66	0.29	1.89	11.28	1.41	4	12	15		35	327	61	55	129	17			245			30	18	8																	
A16	PC-Pl				76.77	0.17	13.10	1.66	0.03	0.12	0.70	1.83	5.48	0.12	1.82	11.66	1.32	5	5	2		45	316	38	54	126	17			261			30	17	8																	
A18	PC-Pl				77.14	0.16	12.70	1.69	0.03	0.10	0.67	2.04	5.34	0.12	1.82	9.81	1.26	5	12	2		42	296	40	51	123	16			250			30	17	7																	
A19	PC-Pl				76.09	0.19	13.34	1.71	0.02	0.13	0.60	2.16	5.62	0.14	1.86	12.27	1.29	6	3	2		39	332	42	54	123	17			227			31	19	9																	
A21	PC-Pl				76.94	0.19	13.04	1.72	0.01	0.11	0.32	2.06	5.49	0.12	1.84	10.54	1.36	7	3	2		24	293	49	46	125	17			255			32	18	5																	
A22	PC-Pl				76.79	0.17	13.10	1.63	0.03	0.11	0.59	1.91	5.54	0.12	1.77	10.90	1.32	4	4	2		38	310	43	51	118	16			272			30	17	7																	
A23	PC-Pl				78.63	0.18	12.11	1.34	0.01	0.09	0.44	1.75	5.33	0.11	1.45	10.95	1.32	6	3	2		32	273	55	41	116	14			332			30	14	4																	
A24	PC-Pl				78.46	0.16	12.25	1.28	0.02	0.09	0.58	1.78	5.24	0.13	1.39	11.51	1.31	6	9	2		34	269	65	46	109	13			301			29	16	5																	
A25	PC-Pl				77.89	0.17	12.30	1.51	0.03	0.10	0.75	1.91	5.21	0.11	1.65	10.83	1.24	5	7	2		36	265	48	44	108	13			310			30	17	6																	
A26	PC-Pl				78.24	0.17	12.27	1.42	0.02	0.10	0.66	1.79	5.22	0.10	1.54	11.53	1.28	5	11	2		36	258	51	45	115	13			308			29	16	5																	
A27	PC-Pl				78.06	0.16	12.13	1.48	0.03	0.11	0.72	2.05	5.15	0.10	1.63	11.92	1.21	3	9	2		36	262	49	44	115	12			331			29	14	6																	
A28	PC-Pl				77.95	0.16	12.26	1.52	0.04	0.10	0.72	1.94	5.20	0.10	1.66	10.72	1.24	6	5	2		36	263	48	43	112	13			325			29	14	5																	
A29	PC-Pl				77.86	0.17	12.41	1.51	0.03	0.11	0.73	1.82	5.26	0.10	1.66	11.85	1.27	5	8	2		37	270	46	45	114	13			309			32	17	7																	
A30	PC-Pl				76.49	0.16	13.03	1.66	0.03	0.11	0.66	2.30	5.43	0.12	1.81	10.80	1.23	5	11	2		47	316	36	54	122	16			209			30	18	8																	
A31	PC-Pl				76.42	0.16	13.18	1.57	0.02	0.10	0.68	2.25	5.50	0.12	1.69	10.49	1.24	4	3	2		42	323	33	57	119	17			205			27	16	7																	
A32	PC-Pl				76.99	0.17	12.67	1.64	0.03	0.12	0.72	2.25	5.29	0.11	1.79	11.84	1.21	7	5	2		41	293	41	50	115	15			270			31	17	8																	
A36	PC-Pl				77.00	0.18	12.65	1.77	0.06	0.13	0.74	1.96	5.39	0.11	1.97	11.88	1.25	7	7	5		36	271	49	47	118	14			339			30	16	7																	
A38	PC-Pl				78.29	0.15	12.19	1.47	0.02	0.11	0.60	1.72	5.34	0.10	1.60	11.98	1.29	4	4	2		33	266	49	43	110	14			328			30	16	6																	
A39	PC-Pl				77.44	0.17	12.57	1.55	0.03	0.11	0.77	1.87	5.37	0.11	1.69	11.48	1.26	6	7	2		41	267	52	45	122	14			341			30	15	6																	
A40	PC-Pl				78.32	0.15	12.23	1.45	0.02	0.07	0.71	1.64	5.29	0.10	1.54	8.07	1.29	5	4	2		32	266	48	44	110	13			318			30	16	6																	

* major and minor oxides normalised to 100 wt% volatile-free and with all Fe expressed as FeO^T; trace elements in ppm by wt

Mg# =100 × mol. Mg / (Mg + Fe)

ASI = mol. Al_2O_3 / (CaO - 3.33P_2O_5 + Na_2O + K_2O)

Table 12: EA1.4 - Bulk-rock analytical data for the Tsaarsbank Ignimbrite from the Postberg eruption centre

Sample	Abbr.	latitude S	longitude E	ht ASL	SiO_2	TiO_2	Al_2O_3	FeO	MnO	MgO	CaO	Na_2O	K_2O	P_2O_5	FM	Mg#	ASI	V	Cr	Ni	Cu	Zn	Rb	Sr	Y	Zr	Nb	Mo	Cs	Ba	Hf	Ta	Pb	Th	U	La	Ce	Pr	Nd	Sm	Eu	Gd	Tb	Dy	Ho	Er	Tm	Yb	Lu
		(deg min sec)	(deg min sec)	(m)																																													
A1	PC-TI				75.22	0.18	13.47	1.57	0.03	0.19	0.76	2.62	5.83	0.12	1.79	17.87	1.15						332	42	62	123	18			271				18	8																	
A2	PC-TI				74.91	0.17	13.68	1.64	0.02	0.19	0.67	2.86	5.73	0.12	1.86	17.13	1.15						313	43	64	136	20			261				20	8																	
A3	PC-TI				75.11	0.17	13.50	1.77	0.04	0.18	0.74	2.71	5.64	0.13	1.99	15.39	1.16						318	37	61	129	19			229				19	9																	
A4	PC-TI				76.99	0.17	12.40	1.57	0.03	0.17	0.79	2.54	5.24	0.10	1.77	16.29	1.12						270	51	44	127	15			356				16	6																	
A5	PC-TI				76.94	0.18	12.48	1.61	0.03	0.18	0.78	2.35	5.27	0.16	1.83	16.84	1.18						260	52	45	134	14			344				16	6																	
A6	PC-TI				78.03	0.16	11.94	1.35	0.02	0.13	0.37	2.46	5.41	0.12	1.51	14.90	1.16	4	3	2		31	284	43	42	116	14			307			30	15	6																	
A20	PC-TI				77.47	0.19	12.74	1.46	0.01	0.14	0.69	1.83	5.36	0.11	1.61	15.01	1.30	7	3	5		37	275	58	45	130	15			357			31	18	8																	
A37	PC-TI				79.04	0.16	12.53	0.51	0.01	0.05	0.34	1.86	5.42	0.08	0.57	15.26	1.34	8	9	4		15	248	70	53	115	14			396			31	17	4																	
Pos1	PC-TI	33 06 20	18 00 14	148	77.11	0.17	12.48	1.41	0.02	0.15	0.57	2.48	5.50	0.11	1.58	16.08	1.16	7.3	20	6.7	13	33	247	47	42	129	14	1.4	12	332	3.7	1.3	23	14	4.1	23	49	5.9	22	5.7	0.72	6.8	1.1	7.4	1.5	4.4	0.60	4.2	0.59
Pos2	PC-TI	33 07 53	17 58 22	0	75.09	0.18	13.34	1.76	0.05	0.18	0.77	2.70	5.80	0.13	1.99	15.52	1.13	7.6	12	11	19	41	297	41	50	126	16	2.3	13	282	4.2	1.6	25	15	7.5	24	51	6.1	24	6.2	0.64	6.4	1.3	8.4	1.7	4.9	0.71	4.6	0.70
LQP1	PC-TI				75.22	0.18	13.47	1.57	0.03	0.19	0.76	2.62	5.83	0.12	1.79	17.87	1.15						332	42	62	123	18			271						12	51		23											
LQP2	PC-TI				74.91	0.17	13.68	1.64	0.02	0.19	0.67	2.86	5.73	0.12	1.86	17.14	1.15						313	43	64	136	20			261						16	45		26											
LQP3	PC-TI				75.11	0.17	13.50	1.77	0.04	0.18	0.74	2.71	5.64	0.13	1.99	15.39	1.16						318	37	61	129	19			229						13	47		21											
LQP4	PC-TI				77.01	0.17	12.40	1.57	0.03	0.17	0.77	2.54	5.24	0.10	1.77	16.30	1.13						270	51	44	127	15			356						26	59	6.94	25	6.19	0.82	5.8	1.1	7.2	1.5	4.0	0.6	4.0	0.58
LQP6	PC-TI				76.78	0.18	12.46	1.61	0.03	0.18	0.78	2.55	5.26	0.16	1.82	16.85	1.14						260	52	45	134	14			344						27	61	7.17	26	6.34	0.82	6.2	1.1	6.9	1.3	3.9	0.6	3.9	0.55
* major and minor oxides normalised to 100 wt% volatile-free and with all Fe expressed as FeO^T; trace elements in ppm by wt																																																
Mg# =100 × mol. Mg / (Mg + Fe)																																																
ASI = mol. Al_2O_3 / (CaO - 3.33P_2O_5 + Na_2O + K_2O)																																																

Table 13: EA1.5 - Control standards used for the calibration procedure for major oxide chemical analysis

Electronic Appendix EA1, Table EA1.5 Control standards used for the calabration procedure for Major Oxide chemical analysis

Sample name		Al2O3	CaO	Cr2O3	Fe2O3	K2O	MgO	MnO	Na2O	P2O5	SiO2	TiO2	L.O.I.	Sum Of Conc.
BHVO-1														
Basalt Reference values		**13.71**	**11.39**	**0.04**	**12.36**	**0.54**	**7.22**	**0.17**	**2.31**	**0.27**	**49.82**	**2.73**	**0.52**	**101.08**
BHVO-1	MajorBasic32+Zn	13.64	11.29	0.03	12.31	0.52	7.13	0.17	2.23	0.27	49.38	2.72	0.52	100.21
BHVO-1 std	MajorBasic32+Zn	13.75	11.40	0.04	12.28	0.52	7.20	0.17	2.22	0.27	49.94	2.73	0.52	101.04
MONITOR BHVO-1	MajorBasic32+Zn	13.79	11.40	0.04	12.29	0.52	7.24	0.17	2.24	0.28	49.89	2.74	0.52	101.12
MONITOR BHVO-1	Majors Acid32	13.49	11.57	0.02	12.36	0.52	7.19	0.17	2.18	0.27	50.36	2.92	0.52	101.57
BHVO-1 MONITOR	Majors Acid32	13.48	11.49	0.02	12.34	0.52	7.17	0.17	2.14	0.27	50.11	2.91	0.52	101.14
BHVO-1 MONITOR	MajorBasic32+Zn	13.75	11.40	0.04	12.26	0.52	7.16	0.17	2.25	0.27	50.00	2.74	0.52	101.08
BHVO-1 MONITOR	Majors Acid32	13.55	11.47	0.02	12.36	0.53	7.18	0.17	2.15	0.28	50.14	2.90	0.52	101.27
MONITOR BHVO-1	MajorBasic32+Zn	13.74	11.42	0.04	12.27	0.53	7.19	0.16	2.20	0.27	49.86	2.74	0.52	100.94
MONITOR BHVO-1	MajorBasic32+Zn	13.72	11.41	0.04	12.30	0.52	7.12	0.17	2.21	0.28	49.95	2.74	0.52	100.98
MONITOR BHVO-1	Majors Acid32	13.48	11.52	0.02	12.35	0.53	7.16	0.17	2.14	0.28	50.46	2.89	0.52	101.52
MONITOR BHVO-1	MajorBasic32+Zn	13.71	11.40	0.04	12.27	0.53	7.19	0.17	2.22	0.28	49.91	2.73	0.52	100.97
MONITOR bhvo-1	MajorBasic32+Zn	13.71	11.39	0.04	12.26	0.52	7.20	0.16	2.28	0.28	50.03	2.73	0.52	101.12
MONITOR BHVO-1	MajorBasic32+Zn	13.73	11.45	0.03	12.33	0.52	7.21	0.17	2.23	0.28	50.12	2.74	0.52	101.33
MONITOR BHVO-1	Majors Acid32	13.44	11.51	0.02	12.35	0.52	7.21	0.17	2.15	0.28	50.25	2.91	0.52	101.33
MONITOR BHVO-1	MajorBasic32+Zn	13.72	11.44	0.04	12.29	0.52	7.15	0.17	2.29	0.27	50.02	2.75	0.52	101.18
MONITOR BHVO-1	MajorBasic32+Zn	13.74	11.42	0.04	12.27	0.52	7.18	0.17	2.21	0.28	50.17	2.73	0.52	101.25
MONITOR bhvo-1	MajorBasic32+Zn	13.78	11.40	0.04	12.32	0.52	7.17	0.17	2.24	0.28	50.29	2.72	0.52	101.45
MONITOR BHVO-1	MajorBasic32+Zn	13.68	11.30	0.04	12.27	0.52	7.15	0.17	1.73	0.27	50.12	2.73	0.52	100.50
MONITOR BHVO-1	MajorBasic32+Zn	13.71	11.40	0.04	12.25	0.53	7.24	0.17	2.24	0.27	49.84	2.73	0.52	100.94
MONITOR bhvo-1	MajorBasic32+Zn	13.81	11.37	0.04	12.27	0.52	7.16	0.17	2.22	0.29	50.09	2.73	0.52	101.19
MONITOR bhvo-1	Majors Acid32	13.55	11.51	0.02	12.33	0.53	7.17	0.17	2.13	0.28	50.18	2.90	0.52	101.29
MONITOR bhvo-1	MajorBasic32+Zn	13.82	11.39	0.04	12.27	0.52	7.19	0.16	2.25	0.28	49.99	2.73	0.52	101.16
MONITOR bhvo-1	Majors Acid32	13.46	11.49	0.02	12.36	0.52	7.20	0.17	2.15	0.28	50.26	2.91	0.52	101.34
MONITOR BHVO-1	MajorBasic32+Zn	13.76	11.42	0.04	12.30	0.52	7.17	0.17	2.23	0.27	50.15	2.75	0.52	101.30
MONITOR BHVO-1	Majors Acid32	13.54	11.50	0.02	12.36	0.53	7.20	0.18	2.15	0.28	50.45	2.91	0.52	101.64
MONITOR BHVO-1	Majors Acid32	13.55	11.49	0.02	12.37	0.53	7.20	0.18	2.19	0.28	50.44	2.90	0.52	101.67
MONITOR BHVO-1	MajorBasic32+Zn	13.67	11.50	0.04	12.30	0.52	7.17	0.17	2.23	0.28	50.18	2.74	0.52	101.32
MONITOR BHVO-1	Majors Acid32	13.48	11.48	0.02	12.35	0.52	7.17	0.17	2.15	0.29	50.39	2.89	0.52	101.43
MONITOR BHVO-1	MajorBasic32+Zn	13.61	11.47	0.03	12.29	0.51	7.18	0.17	2.20	0.28	50.17	2.75	0.52	101.18
MONITOR BHVO-1	MajorBasic32+Zn	13.77	11.46	0.04	12.26	0.51	7.17	0.17	2.27	0.27	49.90	2.72	0.52	101.06
MONITOR BHVO-1	MajorBasic32+Zn	13.69	11.44	0.03	12.30	0.51	7.11	0.17	2.24	0.27	50.10	2.73	0.52	101.11
MONITOR BHV01	MajorBasic32+Zn	13.70	11.52	0.04	12.27	0.52	7.20	0.17	2.24	0.28	50.15	2.76	0.52	101.37
MONITOR bhvo-1	Majors Acid32	13.41	11.50	0.02	12.35	0.52	7.16	0.17	2.05	0.28	50.18	2.90	0.52	101.06
MONITOR BHVO-1	MajorBasic32+Zn	13.73	11.48	0.04	12.31	0.53	7.17	0.18	2.23	0.28	50.00	2.74	0.52	101.21
MONITOR BHVO-1	Majors Acid32	13.44	11.55	0.02	12.36	0.52	7.19	0.17	2.16	0.28	50.48	2.89	0.52	101.58
Average		13.63	11.43		12.32	0.52	7.19	0.17	2.20	0.27	49.94	2.80	0.52	101.02
Relative standard deviation (%)		0.58	0.35		0.36	3.70	0.47	0.00	4.68	0.74	0.23	2.71		0.06

PANalytical

Results quantitative - MajorBasic32+Zn

Major element analysis by XRF, Rh Tube, 3kWatt

BDL = Below Detection Limit

Note: LOI = weight loss or gain at 1000ºC.

LOI (loss on ignition) includes the total of volatiles content of the rock (including the water combined to the lattice of silicate minerals) and the gain on ignition related to the oxidation of the rock (mostly due to Fe).

Concentration in %. LOI: loss on ignition

Table 13: EA1.5 continued - Control standards used for the calibration procedure for Major Oxide chemical analysis

Sample name		Al2O3	CaO	Cr2O3	Fe2O3	K2O	MgO	MnO	Na2O	P2O5	SiO2	TiO2	L.O.I.	Sum Of Conc.
JG-1														
Granodiorite Reference values		14.20	2.18	0.01	2.14	3.97	0.74	0.06	3.39	0.10	72.30	0.26		99.35
JG-1 STD	Majors Interm32	14.14	2.17	0.01	2.12	4.01	0.73	0.07	3.35	0.10	72.95	0.25		99.90
STANDARD JG-1	Majors Acid32	14.34	2.19	0.01	2.12	4.02	0.78	0.07	3.60	0.10	72.13	0.27		99.63
JG-1 std	Majors Acid32	14.44	2.20	0.01	2.14	4.03	0.77	0.07	3.63	0.10	72.80	0.26		100.45
JG-1 std	Majors Acid32	14.37	2.20	0.01	2.13	4.02	0.78	0.07	3.56	0.09	72.72	0.26		100.21
JG-1 STD	Majors Acid32	14.45	2.21	0.01	2.12	4.02	0.77	0.06	3.68	0.10	72.48	0.26		100.16
JG-1 STD	Majors Acid32	14.36	2.21	0.01	2.13	4.03	0.77	0.07	3.67	0.10	72.57	0.27		100.19
JG-1 std	Majors Acid32	14.37	2.21	0.01	2.13	4.02	0.79	0.07	3.66	0.10	72.18	0.26		99.80
JG-1 STD	Majors Acid32	14.34	2.21	0.01	2.13	4.03	0.78	0.06	3.61	0.10	72.19	0.27		99.73
JG-1 std	Majors Acid32	14.13	2.21	0.01	2.13	4.02	0.75	0.07	3.43	0.09	72.03	0.26		99.13
J-G std	Majors Acid32	14.12	2.21	0.01	2.13	3.98	0.75	0.07	3.42	0.10	71.98	0.26		99.03
JG-1 STD	Majors Acid32	14.03	2.20	0.01	2.13	4.00	0.77	0.06	3.46	0.10	71.95	0.26		98.97
JG-1 STD	Majors Acid32	14.11	2.21	0.01	2.13	4.00	0.76	0.07	3.42	0.10	72.13	0.26		99.20
JG-1 STD	Majors Acid32	14.00	2.21	0.01	2.13	3.99	0.75	0.07	3.44	0.10	72.02	0.26		98.98
JG-1 std	Majors Acid32	14.06	2.21	0.01	2.13	4.01	0.76	0.07	3.43	0.10	72.05	0.26		99.09
JG-1 STD	Majors Acid32	14.00	2.20	0.01	2.13	4.01	0.77	0.07	3.44	0.10	71.81	0.26		98.80
JG-1 STD	Majors Acid32	13.99	2.20	0.01	2.13	4.00	0.78	0.06	3.39	0.10	71.98	0.26		98.90
JG-1 std	Majors Acid32	14.04	2.19	0.01	2.13	3.99	0.76	0.07	3.36	0.10	71.80	0.26		98.71
JG-1 std	Majors Acid32	13.98	2.20	0.01	2.13	4.01	0.74	0.07	3.41	0.10	71.66	0.26		98.57
JG-1 std	Majors Acid32	13.95	2.20	0.01	2.13	4.02	0.76	0.07	3.38	0.10	71.97	0.26		98.85
JG-1 std	Majors Acid32	14.01	2.20	0.01	2.13	4.00	0.74	0.06	3.42	0.10	71.88	0.26		98.81
JG-1 STD	Majors Acid32	14.01	2.19	0.01	2.12	3.98	0.75	0.07	3.43	0.10	71.72	0.26		98.64
JG-1 STD	Majors Acid32	14.01	2.20	0.01	2.13	3.99	0.75	0.07	3.39	0.10	71.96	0.26		98.87
JG-1 STD	Majors Acid32	13.94	2.17	0.01	2.12	4.00	0.73	0.07	3.24	0.09	71.76	0.26		98.39
JG-1 STD	Majors Acid32	13.83	2.17	0.01	2.12	3.98	0.74	0.07	3.25	0.10	71.65	0.25		98.17
JG-1 std	Majors Acid32	13.79	2.18	0.01	2.13	3.98	0.73	0.07	3.20	0.10	71.63	0.26		98.08
JG-1 STD	Majors Acid32	13.85	2.19	0.01	2.13	3.98	0.74	0.07	3.29	0.10	71.69	0.26		98.31
Average		14.10	2.20	0.01	2.13	4.00	0.76	0.07	3.44	0.10	72.07	0.26	#DIV/0!	99.14
Relative standard deviation (%)		0.69	0.81	6.38	0.56	0.87	2.39	8.06	1.61	1.90	0.33	0.15		0.21

Table 13: EA1.5 continued - Control standards used for the calibration procedure for Major Oxide chemical analysis

Sample name		Al2O3	CaO	Cr2O3	Fe2O3	K2O	MgO	MnO	Na2O	P2O5	SiO2	TiO2	L.O.I.	Sum Of Conc.
NIM-G														
Granite Reference values		**12.08**	**0.78**	**0.00**	**2.02**	**4.99**	**0.06**	**0.02**	**3.36**	**0.01**	**75.70**	**0.09**		**99.11**
NIM-G STD	Majors Acid32	12.26	0.82	0.00	1.99	5.01	0.08	0.02	3.41	0.01	75.76	0.10		99.46
NIM-G STD	Majors Acid32	12.20	0.82	0.00	1.99	5.01	0.07	0.02	3.37	0.02	75.85	0.09		99.44
NIM-G STD	Majors Acid32	12.25	0.81	0.00	1.98	5.01	0.07	0.02	3.38	0.01	75.70	0.10		99.33
STANDARD Nim-G	Majors Acid32	12.26	0.80	0.00	1.98	4.98	0.08	0.02	3.37	0.01	75.43	0.10		99.03
NIM-G std	Majors Acid32	12.30	0.81	0.00	1.99	5.01	0.07	0.02	3.35	0.01	76.31	0.09		99.96
NIM-G std	Majors Acid32	12.27	0.81	0.00	1.98	5.01	0.07	0.02	3.34	0.01	75.97	0.09		99.57
NIM-G STD	Majors Acid32	12.18	0.81	0.00	1.98	4.98	0.07	0.02	3.36	0.01	76.02	0.10		99.53
NIM-G STD	Majors Acid32	12.14	0.81	0.00	1.98	4.99	0.07	0.02	3.40	0.02	75.74	0.10		99.27
NIM-G std	Majors Acid32	12.16	0.80	0.00	1.99	5.02	0.07	0.02	3.39	0.01	75.77	0.10		99.33
NIM-G STD	Majors Acid32	12.17	0.81	0.00	1.99	5.00	0.07	0.02	3.34	0.02	75.41	0.10		98.93
NIM-G std	Majors Acid32	11.94	0.82	0.00	1.99	4.97	0.07	0.02	3.22	0.01	75.43	0.09		98.56
NIM-G std	Majors Acid32	12.00	0.81	0.00	1.98	4.96	0.07	0.02	3.20	0.01	75.50	0.08		98.63
NIM-G STD	Majors Acid32	11.93	0.80	0.00	1.98	4.97	0.07	0.02	3.19	0.02	75.41	0.08		98.47
NIM-G STD	Majors Acid32	12.03	0.81	0.00	1.99	4.97	0.07	0.02	3.20	0.02	75.17	0.08		98.36
NIM-G STD	Majors Acid32	12.03	0.81	0.00	1.99	4.99	0.07	0.02	3.19	0.02	75.38	0.08		98.58
NIM-G std	Majors Acid32	11.96	0.81	0.00	1.99	4.97	0.06	0.02	3.20	0.01	75.46	0.08		98.56
NIM-G STD	Majors Acid32	12.01	0.81	0.00	1.99	4.97	0.07	0.02	3.22	0.02	75.23	0.08		98.42
NIM-G STD	Majors Acid32	11.96	0.81	0.00	1.98	4.98	0.07	0.02	3.18	0.02	75.29	0.08		98.39
NIM-G std	Majors Acid32	11.96	0.80	0.00	1.99	4.99	0.07	0.02	3.15	0.01	75.34	0.08		98.41
NIM-G std	Majors Acid32	11.90	0.80	0.00	1.99	4.98	0.07	0.02	3.16	0.02	75.13	0.08		98.15
NIM-G std	Majors Acid32	11.95	0.81	0.00	1.99	4.98	0.07	0.02	3.21	0.02	75.20	0.08		98.33
NIM-G std	Majors Acid32	11.91	0.81	0.00	1.98	4.99	0.07	0.02	3.17	0.02	75.15	0.08		98.20
NIM-G STD	Majors Acid32	11.88	0.81	0.00	1.98	4.98	0.07	0.02	3.17	0.02	75.44	0.09		98.46
NIM-G STD	Majors Acid32	11.95	0.81	0.00	1.99	4.97	0.07	0.02	3.19	0.02	75.39	0.08		98.49
Average		12.07	0.81	0.00	1.99	4.99	0.07	0.02	3.27	0.02	75.52	0.09	#DIV/0!	98.83
Relative standard deviation (%)		0.11	3.74	100.00	1.69	0.06	17.36	0.00	2.83	54.17	0.24	2.31		0.29

Table 13: EA1.5 continued - Control standards used for the calibration procedure for Major Oxide chemical analysis

Sample name		Al2O3	CaO	Cr2O3	Fe2O3	K2O	MgO	MnO	Na2O	P2O5	SiO2	TiO2	L.O.I.	Sum Of Conc.
Quality control for 2010-2011														
Average HUSG		**13.75**	**1.52**	**0.00**	**3.78**	**4.66**	**1.04**	**0.06**	**2.57**	**0.21**	**69.77**	**0.54**	**0.73**	**98.65**
STDEV		**0.20**	**0.04**	**0.00**	**0.14**	**0.06**	**0.04**	**0.01**	**0.18**	**0.01**	**0.54**	**0.02**	**0.05**	**0.71**
MIN		**13.04**	**1.48**	**0.00**	**3.64**	**4.55**	**0.94**	**0.05**	**2.30**	**0.20**	**68.42**	**0.52**	**0.53**	**97.23**
MAX		**14.30**	**1.63**	**0.01**	**4.56**	**4.80**	**1.22**	**0.08**	**3.30**	**0.23**	**70.96**	**0.60**	**0.80**	**100.40**
HUSG STD	Majors Acid32	13.87	1.58	0.00	3.75	4.68	1.11	0.06	2.74	0.22	70.73	0.56	0.90	100.20
HUSG STD	Majors Interm32	13.87	1.56	0.01	3.75	4.65	1.11	0.06	2.69	0.23	70.81	0.56	0.90	100.20
HUSG-1 std	Majors Acid32	13.84	1.57	0.00	3.74	4.67	1.11	0.05	2.73	0.22	70.51	0.56	0.90	99.90
HUSG-1 std	Majors Acid32	13.84	1.56	0.01	3.73	4.65	1.11	0.06	2.71	0.22	70.37	0.56	0.90	99.72
HUSG-1 STD	Majors Interm32	13.76	1.57	0.01	3.74	4.65	1.11	0.06	2.71	0.21	70.36	0.54	0.90	99.62
HUSG-1 std	Majors Acid32	13.69	1.58	0.01	3.75	4.68	1.11	0.06	2.64	0.22	70.63	0.56	0.90	99.83
HUS-G std	Majors Acid32	13.68	1.57	0.01	3.74	4.64	1.10	0.05	2.63	0.22	70.58	0.57	0.90	99.69
HUSG-1 STD	Majors Acid32	13.59	1.58	0.01	3.74	4.65	1.11	0.06	2.61	0.23	70.61	0.57	0.90	99.66
HUSG-1 STD	Majors Acid32	13.67	1.57	0.01	3.74	4.62	1.10	0.06	2.63	0.23	70.34	0.56	0.90	99.43
HUSG-1 STD	Majors Acid32	13.69	1.57	0.01	3.75	4.65	1.10	0.06	2.63	0.23	70.39	0.56	0.90	99.54
HUSG-1 std	Majors Acid32	13.69	1.57	0.01	3.76	4.65	1.10	0.06	2.61	0.22	70.41	0.57	0.90	99.55
HUSG-1 STD	Majors Acid32	13.75	1.57	0.00	3.75	4.65	1.08	0.06	2.62	0.22	70.41	0.57	0.90	99.58
HUS-G std	MajorBasic32+Zn	13.90	1.56	0.00	3.72	4.66	1.00	0.05	2.69	0.22	71.37	0.54	0.90	100.61
HUS-G STD	MajorBasic32+Zn	13.87	1.54	0.00	3.71	4.65	1.02	0.05	2.03	0.22	70.36	0.55	0.90	98.90
HUSG-1 STD	Majors Acid32	13.63	1.57	0.00	3.73	4.66	1.10	0.06	2.66	0.23	70.59	0.57	0.90	99.70
HUS-G std	Majors Acid32	13.67	1.55	0.00	3.73	4.64	1.09	0.06	2.60	0.22	70.60	0.58	0.90	99.64
HUSG-1 std	Majors Acid32	13.66	1.57	0.00	3.74	4.67	1.09	0.06	2.61	0.22	70.43	0.57	0.90	99.52
HUSG-1 std	Majors Acid32	13.65	1.57	0.00	3.74	4.67	1.10	0.06	2.61	0.22	70.48	0.56	0.90	99.56
HUSG-1 std	Majors Acid32	13.61	1.57	0.00	3.74	4.63	1.10	0.06	2.62	0.23	70.41	0.56	0.90	99.43
HUSG-1 STD	Majors Acid32	13.67	1.56	0.00	3.74	4.63	1.10	0.06	2.64	0.22	70.52	0.56	0.90	99.60
HUSG-1 STD	Majors Acid32	13.69	1.56	0.00	3.74	4.64	1.10	0.06	2.62	0.22	70.52	0.56	0.90	99.61
HUSG-1 STD	Majors Acid32	13.66	1.57	0.00	3.74	4.64	1.11	0.06	2.60	0.22	70.39	0.56	0.90	99.45
HUS-G STD	Majors Acid32	13.62	1.55	0.00	3.74	4.66	1.08	0.06	2.50	0.22	70.40	0.56	0.90	99.29
HUSG-1 STD	Majors Acid32	13.53	1.54	0.00	3.73	4.66	1.10	0.06	2.54	0.22	70.55	0.56	0.90	99.39
HUSG-1 std	Majors Acid32	13.53	1.55	0.00	3.73	4.63	1.08	0.06	2.47	0.22	70.52	0.56	0.90	99.25
HUSG-1 STD	Majors Acid32	13.63	1.58	0.00	3.75	4.64	1.11	0.05	2.60	0.23	70.63	0.56	0.90	99.68
Average		13.79	1.57	0.01	3.74	4.66	1.11	0.06	2.69	0.22	70.57	0.56	0.90	99.88
Relative standard deviation (%)		0.34	3.20	45.08	0.89	0.10	6.17	11.31	4.82	3.53	1.15	2.98	23.28	1.25

Table 13: EA1.5 continued - Control standards used for the calibration procedure for Major Oxide chemical analysis

Sample name		Al2O3	CaO	Cr2O3	Fe2O3	K2O	MgO	MnO	Na2O	P2O5	SiO2	TiO2	L.O.I.	Sum Of Conc.
WITS-G														
Granite Reference values		**11.53**	**1.51**		**3.58**	**4.46**	**0.10**	**0.05**	**2.97**	**0.04**	**74.53**	**0.29**	**0.08**	**99.14**
WITS-G		**11.73**	**1.44**		**3.43**	**4.29**	**0.21**	**0.03**	**2.39**	**0.05**	**74.26**	**0.29**	**0.07**	**98.19**
WITS-G (AUG)		**12.01**	**1.46**		**3.51**	**4.26**	**0.05**	**0.02**	**2.39**	**0.06**	**74.56**	**0.30**	**0.07**	**98.69**
WITS-G (OCT)		**11.52**	**1.47**		**3.47**	**4.33**	**0.00**	**0.05**	**2.37**	**0.03**	**73.57**	**0.28**	**0.07**	**97.14**
WITS-G (DEC)		**11.45**	**1.47**		**3.50**	**4.39**	**0.06**	**0.05**	**2.45**	**0.04**	**75.45**	**0.28**	**0.07**	**99.22**
Average reference value		**11.65**	**1.47**		**3.50**	**4.34**	**0.08**	**0.04**	**2.51**	**0.04**	**74.47**	**0.29**	**0.07**	**98.48**
WITS-G STD	Majors Acid32	11.77	1.50	0.00	3.46	4.43	0.09	0.05	2.68	0.04	75.13	0.31	0.07	**99.53**
WITS-G STD	Majors Interm32	11.79	1.48	0.00	3.46	4.42	0.08	0.05	2.62	0.03	75.57	0.30	0.07	**99.87**
WITS-G std	Majors Acid32	11.81	1.49	0.00	3.46	4.43	0.09	0.05	2.67	0.04	75.03	0.31	0.07	**99.45**
WITS-G std	Majors Acid32	11.80	1.49	0.00	3.46	4.43	0.08	0.05	2.64	0.04	74.89	0.31	0.07	**99.26**
WITS-G STD	Majors Interm32	11.69	1.47	0.01	3.45	4.41	0.08	0.05	2.61	0.03	75.04	0.30	0.07	**99.21**
WITS-G STD	Majors Acid32	11.73	1.49	0.00	3.45	4.43	0.08	0.05	2.68	0.04	74.92	0.31	0.07	**99.25**
WITS-G std	Majors Acid32	11.63	1.49	0.00	3.46	4.42	0.09	0.05	2.56	0.04	74.90	0.30	0.07	**99.01**
WITS-G STD	Majors Interm32	11.62	1.47	0.00	3.47	4.40	0.08	0.05	2.56	0.03	75.32	0.29	0.07	**99.36**
WITS-G std	Majors Acid32	11.62	1.49	0.00	3.47	4.42	0.10	0.05	2.54	0.04	75.13	0.30	0.07	**99.23**
WITS-G STD	Majors Acid32	11.55	1.48	0.00	3.45	4.41	0.09	0.05	2.55	0.03	75.03	0.30	0.07	**99.01**
WITS-G STD	Majors Acid32	11.59	1.49	0.00	3.46	4.41	0.09	0.05	2.54	0.04	74.99	0.30	0.07	**99.03**
WITS-G STD	Majors Acid32	11.64	1.48	0.00	3.47	4.41	0.10	0.05	2.62	0.04	75.02	0.30	0.07	**99.20**
WITS-G std	Majors Acid32	11.64	1.49	0.00	3.47	4.42	0.09	0.05	2.59	0.04	75.11	0.30	0.07	**99.27**
WITS-G STD	Majors Acid32	11.65	1.49	0.00	3.46	4.41	0.10	0.05	2.56	0.04	74.92	0.31	0.07	**99.06**
WITS-G STD	Majors Acid32	11.61	1.48	0.00	3.45	4.42	0.09	0.05	2.59	0.04	75.06	0.31	0.07	**99.17**
WITS-G std	Majors Acid32	11.70	1.48	0.00	3.46	4.40	0.10	0.05	2.56	0.04	75.21	0.30	0.07	**99.37**
WITS-G std	Majors Acid32	11.65	1.48	0.00	3.47	4.43	0.10	0.05	2.58	0.04	74.83	0.30	0.07	**99.00**
WITS-G std	Majors Acid32	11.63	1.49	0.00	3.47	4.44	0.09	0.05	2.60	0.04	75.14	0.31	0.07	**99.33**
WITS-G std	Majors Acid32	11.71	1.49	0.00	3.47	4.42	0.10	0.05	2.58	0.04	75.30	0.30	0.07	**99.53**
WITS-G STD	Majors Acid32	11.62	1.47	0.00	3.46	4.43	0.09	0.05	2.58	0.04	75.27	0.30	0.07	**99.38**
WITS-G STD	Majors Acid32	11.70	1.48	0.00	3.47	4.42	0.10	0.05	2.59	0.04	75.19	0.30	0.07	**99.41**
WITS-G STD	Majors Acid32	11.57	1.49	0.00	3.47	4.44	0.09	0.05	2.60	0.04	75.21	0.30	0.07	**99.33**
WITS-G STD	Majors Acid32	11.50	1.48	0.00	3.47	4.43	0.10	0.05	2.47	0.04	75.19	0.30	0.07	**99.10**
WITS-G STD	Majors Acid32	11.53	1.47	0.00	3.45	4.41	0.10	0.05	2.44	0.04	74.92	0.30	0.07	**98.78**
WITS-G std	Majors Acid32	11.48	1.47	0.00	3.47	4.40	0.10	0.05	2.49	0.04	75.09	0.29	0.07	**98.95**
WITS-G STD	Majors Acid32	11.61	1.49	0.00	3.46	4.41	0.10	0.05	2.57	0.04	74.94	0.31	0.07	**99.05**
Average		11.69	1.49	0.00	3.46	4.42	0.08	0.05	2.64	0.04	75.13	0.31	0.07	99.46
Relative standard deviation (%)		1.36	1.59		3.41	0.81	16.00	0.00	10.98	10.00	0.81	5.52	12.50	0.33

Table 14: EA1.6 - Control standards used for the calibration procedure for Trace Element chemical analysis

	Values in ppm	Sc	Sc 2σ	V	V 2σ	Cr	Cr 2σ	Co	Co 2σ	Ni	Ni 2σ	Cu	Cu 2σ	Zn	Zn 2σ	Rb	Rb 2σ	Sr	Sr 2σ	Y	Y 2σ	Zr	Zr 2σ	Nb	Nb 2σ	Mo	Mo 2σ	Cs	Cs 2σ
	Instrument DL	*0.035*		*0.021*		*0.210*		*0.009*		*0.168*		*0.027*		*0.140*		*0.012*		*0.006*		*0.002*		*0.004*		*0.002*		*0.012*		*0.004*	
	Method DL	*0.694*		*0.418*		*4.200*		*0.180*		*3.360*		*0.546*		*2.792*		*0.245*		*0.121*		*0.039*		*0.071*		*0.043*		*0.245*		*0.085*	
Certified BHVO glass		**33.00**		**308**		**293**		**44**		**116**		**127**		**102**		**9.2**		**396**		**26**		**170**		**18.3**		**3.8**		**0.10**	
	Repl 1	30.79	0.44	312.8	3.6	277.6	3.2	44.01	0.66	119.7	2	123.7	1.4	136	5.6	8.87	0.24	373.7	4.4	22.84	0.32	155.5	1.7	16.78	0.26	3.86	0.16	0.111	0.01
	Repl 2	30.84	0.58	311.9	2.6	278.4	3	43.68	0.55	118.7	1.7	124.7	1.7	128.5	3.6	8.96	0.29	381.6	4.2	22.96	0.33	152.9	1.4	16.61	0.24	4.02	0.23	0.099	0.02
	Repl 3	30.04	0.49	312.2	4.3	273.3	3.6	43.58	0.65	116	2.1	124.6	2.2	113.4	3.4	8.94	0.26	365.2	5.3	22.36	0.37	149.9	1.9	16.34	0.26	3.97	0.17	0.119	0.02
	Repl 4	30.77	0.42	314.7	2.9	280.7	3.1	43.58	0.54	120.2	1.8	124.8	1.3	111.6	3.6	9.03	0.25	378.2	5	23.21	0.27	154.1	2.5	16.53	0.24	3.95	0.17	0.085	0.01
	Average Analysed	**30.61**		**312.90**		**277.50**		**43.71**		**118.65**		**124.45**		**122.38**		**8.95**		**374.68**		**22.84**		**153.10**		**16.57**		**3.95**		**0.10**	
	% Deviation	*7.2*		*1.6*		*5.3*		*0.7*		*2.3*		*2.0*		*20.0*		*2.7*		*5.4*		*12.1*		*9.9*		*9.5*		*3.9*		*0.4*	
Certified BHVO powder		**31.42**		**313.80**		**287.60**		**44.90**		**120.00**		**137.20**		**105.10**		**9.52**		**399.20**		**26.23**		**174.60**		**18.53**		**1.06**		**0.10**	
	Repl 1	32.2	1.6	318.5	4.3	294.6	5.3	44.5	2	127.4	5	133.6	3.7	121.3	8.9	8.31	0.94	398.9	6.3	24.46	0.75	160.7	2.1	16.72	0.5	1.95	0.42	0.46	0.12
	Repl 2	31.4	1.2	319.7	5.3	295	4.5	44.4	1.4	130.3	5.5	137.8	3.8	124.2	7.9	8.69	0.82	392.8	6.3	24.01	0.72	160.4	3.1	17.32	0.5	1.58	0.38	0.293	0.09
	Repl 3	33.4	1.1	318.8	3.8	299.9	4.9	44.7	1	130.8	6	138.6	3.5	127.1	8.4	8.75	0.63	407.9	5.1	24.2	0.56	161.7	2.5	17.39	0.57	1.28	0.28	0.3	0.10
	Repl 4	32	1	323.4	4.5	294.1	5.5	44.7	1.4	137.4	6.1	141.8	3.7	123.5	8.4	9.2	0.75	392.1	5.9	24.48	0.6	161.3	2.6	17.43	0.55	1.45	0.39	0.296	0.10
	Repl 5	32.6	1	321.1	4.1	293.4	4.7	42.23	0.9	127.3	4.9	132	2.3	113.2	7	9.26	0.82	396.8	5.3	24.02	0.62	161.4	2.8	17.9	0.63	1.57	0.38	0.276	0.08
	Repl 6	32.9	1.1	323.8	4.1	291	4.3	43.4	1.6	138.1	5.8	137	3.3	120	6.2	9.64	0.83	395.9	5.1	24.51	0.71	160.3	2.6	17.38	0.66	1.4	0.28	0.265	0.09
	Repl 7	33.2	1.2	323.7	4.9	296.3	5.5	44.3	1.8	136.5	5.7	134.2	3.8	117	7.9	8.51	0.62	399.3	5.2	24.48	0.65	164.4	2.7	17.59	0.56	1.44	0.34	0.274	0.06
	Repl 8	32.1	1.2	324.6	4.7	292.1	4.3	44.2	1.7	136.3	4.6	131.4	3.2	114	5.7	9.13	0.88	391.7	4.6	23.83	0.67	161.9	2.2	17.41	0.56	1.55	0.35	0.319	0.09
	Repl 9	32	1.3	327.9	5.7	293.3	5.1	43.6	1.5	140.1	5.1	141.7	3	116.6	7.1	8.75	0.65	403.4	5.3	25.22	0.8	165.4	2.4	17.25	0.48	1.47	0.39	0.302	0.07
	Average Analysed	**32.42**		**322.39**		**294.41**		**44.00**		**133.80**		**136.46**		**119.66**		**8.92**		**397.64**		**24.36**		**161.94**		**17.38**		**1.52**		**0.31**	
	% Deviation	*0.5*		*0.4*		*0.3*		*4.2*		*5.1*		*3.4*		*5.7*		*3.7*		*0.2*		*1.4*		*0.3*		*2.9*		*3.1*		*12.1*	

	Values in ppm	Ba	Ba 2σ	La	La 2σ	Ce	Ce 2σ	Pr	Pr 2σ	Nd	Nd 2σ	Sm	Sm 2σ	Eu	Eu 2σ	Gd	Gd 2σ	Tb	Tb 2σ	Dy	Dy 2σ	Ho	Ho 2σ	Er	Er 2σ	Tm	Tm 2σ	Yb	Yb 2σ	Lu	Lu 2σ
	Instrument DL	*0.053*		*0.001*		*0.001*		*0.002*		*0.013*		*0.010*		*0.003*		*0.008*		*0.001*		*0.007*		*0.001*		*0.004*		*0.001*		*0.005*		*0.001*	
	Method DL	*1.060*		*0.026*		*0.026*		*0.040*		*0.260*		*0.210*		*0.067*		*0.152*		*0.026*		*0.148*		*0.029*		*0.082*		*0.025*		*0.098*		*0.028*	
Certified BHVO glass		**131**		**15.2**		**37.6**		**5.35**		**24.50**		**6.1**		**2.07**		**6.16**		**0.919**		**5.28**		**0.98**		**2.56**		**0.34**		**2.01**		**0.28**	
	Repl 1	124.7	2.4	14.56	0.24	35.39	0.5	4.895	0.09	23.19	0.34	5.71	0.22	1.93	0.06	6.00	0.24	0.88	0.03	4.89	0.12	0.93	0.03	2.41	0.09	0.31	0.02	1.94	0.10	0.27	0.02
	Repl 2	125	2.2	14.6	0.21	35.41	0.36	5.02	0.12	23.01	0.43	5.95	0.28	2.00	0.07	5.55	0.25	0.85	0.03	4.93	0.17	0.93	0.03	2.29	0.09	0.30	0.02	1.85	0.10	0.26	0.02
	Repl 3	123.3	2.1	14.2	0.17	34.83	0.48	4.9	0.10	22.42	0.45	5.68	0.21	1.90	0.06	5.73	0.21	0.82	0.03	4.68	0.13	0.92	0.03	2.28	0.07	0.29	0.02	1.84	0.09	0.26	0.02
	Repl 4	124	1.8	14.49	0.18	35.7	0.43	5.005	0.09	22.85	0.44	5.78	0.20	1.96	0.07	5.87	0.19	0.88	0.03	4.97	0.12	0.92	0.03	2.40	0.07	0.32	0.02	1.89	0.06	0.27	0.02
	Average Analysed	**124.25**		**14.46**		**35.33**		**4.96**		**22.87**		**5.78**		**1.95**		**5.79**		**0.86**		**4.87**		**0.93**		**2.34**		**0.30**		**1.88**		**0.26**	
	% Deviation	*5.2*		*4.9*		*6.0*		*7.4*		*6.7*		*5.2*		*5.8*		*6.0*		*6.7*		*7.8*		*5.1*		*8.5*		*9.5*		*6.5*		*5.5*	
Certified BHVO powder		**134.40**		**15.44**		**38.08**		**5.42**		**24.78**		**6.17**		**2.05**		**6.29**		**0.95**		**5.27**		**0.98**		**2.50**		0.33		1.99		0.28	
	Repl 1	129.9	7.7	15.14	0.55	37.27	0.73	5.12	0.27	24.21	0.92	6.18	0.57	2.14	0.23	6.56	0.62	1.03	0.13	5.14	0.49	0.89	0.09	2.44	0.27	0.34	0.07	1.92	0.31	0.29	0.06
	Repl 2	132	6.7	14.65	0.48	37.48	0.81	5.34	0.21	23.8	1.1	6.37	0.63	1.92	0.21	5.39	0.68	0.85	0.10	4.94	0.51	0.92	0.09	2.47	0.27	0.33	0.05	1.72	0.29	0.28	0.06
	Repl 3	133	5.8	15.53	0.5	36.88	0.54	5.13	0.29	23.8	1.3	6.11	0.65	2.14	0.23	5.82	0.85	0.92	0.09	5.27	0.48	1.00	0.09	2.56	0.27	0.31	0.06	1.96	0.32	0.23	0.04
	Repl 4	129.4	6.5	15.72	0.64	37.21	0.82	5.44	0.3	24	1.1	5.93	0.68	2.11	0.20	6.60	0.86	0.88	0.09	4.77	0.37	1.02	0.09	2.53	0.22	0.26	0.04	2.16	0.28	0.27	0.05
	Repl 5	136.3	5.4	15.66	0.43	37.61	0.7	5.24	0.24	26	1.4	6.59	0.63	2.16	0.23	5.79	0.55	0.94	0.10	5.74	0.43	1.04	0.11	2.54	0.29	0.30	0.05	2.11	0.33	0.23	0.05
	Repl 6	130.3	6.1	15.17	0.59	37.62	0.67	5.03	0.29	24.4	1.4	5.86	0.69	1.96	0.17	5.69	0.60	0.97	0.10	5.26	0.40	0.99	0.10	2.42	0.26	0.27	0.05	1.82	0.31	0.24	0.04
	Repl 7	131.8	7.5	15.13	0.49	37.88	0.72	5.23	0.26	23.7	1.2	6.33	0.71	1.99	0.20	5.96	0.65	0.87	0.10	5.66	0.46	1.00	0.09	2.18	0.28	0.29	0.05	1.92	0.28	0.27	0.05
	Repl 8	138.2	5.9	15.73	0.43	36.98	0.8	5.16	0.27	24.4	1.2	6.59	0.67	2.12	0.23	5.83	0.56	0.89	0.10	5.32	0.45	0.95	0.08	2.46	0.18	0.39	0.07	2.03	0.29	0.27	0.05
	Repl 9	129.2	5.7	15.56	0.55	38.39	0.92	5.36	0.26	24.6	1.5	6.16	0.68	2.14	0.22	6.29	0.68	0.92	0.10	4.97	0.55	0.95	0.11	2.44	0.33	0.31	0.06	1.94	0.32	0.28	0.05
	Average Analysed	**132.23**		**15.37**		**37.48**		**5.23**		**24.32**		**6.24**		**2.08**		**5.99**		**0.92**		**5.23**		**0.97**		**2.45**		**0.31**		**1.95**		**0.26**	
	% Deviation	*3.0*		*1.9*		*0.3*		*0.2*		*6.4*		*5.4*		*3.9*		*3.5*		*2.3*		*8.9*		*6.4*		*3.6*		*4.9*		*7.4*		*13.0*	

Table 14: EA1.6 continued - Control standards used for the calibration procedure for Trace Element chemical analysis

	Values in ppm	Hf	Hf 2σ	Ta	Ta 2σ	Pb	Pb 2σ	Th	Th 2σ	U	U 2σ
	Instrument DL	*0.004*		*0.001*		*0.005*		*0.002*		*0.002*	
	Method DL	*0.070*		*0.017*		*0.090*		*0.048*		*0.036*	
Certified BHVO glass		**4.32**		**1.15**		**1.70**		**1.22**		**0.40**	
	Repl 1	4.17	0.13	1.01	0.03	1.83	0.07	1.16	0.04	0.45	0.02
	Repl 2	4.17	0.15	1.01	0.03	1.78	0.09	1.17	0.04	0.41	0.03
	Repl 3	4.13	0.13	1.02	0.03	1.72	0.07	1.10	0.04	0.40	0.03
	Repl 4	4.24	0.12	1.03	0.03	1.72	0.08	1.15	0.03	0.41	0.01
	Average Analysed	**4.18**		**1.02**		**1.76**		**1.14**		**0.42**	
	% Deviation	*3.4*		*11.9*		*3.7*		*6.0*		*4.1*	
Certified BHVO powder		4.44		1.17		2.04		1.23		0.42	
	Repl 1	4.51	0.39	1.15	0.12	2.77	0.29	1.16	0.12	0.46	0.08
	Repl 2	4.25	0.43	1.10	0.09	2.78	0.27	1.12	0.15	0.36	0.07
	Repl 3	4.27	0.36	1.04	0.09	2.81	0.26	1.23	0.12	0.51	0.07
	Repl 4	4.32	0.39	1.03	0.12	2.64	0.28	1.24	0.13	0.40	0.05
	Repl 5	4.40	0.35	1.04	0.08	2.59	0.23	1.20	0.12	0.52	0.07
	Repl 6	4.31	0.35	1.02	0.09	2.54	0.23	1.22	0.10	0.44	0.07
	Repl 7	4.45	0.39	1.06	0.11	2.49	0.23	1.26	0.14	0.40	0.07
	Repl 8	4.22	0.30	1.14	0.09	2.58	0.29	1.29	0.13	0.39	0.07
	Repl 9	4.34	0.29	1.06	0.09	2.73	0.26	1.26	0.12	0.39	0.08
	Average Analysed	**4.34**		**1.07**		**2.66**		**1.22**		**0.43**	
	% Deviation	*1.3*		*3.1*		*2.7*		*1.7*		*17.4*	

7.2 Electronic Appendix EA2- Geochemical data of the Ignimbrites from the Saldanha Centre in the Saldanha Bay Volcanic Complex.

Table 15: EA2.1 - Bulk-rock analytical data for the Saldanha Ignimbrite in the Saldanha eruption centre

Electronic Appendix EA2, Table EA2.1 Bulk-rock analytical data for the Saldanha Ignimbrite in the Saldanha eruption centre

Sample	Abbr.	latitude S	longitude E	ht ASL	SiO_2	TiO_2	Al_2O_3	FeO	MnO	MgO	CaO	Na_2O	K_2O	P_2O_5	FM	Mg#	ASI	V	Cr	Ni	Cu	Zn	Rb	Sr	Y	Zr	Nb	Mo	Cs	Ba	Hf	Ta	Pb	Th	U	La	Ce	Pr	Nd	Sm	Eu	Gd	Tb	Dy	Ho	Er	Tm	Yb	Lu
		(deg min sec)	(deg min sec)	(m)																																														
B1	SC-SI				75.12	0.24	13.67	1.87	0.03	0.20	0.98	2.10	5.66	0.12	2.10	15.70	1.23	10	5	2.0		42	225	88	45	169	15	1.0		642			34	21	5.0																	
B2	SC-SI				74.48	0.26	13.91	2.00	0.03	0.21	1.19	2.03	5.77	0.12	2.24	15.62	1.22	12	11	2.0		42	240	90	44	187	15	1.0		673			35	21	3.0																	
B3	SC-SI				74.27	0.27	13.98	2.11	0.04	0.22	1.26	2.01	5.71	0.12	2.37	15.48	1.22	13	22	2.0		45	237	94	44	193	15	1.0		704			36	22	5.0																	
B6	SC-SI				74.46	0.26	14.00	1.98	0.03	0.23	1.21	1.99	5.73	0.11	2.23	16.92	1.23	12	12	2.0		43	242	89	44	177	15	1.0		682			36	21	4.0																	
B7	SC-SI				73.90	0.27	14.34	2.12	0.03	0.25	1.19	1.84	5.93	0.13	2.40	17.46	1.27	14	7.0	2.0		44	240	89	45	199	16	1.0		708			35	22	4.0																	
B8	SC-SI				77.49	0.17	12.71	1.53	0.02	0.14	0.76	1.69	5.38	0.11	1.69	14.02	1.31	6.0	13	2.0		36	262	50	46	117	14	1.0		325			30	15	5.0																	
B10, QP4	SC-SI				73.65	0.26	13.89	2.05	0.03	0.27	1.20	2.83	5.67	0.15	2.36	19.20	1.10						235	92	44	222	16			731				20	5.0	45	98	12	42	8.8	1.4	7.9	1.2	7.4	1.4	3.7	0.60	4.0	0.54
B11, QP5	SC-SI				73.67	0.26	13.88	2.06	0.02	0.28	1.17	2.82	5.70	0.13	2.36	19.70	1.10						247	86	43	197	16			739				21	5.0	46	100	12	42	8.3	1.4	8.3	1.3	7.7	1.4	3.9	0.55	3.6	0.51
B12, QP6	SC-SI				73.74	0.27	13.83	2.06	0.03	0.25	1.17	2.79	5.69	0.15	2.35	18.04	1.11						233	88	43	211	16			706				19	5.0	41	87	10	39	8.2	1.4	7.3	1.2	7.0	1.3	3.4	0.51	3.5	0.52
B13, QP7	SC-SI				73.73	0.27	13.84	2.07	0.02	0.24	1.19	2.80	5.67	0.16	2.33	17.25	1.11						239	90	44	218	16			697				20	5.0	41	90	11	39	7.9	1.4	7.3	1.2	7.2	1.3	3.6	0.60	3.9	0.48
B14, QP11	SC-SI				74.98	0.21	13.40	1.80	0.02	0.21	0.97	2.76	5.55	0.09	2.04	17.36	1.11						269	76	44	167	16			558				18	6.0	35	76	8.5	33	7.6	1.2	6.6	1.1	7.1	1.4	3.7	0.58	4.0	0.55
B15, QP16	SC-SI				74.53	0.22	13.55	1.82	0.02	0.22	1.07	2.74	5.73	0.10	2.06	17.89	1.09						247	87	39	168	15			702				19	5.0	41	85	10	35	7.9	1.3	7.3	1.2	7.2	1.3	3.6	0.61	3.9	0.48
B16, QP17	SC-SI				74.68	0.23	13.50	1.81	0.03	0.23	1.07	2.74	5.56	0.15	2.07	18.11	1.11						237	89	41	198	15			702				18	5.0	39	83	9.6	35	7.3	1.4	6.8	1.1	6.8	1.4	3.7	0.55	3.8	0.52
B24, QP41	SC-SI				74.36	0.22	13.62	1.83	0.02	0.25	0.95	2.77	5.83	0.14	2.10	19.84	1.11						231	87	41	175	15			648				18	3.0	35	77	9.1	34	7.5	1.3	6.9	1.2	6.8	1.3	3.7	0.57	3.7	0.53
B25, QP44	SC-SI				75.07	0.23	13.47	1.76	0.02	0.27	0.73	2.60	5.66	0.18	2.05	21.15	1.19						249	85	42	178	16			631				18	3.0	36	80	9.0	34	6.9	1.2	6.0	1.0	6.6	1.3	3.5	0.54	3.6	0.53
B26, QP46	SC-SI				75.22	0.22	13.42	1.70	0.02	0.25	0.70	2.63	5.67	0.16	1.97	20.44	1.18						257	84	39	175	16			627				18	3.0	36	75	9	32	7.1	1.2	6.0	1.0	6.3	1.2	3.3	0.51	3.5	0.52
CJA1	SC-SI	33 01 29.8	17 57 13.1	12	77.01	0.17	12.45	1.51	0.02	0.16	0.79	2.41	5.37	0.11	1.69	16.28	1.14	11	9.8	5.7	14	34	216	41	28	87		2.1	7.9	303	2.5	1.0	29	10	5.9	19	46	5.1	18	4.3	0.62	4.6	0.76	4.8	1.0	2.9	0.41	2.7	0.38
CJA3A5	SC-SI	33 00 23.2	17 56 21.5	44	77.12	0.17	12.46	1.49	0.03	0.14	0.78	2.35	5.34	0.11	1.66	14.61	1.15	10		4.0	16	41	285	46	35	105		2.4	12	339	3.5	1.4	39	14	8.3	23	56	6.2	23	6.0	0.74	5.8	1.0	6.7	1.4	3.8	0.54	3.9	0.50
CJA7	SC-SI	33 01 29.7	17 57 13.1	12	76.72	0.17	12.64	1.52	0.03	0.15	0.79	2.40	5.45	0.12	1.70	15.18	1.15	11	8.9	4.5	24	45	292	50	35	106		2.7	11	408	3.6	1.4	42	14	8.6	24	59	6.6	24	6.0	0.92	6.1	1.1	6.7	1.4	4.2	0.61	4.0	0.53
CJB9	SC-SI	33 01 43.1	17 57 15.2	7	77.08	0.17	12.49	1.45	0.02	0.14	0.70	2.43	5.39	0.12	1.61	14.93	1.16	8.2	9.9	6.0	13	48	273	41	33	90		0.84	12	301	2.7	1.2	33	12	4.7	20	49	5.6	20	5.0	0.59	4.5	0.88	5.4	1.2	3.3	0.46	3.1	0.44
CJB13A	SC-SI	33 02 00.4	17 56 02.3	5	77.61	0.17	12.30	1.44	0.02	0.16	0.60	2.33	5.27	0.11	1.61	16.17	1.19	8.6	12	114	15	44	234	37	30	85	15	2.3	7.6	287	2.7	1.1	31	11	6.8	19	47	5.1	19	4.6	0.59	4.4	0.82	5.5	1.1	3.1	0.45	3.0	0.38
CJB18A	SC-SI	33 02 50.4	17 54 29.2	10	75.58	0.21	13.28	1.63	0.03	0.19	0.90	2.42	5.62	0.12	1.86	17.37	1.16	13	8.3	5.7	15	46	243	58	30	113		1.1	11	478	3.3	1.1	36	12	4.5	25	60	6.5	23	5.3	0.90	4.8	0.86	5.4	1.1	3.1	0.43	2.8	0.38
CJB18B	SC-SI	33 02 47.0	17 54 10.9	4	74.97	0.22	13.27	1.61	0.02	0.20	0.91	2.89	5.77	0.13	1.83	18.04	1.07	11	12	122	7.7	44	228	54	30	112	14	1.1	9.9	462	3.3	1.0	33	12	4.1	25	59	6.6	23	5.3	0.89	4.9	0.89	5.4	1.1	3.1	0.45	2.8	0.37
CJB23	SC-SI	33 01 35.0	17 56 29.7	6	74.34	0.24	13.67	1.83	0.03	0.22	1.03	2.70	5.80	0.13	2.08	17.43	1.11	13	12	134	6.9	51	225	62	29	125	16	0.84	11	554	3.7	1.1	34	13	3.4	27	66	7.4	26	5.8	0.96	5.1	0.87	5.5	1.1	2.8	0.39	2.9	0.37
CJB26	SC-SI	33 01 42.1	17 57 20.3	11	77.14	0.17	12.42	1.57	0.02	0.15	0.75	2.38	5.28	0.11	1.74	14.88	1.16	9.8	9.2	117	19	50	246	40	33	96	16	2.2	9.4	284	3.0	1.3	35	12	6.6	20	49	5.4	20	5.2	0.61	4.8	0.88	6.0	1.2	3.4	0.48	3.3	0.42
CJB27	SC-SI	33 01 43.0	17 57 21.5	9	76.80	0.17	12.56	1.58	0.03	0.17	0.64	2.56	5.36	0.11	1.79	16.37	1.15	9.4	5.5	112	17	48	247	42	31	92	15	2.1	8.1	302	2.7	1.2	35	12	7.0	20	49	5.4	19	4.8	0.62	4.7	0.88	5.5	1.1	3.3	0.45	3.1	0.42
CJB28	SC-SI	33 01 44.2	17 57 21.4	5	77.00	0.16	12.54	1.46	0.02	0.14	0.74	2.39	5.44	0.11	1.62	14.93	1.15	9.9	9.1	119	7.3	44	253	41	31	87	16	1.6	11	291	2.7	1.1	33	11	5.8	19	47	5.3	19	5.0	0.63	4.3	0.82	5.4	1.2	3.2	0.45	3.2	0.40
MB10	SC-SI	33 01 41.8	17 57 14.3	9	77.12	0.16	12.49	1.45	0.03	0.14	0.72	2.36	5.41	0.11	1.62	14.93	1.16	8.1	14	5.2	7.3	48	241	42	32	91		0.73	10	320	2.8	1.2	35	12	4.5	20	48	5.4	20	4.9	0.65	4.7	0.89	5.5	1.2	3.4	0.45	3.2	0.42
MB11	SC-SI	33 01 41.4	17 57 13.5	9	77.18	0.16	12.54	1.42	0.02	0.14	0.70	2.35	5.38	0.11	1.58	15.26	1.17	8.8	9.5	5.1	8.4	43	252	41	30	85		2.0	9.9	298	2.7	1.1	33	11	6.9	19	47	5.4	18	4.8	0.61	4.3	0.82	5.3	1.1	3.3	0.45	3.0	0.40
MB12	SC-SI	33 02 01.2	17 56 05.8	5	76.86	0.18	12.67	1.49	0.02	0.15	0.73	2.42	5.36	0.11	1.66	15.50	1.17	24	8.1	71	9.5	71	203	100	36	240	19	2.2	8.3	851	4.6	1.2	43	16	3.2	50	109	9.2	34	7.2	1.30	6.0	0.95	6.1	1.2	3.4	0.46	3.1	0.41
MB22	SC-SI	33 01 35.9	17 56 27.2	7	73.19	0.27	14.34	1.94	0.03	0.29	1.18	2.67	5.97	0.13	2.26	20.81	1.13	16	11	135	8.1	53	222	88	32	164	17	0.63	7.4	753	6.5	1.2	40	20	4.8	37	84	12	45	9.1	1.4	7.9	1.2	7.1	1.3	3.6	0.50	3.2	0.46
MB26	SC-SI	33 01 43.0	17 57 19.8	8	76.51	0.18	12.81	1.61	0.02	0.15	0.77	2.48	5.35	0.11	1.78	14.51	1.16	9.4	11	81	8.4	47	248	39	33	92	16	2.4	11	267	2.9	1.3	33	12	7.6	20	49	5.5	20	5.0	0.55	4.7	0.89	6.0	1.3	3.5	0.53	3.3	0.47
WIG	SC-SI	32 59 52.0	17 52 24.0	3	73.47	0.27	14.21	2.03	0.03	0.29	1.14	2.58	5.85	0.13	2.35	20.06	1.15	16	32	101	14	41	209	72	29	152	15	1.0	8.9	596	4.0	1.0	33	14	3.8	31	71	7.7	29	6.0	1.1	5.7	0.90	5.1	1.0	2.9	0.43	2.7	0.39
WP8	SC-SI				76.67	0.17	12.67	1.50	0.02	0.14	0.80	2.43	5.48	0.11	1.67	14.54	1.14	9.4	8.1	108	18	49	249	49	33	106	14	2.4	12	380	3.3	1.2	37	13	7.0	23	54	6.1	22	5.3	0.71	5.2	0.89	6.0	1.2	3.5	0.49	3.2	0.41
WP12A	SC-SI	32 58 35.7	17 52 52.1	2	75.56	0.21	13.20	1.68	0.03	0.20	0.92	2.46	5.61	0.12	1.91	17.87	1.15	13		134	25	52	274	67	38	137	18	1.0	12	553	4.3	1.5	44	17	5.4	32	75	8.4	31	7.0	1.0	7.2	1.1	7.2	1.4	4.2	0.60	4.0	0.53
WP12B	SC-SI	32 58 35.7	17 52 52.1	2	75.87	0.21	12.97	1.65	0.02	0.20	0.87	2.49	5.59	0.12	1.86	17.61	1.13	22	14	94	12	58	265	91	36	212	21	1.8	12	779	4.3	1.4	41	16	8.1	46	107	7.8	29	6.7	1.0	7.0	1.1	7.0	1.4	4.0	0.57	3.7	0.54
WP18	SC-SI	33 01 38.6	17 57 09.2	4	74.80	0.22	13.49	1.79	0.03	0.20	1.02	2.54	5.76	0.12	2.03	16.88	1.13	14	14	138	14	49	280	68	35	132	18	0.63	13	572	4.1	1.4	46	17	4.6	32	76	8.6	31	7.5	1.2	6.7	1.1	6.8	1.3	4.0	0.55	3.6	0.48
Sal1	SC-SI	33 01 43.7	17 57 21.6	7	76.79	0.18	12.49	1.49	0.03	0.17	0.76	2.59	5.38	0.12	1.69	17.03	1.12	12	12	5.1	14	40	241	48	46	120	15	2.1	9.6	317	4.1	1.4	24	16	6.6	26	54	6.7	25	6.1	0.69	6.3	1.1	7.7	1.7	4.9	0.66	4.7	0.66
Sal 3	SC-SI	33 01 35.9	17 56 27.2	7	74.27	0.24	13.62	1.80	0.03	0.24	1.04	2.77	5.86	0.12	2.08	19.36	1.09	14	22	6.1	15	38	211	67	40	157	15	0.62	9.6	544	4.9	1.2	26	17	3.2	33	68	8.1	32	7.4	1.06	6.9	1.1	7.4	1.4	4.3	0.57	3.8	0.57
Sal3B	SC-SI	33 01 35.9	17 56 27.2	7	74.64	0.23	13.42	1.75	0.03	0.26	0.87	2.67	6.01	0.11	2.04	21.23	1.10	16	11	6.4	10	40	243	75	44	179	15	1.0	11	600	5.5	1.1	29	18	3.2	36	74	9.0	34	8.1	1.19	8.1	1.4	8.3	1.6	4.6	0.63	4.3	0.55

* major and minor oxides normalised to 100 wt% volatile-free and with all Fe expressed as FeO^T; trace elements in ppm by wt

Mg# =100 × mol. Mg / (Mg + Fe)

ASI = mol. Al_2O_3 / (CaO - 3.33P_2O_5 + Na_2O + K_2O)

Table 16: EA2.2 - Bulk-rock analytical data for the Jacob's Bay Ignimbrite in the Saldanha eruption centre

Electronic Appendix EA2, Table EA2.2 Bulk-rock analytical data for the Jacob's Bay Ignimbrite in the Saldanha eruption centre

Sample	Abbr.	latitude S	longitude E	ht ASL	SiO_2	TiO_2	Al_2O_3	FeO	MnO	MgO	CaO	Na_2O	K_2O	P_2O_5	FM	Mg#	ASI	V	Cr	Ni	Cu	Zn	Rb	Sr	Y	Zr	Nb	Mo	Cs	Ba	Hf	Ta	Pb	Th	U	La	Ce	Pr	Nd	Sm	Eu	Gd	Tb	Dy	Ho	Er	Tm	Yb	Lu
		(deg min sec)	(deg min sec)	(m)																																													
B4	SC-JI				72.74	0.35	14.59	2.55	0.05	0.33	1.51	2.06	5.67	0.14	2.94	18.73	1.22	18	6	2		51	232	109	48	258	17	2.0		795			35	24	4.0																	
B5	SC-JI				72.74	0.35	14.58	2.58	0.04	0.35	1.54	2.12	5.56	0.14	2.97	19.56	1.22	19	8	2		53	232	106	49	261	18	2.0		753			35	27	5.0																	
B9, QP3	SC-JI				72.82	0.35	14.16	2.55	0.04	0.39	1.03	2.55	5.95	0.16	2.98	21.43	1.17						250	101	33	244	16			878				20	4.0	46	98	11	41	8.0	1.5	6.3	0.96	5.5	1.1	2.8	0.43	3.0	0.45
B17, QP18	SC-JI				71.01	0.41	14.77	2.85	0.03	0.46	1.67	3.07	5.52	0.20	3.34	22.22	1.09						235	125	49	316	21			987				26	4.0	68	138	16	59	11	1.9	9.6	1.5	8.1	1.6	4.1	0.64	3.9	0.61
B18, QP19	SC-JI				71.05	0.41	14.74	2.89	0.03	0.48	1.66	3.07	5.49	0.19	3.40	22.70	1.09						216	120	46	325	20			929				23	4.0	62	130	14	54	10	1.9	9.4	1.4	8.1	1.5	3.9	0.63	3.7	0.58
B19, QP20	SC-JI				71.22	0.42	14.66	2.81	0.04	0.47	1.67	3.06	5.45	0.21	3.32	22.88	1.09						229	125	47	336	20			1002				25	4.0	67	138	16	58	11	1.9	9.2	1.4	8.3	1.5	4.0	0.60	4.0	0.60
B20, QP21	SC-JI				71.22	0.40	14.67	2.80	0.04	0.46	1.67	3.08	5.47	0.20	3.29	22.61	1.08						221	126	47	329	20			990				25	4.0	66	135	16	58	11	1.9	9.2	1.4	8.3	1.6	4.0	0.58	4.0	0.56
B21, QP23	SC-JI				71.78	0.39	14.51	2.70	0.03	0.38	1.47	2.92	5.67	0.13	3.12	20.22	1.09						233	110	46	295	21			874				26	5.0	60	124	14	54	11	1.7	10	1.5	7.9	1.5	4.2	0.59	3.9	0.58
B22, QP24	SC-JI				72.04	0.38	14.44	2.71	0.04	0.39	1.48	2.89	5.44	0.17	3.15	20.58	1.12						227	116	48	306	20			879				25	5.0	58	120	14	54	10	1.7	8.8	1.4	8.0	1.5	4.1	0.65	4.1	0.55
B23, QP25	SC-JI				71.82	0.38	14.53	2.66	0.04	0.40	1.52	2.94	5.53	0.18	3.10	21.03	1.11						225	117	48	398	20			931				24	5.0	61	127	15	55	11	1.9	9.8	1.5	8.5	1.7	4.2	0.60	4.2	0.61
B27, QP52	SC-JI				72.70	0.32	14.21	2.42	0.02	0.34	1.38	2.93	5.60	0.09	2.78	19.84	1.08						247	100	46	243	18			757				23	4.0	53	110	12	48	9.4	1.5	8.5	1.3	7.7	1.5	4.1	0.55	3.7	0.55
B28, QP53	SC-JI				72.57	0.31	14.26	2.44	0.02	0.35	1.38	2.95	5.58	0.12	2.82	20.49	1.09						233	98	45	272	17			766				24	4.0	54	114	14	50	10	1.6	8.6	1.4	7.8	1.5	4.2	0.58	4.1	0.63
B29, QP54	SC-JI				72.66	0.35	14.15	2.41	0.03	0.37	1.38	2.92	5.59	0.13	2.82	21.66	1.08						233	98	44	241	19			799				24	5.0	54	111	13	46	9.4	1.5	8.0	1.4	7.5	1.5	4.3	0.59	3.8	0.58
B30, QP58	SC-JI				72.99	0.33	13.98	2.45	0.04	0.38	1.36	2.89	5.40	0.17	2.87	21.86	1.10						231	97	46	268	18			724				23	6.0	51	108	12	47	9.1	1.5	8.4	1.4	7.6	1.5	3.8	0.60	4.1	0.57
B31, QP60	SC-JI				72.91	0.32	14.02	2.43	0.03	0.38	1.38	2.93	5.45	0.15	2.85	21.86	1.09						245	95	45	267	19			727				21	6.0	49	104	12	44	9.1	1.6	8.6	1.3	7.8	1.5	4.0	0.57	3.7	0.59
B32, QP63	SC-JI				73.48	0.31	13.67	2.37	0.03	0.36	1.24	2.87	5.47	0.19	2.76	21.52	1.10						234	103	45	244	17			760				24	5.0	52	108	13	47	9.2	1.6	8.0	1.3	7.7	1.6	4.1	0.63	4.2	0.59
CJA3	SC-JI	33 00 18.1	17 56 22.1	53	71.31	0.41	14.80	2.84	0.04	0.45	1.69	2.76	5.53	0.17	3.33	22.05	1.12	29	12	8	18	55	203	100	34	237		1.9	8.5	852	6.1	1.3	34	19	4.3	51	115	13	45	8.8	1.6	8.0	1.2	6.5	1.2	3.3	0.48	3.2	0.44
CJA5	SC-JI	33 00 18.1	17 56 22.1	53	71.16	0.39	14.86	2.84	0.04	0.42	1.60	2.81	5.72	0.16	3.30	20.92	1.11	30	17	117	17	75	264	118	42	274	26	2.4	13	1143	7.87	1.8	51	25	6.8	62	140	15	56	11	1.9	11	1.5	8.5	1.7	4.5	0.62	4.4	0.56
CJB13B	SC-JI	33 01 14.9	17 55 04.3	44	70.20	0.46	15.22	3.09	0.04	0.51	1.91	2.87	5.52	0.17	3.64	22.76	1.11	30	13	7	10	68	201	109	34	277		2.5	9.1	935	7.07	1.3	38	21	5.0	57	132	14	52	9.4	1.6	7.7	1.1	6.7	1.3	3.5	0.45	3.0	0.44
CJB15	SC-JI	33 02 28.2	17 55 45.4	5	70.82	0.45	14.92	3.09	0.05	0.51	1.79	2.76	5.43	0.18	3.65	22.57	1.12	30	19	83	19	54	203	117	44	345	24	2.2	9.4	926	8.74	1.6	32	25	5.2	68	139	16	61	11	1.8	9.5	1.5	8.4	1.8	4.6	0.62	4.1	0.57
CJB16	SC-JI	33 02 50.4	17 54 58.7	6	71.59	0.39	14.83	2.64	0.04	0.39	1.44	2.73	5.78	0.17	3.07	20.83	1.15	26	11	84	18	64	213	97	32	217	20	2.0	7.8	826	5.65	1.2	40	18	4.2	46	104	11	41	8.2	1.4	6.6	1.0	6.2	1.2	3.3	0.43	3.0	0.41
CJB17	SC-JI	33 03 04.4	17 54 38.3	6	71.12	0.39	15.00	2.67	0.04	0.40	1.58	2.78	5.85	0.16	3.11	21.09	1.12	25	15	99	15	69	216	105	36	243	21	2.3	8.6	952	6.51	1.4	42	21	5.6	51	113	13	46	9.6	1.6	7.6	1.1	6.9	1.3	3.5	0.51	3.5	0.45
CJB19	SC-JI	33 02 21.8	17 53 48.7	3	71.30	0.39	14.82	2.73	0.04	0.46	1.67	2.75	5.67	0.16	3.24	23.08	1.11	25	21	92	22	45	199	132	47	322	21	1.7	8.3	1031	8.55	1.5	29	26	4.7	66	131	16	58	12	1.9	10	1.4	8.5	1.8	4.8	0.69	4.3	0.63
CJB20	SC-JI	33 01 45.6	17 53 30.9	3	70.90	0.41	15.03	2.80	0.04	0.46	1.74	2.82	5.63	0.16	3.31	22.73	1.11	27	14	94	14	65	204	105	35	249	21	1.7	8.5	923	6.55	1.3	40	20	4.3	53	121	13	47	9.6	1.6	7.7	1.1	6.6	1.3	3.5	0.48	3.2	0.45
CJB22	SC-JI	33 01 35.6	17 56 23.8	10	72.87	0.30	14.39	2.15	0.03	0.32	1.26	2.70	5.84	0.14	2.50	20.71	1.13	19	14	111	15	51	221	85	32	193	18	0.79	8.2	721	5.45	1.2	40	17	3.4	38	87	10	35	7.5	1.3	6.3	1.1	5.9	1.2	3.2	0.44	3.0	0.41
CJB30	SC-JI	33 01 18.0	17 54 52.6	48	70.63	0.45	15.04	3.03	0.05	0.51	1.78	2.81	5.52	0.18	3.60	23.08	1.12	30	21	104	16	65	208	105	34	270	22	2.4	9.0	851	6.84	1.3	40	21	5.0	56	128	14	50	9.6	1.5	7.4	1.2	6.6	1.3	3.5	0.47	3.1	0.43
MB1	SC-JI	33 02 58.0	17 55 41.9	91	70.95	0.42	14.90	2.97	0.05	0.46	1.68	2.75	5.64	0.17	3.48	21.68	1.12	29	19	74	8	71	202	108	41	287	22	1.9	9.2	877	7.58	1.4	37	22	5.3	57	124	14	53	10	1.6	8.3	1.2	7.6	1.6	4.1	0.59	3.8	0.51
MB2	SC-JI	33 02 03.0	17 55 37.3	70	70.94	0.41	14.92	2.73	0.04	0.43	1.67	2.89	5.81	0.16	3.20	21.75	1.09	10	10	124	6	46	236	42	31	95	15	1.7	8.4	303	3.13	1.2	33	12	6.6	21	50	6	20	5.1	0.61	4.8	0.9	5.8	1.1	3.3	0.47	3.2	0.44
MB5	SC-JI	33 02 16.3	17 55 41.8	61	70.25	0.43	15.32	2.99	0.04	0.49	1.87	2.86	5.57	0.17	3.52	22.74	1.12	29	10	86	12	74	202	110	35	268	22	2.0	8.8	901	7.12	1.3	40	21	5.1	56	126	14	50	9.5	1.6	7.8	1.2	7.0	1.3	3.5	0.48	3.4	0.47
MB6	SC-JI	33 02 04.7	17 55 47.3	64	70.96	0.44	14.85	3.03	0.04	0.50	1.69	2.75	5.57	0.17	3.57	22.78	1.12	31	25	80	13	76	205	111	43	318	24	1.6	8.4	909	8.21	1.6	37	25	4.5	62	135	15	56	11	1.6	9.6	1.4	8.3	1.6	4.5	0.59	3.9	0.53
MB7A	SC-JI	33 02 06.9	17 55 32.7	94	71.53	0.39	14.76	2.71	0.04	0.43	1.53	2.75	5.70	0.16	3.18	21.99	1.13	24	10	102	12	67	212	97	34	232	21	2.2	9.5	818	6.38	1.3	41	20	5.4	49	112	12	45	9.2	1.4	7.5	1.2	6.8	1.3	3.3	0.49	3.3	0.48
MB7B	SC-JI	33 02 08.4	17 55 18.2	91	71.51	0.39	14.86	2.66	0.04	0.41	1.67	2.80	5.50	0.15	3.11	21.46	1.12	25	15	109	8	67	211	98	34	239	20	2.0	9.6	769	6.27	1.2	41	19	4.7	49	111	12	45	8.8	1.4	7.1	1.1	6.6	1.3	3.3	0.45	3.1	0.44
WP11	SC-JI	32 58 52.6	17 52 52.3	2	72.33	0.36	14.42	2.60	0.04	0.37	1.40	2.67	5.67	0.15	3.00	20.18	1.14	27		115	20	62	260	96	40	240	23	2.2	12	851	7.01	1.6	48	22	6.4	52	122	13	48	9.9	1.6	9.2	1.4	8.0	1.5	4.4	0.62	4.1	0.61
WP16	SC-JI	32 58 11.0	17 53 08.0	5	73.36	0.32	13.87	2.38	0.03	0.33	1.33	2.63	5.60	0.15	2.74	19.72	1.11	13	11	138	16	47	268	61	37	133	17	2.6	11	492	6.15	1.5	48	20	5.4	30	70	12	43	8.5	1.5	8.6	1.2	7.3	1.5	4.1	0.60	3.9	0.50
WP25A	SC-JI	32 56 26.0	17 53 11.0	5	71.45	0.40	14.70	2.85	0.04	0.45	1.61	2.72	5.61	0.16	3.34	21.94	1.12	27		102	21	62	213	96	35	239	21	2.3	9.0	774	6.21	1.3	38	19	5.5	50	110	12	45	8.9	1.4	8.1	1.2	6.6	1.3	3.5	0.49	3.3	0.46
WP25B	SC-JI	32 56 26.0	17 53 11.0	5	71.69	0.40	14.60	2.78	0.04	0.43	1.55	2.71	5.64	0.16	3.25	21.60	1.12	26	25	89	24	60	204	91	33	230	20	1.9	8.2	712	6.04	1.2	36	18	4.8	46	106	12	43	8.2	1.4	7.7	1.2	6.4	1.1	3.3	0.45	3.1	0.42
WP29	SC-JI	32 59 52.0	17 52 24.0	3	69.96	0.46	15.31	3.16	0.05	0.52	1.88	2.86	5.61	0.18	3.73	22.75	1.11	31	14	104	21	66	195	114	36	283	22	1.9	7.2	934	7.26	1.3	37	21	4.7	57	125	14	51	9.6	1.7	8.7	1.2	6.8	1.3	3.3	0.52	3.3	0.49
WP30	SC-JI	32 59 52.0	17 52 24.0	3	72.03	0.36	14.56	2.57	0.05	0.36	1.49	2.75	5.67	0.16	2.98	19.84	1.12	22		82	22	55	227	84	33	200	19	1.9	8.9	684	5.23	1.2	36	17	4.9	42	96	10	39	8.2	1.3	7.5	1.1	6.2	1.2	3.3	0.45	3.0	0.41
WP31A	SC-JI	32 59 25.0	17 52 55.0	14	73.73	0.31	13.82	2.24	0.04	0.32	1.14	2.53	5.72	0.14	2.60	20.10	1.14	24	12	99	13	54	213	86	33	215	19	1.8	9.2	674	5.79	1.3	36	18	5.3	43	96	11	39	8.3	1.3	7.6	1.1	6.1	1.3	3.4	0.49	3.2	0.43
WP31B	SC-JI	32 59 25.0	17 52 55.0	14	72.20	0.36	14.41	2.58	0.04	0.39	1.52	2.75	5.58	0.16	3.01	21.24	1.11	18		106	10	43	210	72	31	168	16	1.4	8.9	580	4.37	1.1	34	15	3.8	34	78	9	32	6.6	1.1	6.5	0.9	5.8	1.1	3.1	0.44	3.0	0.41
Sal5	SC-JI	33 02 01.6	17 56 03.4	7	71.17	0.40	14.64	2.79	0.05	0.49	1.62	3.04	5.63	0.16	3.33	23.64	1.07	27	18	10	27	66	196	108	48	336	21	1.9	8.0	862	9.4	1.6	31	26	4.6	64	128	15	58	11	1.7	10	1.6	8.9	1.7	4.8	0.69	4.5	0.64
Sal 6	SC-JI	33 02 01.2	17 56 05.9	5	71.60	0.40	14.43	2.81	0.06	0.52	1.46	2.94	5.59	0.19	3.39	24.70	1.10	27	17	11	20	60	196	111	48	311	21	1.1	6.2	809	9.0	1.6	31	27	3.7	64	129	15	58	12	1.6	11	1.6	9.1	1.8	5.0	0.64	4.4	0.67
Sal 7	SC-JI	32 59 23.8	17 52 55.0	14	71.89	0.38	14.35	2.67	0.04	0.45	1.55	2.97	5.52	0.16	3.17	23.26	1.08	27	20	16	19	61	208	104	48	308	20	2.0	9.4	816	8.6	1.6	30	26	4.7	62	125	15	56	11	1.8	10	1.6	8.9	1.8	5.0	0.68	4.6	0.64
Sal8	SC-JI	32 59 51.5	17 52 24.6	3	70.16	0.49	15.08	2.98	0.05	0.52	1.86	3.12	5.57	0.17	3.54	23.60	1.07	31	17	8	25	66	182	120	48	360	21	2.0	7.3	921	9.5	1.5	30	28	4.6	73	144	17	64	12	2.0	11	1.6	9.5	1.8	4.8	0.69	4.4	0.64

* major and minor oxides normalised to 100 wt% volatile-free and with all Fe expressed as FeO^T; trace elements in ppm by wt

Mg# =100 × mol. Mg / (Mg + Fe)

ASI = mol. Al_2O_3 / (CaO - 3.33P_2O_5 + Na_2O + K_2O)

7.3 Electronic Appendix EA3 – Geochemical summary tables of all the ignimbrites from the Saldanha Bay Volcanic Complex (modified after Clemens et al., 2017).

Table 17: EA3.1 - Summary table of all Ignimbrites from the Postberg Eruption Centre

Sample	Abbr.	latitude S (deg min sec)	longitude E (deg min sec)	ht ASL (m)	SiO_2	TiO_2	Al_2O_3	FeO	MnO	MgO	CaO	Na_2O	K_2O	P_2O_5	FM	Mg#	ASI
A35	PC-SI				74.18	0.26	14.20	1.97	0.03	0.23	1.13	1.99	5.88	0.12	2.23	17.03	1.24
A33	PC-JI				71.91	0.40	14.89	2.78	0.05	0.41	1.64	2.21	5.56	0.16	3.24	21.00	1.22
A34	PC-JI				69.92	0.48	15.61	3.34	0.05	0.52	2.03	2.39	5.48	0.17	3.92	21.86	1.19
MM01	PC-JI	33 08 43	17 59 34	2	73.55	0.33	13.85	2.35	0.04	0.37	0.77	2.61	6.00	0.14	2.76	21.79	1.17
MM02	PC-JI	33 08 54	18 00 06	1	73.38	0.35	13.68	2.47	0.04	0.37	1.42	2.63	5.52	0.14	2.88	20.90	1.09
MM03	PC-JI	33 08 02	17 58 20	5	72.20	0.36	14.28	2.61	0.04	0.43	1.52	2.72	5.70	0.14	3.08	22.66	1.09
A7	PC PI				77.73	0.16	12.50	1.41	0.01	0.10	0.42	2.15	5.38	0.13	1.52	11.53	1.27
A8	PC PI				78.48	0.17	12.04	1.46	0.02	0.11	0.41	1.75	5.45	0.10	1.59	12.19	1.30
A9	PC PI				77.81	0.16	12.30	1.43	0.02	0.11	0.62	2.08	5.27	0.18	1.56	12.32	1.25
A10	PC PI				78.03	0.17	12.66	1.25	0.01	0.10	0.38	1.82	5.45	0.12	1.36	12.79	1.36
A11	PC PI				77.46	0.16	12.59	1.50	0.02	0.10	0.69	2.01	5.34	0.11	1.62	10.89	1.25
A12	PC PI				77.60	0.17	12.64	1.48	0.02	0.09	0.60	1.89	5.38	0.12	1.59	10.08	1.30
A13	PC PI				78.23	0.18	12.28	1.47	0.01	0.08	0.37	1.87	5.37	0.13	1.56	9.11	1.33
A14	PC PI				77.65	0.16	12.55	1.53	0.02	0.12	0.62	1.91	5.29	0.13	1.67	12.59	1.30
A15	PC PI				76.58	0.18	13.12	1.74	0.02	0.12	0.59	1.70	5.66	0.29	1.89	11.28	1.41
A16	PC PI				76.77	0.17	13.10	1.66	0.03	0.12	0.70	1.83	5.48	0.12	1.82	11.66	1.32
A18	PC PI				77.14	0.16	12.70	1.69	0.03	0.10	0.67	2.04	5.34	0.12	1.82	9.81	1.26
A19	PC PI				76.09	0.19	13.34	1.71	0.02	0.13	0.60	2.16	5.62	0.14	1.86	12.27	1.29
A21	PC PI				76.94	0.19	13.04	1.72	0.01	0.11	0.32	2.06	5.49	0.12	1.84	10.54	1.36
A22	PC PI				76.79	0.17	13.10	1.63	0.03	0.11	0.59	1.91	5.54	0.12	1.77	10.90	1.32
A23	PC PI				78.63	0.18	12.11	1.34	0.01	0.09	0.44	1.75	5.33	0.11	1.45	10.95	1.32
A24	PC PI				78.46	0.16	12.25	1.28	0.02	0.09	0.58	1.78	5.24	0.13	1.39	11.51	1.31
A25	PC PI				77.89	0.17	12.30	1.51	0.03	0.10	0.75	1.91	5.21	0.11	1.65	10.83	1.24
A26	PC PI				78.24	0.17	12.27	1.42	0.02	0.10	0.66	1.79	5.22	0.10	1.54	11.53	1.28
A27	PC PI				78.06	0.16	12.13	1.48	0.03	0.11	0.72	2.05	5.15	0.10	1.63	11.92	1.21
A28	PC PI				77.95	0.16	12.26	1.52	0.04	0.10	0.72	1.94	5.20	0.10	1.66	10.72	1.24
A29	PC PI				77.86	0.17	12.41	1.51	0.03	0.11	0.73	1.82	5.26	0.10	1.66	11.85	1.27
A30	PC PI				76.49	0.16	13.03	1.66	0.03	0.11	0.66	2.30	5.43	0.12	1.81	10.80	1.23
A31	PC PI				76.42	0.16	13.18	1.57	0.02	0.10	0.68	2.25	5.50	0.12	1.69	10.49	1.24
A32	PC PI				76.99	0.17	12.67	1.64	0.03	0.12	0.72	2.25	5.29	0.11	1.79	11.84	1.21
A36	PC PI				77.00	0.18	12.65	1.77	0.06	0.13	0.74	1.96	5.39	0.11	1.97	11.88	1.25
A38	PC PI				78.29	0.15	12.19	1.47	0.02	0.11	0.60	1.72	5.34	0.10	1.60	11.98	1.29
A39	PC PI				77.44	0.17	12.57	1.55	0.03	0.11	0.77	1.87	5.37	0.11	1.69	11.48	1.26
A40	PC PI				78.32	0.15	12.23	1.45	0.02	0.07	0.71	1.64	5.29	0.10	1.54	8.07	1.29
A1	PC-TI				75.22	0.18	13.47	1.57	0.03	0.19	0.76	2.62	5.83	0.12	1.79	17.87	1.15
A2	PC-TI				74.91	0.17	13.68	1.64	0.02	0.19	0.67	2.86	5.73	0.12	1.86	17.13	1.15
A3	PC-TI				75.11	0.17	13.50	1.77	0.04	0.18	0.74	2.71	5.64	0.13	1.99	15.39	1.16
A4	PC-TI				76.99	0.17	12.40	1.57	0.03	0.17	0.79	2.54	5.24	0.10	1.77	16.29	1.12
A5	PC-TI				76.94	0.18	12.48	1.61	0.03	0.18	0.78	2.35	5.27	0.16	1.83	16.84	1.18
A6	PC-TI				78.03	0.16	11.94	1.35	0.02	0.13	0.37	2.46	5.41	0.12	1.51	14.90	1.16
A20	PC-TI				77.47	0.19	12.74	1.46	0.01	0.14	0.69	1.83	5.36	0.11	1.61	15.01	1.30
A37	PC-TI				79.04	0.16	12.53	0.51	0.01	0.05	0.34	1.86	5.42	0.08	0.57	15.26	1.34
Pos1	PC-TI	33 06 20	18 00 14	148	77.11	0.17	12.48	1.41	0.02	0.15	0.57	2.48	5.50	0.11	1.58	16.08	1.16
Pos2	PC-TI	33 07 53	17 58 22	0	75.09	0.18	13.34	1.76	0.05	0.18	0.77	2.70	5.80	0.13	1.99	15.52	1.13
LQP1	PC-TI				75.22	0.18	13.47	1.57	0.03	0.19	0.76	2.62	5.83	0.12	1.79	17.87	1.15
LQP2	PC-TI				74.91	0.17	13.68	1.64	0.02	0.19	0.67	2.86	5.73	0.12	1.86	17.14	1.15
LQP3	PC-TI				75.11	0.17	13.50	1.77	0.04	0.18	0.74	2.71	5.64	0.13	1.99	15.39	1.16
LQP4	PC-TI				77.01	0.17	12.40	1.57	0.03	0.17	0.77	2.54	5.24	0.10	1.77	16.30	1.13
LQP6	PC-TI				76.78	0.18	12.46	1.61	0.03	0.18	0.78	2.55	5.26	0.16	1.82	16.85	1.14

* major and minor oxides normalised to 100 wt% volatile-free and with all Fe expressed as FeO^T; trace elements in ppm by wt

Mg# =100 × mol. Mg / (Mg + Fe)

ASI = mol. Al_2O_3 / (CaO - $3.33P_2O_5$ + Na_2O + K_2O)

Table 17: EA3.1 continued - Summary table of all Ignimbrites from the Postberg Eruption Centre

Sample	Abbr.	latitude S	longitude E	ht ASL	V	Cr	Ni	Cu	Zn	Rb	Sr	Y	Zr	Nb	Mo	Cs	Ba	Hf	Ta	Pb	Th	U	La	Ce	Pr	Nd	Sm	Eu	Gd	Tb	Dy	Ho	Er	Tm	Yb	Lu
		(deg min sec)	(deg min sec)	(m)																																
A35	PC-SI				11.00	7.00	2.00		40.00	238.00	86.00	41.00	176.00	15.00			717.00			33.00	19.00	3.00															
A33	PC-JI				22.00	9.00	2.00		53.00	217.00	124.00	48.00	290.00	19.00			943.00			36.00	26.00	3.00															
A34	PC-JI				31.00	11.00	7.00		60.00	198.00	141.00	52.00	380.00	21.00			1074.00			34.00	31.00	4.00															
MM01	PC-JI	33 08 43	17 59 34	2	22.80	87.00	15.05	13.50	63.00	219.65	93.90	39.65	235.90	21.95	5.46	6.35	808.50	6.86	1.37	34.75	19.39	3.72	48.15	101.65	11.77	44.90	8.95	1.36	7.91	1.23	7.14	1.43	4.23	0.65	3.59	0.59
MM02	PC-JI	33 08 54	18 00 06	1	29.70	144.15	15.10	14.90	60.65	204.55	94.80	39.70	257.45	21.25	10.25	8.63	719.00	7.41	1.29	32.25	19.05	5.43	48.40	103.30	11.59	42.60	8.30	1.51	7.51	1.28	7.56	1.55	4.11	0.55	4.23	0.52
MM03	PC-JI	33 08 02	17 58 20	5	35.90	213.20	11.85	16.05	56.60	196.95	121.25	41.65	260.00	20.40	13.90	6.44	896.50	7.24	1.41	32.50	22.23	3.93	56.65	117.85	13.68	50.80	9.85	1.76	8.80	1.46	8.10	1.62	4.77	0.53	3.92	0.55
A7	PC PI				5.00	3.00	2.00		32.00	271.00	51.00	43.00	114.00	13.00			322.00			29.00	17.00	5.00															
A8	PC PI				5.00	3.00	2.00		27.00	279.00	49.00	39.00	111.00	13.00			340.00			30.00	15.00	4.00															
A9	PC PI				6.00	3.00	2.00		32.00	275.00	63.00	45.00	113.00	14.00			320.00			31.00	17.00	4.00															
A10	PC PI				6.00	4.00	2.00		26.00	296.00	63.00	42.00	117.00	15.00			238.00			29.00	13.00	1.00															
A11	PC PI				4.00	7.00	2.00		38.00	293.00	42.00	49.00	116.00	15.00			266.00			30.00	18.00	6.00															
A12	PC PI				3.00	6.00	2.00		38.00	288.00	45.00	48.00	115.00	15.00			270.00			29.00	17.00	5.00															
A13	PC PI				4.00	3.00	2.00		27.00	296.00	48.00	46.00	122.00	16.00			255.00			29.00	17.00	6.00															
A14	PC PI				3.00	3.00	2.00		41.00	285.00	55.00	50.00	115.00	15.00			272.00			29.00	16.00	6.00															
A15	PC PI				4.00	12.00	15.00		35.00	327.00	61.00	55.00	129.00	17.00			245.00			30.00	18.00	8.00															
A16	PC PI				5.00	5.00	2.00		45.00	316.00	38.00	54.00	126.00	17.00			261.00			30.00	17.00	8.00															
A18	PC PI				5.00	12.00	2.00		42.00	296.00	40.00	51.00	123.00	16.00			250.00			30.00	17.00	7.00															
A19	PC PI				6.00	3.00	2.00		39.00	332.00	42.00	54.00	123.00	17.00			227.00			31.00	19.00	9.00															
A21	PC PI				7.00	3.00	2.00		24.00	293.00	49.00	46.00	125.00	17.00			255.00			32.00	18.00	5.00															
A22	PC PI				4.00	4.00	2.00		38.00	310.00	43.00	51.00	118.00	16.00			272.00			30.00	17.00	7.00															
A23	PC PI				6.00	3.00	2.00		32.00	273.00	55.00	41.00	116.00	14.00			332.00			30.00	14.00	4.00															
A24	PC PI				6.00	9.00	2.00		34.00	269.00	65.00	46.00	109.00	13.00			301.00			29.00	16.00	5.00															
A25	PC PI				5.00	7.00	2.00		36.00	265.00	48.00	44.00	108.00	13.00			310.00			30.00	17.00	6.00															
A26	PC PI				5.00	11.00	2.00		36.00	258.00	51.00	45.00	115.00	13.00			308.00			29.00	16.00	5.00															
A27	PC PI				3.00	9.00	2.00		36.00	262.00	49.00	44.00	115.00	12.00			331.00			29.00	14.00	6.00															
A28	PC PI				6.00	5.00	2.00		36.00	263.00	48.00	43.00	112.00	13.00			325.00			29.00	14.00	5.00															
A29	PC PI				5.00	8.00	2.00		37.00	270.00	46.00	45.00	114.00	13.00			309.00			32.00	17.00	7.00															
A30	PC PI				5.00	11.00	2.00		47.00	316.00	36.00	54.00	122.00	16.00			209.00			30.00	18.00	8.00															
A31	PC PI				4.00	3.00	2.00		42.00	323.00	33.00	57.00	119.00	17.00			205.00			27.00	16.00	7.00															
A32	PC PI				7.00	5.00	2.00		41.00	293.00	41.00	50.00	115.00	15.00			270.00			31.00	17.00	8.00															
A36	PC PI				7.00	7.00	5.00		36.00	271.00	49.00	47.00	118.00	14.00			339.00			30.00	16.00	7.00															
A38	PC PI				4.00	4.00	2.00		33.00	266.00	49.00	43.00	110.00	14.00			328.00			30.00	16.00	6.00															
A39	PC PI				6.00	7.00	2.00		41.00	267.00	52.00	45.00	122.00	14.00			341.00			30.00	15.00	6.00															
A40	PC PI				5.00	4.00	2.00		32.00	266.00	48.00	44.00	110.00	13.00			318.00			30.00	16.00	6.00															
A1	PC-TI									332.00	42.00	62.00	123.00	18.00			271.00				18.00	8.00															
A2	PC-TI									313.00	43.00	64.00	136.00	20.00			261.00				20.00	8.00															
A3	PC-TI									318.00	37.00	61.00	129.00	19.00			229.00				19.00	9.00															
A4	PC-TI									270.00	51.00	44.00	127.00	15.00			356.00				16.00	6.00															
A5	PC-TI									260.00	52.00	45.00	134.00	14.00			344.00				16.00	6.00															
A6	PC-TI				4.00	3.00	2.00		31.00	284.00	43.00	42.00	116.00	14.00			307.00			30.00	15.00	6.00															
A20	PC-TI				7.00	3.00	5.00		37.00	275.00	58.00	45.00	130.00	15.00			357.00			31.00	18.00	8.00															
A37	PC-TI				8.00	9.00	4.00		15.00	248.00	70.00	53.00	115.00	14.00			396.00			31.00	17.00	4.00															
Pos1	PC-TI	33 06 20	18 00 14	148	7.29	19.57	6.70	13.24	32.82	246.50	46.50	42.06	128.85	14.39	1.39	12.28	331.75	3.65	1.25	23.15	14.13	4.14	23.03	48.57	5.89	21.70	5.65	0.72	6.79	1.13	7.35	1.52	4.37	0.60	4.20	0.59
Pos2	PC-TI	33 07 53	17 58 22	0	7.55	11.65	11.13	19.14	41.20	296.78	41.29	50.38	125.93	15.93	2.31	12.62	282.39	4.17	1.57	25.06	15.29	7.52	23.88	50.84	6.09	24.49	6.17	0.64	6.41	1.25	8.38	1.73	4.94	0.71	4.63	0.70
LQP1	PC-TI									332.00	42.00	62.00	123.00	18.00			271.00						12.00	51.00		23.00										
LQP2	PC-TI									313.00	43.00	64.00	136.00	20.00			261.00						16.00	45.00		26.00										
LQP3	PC-TI									318.00	37.00	61.00	129.00	19.00			229.00						12.80	47.00		21.00										
LQP4	PC-TI									270.00	51.00	44.00	127.00	15.00			356.00						26.14	58.66	6.94	24.51	6.19	0.82	5.82	1.13	7.21	1.48	3.95	0.63	3.97	0.58
LQP6	PC-TI									260.00	52.00	45.00	134.00	14.00			344.00						27.15	60.94	7.17	26.49	6.34	0.82	6.17	1.07	6.88	1.34	3.86	0.61	3.93	0.55

Table 18: Table EA3.2 - Summary table of all Ignimbrites from the Saldanha Eruption Centre

Sample	Abbr.	latitude S	longitude E	ht ASL	SiO_2	TiO_2	Al_2O_3	FeO	MnO	MgO	CaO	Na_2O	K_2O	P_2O_5	FM	Mg#	ASI
		(deg min sec)	(deg min sec)	(m)													
B1	SC-SI				75.12	0.24	13.67	1.87	0.03	0.20	0.98	2.10	5.66	0.12	2.10	15.70	1.23
B2	SC-SI				74.48	0.26	13.91	2.00	0.03	0.21	1.19	2.03	5.77	0.12	2.24	15.62	1.22
B3	SC-SI				74.27	0.27	13.98	2.11	0.04	0.22	1.26	2.01	5.71	0.12	2.37	15.48	1.22
B6	SC-SI				74.46	0.26	14.00	1.98	0.03	0.23	1.21	1.99	5.73	0.11	2.23	16.92	1.23
B7	SC-SI				73.90	0.27	14.34	2.12	0.03	0.25	1.19	1.84	5.93	0.13	2.40	17.46	1.27
B8	SC-SI				77.49	0.17	12.71	1.53	0.02	0.14	0.76	1.69	5.38	0.11	1.69	14.02	1.31
B10, QP4	SC-SI				73.65	0.26	13.89	2.05	0.03	0.27	1.20	2.83	5.67	0.15	2.36	19.20	1.10
B11, QP5	SC-SI				73.67	0.26	13.88	2.06	0.02	0.28	1.17	2.82	5.70	0.13	2.36	19.70	1.10
B12, QP6	SC-SI				73.74	0.27	13.83	2.06	0.03	0.25	1.17	2.79	5.69	0.15	2.35	18.04	1.11
B13, QP7	SC-SI				73.73	0.27	13.84	2.07	0.02	0.24	1.19	2.80	5.67	0.16	2.33	17.25	1.11
B14, QP11	SC-SI				74.98	0.21	13.40	1.80	0.02	0.21	0.97	2.76	5.55	0.09	2.04	17.36	1.11
B15, QP16	SC-SI				74.53	0.22	13.55	1.82	0.02	0.22	1.07	2.74	5.73	0.10	2.06	17.89	1.09
B16, QP17	SC-SI				74.68	0.23	13.50	1.81	0.03	0.23	1.07	2.74	5.56	0.15	2.07	18.11	1.11
B24, QP41	SC-SI				74.36	0.22	13.62	1.83	0.02	0.25	0.95	2.77	5.83	0.14	2.10	19.84	1.11
B25, QP44	SC-SI				75.07	0.23	13.47	1.76	0.02	0.27	0.73	2.60	5.66	0.18	2.05	21.15	1.19
B26, QP46	SC-SI				75.22	0.22	13.42	1.70	0.02	0.25	0.70	2.63	5.67	0.16	1.97	20.44	1.18
CJA1	SC-SI	33 01 29.8	17 57 13.1	12	77.01	0.17	12.45	1.51	0.02	0.16	0.79	2.41	5.37	0.11	1.69	16.28	1.14
CJA3A5	SC-SI	33 00 23.2	17 56 21.5	44	77.12	0.17	12.46	1.49	0.03	0.14	0.78	2.35	5.34	0.11	1.66	14.61	1.15
CJA7	SC-SI	33 01 29.7	17 57 13.1	12	76.72	0.17	12.64	1.52	0.03	0.15	0.79	2.40	5.45	0.12	1.70	15.18	1.15
CJB9	SC-SI	33 01 43.1	17 57 15.2	7	77.08	0.17	12.49	1.45	0.02	0.14	0.70	2.43	5.39	0.12	1.61	14.93	1.16
CJB13A	SC-SI	33 02 00.4	17 56 02.3	5	77.61	0.17	12.30	1.44	0.02	0.16	0.60	2.33	5.27	0.11	1.61	16.17	1.19
CJB18A	SC-SI	33 02 50.4	17 54 29.2	10	75.58	0.21	13.28	1.63	0.03	0.19	0.90	2.42	5.62	0.12	1.86	17.37	1.16
CJB18B	SC-SI	33 02 47.0	17 54 10.9	4	74.97	0.22	13.27	1.61	0.02	0.20	0.91	2.89	5.77	0.13	1.83	18.04	1.07
CJB23	SC-SI	33 01 35.0	17 56 29.7	6	74.34	0.24	13.67	1.83	0.03	0.22	1.03	2.70	5.80	0.13	2.08	17.43	1.11
CJB26	SC-SI	33 01 42.1	17 57 20.3	11	77.14	0.17	12.42	1.57	0.02	0.15	0.75	2.38	5.28	0.11	1.74	14.88	1.16
CJB27	SC-SI	33 01 43.0	17 57 21.5	9	76.80	0.17	12.56	1.58	0.03	0.17	0.64	2.56	5.36	0.11	1.79	16.37	1.15
CJB28	SC-SI	33 01 44.2	17 57 21.4	5	77.00	0.16	12.54	1.46	0.02	0.14	0.74	2.39	5.44	0.11	1.62	14.93	1.15
MB10	SC-SI	33 01 41.8	17 57 14.3	9	77.12	0.16	12.49	1.45	0.03	0.14	0.72	2.36	5.41	0.11	1.62	14.93	1.16
MB11	SC-SI	33 01 41.4	17 57 13.5	9	77.18	0.16	12.54	1.42	0.02	0.14	0.70	2.35	5.38	0.11	1.58	15.26	1.17
MB12	SC-SI	33 02 01.2	17 56 05.8	5	76.86	0.18	12.67	1.49	0.02	0.15	0.73	2.42	5.36	0.11	1.66	15.50	1.17
MB22	SC-SI	33 01 35.9	17 56 27.2	7	73.19	0.27	14.34	1.94	0.03	0.29	1.18	2.67	5.97	0.13	2.26	20.81	1.13
MB26	SC-SI	33 01 43.0	17 57 19.8	8	76.51	0.18	12.81	1.61	0.02	0.15	0.77	2.48	5.35	0.11	1.78	14.51	1.16
WIG	SC-SI	32 59 52.0	17 52 24.0	3	73.47	0.27	14.21	2.03	0.03	0.29	1.14	2.58	5.85	0.13	2.35	20.06	1.15
WP8	SC-SI				76.67	0.17	12.67	1.50	0.02	0.14	0.80	2.43	5.48	0.11	1.67	14.54	1.14
WP12A	SC-SI	32 58 35.7	17 52 52.1	2	75.56	0.21	13.20	1.68	0.03	0.20	0.92	2.46	5.61	0.12	1.91	17.87	1.15
WP12B	SC-SI	32 58 35.7	17 52 52.1	2	75.87	0.21	12.97	1.65	0.02	0.20	0.87	2.49	5.59	0.12	1.86	17.61	1.13
WP18	SC-SI	33 01 38.6	17 57 09.2	4	74.80	0.22	13.49	1.79	0.03	0.20	1.02	2.54	5.76	0.12	2.03	16.88	1.13
Sal1	SC-SI	33 01 43.7	17 57 21.6	7	76.79	0.18	12.49	1.49	0.03	0.17	0.76	2.59	5.38	0.12	1.69	17.03	1.12
Sal 3	SC-SI	33 01 35.9	17 56 27.2	7	74.27	0.24	13.62	1.80	0.03	0.24	1.04	2.77	5.86	0.12	2.08	19.36	1.09
Sal3B	SC-SI	33 01 35.9	17 56 27.2	7	74.64	0.23	13.42	1.75	0.03	0.26	0.87	2.67	6.01	0.11	2.04	21.23	1.10

* major and minor oxides normalised to 100 wt% volatile-free and with all Fe expressed as FeO^T; trace elements in ppm by wt

Mg# =100 × mol. Mg / (Mg + Fe)

ASI = mol. Al_2O_3 / (CaO - $3.33P_2O_5$ + Na_2O + K_2O)

Table 18: EA3.2 continued - Summary table of all Ignimbrites from the Saldanha Eruption Centre

Sample	Abbr.	latitude S	longitude E	ht ASL	SiO_2	TiO_2	Al_2O_3	FeO	MnO	MgO	CaO	Na_2O	K_2O	P_2O_5	FM	Mg#	ASI
		(deg min sec)	(deg min sec)	(m)													
B4	SC-JI				72.74	0.35	14.59	2.55	0.05	0.33	1.51	2.06	5.67	0.14	2.94	18.73	1.22
B5	SC-JI				72.74	0.35	14.58	2.58	0.04	0.35	1.54	2.12	5.56	0.14	2.97	19.56	1.22
B9, QP3	SC-JI				72.82	0.35	14.16	2.55	0.04	0.39	1.03	2.55	5.95	0.16	2.98	21.43	1.17
B17, QP18	SC-JI				71.01	0.41	14.77	2.85	0.03	0.46	1.67	3.07	5.52	0.20	3.34	22.22	1.09
B18, QP19	SC-JI				71.05	0.41	14.74	2.89	0.03	0.48	1.66	3.07	5.49	0.19	3.40	22.70	1.09
B19, QP20	SC-JI				71.22	0.42	14.66	2.81	0.04	0.47	1.67	3.06	5.45	0.21	3.32	22.88	1.09
B20, QP21	SC-JI				71.22	0.40	14.67	2.80	0.04	0.46	1.67	3.08	5.47	0.20	3.29	22.61	1.08
B21, QP23	SC-JI				71.78	0.39	14.51	2.70	0.03	0.38	1.47	2.92	5.67	0.13	3.12	20.22	1.09
B22, QP24	SC-JI				72.04	0.38	14.44	2.71	0.04	0.39	1.48	2.89	5.44	0.17	3.15	20.58	1.12
B23, QP25	SC-JI				71.82	0.38	14.53	2.66	0.04	0.40	1.52	2.94	5.53	0.18	3.10	21.03	1.11
B27, QP52	SC-JI				72.70	0.32	14.21	2.42	0.02	0.34	1.38	2.93	5.60	0.09	2.78	19.84	1.08
B28, QP53	SC-JI				72.57	0.31	14.26	2.44	0.02	0.35	1.38	2.95	5.58	0.12	2.82	20.49	1.09
B29, QP54	SC-JI				72.66	0.35	14.15	2.41	0.03	0.37	1.38	2.92	5.59	0.13	2.82	21.66	1.08
B30, QP58	SC-JI				72.99	0.33	13.98	2.45	0.04	0.38	1.36	2.89	5.40	0.17	2.87	21.86	1.10
B31, QP60	SC-JI				72.91	0.32	14.02	2.43	0.03	0.38	1.38	2.93	5.45	0.15	2.85	21.86	1.09
B32, QP63	SC-JI				73.48	0.31	13.67	2.37	0.03	0.36	1.24	2.87	5.47	0.19	2.76	21.52	1.10
CJA3	SC-JI	33 00 18.1	17 56 22.1	53	71.31	0.41	14.80	2.84	0.04	0.45	1.69	2.76	5.53	0.17	3.33	22.05	1.12
CJA5	SC-JI	33 00 18.1	17 56 22.1	53	71.16	0.39	14.86	2.84	0.04	0.42	1.60	2.81	5.72	0.16	3.30	20.92	1.11
CJB13B	SC-JI	33 01 14.9	17 55 04.3	44	70.20	0.46	15.22	3.09	0.04	0.51	1.91	2.87	5.52	0.17	3.64	22.76	1.11
CJB15	SC-JI	33 02 28.2	17 55 45.4	5	70.82	0.45	14.92	3.09	0.05	0.51	1.79	2.76	5.43	0.18	3.65	22.57	1.12
CJB16	SC-JI	33 02 50.4	17 54 58.7	6	71.59	0.39	14.83	2.64	0.04	0.39	1.44	2.73	5.78	0.17	3.07	20.83	1.15
CJB17	SC-JI	33 03 04.4	17 54 38.3	6	71.12	0.39	15.00	2.67	0.04	0.40	1.58	2.78	5.85	0.16	3.11	21.09	1.12
CJB19	SC-JI	33 02 21.8	17 53 48.7	3	71.30	0.39	14.82	2.73	0.04	0.46	1.67	2.75	5.67	0.16	3.24	23.08	1.11
CJB20	SC-JI	33 01 45.6	17 53 30.9	3	70.90	0.41	15.03	2.80	0.04	0.46	1.74	2.82	5.63	0.16	3.31	22.73	1.11
CJB22	SC-JI	33 01 35.6	17 56 23.8	10	72.87	0.30	14.39	2.15	0.03	0.32	1.26	2.70	5.84	0.14	2.50	20.71	1.13
CJB30	SC-JI	33 01 18.0	17 54 52.6	48	70.63	0.45	15.04	3.03	0.05	0.51	1.78	2.81	5.52	0.18	3.60	23.08	1.12
MB1	SC-JI	33 02 58.0	17 55 41.9	91	70.95	0.42	14.90	2.97	0.05	0.46	1.68	2.75	5.64	0.17	3.48	21.68	1.12
MB2	SC-JI	33 02 03.0	17 55 37.3	70	70.94	0.41	14.92	2.73	0.04	0.43	1.67	2.89	5.81	0.16	3.20	21.75	1.09
MB5	SC-JI	33 02 16.3	17 55 41.8	61	70.25	0.43	15.32	2.99	0.04	0.49	1.87	2.86	5.57	0.17	3.52	22.74	1.12
MB6	SC-JI	33 02 04.7	17 55 47.3	64	70.96	0.44	14.85	3.03	0.04	0.50	1.69	2.75	5.57	0.17	3.57	22.78	1.12
MB7A	SC-JI	33 02 06.9	17 55 32.7	94	71.53	0.39	14.76	2.71	0.04	0.43	1.53	2.75	5.70	0.16	3.18	21.99	1.13
MB7B	SC-JI	33 02 08.4	17 55 18.2	91	71.51	0.39	14.86	2.66	0.04	0.41	1.67	2.80	5.50	0.15	3.11	21.46	1.12
WP11	SC-JI	32 58 52.6	17 52 52.3	2	72.33	0.36	14.42	2.60	0.04	0.37	1.40	2.67	5.67	0.15	3.00	20.18	1.14
WP16	SC-JI	32 58 11.0	17 53 08.0	5	73.36	0.32	13.87	2.38	0.03	0.33	1.33	2.63	5.60	0.15	2.74	19.72	1.11
WP25A	SC-JI	32 56 26.0	17 53 11.0	5	71.45	0.40	14.70	2.85	0.04	0.45	1.61	2.72	5.61	0.16	3.34	21.94	1.12
WP25B	SC-JI	32 56 26.0	17 53 11.0	5	71.69	0.40	14.60	2.78	0.04	0.43	1.55	2.71	5.64	0.16	3.25	21.60	1.12
WP29	SC-JI	32 59 52.0	17 52 24.0	3	69.96	0.46	15.31	3.16	0.05	0.52	1.88	2.86	5.61	0.18	3.73	22.75	1.11
WP30	SC-JI	32 59 52.0	17 52 24.0	3	72.03	0.36	14.56	2.57	0.05	0.36	1.49	2.75	5.67	0.16	2.98	19.84	1.12
WP31A	SC-JI	32 59 25.0	17 52 55.0	14	73.73	0.31	13.82	2.24	0.04	0.32	1.14	2.53	5.72	0.14	2.60	20.10	1.14
WP31B	SC-JI	32 59 25.0	17 52 55.0	14	72.20	0.36	14.41	2.58	0.04	0.39	1.52	2.75	5.58	0.16	3.01	21.24	1.11
Sal5	SC-JI	33 02 01.6	17 56 03.4	7	71.17	0.40	14.64	2.79	0.05	0.49	1.62	3.04	5.63	0.16	3.33	23.64	1.07
Sal 6	SC-JI	33 02 01.2	17 56 05.9	5	71.60	0.40	14.43	2.81	0.06	0.52	1.46	2.94	5.59	0.19	3.39	24.70	1.10
Sal 7	SC-JI	32 59 23.8	17 52 55.0	14	71.89	0.38	14.35	2.67	0.04	0.45	1.55	2.97	5.52	0.16	3.17	23.26	1.08
Sal8	SC-JI	32 59 51.5	17 52 24.6	3	70.16	0.49	15.08	2.98	0.05	0.52	1.86	3.12	5.57	0.17	3.54	23.60	1.07

Table 18: EA3.2 continued - Summary table of all Ignimbrites from the Saldanha Eruption Centre

Sample	Abbr.	latitude S	longitude E	ht ASL	V	Cr	Ni	Cu	Zn	Rb	Sr	Y	Zr	Nb	Mo	Cs	Ba	Hf	Ta	Pb	Th	U	La	Ce	Pr	Nd	Sm	Eu	Gd	Tb	Dy	Ho	Er	Tm	Yb	Lu
		(deg min sec)	(deg min sec)	(m)																																
B1	SC-SI				10	5	2.0		42	225	88	45	169	15	1.0		642			34	21	5.0															
B2	SC-SI				12	11	2.0		42	240	90	44	187	15	1.0		673			35	21	3.0															
B3	SC-SI				13	22	2.0		45	237	94	44	193	15	1.0		704			36	22	5.0															
B6	SC-SI				12	12	2.0		43	242	89	44	177	15	1.0		682			36	21	4.0															
B7	SC-SI				14	7.0	2.0		44	240	89	45	199	16	1.0		708			35	22	4.0															
B8	SC-SI				6.0	13	2.0		36	262	50	46	117	14	1.0		325			30	15	5.0															
B10, QP4	SC-SI									235	92	44	222	16			731				20	5.0	45	98	12	42	8.8	1.4	7.9	1.2	7.4	1.4	3.7	0.60	4.0	0.54
B11, QP5	SC-SI									247	86	43	197	16			739				21	5.0	46	100	12	42	8.3	1.4	8.3	1.3	7.7	1.4	3.9	0.55	3.6	0.51
B12, QP6	SC-SI									233	88	43	211	16			706				19	5.0	41	87	10	39	8.2	1.4	7.3	1.2	7.0	1.3	3.4	0.51	3.5	0.52
B13, QP7	SC-SI									239	90	44	218	16			697				20	5.0	41	90	11	39	7.9	1.4	7.3	1.2	7.2	1.3	3.6	0.60	3.9	0.48
B14, QP11	SC-SI									269	76	44	167	16			558				18	6.0	35	76	8.5	33	7.6	1.2	6.6	1.1	7.1	1.4	3.7	0.58	4.0	0.55
B15, QP16	SC-SI									247	87	39	168	15			702				19	5.0	41	85	10	35	7.9	1.3	7.3	1.2	7.2	1.3	3.6	0.61	3.9	0.48
B16, QP17	SC-SI									237	89	41	198	15			702				18	5.0	39	83	9.6	35	7.3	1.4	6.8	1.1	6.8	1.4	3.7	0.55	3.8	0.52
B24, QP41	SC-SI									231	87	41	175	15			648				18	3.0	35	77	9.1	34	7.5	1.3	6.9	1.2	6.8	1.3	3.7	0.57	3.7	0.53
B25, QP44	SC-SI									249	85	42	178	16			631				18	3.0	36	80	9.0	34	6.9	1.2	6.0	1.0	6.6	1.3	3.5	0.54	3.6	0.53
B26, QP46	SC-SI									257	84	39	175	16			627				18	3.0	36	75	9	32	7.1	1.2	6.0	1.0	6.3	1.2	3.3	0.51	3.5	0.52
CJA1	SC-SI	33 01 29.8	17 57 13.1	12	11	9.8	5.7	14	34	216	41	28	87		2.1	7.9	303	2.5	1.0	29	10	5.9	19	46	5.1	18	4.3	0.62	4.6	0.76	4.8	1.0	2.9	0.41	2.7	0.38
CJA3A5	SC-SI	33 00 23.2	17 56 21.5	44	10		4.0	16	41	285	46	35	105		2.4	12	339	3.5	1.4	39	14	8.3	23	56	6.2	23	6.0	0.74	5.8	1.0	6.7	1.4	3.8	0.54	3.9	0.50
CJA7	SC-SI	33 01 29.7	17 57 13.1	12	11	8.9	4.5	24	45	292	50	35	106		2.7	11	408	3.6	1.4	42	14	8.6	24	59	6.6	24	6.0	0.92	6.1	1.1	6.7	1.4	4.2	0.61	4.0	0.53
CJB9	SC-SI	33 01 43.1	17 57 15.2	7	8.2	9.9	6.0	13	48	273	41	33	90		0.84	12	301	2.7	1.2	33	12	4.7	20	49	5.6	20	5.0	0.59	4.5	0.88	5.4	1.2	3.3	0.46	3.1	0.44
CJB13A	SC-SI	33 02 00.4	17 56 02.3	5	8.6	12	114	15	44	234	37	30	85	15	2.3	7.6	287	2.7	1.1	31	11	6.8	19	47	5.1	19	4.6	0.59	4.4	0.82	5.5	1.1	3.1	0.45	3.0	0.38
CJB18A	SC-SI	33 02 50.4	17 54 29.2	10	13	8.3	5.7	15	46	243	58	30	113		1.1	11	478	3.3	1.1	36	12	4.5	25	60	6.5	23	5.3	0.90	4.8	0.86	5.4	1.1	3.1	0.43	2.8	0.38
CJB18B	SC-SI	33 02 47.0	17 54 10.9	4	11	12	122	7.7	44	228	54	30	112	14	1.1	9.9	462	3.3	1.0	33	12	4.1	25	59	6.6	23	5.3	0.89	4.9	0.89	5.4	1.1	3.1	0.45	2.8	0.37
CJB23	SC-SI	33 01 35.0	17 56 29.7	6	13	12	134	6.9	51	225	62	29	125	16	0.84	11	554	3.7	1.1	34	13	3.4	27	66	7.4	26	5.8	0.96	5.1	0.87	5.5	1.1	2.8	0.39	2.9	0.37
CJB26	SC-SI	33 01 42.1	17 57 20.3	11	9.8	9.2	117	19	50	246	40	33	96	16	2.2	9.4	284	3.0	1.3	35	12	6.6	20	49	5.4	20	5.2	0.61	4.8	0.88	6.0	1.2	3.4	0.48	3.3	0.42
CJB27	SC-SI	33 01 43.0	17 57 21.5	9	9.4	5.5	112	17	48	247	42	31	92	15	2.1	8.1	302	2.7	1.2	35	12	7.0	20	49	5.4	19	4.8	0.62	4.7	0.88	5.5	1.1	3.3	0.45	3.1	0.42
CJB28	SC-SI	33 01 44.2	17 57 21.4	5	9.9	9.1	119	7.3	44	253	41	31	87	16	1.6	11	291	2.7	1.1	33	11	5.8	19	47	5.3	19	5.0	0.63	4.3	0.82	5.4	1.2	3.2	0.45	3.2	0.40
MB10	SC-SI	33 01 41.8	17 57 14.3	9	8.1	14	5.2	7.3	48	241	42	32	91		0.73	10	320	2.8	1.2	35	12	4.5	20	48	5.4	20	4.9	0.65	4.7	0.89	5.5	1.2	3.4	0.45	3.2	0.42
MB11	SC-SI	33 01 41.4	17 57 13.5	9	8.8	9.5	5.1	8.4	43	252	41	30	85		2.0	9.9	298	2.7	1.1	33	11	6.9	19	47	5.4	18	4.8	0.61	4.3	0.82	5.3	1.1	3.3	0.45	3.0	0.40
MB12	SC-SI	33 02 01.2	17 56 05.8	5	24	8.1	71	9.5	71	203	100	36	240	19	2.2	8.3	851	4.6	1.2	43	16	3.2	50	109	9.2	34	7.2	1.30	6.0	0.95	6.1	1.2	3.4	0.46	3.1	0.41
MB22	SC-SI	33 01 35.9	17 56 27.2	7	16	11	135	8.1	53	222	88	32	164	17	0.63	7.4	753	6.5	1.2	40	20	4.8	37	84	12	45	9.1	1.4	7.9	1.2	7.1	1.3	3.6	0.50	3.2	0.46
MB26	SC-SI	33 01 43.0	17 57 19.8	8	9.4	11	81	8.4	47	248	39	33	92	16	2.4	11	267	2.9	1.3	33	12	7.6	20	49	5.5	20	5.0	0.55	4.7	0.89	6.0	1.3	3.5	0.53	3.3	0.47
WIG	SC-SI	32 59 52.0	17 52 24.0	3	16	32	101	14	41	209	72	29	152	15	1.0	8.9	596	4.0	1.0	33	14	3.8	31	71	7.7	29	6.0	1.1	5.7	0.90	5.1	1.0	2.9	0.43	2.7	0.39
WP8	SC-SI				9.4	8.1	108	18	49	249	49	33	106	14	2.4	12	380	3.3	1.2	37	13	7.0	23	54	6.1	22	5.3	0.71	5.2	0.89	6.0	1.2	3.5	0.49	3.2	0.41
WP12A	SC-SI	32 58 35.7	17 52 52.1	2	13		134	25	52	274	67	38	137	18	1.0	12	553	4.3	1.5	44	17	5.4	32	75	8.4	31	7.0	1.0	7.2	1.1	7.2	1.4	4.2	0.60	4.0	0.53
WP12B	SC-SI	32 58 35.7	17 52 52.1	2	22	14	94	12	58	265	91	36	212	21	1.8	12	779	4.3	1.4	41	16	8.1	46	107	7.8	29	6.7	1.0	7.0	1.1	7.0	1.4	4.0	0.57	3.7	0.54
WP18	SC-SI	33 01 38.6	17 57 09.2	4	14	14	138	14	49	280	68	35	132	18	0.63	13	572	4.1	1.4	46	17	4.6	32	76	8.6	31	7.5	1.2	6.7	1.1	6.8	1.3	4.0	0.55	3.6	0.48
Sal1	SC-SI	33 01 43.7	17 57 21.6	7	12	12	5.1	14	40	241	48	46	120	15	2.1	9.6	317	4.1	1.4	24	16	6.6	26	54	6.7	25	6.1	0.69	6.3	1.1	7.7	1.7	4.9	0.66	4.7	0.66
Sal 3	SC-SI	33 01 35.9	17 56 27.2	7	14	22	6.1	15	38	211	67	40	157	15	0.62	9.6	544	4.9	1.2	26	17	3.2	33	68	8.1	32	7.4	1.06	6.9	1.1	7.4	1.4	4.3	0.57	3.8	0.57
Sal3B	SC-SI	33 01 35.9	17 56 27.2	7	16	11	6.4	10	40	243	75	44	179	15	1.0	11	600	5.5	1.1	29	18	3.2	36	74	9.0	34	8.1	1.19	8.1	1.4	8.3	1.6	4.6	0.63	4.3	0.55

Table 18: EA3.2 continued - Summary table of all Ignimbrites from the Saldanha Eruption Centre

Sample	Abbr.	latitude S	longitude E	ht ASL	V	Cr	Ni	Cu	Zn	Rb	Sr	Y	Zr	Nb	Mo	Cs	Ba	Hf	Ta	Pb	Th	U	La	Ce	Pr	Nd	Sm	Eu	Gd	Tb	Dy	Ho	Er	Tm	Yb	Lu
		(deg min sec)	(deg min sec)	(m)																																
B4	SC-JI				18	6	2		51	232	109	48	258	17	2.0		795			35	24	4.0															
B5	SC-JI				19	8	2		53	232	106	49	261	18	2.0		753			35	27	5.0															
B9, QP3	SC-JI									250	101	33	244	16			878				20	4.0	46	98	11	41	8.0	1.5	6.3	0.96	5.5	1.1	2.8	0.43	3.0	0.45
B17, QP18	SC-JI									235	125	49	316	21			987				26	4.0	68	138	16	59	11	1.9	9.6	1.5	8.1	1.6	4.1	0.64	3.9	0.61
B18, QP19	SC-JI									216	120	46	325	20			929				23	4.0	62	130	14	54	10	1.9	9.4	1.4	8.1	1.5	3.9	0.63	3.7	0.58
B19, QP20	SC-JI									229	125	47	336	20			1002				25	4.0	67	138	16	58	11	1.9	9.2	1.4	8.3	1.5	4.0	0.60	4.0	0.60
B20, QP21	SC-JI									221	126	47	329	20			990				25	4.0	66	135	16	58	11	1.9	9.2	1.4	8.3	1.6	4.0	0.58	4.0	0.56
B21, QP23	SC-JI									233	110	46	295	21			874				26	5.0	60	124	14	54	11	1.7	10	1.5	7.9	1.5	4.2	0.59	3.9	0.58
B22, QP24	SC-JI									227	116	48	306	20			879				25	5.0	58	120	14	54	10	1.7	8.8	1.4	8.0	1.5	4.1	0.65	4.1	0.55
B23, QP25	SC-JI									225	117	48	398	20			931				24	5.0	61	127	15	55	11	1.9	9.8	1.5	8.5	1.7	4.2	0.60	4.2	0.61
B27, QP52	SC-JI									247	100	46	243	18			757				23	4.0	53	110	12	48	9.4	1.5	8.5	1.3	7.7	1.5	4.1	0.55	3.7	0.55
B28, QP53	SC-JI									233	98	45	272	17			766				24	4.0	54	114	14	50	10	1.6	8.6	1.4	7.8	1.5	4.2	0.58	4.1	0.63
B29, QP54	SC-JI									233	98	44	241	19			799				24	5.0	54	111	13	46	9.4	1.5	8.0	1.4	7.5	1.5	4.3	0.59	3.8	0.58
B30, QP58	SC-JI									231	97	46	268	18			724				23	6.0	51	108	12	47	9.1	1.5	8.4	1.4	7.6	1.5	3.8	0.60	4.1	0.57
B31, QP60	SC-JI									245	95	45	267	19			727				21	6.0	49	104	12	44	9.1	1.6	8.6	1.3	7.8	1.5	4.0	0.57	3.7	0.59
B32, QP63	SC-JI									234	103	45	244	17			760				24	5.0	52	108	13	47	9.2	1.6	8.0	1.3	7.7	1.6	4.1	0.63	4.2	0.59
CJA3	SC-JI	33 00 18.1	17 56 22.1	53	29	12	8	18	55	203	100	34	237		1.9	8.5	852	6.1	1.3	34	19	4.3	51	115	13	45	8.8	1.6	8.0	1.2	6.5	1.2	3.3	0.48	3.2	0.44
CJA5	SC-JI	33 00 18.1	17 56 22.1	53	30	17	117	17	75	264	118	42	274	26	2.4	13	1143	7.87	1.8	51	25	6.8	62	140	15	56	11	1.9	11	1.5	8.5	1.7	4.5	0.62	4.4	0.56
CJB13B	SC-JI	33 01 14.9	17 55 04.3	44	30	13	7	10	68	201	109	34	277		2.5	9.1	935	7.07	1.3	38	21	5.0	57	132	14	52	9.4	1.6	7.7	1.1	6.7	1.3	3.5	0.45	3.0	0.44
CJB15	SC-JI	33 02 28.2	17 55 45.4	5	30	19	83	19	54	203	117	44	345	24	2.2	9.4	926	8.74	1.6	32	25	5.2	68	139	16	61	11	1.8	9.5	1.5	8.4	1.8	4.6	0.62	4.1	0.57
CJB16	SC-JI	33 02 50.4	17 54 58.7	6	26	11	84	18	64	213	97	32	217	20	2.0	7.8	826	5.65	1.2	40	18	4.2	46	104	11	41	8.2	1.4	6.6	1.0	6.2	1.2	3.3	0.43	3.0	0.41
CJB17	SC-JI	33 03 04.4	17 54 38.3	6	25	15	99	15	69	216	105	36	243	21	2.3	8.6	952	6.51	1.4	42	21	5.6	51	113	13	46	9.6	1.6	7.6	1.1	6.9	1.3	3.5	0.51	3.5	0.45
CJB19	SC-JI	33 02 21.8	17 53 48.7	3	25	21	92	22	45	199	132	47	322	21	1.7	8.3	1031	8.55	1.5	29	26	4.7	66	131	16	58	12	1.9	10	1.4	8.5	1.8	4.8	0.69	4.3	0.63
CJB20	SC-JI	33 01 45.6	17 53 30.9	3	27	14	94	14	65	204	105	35	249	21	1.7	8.5	923	6.55	1.3	40	20	4.3	53	121	13	47	9.6	1.6	7.7	1.1	6.6	1.3	3.5	0.48	3.2	0.45
CJB22	SC-JI	33 01 35.6	17 56 23.8	10	19	14	111	15	51	221	85	32	193	18	0.79	8.2	721	5.45	1.2	40	17	3.4	38	87	10	35	7.5	1.3	6.3	1.1	5.9	1.2	3.2	0.44	3.0	0.41
CJB30	SC-JI	33 01 18.0	17 54 52.6	48	30	21	104	16	65	208	105	34	270	22	2.4	9.0	851	6.84	1.3	40	21	5.0	56	128	14	50	9.6	1.5	7.4	1.2	6.6	1.3	3.5	0.47	3.1	0.43
MB1	SC-JI	33 02 58.0	17 55 41.9	91	29	19	74	8	71	202	108	41	287	22	1.9	9.2	877	7.58	1.4	37	22	5.3	57	124	14	53	10	1.6	8.3	1.2	7.6	1.6	4.1	0.59	3.8	0.51
MB2	SC-JI	33 02 03.0	17 55 37.3	70	10	10	124	6	46	236	42	31	95	15	1.7	8.4	303	3.13	1.2	33	12	6.6	21	50	6	20	5.1	0.61	4.8	0.9	5.8	1.1	3.3	0.47	3.2	0.44
MB5	SC-JI	33 02 16.3	17 55 41.8	61	29	10	86	12	74	202	110	35	268	22	2.0	8.8	901	7.12	1.3	40	21	5.1	56	126	14	50	9.5	1.6	7.8	1.2	7.0	1.3	3.5	0.48	3.4	0.47
MB6	SC-JI	33 02 04.7	17 55 47.3	64	31	25	80	13	76	205	111	43	318	24	1.6	8.4	909	8.21	1.6	37	25	4.5	62	135	15	56	11	1.6	9.6	1.4	8.3	1.6	4.5	0.59	3.9	0.53
MB7A	SC-JI	33 02 06.9	17 55 32.7	94	24	10	102	12	67	212	97	34	232	21	2.2	9.5	818	6.38	1.3	41	20	5.4	49	112	12	45	9.2	1.4	7.5	1.2	6.8	1.3	3.3	0.49	3.3	0.48
MB7B	SC-JI	33 02 08.4	17 55 18.2	91	25	15	109	8	67	211	98	34	239	20	2.0	9.6	769	6.27	1.2	41	19	4.7	49	111	12	45	8.8	1.4	7.1	1.1	6.6	1.3	3.3	0.45	3.1	0.44
WP11	SC-JI	32 58 52.6	17 52 52.3	2	27		115	20	62	260	96	40	240	23	2.2	12	851	7.01	1.6	48	22	6.4	52	122	13	48	9.9	1.6	9.2	1.4	8.0	1.5	4.4	0.62	4.1	0.61
WP16	SC-JI	32 58 11.0	17 53 08.0	5	13	11	138	16	47	268	61	37	133	17	2.6	11	492	6.15	1.5	48	20	5.4	30	70	12	43	8.5	1.5	8.6	1.2	7.3	1.5	4.1	0.60	3.9	0.50
WP25A	SC-JI	32 56 26.0	17 53 11.0	5	27		102	21	62	213	96	35	239	21	2.3	9.0	774	6.21	1.3	38	19	5.5	50	110	12	45	8.9	1.4	8.1	1.2	6.6	1.3	3.5	0.49	3.3	0.46
WP25B	SC-JI	32 56 26.0	17 53 11.0	5	26	25	89	24	60	204	91	33	230	20	1.9	8.2	712	6.04	1.2	36	18	4.8	46	106	12	43	8.2	1.4	7.7	1.2	6.4	1.1	3.3	0.45	3.1	0.42
WP29	SC-JI	32 59 52.0	17 52 24.0	3	31	14	104	21	66	195	114	36	283	22	1.9	7.2	934	7.26	1.3	37	21	4.7	57	125	14	51	9.6	1.7	8.7	1.2	6.8	1.3	3.3	0.52	3.3	0.49
WP30	SC-JI	32 59 52.0	17 52 24.0	3	22		82	22	55	227	84	33	200	19	1.9	8.9	684	5.23	1.2	36	17	4.9	42	96	10	39	8.2	1.3	7.5	1.1	6.2	1.2	3.3	0.45	3.0	0.41
WP31A	SC-JI	32 59 25.0	17 52 55.0	14	24	12	99	13	54	213	86	33	215	19	1.8	9.2	674	5.79	1.3	36	18	5.3	43	96	11	39	8.3	1.3	7.6	1.1	6.1	1.3	3.4	0.49	3.2	0.43
WP31B	SC-JI	32 59 25.0	17 52 55.0	14	18		106	10	43	210	72	31	168	16	1.4	8.9	580	4.37	1.1	34	15	3.8	34	78	9	32	6.6	1.1	6.5	0.9	5.8	1.1	3.1	0.44	3.0	0.41
Sal5	SC-JI	33 02 01.6	17 56 03.4	7	27	18	10	27	66	196	108	48	336	21	1.9	8.0	862	9.4	1.6	31	26	4.6	64	128	15	58	11	1.7	10	1.6	8.9	1.7	4.8	0.69	4.5	0.64
Sal 6	SC-JI	33 02 01.2	17 56 05.9	5	27	17	11	20	60	196	111	48	311	21	1.1	6.2	809	9.0	1.6	31	27	3.7	64	129	15	58	12	1.6	11	1.6	9.1	1.8	5.0	0.64	4.4	0.67
Sal 7	SC-JI	32 59 23.8	17 52 55.0	14	27	20	16	19	61	208	104	48	308	20	2.0	9.4	816	8.6	1.6	30	26	4.7	62	125	15	56	11	1.8	10	1.6	8.9	1.8	5.0	0.68	4.6	0.64
Sal8	SC-JI	32 59 51.5	17 52 24.6	3	31	17	8	25	66	182	120	48	360	21	2.0	7.3	921	9.5	1.5	30	28	4.6	73	144	17	64	12	2.0	11	1.6	9.5	1.8	4.8	0.69	4.4	0.64

7.4 Electronic Appendix EA4 – Whole-rock control standards for major and trace elements used to calibrate XRF and LA-ICP-MS instruments at the University of Stellenbosch.

Table 19: EA4.1 - Whole-rock Analytical details- Internal standards/ Control standards for Major Elements

Electronic Appendix EA4, Table 4.1 Whole-rock Analytical details- Internal standards/ Control standards for Major Elements

Sample name		Al2O3	CaO	Cr2O3	Fe2O3	K2O	MgO	MnO	Na2O	P2O5	SiO2	TiO2	L.O.I.	Sum Of Conc.
Basalt Reference values														
Basalt Reference values		**13.71**	**11.4**	**0.04**	**12.36**	**0.54**	**7.22**	**0.17**	**2.31**	**0.27**	**49.82**	**2.73**	**0.52**	**101.08**
BHVO-1	MajorBasic32+Zn	13.64	11.3	0.03	12.31	0.52	7.13	0.17	2.23	0.27	49.38	2.72	0.52	100.21
BHVO-1 std	MajorBasic32+Zn	13.75	11.4	0.04	12.28	0.52	7.20	0.17	2.22	0.27	49.94	2.73	0.52	101.04
MONITOR BHVO-1	MajorBasic32+Zn	13.79	11.4	0.04	12.29	0.52	7.24	0.17	2.24	0.28	49.89	2.74	0.52	101.12
MONITOR BHVO-1	Majors Acid32	13.49	11.6	0.02	12.36	0.52	7.19	0.17	2.18	0.27	50.36	2.92	0.52	101.57
BHVO-1 MONITOR	Majors Acid32	13.48	11.5	0.02	12.34	0.52	7.17	0.17	2.14	0.27	50.11	2.91	0.52	101.14
BHVO-1 MONITOR	MajorBasic32+Zn	13.75	11.4	0.04	12.26	0.52	7.16	0.17	2.25	0.27	50.00	2.74	0.52	101.08
BHVO-1 MONITOR	Majors Acid32	13.55	11.5	0.02	12.36	0.53	7.18	0.17	2.15	0.28	50.14	2.90	0.52	101.27
MONITOR BHVO-1	MajorBasic32+Zn	13.74	11.4	0.04	12.27	0.53	7.19	0.16	2.20	0.27	49.86	2.74	0.52	100.94
MONITOR BHVO-1	MajorBasic32+Zn	13.72	11.4	0.04	12.30	0.52	7.12	0.17	2.21	0.28	49.95	2.74	0.52	100.98
MONITOR BHVO-1	Majors Acid32	13.48	11.5	0.02	12.35	0.53	7.16	0.17	2.14	0.28	50.46	2.89	0.52	101.52
MONITOR BHVO-1	MajorBasic32+Zn	13.71	11.4	0.04	12.27	0.53	7.19	0.17	2.22	0.28	49.91	2.73	0.52	100.97
MONITOR bhvo-1	MajorBasic32+Zn	13.71	11.4	0.04	12.26	0.52	7.20	0.16	2.28	0.28	50.03	2.73	0.52	101.12
MONITOR BHVO-1	MajorBasic32+Zn	13.73	11.5	0.03	12.33	0.52	7.21	0.17	2.23	0.28	50.12	2.74	0.52	101.33
MONITOR BHVO-1	Majors Acid32	13.44	11.5	0.02	12.35	0.52	7.21	0.17	2.15	0.28	50.25	2.91	0.52	101.33
MONITOR BHVO-1	MajorBasic32+Zn	13.72	11.4	0.04	12.29	0.52	7.15	0.17	2.29	0.27	50.02	2.75	0.52	101.18
MONITOR BHVO-1	MajorBasic32+Zn	13.74	11.4	0.04	12.27	0.52	7.18	0.17	2.21	0.28	50.17	2.73	0.52	101.25
MONITOR bhvo-1	MajorBasic32+Zn	13.78	11.4	0.04	12.32	0.52	7.17	0.17	2.24	0.28	50.29	2.72	0.52	101.45
MONITOR BHVO-1	MajorBasic32+Zn	13.68	11.3	0.04	12.27	0.52	7.15	0.17	1.73	0.27	50.12	2.73	0.52	100.50
MONITOR BHVO-1	MajorBasic32+Zn	13.71	11.4	0.04	12.25	0.53	7.24	0.17	2.24	0.27	49.84	2.73	0.52	100.94
MONITOR bhvo-1	MajorBasic32+Zn	13.81	11.4	0.04	12.27	0.52	7.16	0.17	2.22	0.29	50.09	2.73	0.52	101.19
MONITOR bhvo-1	Majors Acid32	13.55	11.5	0.02	12.33	0.53	7.17	0.17	2.13	0.28	50.18	2.90	0.52	101.29
MONITOR bhvo-1	MajorBasic32+Zn	13.82	11.4	0.04	12.27	0.52	7.19	0.16	2.25	0.28	49.99	2.73	0.52	101.16
MONITOR bhvo-1	Majors Acid32	13.46	11.5	0.02	12.36	0.52	7.20	0.17	2.15	0.28	50.26	2.91	0.52	101.34
MONITOR BHVO-1	MajorBasic32+Zn	13.76	11.4	0.04	12.30	0.52	7.17	0.17	2.23	0.27	50.15	2.75	0.52	101.30
MONITOR BHVO-1	Majors Acid32	13.54	11.5	0.02	12.36	0.53	7.20	0.18	2.15	0.28	50.45	2.91	0.52	101.64
MONITOR BHVO-1	Majors Acid32	13.55	11.5	0.02	12.37	0.53	7.20	0.18	2.19	0.28	50.44	2.90	0.52	101.67
MONITOR BHVO-1	MajorBasic32+Zn	13.67	11.5	0.04	12.30	0.52	7.17	0.17	2.23	0.28	50.18	2.74	0.52	101.32
MONITOR BHVO-1	Majors Acid32	13.48	11.5	0.02	12.35	0.52	7.17	0.17	2.15	0.29	50.39	2.89	0.52	101.43
MONITOR BHVO-1	MajorBasic32+Zn	13.61	11.5	0.03	12.29	0.51	7.18	0.17	2.20	0.28	50.17	2.75	0.52	101.18
MONITOR BHVO-1	MajorBasic32+Zn	13.77	11.5	0.04	12.26	0.51	7.17	0.17	2.27	0.27	49.90	2.72	0.52	101.06
MONITOR BHVO-1	MajorBasic32+Zn	13.69	11.4	0.03	12.30	0.51	7.11	0.17	2.24	0.27	50.10	2.73	0.52	101.11
MONITOR BHV01	MajorBasic32+Zn	13.70	11.5	0.04	12.27	0.52	7.20	0.17	2.24	0.28	50.15	2.76	0.52	101.37
MONITOR bhvo-1	Majors Acid32	13.41	11.5	0.02	12.35	0.52	7.16	0.17	2.05	0.28	50.18	2.90	0.52	101.06
MONITOR BHVO-1	MajorBasic32+Zn	13.73	11.5	0.04	12.31	0.53	7.17	0.18	2.23	0.28	50.00	2.74	0.52	101.21
MONITOR BHVO-1	Majors Acid32	13.44	11.6	0.02	12.36	0.52	7.19	0.17	2.16	0.28	50.48	2.89	0.52	101.58
Average		13.63	11.4		12.32	0.52	7.19	0.17	2.20	0.27	49.94	2.80	0.52	101.02
Relative standard deviation (%)		0.58	0.35		0.36	3.70	0.47	0.00	4.68	0.74	0.23	2.71		0.06

PANalytical

Results quantitative - MajorBasic32+Zn

Major element analysis by XRF, Rh Tube, 3kWatt

BDL = Below Detection Limit

Note: LOI = weight loss or gain at 1000ºC.

LOI (loss on ignition) includes the total of volatiles content of the rock (including the water combined to the lattice of silicate minerals) and the gain on ignition related to the oxidation of the rock (mostly due to Fe).

Concentration in %. LOI: loss on ignition

Table 19: EA4.1 continued - Whole-rock Analytical details- Internal standards/ Control standards for Major Elements

Sample name		Al2O3	CaO	Cr2O3	Fe2O3	K2O	MgO	MnO	Na2O	P2O5	SiO2	TiO2	L.O.I.	Sum Of Conc.
JG-1														
Granodiorite Reference values		**14.20**	**2.18**	**0.01**	**2.14**	**3.97**	**0.74**	**0.06**	**3.39**	**0.10**	**72.30**	**0.26**		**99.35**
JG-1 STD	Majors Interm32	14.14	2.17	0.01	2.12	4.01	0.73	0.07	3.35	0.10	72.95	0.25		99.90
STANDARD JG-1	Majors Acid32	14.34	2.19	0.01	2.12	4.02	0.78	0.07	3.60	0.10	72.13	0.27		99.63
JG-1 std	Majors Acid32	14.44	2.20	0.01	2.14	4.03	0.77	0.07	3.63	0.10	72.80	0.26		100.45
JG-1 std	Majors Acid32	14.37	2.20	0.01	2.13	4.02	0.78	0.07	3.56	0.09	72.72	0.26		100.21
JG-1 STD	Majors Acid32	14.45	2.21	0.01	2.12	4.02	0.77	0.06	3.68	0.10	72.48	0.26		100.16
JG-1 STD	Majors Acid32	14.36	2.21	0.01	2.13	4.03	0.77	0.07	3.67	0.10	72.57	0.27		100.19
JG-1 std	Majors Acid32	14.37	2.21	0.01	2.13	4.02	0.79	0.07	3.66	0.10	72.18	0.26		99.80
JG-1 STD	Majors Acid32	14.34	2.21	0.01	2.13	4.03	0.78	0.06	3.61	0.10	72.19	0.27		99.73
JG-1 std	Majors Acid32	14.13	2.21	0.01	2.13	4.02	0.75	0.07	3.43	0.09	72.03	0.26		99.13
J-G std	Majors Acid32	14.12	2.21	0.01	2.13	3.98	0.75	0.07	3.42	0.10	71.98	0.26		99.03
JG-1 STD	Majors Acid32	14.03	2.20	0.01	2.13	4.00	0.77	0.06	3.46	0.10	71.95	0.26		98.97
JG-1 STD	Majors Acid32	14.11	2.21	0.01	2.13	4.00	0.76	0.07	3.42	0.10	72.13	0.26		99.20
JG-1 STD	Majors Acid32	14.00	2.21	0.01	2.13	3.99	0.75	0.07	3.44	0.10	72.02	0.26		98.98
JG-1 std	Majors Acid32	14.06	2.21	0.01	2.13	4.01	0.76	0.07	3.43	0.10	72.05	0.26		99.09
JG-1 STD	Majors Acid32	14.00	2.20	0.01	2.13	4.01	0.77	0.07	3.44	0.10	71.81	0.26		98.80
JG-1 STD	Majors Acid32	13.99	2.20	0.01	2.13	4.00	0.78	0.06	3.39	0.10	71.98	0.26		98.90
JG-1 std	Majors Acid32	14.04	2.19	0.01	2.13	3.99	0.76	0.07	3.36	0.10	71.80	0.26		98.71
JG-1 std	Majors Acid32	13.98	2.20	0.01	2.13	4.01	0.74	0.07	3.41	0.10	71.66	0.26		98.57
JG-1 std	Majors Acid32	13.95	2.20	0.01	2.13	4.02	0.76	0.07	3.38	0.10	71.97	0.26		98.85
JG-1 std	Majors Acid32	14.01	2.20	0.01	2.13	4.00	0.74	0.06	3.42	0.10	71.88	0.26		98.81
JG-1 STD	Majors Acid32	14.01	2.19	0.01	2.12	3.98	0.75	0.07	3.43	0.10	71.72	0.26		98.64
JG-1 STD	Majors Acid32	14.01	2.20	0.01	2.13	3.99	0.75	0.07	3.39	0.10	71.96	0.26		98.87
JG-1 STD	Majors Acid32	13.94	2.17	0.01	2.12	4.00	0.73	0.07	3.24	0.09	71.76	0.26		98.39
JG-1 STD	Majors Acid32	13.83	2.17	0.01	2.12	3.98	0.74	0.07	3.25	0.10	71.65	0.25		98.17
JG-1 std	Majors Acid32	13.79	2.18	0.01	2.13	3.98	0.73	0.07	3.20	0.10	71.63	0.26		98.08
JG-1 STD	Majors Acid32	13.85	2.19	0.01	2.13	3.98	0.74	0.07	3.29	0.10	71.69	0.26		98.31
Average		14.10	2.20	0.01	2.13	4.00	0.76	0.07	3.44	0.10	72.07	0.26	#DIV/0!	99.14
Relative standard deviation (%)		0.69	0.81	6.38	0.56	0.87	2.39	8.06	1.61	1.90	0.33	0.15		0.21

Table 19: EA4.1 continued - Whole-rock Analytical details- Internal standards/ Control standards for Major Elements

Sample name		Al2O3	CaO	Cr2O3	Fe2O3	K2O	MgO	MnO	Na2O	P2O5	SiO2	TiO2	L.O.I.	Sum Of Conc.
NIM-G Granite Reference values		**12.08**	**0.78**	**0.00**	**2.02**	**4.99**	**0.06**	**0.02**	**3.36**	**0.01**	**75.70**	**0.09**		**99.11**
NIM-G STD	Majors Acid32	12.26	0.82	0.00	1.99	5.01	0.08	0.02	3.41	0.01	75.76	0.10		99.46
NIM-G STD	Majors Acid32	12.20	0.82	0.00	1.99	5.01	0.07	0.02	3.37	0.02	75.85	0.09		99.44
NIM-G STD	Majors Acid32	12.25	0.81	0.00	1.98	5.01	0.07	0.02	3.38	0.01	75.70	0.10		99.33
STANDARD Nim-G	Majors Acid32	12.26	0.80	0.00	1.98	4.98	0.08	0.02	3.37	0.01	75.43	0.10		99.03
NIM-G std	Majors Acid32	12.30	0.81	0.00	1.99	5.01	0.07	0.02	3.35	0.01	76.31	0.09		99.96
NIM-G std	Majors Acid32	12.27	0.81	0.00	1.98	5.01	0.07	0.02	3.34	0.01	75.97	0.09		99.57
NIM-G STD	Majors Acid32	12.18	0.81	0.00	1.98	4.98	0.07	0.02	3.36	0.01	76.02	0.10		99.53
NIM-G STD	Majors Acid32	12.14	0.81	0.00	1.98	4.99	0.07	0.02	3.40	0.02	75.74	0.10		99.27
NIM-G std	Majors Acid32	12.16	0.80	0.00	1.99	5.02	0.07	0.02	3.39	0.01	75.77	0.10		99.33
NIM-G STD	Majors Acid32	12.17	0.81	0.00	1.99	5.00	0.07	0.02	3.34	0.02	75.41	0.10		98.93
NIM-G std	Majors Acid32	11.94	0.82	0.00	1.99	4.97	0.07	0.02	3.22	0.01	75.43	0.09		98.56
NIM-G std	Majors Acid32	12.00	0.81	0.00	1.98	4.96	0.07	0.02	3.20	0.01	75.50	0.08		98.63
NIM-G STD	Majors Acid32	11.93	0.80	0.00	1.98	4.97	0.07	0.02	3.19	0.02	75.41	0.08		98.47
NIM-G STD	Majors Acid32	12.03	0.81	0.00	1.99	4.97	0.07	0.02	3.20	0.02	75.17	0.08		98.36
NIM-G STD	Majors Acid32	12.03	0.81	0.00	1.99	4.99	0.07	0.02	3.19	0.02	75.38	0.08		98.58
NIM-G std	Majors Acid32	11.96	0.81	0.00	1.99	4.97	0.06	0.02	3.20	0.01	75.46	0.08		98.56
NIM-G STD	Majors Acid32	12.01	0.81	0.00	1.99	4.97	0.07	0.02	3.22	0.02	75.23	0.08		98.42
NIM-G STD	Majors Acid32	11.96	0.81	0.00	1.98	4.98	0.07	0.02	3.18	0.02	75.29	0.08		98.39
NIM-G std	Majors Acid32	11.96	0.80	0.00	1.99	4.99	0.07	0.02	3.15	0.01	75.34	0.08		98.41
NIM-G std	Majors Acid32	11.90	0.80	0.00	1.99	4.98	0.07	0.02	3.16	0.02	75.13	0.08		98.15
NIM-G std	Majors Acid32	11.95	0.81	0.00	1.99	4.98	0.07	0.02	3.21	0.02	75.20	0.08		98.33
NIM-G std	Majors Acid32	11.91	0.81	0.00	1.98	4.99	0.07	0.02	3.17	0.02	75.15	0.08		98.20
NIM-G STD	Majors Acid32	11.88	0.81	0.00	1.98	4.98	0.07	0.02	3.17	0.02	75.44	0.09		98.46
NIM-G STD	Majors Acid32	11.95	0.81	0.00	1.99	4.97	0.07	0.02	3.19	0.02	75.39	0.08		98.49
Average		12.07	0.81	0.00	1.99	4.99	0.07	0.02	3.27	0.02	75.52	0.09	#DIV/0!	98.83
Relative standard deviation (%)		0.11	3.74	100.00	1.69	0.06	17.36	0.00	2.83	54.17	0.24	2.31		0.29

Table 19: EA4.1 continued - Whole-rock Analytical details- Internal standards/ Control standards for Major Elements

Sample name		Al2O3	CaO	Cr2O3	Fe2O3	K2O	MgO	MnO	Na2O	P2O5	SiO2	TiO2	L.O.I.	Sum Of Conc.
Quality control for 2010-2011														
Average HUSG		**13.75**	**1.52**	**0.00**	**3.78**	**4.66**	**1.04**	**0.06**	**2.57**	**0.21**	**69.77**	**0.54**	**0.73**	**98.65**
STDEV		**0.20**	**0.04**	**0.00**	**0.14**	**0.06**	**0.04**	**0.01**	**0.18**	**0.01**	**0.54**	**0.02**	**0.05**	**0.71**
MIN		**13.04**	**1.48**	**0.00**	**3.64**	**4.55**	**0.94**	**0.05**	**2.30**	**0.20**	**68.42**	**0.52**	**0.53**	**97.23**
MAX		**14.30**	**1.63**	**0.01**	**4.56**	**4.80**	**1.22**	**0.08**	**3.30**	**0.23**	**70.96**	**0.60**	**0.80**	**100.40**
HUSG STD	Majors Acid32	13.87	1.58	0.00	3.75	4.68	1.11	0.06	2.74	0.22	70.73	0.56	0.90	100.20
HUSG STD	Majors Interm32	13.87	1.56	0.01	3.75	4.65	1.11	0.06	2.69	0.23	70.81	0.56	0.90	100.20
HUSG-1 std	Majors Acid32	13.84	1.57	0.00	3.74	4.67	1.11	0.05	2.73	0.22	70.51	0.56	0.90	99.90
HUSG-1 std	Majors Acid32	13.84	1.56	0.01	3.73	4.65	1.11	0.06	2.71	0.22	70.37	0.56	0.90	99.72
HUSG-1 STD	Majors Interm32	13.76	1.57	0.01	3.74	4.65	1.11	0.06	2.71	0.21	70.36	0.54	0.90	99.62
HUSG-1 std	Majors Acid32	13.69	1.58	0.01	3.75	4.68	1.11	0.06	2.64	0.22	70.63	0.56	0.90	99.83
HUS-G std	Majors Acid32	13.68	1.57	0.01	3.74	4.64	1.10	0.05	2.63	0.22	70.58	0.57	0.90	99.69
HUSG-1 STD	Majors Acid32	13.59	1.58	0.01	3.74	4.65	1.11	0.06	2.61	0.23	70.61	0.57	0.90	99.66
HUSG-1 STD	Majors Acid32	13.67	1.57	0.01	3.74	4.62	1.10	0.06	2.63	0.23	70.34	0.56	0.90	99.43
HUSG-1 STD	Majors Acid32	13.69	1.57	0.01	3.75	4.65	1.10	0.06	2.63	0.23	70.39	0.56	0.90	99.54
HUSG-1 std	Majors Acid32	13.69	1.57	0.01	3.76	4.65	1.10	0.06	2.61	0.22	70.41	0.57	0.90	99.55
HUSG-1 STD	Majors Acid32	13.75	1.57	0.00	3.75	4.65	1.08	0.06	2.62	0.22	70.41	0.57	0.90	99.58
HUS-G std	MajorBasic32+Zn	13.90	1.56	0.00	3.72	4.66	1.00	0.05	2.69	0.22	71.37	0.54	0.90	100.61
HUS-G STD	MajorBasic32+Zn	13.87	1.54	0.00	3.71	4.65	1.02	0.05	2.03	0.22	70.36	0.55	0.90	98.90
HUSG-1 STD	Majors Acid32	13.63	1.57	0.00	3.73	4.66	1.10	0.06	2.66	0.23	70.59	0.57	0.90	99.70
HUS-G std	Majors Acid32	13.67	1.55	0.00	3.73	4.64	1.09	0.06	2.60	0.22	70.60	0.58	0.90	99.64
HUSG-1 std	Majors Acid32	13.66	1.57	0.00	3.74	4.67	1.09	0.06	2.61	0.22	70.43	0.57	0.90	99.52
HUSG-1 std	Majors Acid32	13.65	1.57	0.00	3.74	4.67	1.10	0.06	2.61	0.22	70.48	0.56	0.90	99.56
HUSG-1 std	Majors Acid32	13.61	1.57	0.00	3.74	4.63	1.10	0.06	2.62	0.23	70.41	0.56	0.90	99.43
HUSG-1 STD	Majors Acid32	13.67	1.56	0.00	3.74	4.63	1.10	0.06	2.64	0.22	70.52	0.56	0.90	99.60
HUSG-1 STD	Majors Acid32	13.69	1.56	0.00	3.74	4.64	1.10	0.06	2.62	0.22	70.52	0.56	0.90	99.61
HUSG-1 STD	Majors Acid32	13.66	1.57	0.00	3.74	4.64	1.11	0.06	2.60	0.22	70.39	0.56	0.90	99.45
HUS-G STD	Majors Acid32	13.62	1.55	0.00	3.74	4.66	1.08	0.06	2.50	0.22	70.40	0.56	0.90	99.29
HUSG-1 STD	Majors Acid32	13.53	1.54	0.00	3.73	4.66	1.10	0.06	2.54	0.22	70.55	0.56	0.90	99.39
HUSG-1 std	Majors Acid32	13.53	1.55	0.00	3.73	4.63	1.08	0.06	2.47	0.22	70.52	0.56	0.90	99.25
HUSG-1 STD	Majors Acid32	13.63	1.58	0.00	3.75	4.64	1.11	0.05	2.60	0.23	70.63	0.56	0.90	99.68
Average		13.79	1.57	0.01	3.74	4.66	1.11	0.06	2.69	0.22	70.57	0.56	0.90	99.88
Relative standard deviation (%)		0.34	3.20	45.08	0.89	0.10	6.17	11.31	4.82	3.53	1.15	2.98	23.28	1.25

Table 19: EA4.1 continued - Whole-rock Analytical details- Internal standards/ Control standards for Major Elements

Sample name		Al2O3	CaO	Cr2O3	Fe2O3	K2O	MgO	MnO	Na2O	P2O5	SiO2	TiO2	L.O.I.	Sum Of Conc.
WITS-G														
Granite Reference values		**11.53**	**1.51**		**3.58**	**4.46**	**0.10**	**0.05**	**2.97**	**0.04**	**74.53**	**0.29**	**0.08**	**99.14**
WITS-G		**11.73**	**1.44**		**3.43**	**4.29**	**0.21**	**0.03**	**2.39**	**0.05**	**74.26**	**0.29**	**0.07**	**98.19**
WITS-G (AUG)		**12.01**	**1.46**		**3.51**	**4.26**	**0.05**	**0.02**	**2.39**	**0.06**	**74.56**	**0.30**	**0.07**	**98.69**
WITS-G (OCT)		**11.52**	**1.47**		**3.47**	**4.33**	**0.00**	**0.05**	**2.37**	**0.03**	**73.57**	**0.28**	**0.07**	**97.14**
WITS-G (DEC)		**11.45**	**1.47**		**3.50**	**4.39**	**0.06**	**0.05**	**2.45**	**0.04**	**75.45**	**0.28**	**0.07**	**99.22**
Average reference value		**11.65**	**1.47**		**3.50**	**4.34**	**0.08**	**0.04**	**2.51**	**0.04**	**74.47**	**0.29**	**0.07**	**98.48**
WITS-G STD	Majors Acid32	11.77	1.50	0.00	3.46	4.43	0.09	0.05	2.68	0.04	75.13	0.31	0.07	**99.53**
WITS-G STD	Majors Interm32	11.79	1.48	0.00	3.46	4.42	0.08	0.05	2.62	0.03	75.57	0.30	0.07	**99.87**
WITS-G std	Majors Acid32	11.81	1.49	0.00	3.46	4.43	0.09	0.05	2.67	0.04	75.03	0.31	0.07	**99.45**
WITS-G std	Majors Acid32	11.80	1.49	0.00	3.46	4.43	0.08	0.05	2.64	0.04	74.89	0.31	0.07	**99.26**
WITS-G STD	Majors Interm32	11.69	1.47	0.01	3.45	4.41	0.08	0.05	2.61	0.03	75.04	0.30	0.07	**99.21**
WITS-G STD	Majors Acid32	11.73	1.49	0.00	3.45	4.43	0.08	0.05	2.68	0.04	74.92	0.31	0.07	**99.25**
WITS-G std	Majors Acid32	11.63	1.49	0.00	3.46	4.42	0.09	0.05	2.56	0.04	74.90	0.30	0.07	**99.01**
WITS-G STD	Majors Interm32	11.62	1.47	0.00	3.47	4.40	0.08	0.05	2.56	0.03	75.32	0.29	0.07	**99.36**
WITS-G std	Majors Acid32	11.62	1.49	0.00	3.47	4.42	0.10	0.05	2.54	0.04	75.13	0.30	0.07	**99.23**
WITS-G STD	Majors Acid32	11.55	1.48	0.00	3.45	4.41	0.09	0.05	2.55	0.03	75.03	0.30	0.07	**99.01**
WITS-G STD	Majors Acid32	11.59	1.49	0.00	3.46	4.41	0.09	0.05	2.54	0.04	74.99	0.30	0.07	**99.03**
WITS-G STD	Majors Acid32	11.64	1.48	0.00	3.47	4.41	0.10	0.05	2.62	0.04	75.02	0.30	0.07	**99.20**
WITS-G std	Majors Acid32	11.64	1.49	0.00	3.47	4.42	0.09	0.05	2.59	0.04	75.11	0.30	0.07	**99.27**
WITS-G STD	Majors Acid32	11.65	1.49	0.00	3.46	4.41	0.10	0.05	2.56	0.04	74.92	0.31	0.07	**99.06**
WITS-G STD	Majors Acid32	11.61	1.48	0.00	3.45	4.42	0.09	0.05	2.59	0.04	75.06	0.31	0.07	**99.17**
WITS-G std	Majors Acid32	11.70	1.48	0.00	3.46	4.40	0.10	0.05	2.56	0.04	75.21	0.30	0.07	**99.37**
WITS-G std	Majors Acid32	11.65	1.48	0.00	3.47	4.43	0.10	0.05	2.58	0.04	74.83	0.30	0.07	**99.00**
WITS-G std	Majors Acid32	11.63	1.49	0.00	3.47	4.44	0.09	0.05	2.60	0.04	75.14	0.31	0.07	**99.33**
WITS-G std	Majors Acid32	11.71	1.49	0.00	3.47	4.42	0.10	0.05	2.58	0.04	75.30	0.30	0.07	**99.53**
WITS-G STD	Majors Acid32	11.62	1.47	0.00	3.46	4.43	0.09	0.05	2.58	0.04	75.27	0.30	0.07	**99.38**
WITS-G STD	Majors Acid32	11.70	1.48	0.00	3.47	4.42	0.10	0.05	2.59	0.04	75.19	0.30	0.07	**99.41**
WITS-G STD	Majors Acid32	11.57	1.49	0.00	3.47	4.44	0.09	0.05	2.60	0.04	75.21	0.30	0.07	**99.33**
WITS-G STD	Majors Acid32	11.50	1.48	0.00	3.47	4.43	0.10	0.05	2.47	0.04	75.19	0.30	0.07	**99.10**
WITS-G STD	Majors Acid32	11.53	1.47	0.00	3.45	4.41	0.10	0.05	2.44	0.04	74.92	0.30	0.07	**98.78**
WITS-G std	Majors Acid32	11.48	1.47	0.00	3.47	4.40	0.10	0.05	2.49	0.04	75.09	0.29	0.07	**98.95**
WITS-G STD	Majors Acid32	11.61	1.49	0.00	3.46	4.41	0.10	0.05	2.57	0.04	74.94	0.31	0.07	**99.05**
Average		11.69	1.49	0.00	3.46	4.42	0.08	0.05	2.64	0.04	75.13	0.31	0.07	99.46
Relative standard deviation (%)		1.36	1.59		3.41	0.81	16.00	0.00	10.98	10.00	0.81	5.52	12.50	0.33

7.5 Electronic Appendix EA5 – U-Pb Dating quality control data tables.

Table 20: EA5.1 - Quality Control result summary for MM samples displaying Plesovice U-Pb results summary

Electronic Appendix EA5, Table EA5.1 Quality Control result summary for MM samples displaying Plesovice U-Pb results summary

						RATIOS							AGES [Ma]						Conc.
Sample	Analysis	U [ppm][a]	Pb [ppm][a]	$^{206}Pb/^{204}Pb$	Th/U meas	$^{207}Pb/^{235}U$[b]	2 s[d]	$^{206}Pb/^{238}U$[b]	2 s[d]	rho[c]	$^{207}Pb/^{206}Pb$[e]	2 s[d]	$^{207}Pb/^{235}U$	2 s	$^{206}Pb/^{238}U$	2 s	$^{207}Pb/^{206}Pb$	2 s	%
PL	A_009	829	45	14095	0.08	0.399	0.014	0.0538	0.0011	0.61	0.0537	0.0015	341	12	338	7	360	62	94
PL	A_010	796	43	13985	0.08	0.400	0.014	0.0544	0.0011	0.62	0.0534	0.0014	342	12	341	7	346	60	99
PL	A_011	811	44	20776	0.08	0.403	0.014	0.0544	0.0011	0.62	0.0537	0.0014	344	12	341	7	358	61	95
PL	A_038	653	35	211808	0.08	0.395	0.013	0.0542	0.0011	0.62	0.0528	0.0014	338	11	340	7	321	59	106
PL	A_039	644	35	208829	0.08	0.398	0.013	0.0542	0.0011	0.62	0.0532	0.0014	340	11	340	7	337	59	101
PL	A_072	594	32	21774	0.08	0.396	0.013	0.0540	0.0011	0.61	0.0532	0.0014	339	11	339	7	339	60	100
PL	A_073	666	36	215591	0.10	0.394	0.013	0.0539	0.0011	0.62	0.0530	0.0014	337	11	338	7	331	59	102
PL	A_135	600	33	55995	0.08	0.404	0.020	0.0546	0.0012	0.46	0.0537	0.0023	344	17	343	8	357	98	96
PL	A_136	641	35	196769	0.08	0.397	0.015	0.0539	0.0012	0.58	0.0535	0.0017	340	13	338	8	348	70	97
PL	A_137	426	23	131437	0.08	0.395	0.017	0.0542	0.0012	0.51	0.0528	0.0020	338	15	340	8	322	86	106
PL	A_097	504	27	198214	0.08	0.395	0.015	0.0540	0.0012	0.60	0.0530	0.0016	338	13	339	8	329	68	103
PL	A_098	504	28	6760	0.08	0.402	0.015	0.0545	0.0012	0.60	0.0535	0.0016	343	13	342	8	349	67	98
PL	A_100	457	25	6926	0.08	0.405	0.015	0.0547	0.0012	0.60	0.0537	0.0016	345	13	343	8	360	66	95
PL	A_101	587	32	16542	0.12	0.406	0.014	0.0537	0.0012	0.63	0.0549	0.0015	346	12	337	7	407	61	83
PL	A_102	553	30	216227	0.10	0.402	0.015	0.0538	0.0012	0.61	0.0543	0.0016	343	12	338	8	381	65	89
PL	A_103	523	28	8836	0.09	0.408	0.015	0.0544	0.0012	0.60	0.0544	0.0016	348	13	342	8	387	65	88
average						0.400		0.0542			0.0535		342		340		352		

[a]U and Pb concentrations and Th/U ratios are calculated relative to GJ-1 reference zircon

[b]Corrected for background and within-run Pb/U fractionation and normalised to reference zircon GJ-1 (ID-TIMS values/measured value); $^{207}Pb/^{235}U$ calculated using ($^{207}Pb/^{206}Pb$)/($^{238}U/^{206}Pb$ * 1/137.88)

[c]Rho is the error correlation defined as the quotient of the propagated errors of the $^{206}Pb/^{238}U$ and the $^{207}/^{235}U$ ratio

[d]Quadratic addition of within-run errors (2 SD) and daily reproducibility of GJ-1 (2 SD)

[e]Corrected for mass-bias by normalising to GJ-1 reference zircon (~0.6 per atomic mass unit) and common Pb using the model Pb composition of Stacey & Kramers (1975)

Table 21: EA5.2 - Quality Control result summary for MM samples displaying M127 U-Pb results summary

Electronic Appendix EA5, Table EA5.2 Quality Control result summary for MM samples displaying M127 U-Pb results summary

						RATIOS							AGES [Ma]						Conc.
Sample	Analysis	U [ppm][a]	Pb [ppm][a]	$^{206}Pb/^{204}Pb$	Th/U meas	$^{207}Pb/^{235}U$[b]	2 s[d]	$^{206}Pb/^{238}U$[b]	2 s[d]	rho[c]	$^{207}Pb/^{206}Pb$[e]	2 s[d]	$^{207}Pb/^{235}U$	2 s	$^{206}Pb/^{238}U$	2 s	$^{207}Pb/^{206}Pb$	2 s	%
M127	A_012	1020	87	49963	0.42	0.677	0.022	0.0848	0.0018	0.65	0.0579	0.0014	525	17	525	11	526	54	100
M127	A_013	1026	88	24211	0.42	0.695	0.022	0.0860	0.0018	0.65	0.0586	0.0014	536	17	532	11	553	53	96
M127	A_040	854	73	67218	0.42	0.682	0.021	0.0857	0.0018	0.65	0.0577	0.0014	528	17	530	11	519	52	102
M127	A_041	859	73	7730	0.42	0.688	0.022	0.0853	0.0018	0.65	0.0586	0.0014	532	17	527	11	550	52	96
M127	A_042	832	72	429552	0.42	0.689	0.022	0.0863	0.0018	0.65	0.0579	0.0014	532	17	533	11	527	52	101
M127	A_074	855	73	309392	0.42	0.681	0.021	0.0854	0.0018	0.65	0.0579	0.0014	528	17	528	11	526	52	100
M127	A_075	838	72	110352	0.43	0.681	0.021	0.0856	0.0018	0.65	0.0577	0.0014	527	17	530	11	518	53	102
M127	A_076	880	75	26043	0.43	0.678	0.022	0.0849	0.0018	0.65	0.0580	0.0014	526	17	525	11	528	53	99
M127	A_099	716	61	443010	0.42	0.684	0.023	0.0850	0.0019	0.64	0.0583	0.0015	529	18	526	12	542	57	97
average						0.684		0.0854			0.0581		529		528		532		

[a]U and Pb concentrations and Th/U ratios are calculated relative to GJ-1 reference zircon

[b]Corrected for background and within-run Pb/U fractionation and normalised to reference zircon GJ-1 (ID-TIMS values/measured value); $^{207}Pb/^{235}U$ calculated using $(^{207}Pb/^{206}Pb)/(^{238}U/^{206}Pb * 1/137.88)$

[c]Rho is the error correlation defined as the quotient of the propagated errors of the $^{206}Pb/^{238}U$ and the $^{207}/^{235}U$ ratio

[d]Quadratic addition of within-run errors (2 SD) and daily reproducibility of GJ-1 (2 SD)

[e]Corrected for mass-bias by normalising to GJ-1 reference zircon (~0.6 per atomic mass unit) and common Pb using the model Pb composition of Stacey & Kramers (1975)

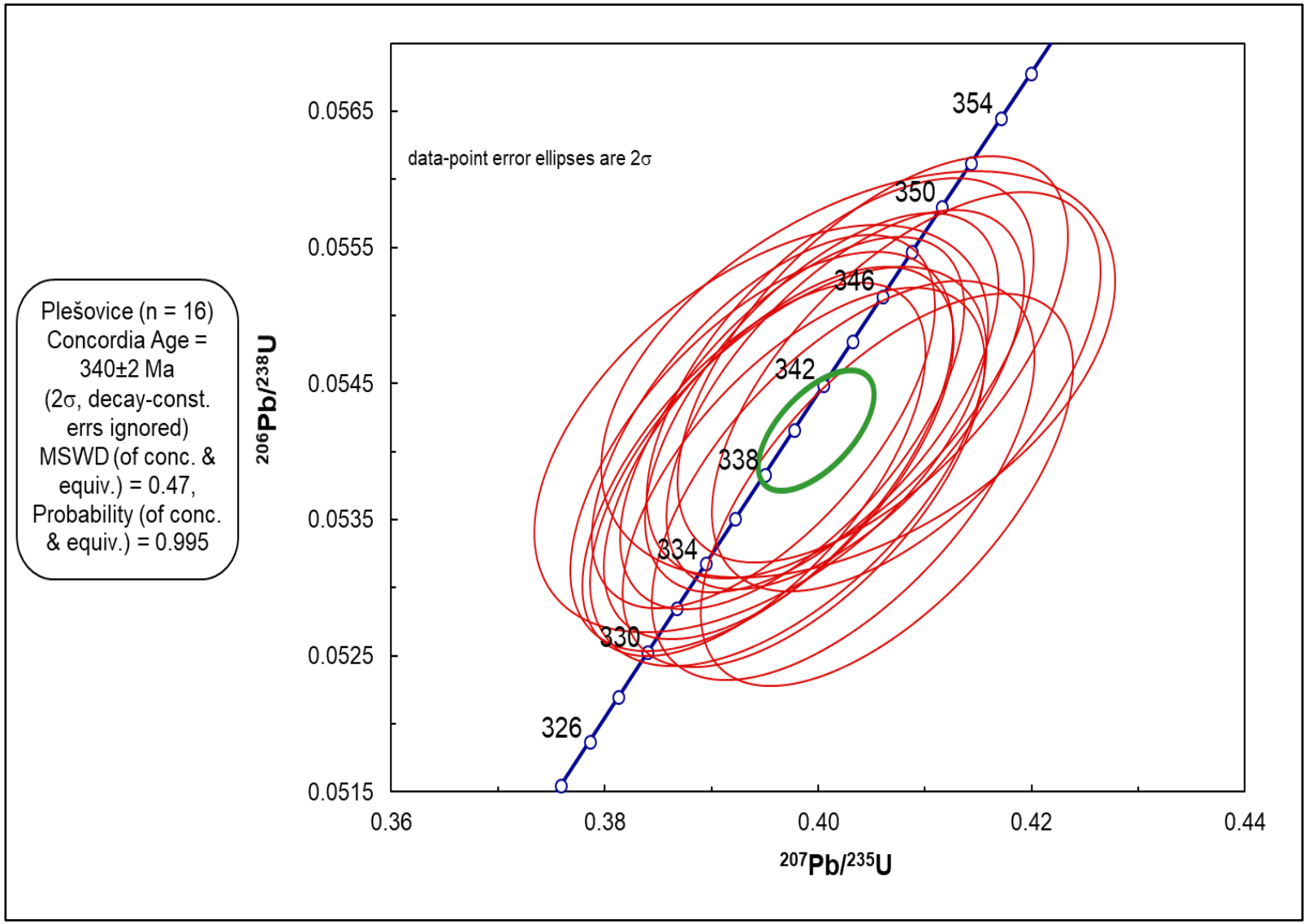

Figure 37: Quality control Concordia diagram for samples MM1, 2 & 3 displaying the Plešovice (Sláma et al., 2008) zircon reference material This was done using methods for analysis and data processing described by Frei and Gerdes (2009) and Cornell et al. (2016).

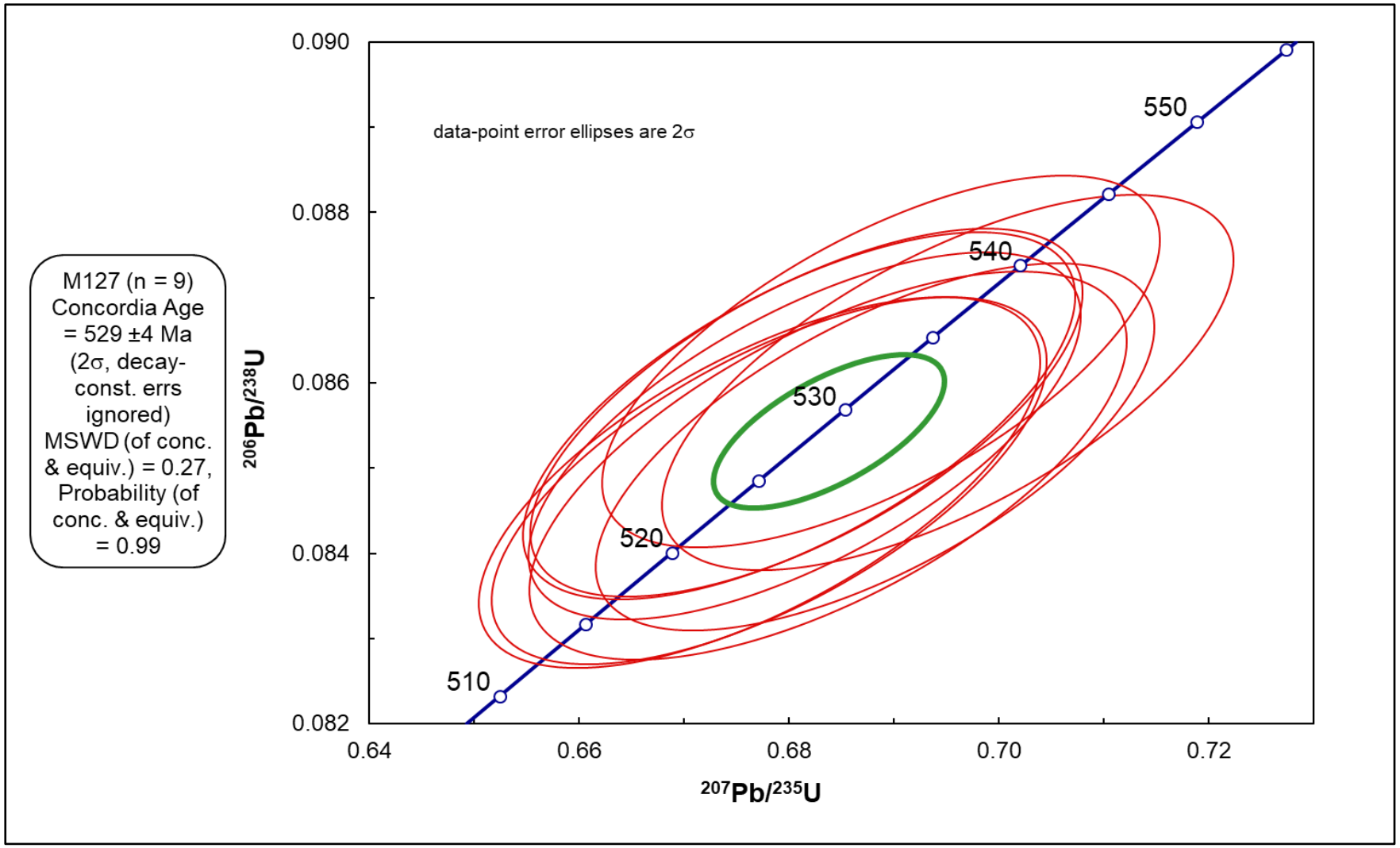

Figure 38: Quality control Concordia diagram for samples MM1, 2 & 3 displaying M127 (Nasdala et al., 2008; Mattinson, 2010) zircon reference material. This was done using methods for analysis and data processing described by Frei and Gerdes (2009) and Cornell et al. (2016).

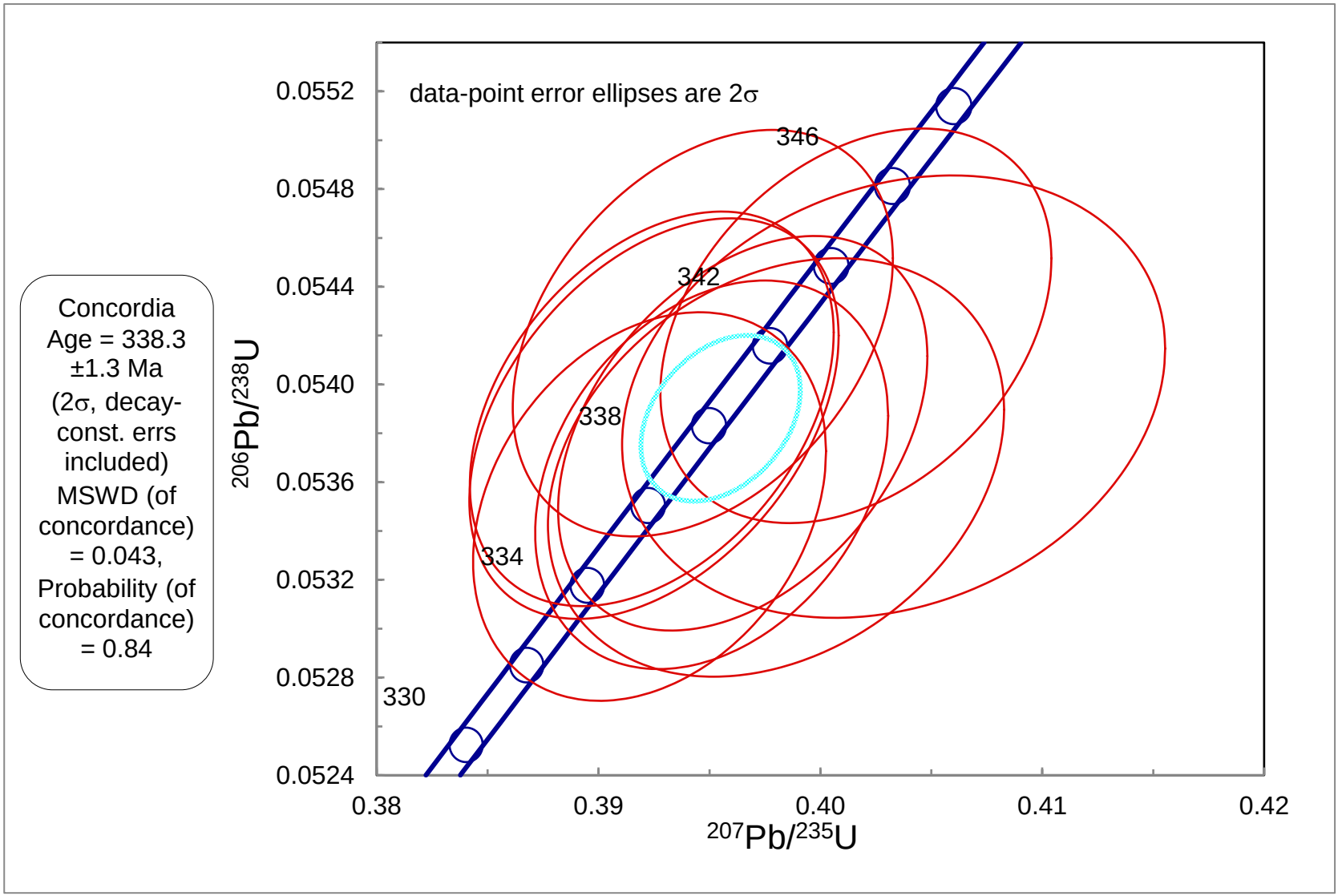

Figure 39: Quality control diagram of samples Pos 1 and Pos 2 displaying the Plešovice (Sláma et al., 2008) zircon reference material This was done using methods for analysis and data processing described by Frei and Gerdes (2009) and Cornell et al. (2016).

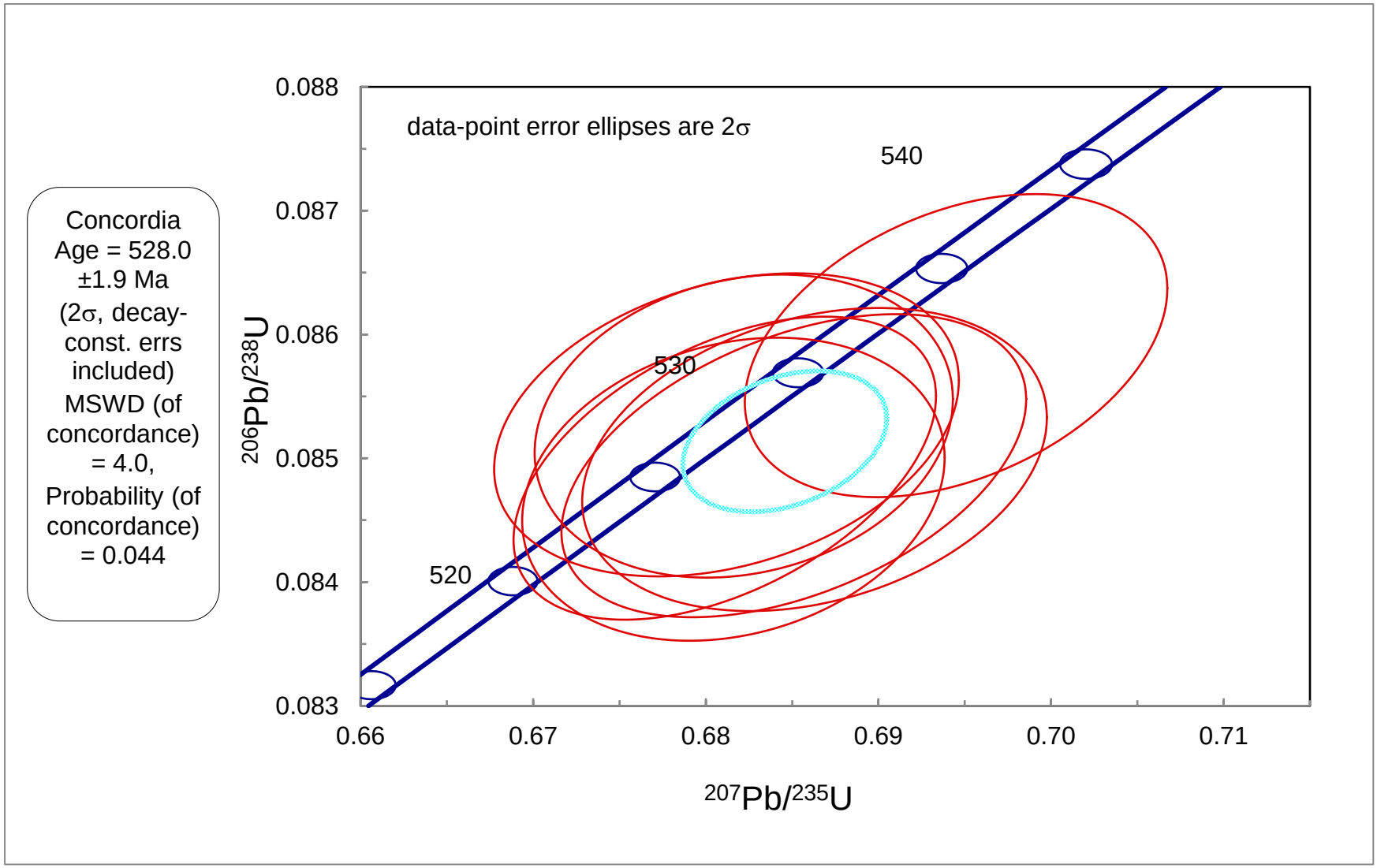

Figure 40: Quality control Concordia diagrams of samples Pos 1 and Pos 2 displaying M127 (Nasdala et al., 2008; Mattinson, 2010) zircon reference material. This was done using methods for analysis and data processing described by Frei and Gerdes (2009) and Cornell et al. (2016).

Table 22: EA5.5 - Quality Control result summary for MM and Pos samples displaying GJ1 U-Pb results summary

Electronic Appendix EA5, Table EA5.5 Quality Control result summary for MM and Pos samples displaying GJ1 U-Pb results summary

					RATIOS							AGES [Ma]						Conc.
Analysis	Sample	U [ppm][a]	Pb [ppm][a]	Th/U[a]	$^{207}Pb/^{235}U$[b]	2 σ[d]	$^{206}Pb/^{238}U$[b]	2 σ[d]	rho[c]	$^{207}Pb/^{206}Pb$[e]	2 σ[d]	$^{207}Pb/^{235}U$	2 σ	$^{206}Pb/^{238}U$	2 σ	$^{207}Pb/^{206}Pb$	2 σ	%
GJ1_105.FIN2	GJ1	291	26	0.03	0.8181	0.0130	0.0988	0.0012	0.3986	0.0599	0.0007	607	7	608	7	601	24	101
GJ1_291.FIN2	GJ1	283	26	0.03	0.8235	0.0140	0.0988	0.0012	0.2774	0.0606	0.0008	610	8	607	7	620	27	98
GJ1_001.FIN2	GJ1	284	26	0.03	0.8172	0.0130	0.0986	0.0012	0.1853	0.0602	0.0008	606	7	606	7	611	27	99
GJ1_003.FIN2	GJ1	284	27	0.03	0.8193	0.0130	0.0986	0.0012	0.2814	0.0607	0.0007	607	8	606	7	624	26	97
GJ1_275.FIN2	GJ1	284	24	0.03	0.8111	0.0130	0.0984	0.0012	0.3229	0.0599	0.0007	603	7	605	7	599	25	101
GJ1_274.FIN2	GJ1	293	28	0.03	0.8111	0.0130	0.0984	0.0012	0.3484	0.0599	0.0007	603	7	605	7	598	24	101
GJ1_054.FIN2	GJ1	282	26	0.03	0.8212	0.0130	0.0983	0.0012	0.1439	0.0606	0.0007	609	7	605	7	619	26	98
GJ1_343.FIN2	GJ1	290	23	0.03	0.8095	0.0140	0.0983	0.0012	0.3758	0.0597	0.0008	602	8	605	7	594	29	102
GJ1_019.FIN2	GJ1	292	27	0.03	0.8188	0.0130	0.0983	0.0012	0.1575	0.0606	0.0007	607	7	605	7	620	26	98
GJ1_292.FIN2	GJ1	292	27	0.03	0.8130	0.0130	0.0983	0.0012	0.1600	0.0600	0.0007	604	7	604	7	602	26	100
GJ1_223.FIN2	GJ1	282	25	0.03	0.8167	0.0130	0.0983	0.0012	0.2593	0.0603	0.0007	606	7	604	7	616	24	98
GJ1_309.FIN2	GJ1	290	27	0.03	0.8157	0.0130	0.0983	0.0012	0.2269	0.0602	0.0008	605	7	604	7	615	27	98
GJ1_342.FIN2	GJ1	288	23	0.03	0.8249	0.0130	0.0983	0.0012	0.2797	0.0609	0.0007	611	7	604	7	634	25	95
GJ1_104.FIN2	GJ1	301	24	0.03	0.8176	0.0130	0.0983	0.0012	0.3815	0.0603	0.0007	607	8	604	7	616	27	98
GJ1_053.FIN2	GJ1	290	27	0.03	0.8217	0.0130	0.0982	0.0012	0.3589	0.0604	0.0007	609	7	604	7	619	26	98
GJ1_087.FIN2	GJ1	280	24	0.03	0.8284	0.0140	0.0982	0.0012	0.2672	0.0611	0.0008	612	8	604	7	639	27	94
GJ1_002.FIN2	GJ1	292	26	0.03	0.8195	0.0130	0.0981	0.0012	0.1433	0.0605	0.0007	608	7	603	7	623	25	97
GJ1_308.FIN2	GJ1	287	26	0.03	0.8163	0.0130	0.0981	0.0012	0.3949	0.0604	0.0007	606	8	603	7	616	26	98
GJ1_070.FIN2	GJ1	289	25	0.03	0.8129	0.0130	0.0978	0.0012	0.1751	0.0601	0.0007	604	7	602	7	603	27	100
GJ1_189.FIN2	GJ1	286	26	0.03	0.8153	0.0130	0.0978	0.0012	0.3615	0.0605	0.0007	605	7	602	7	625	25	96
GJ1_240.FIN2	GJ1	287	29	0.03	0.8202	0.0120	0.0978	0.0011	0.1953	0.0607	0.0007	608	7	601	7	626	24	96
GJ1_036.FIN2	GJ1	284	26	0.03	0.8107	0.0130	0.0978	0.0012	0.2340	0.0603	0.0008	603	7	601	7	615	26	98
GJ1_325.FIN2	GJ1	288	27	0.03	0.8228	0.0140	0.0978	0.0012	0.1385	0.0609	0.0009	610	8	601	7	628	30	96
GJ1_206.FIN2	GJ1	314	29	0.03	0.8260	0.0150	0.0977	0.0013	0.1203	0.0612	0.0009	612	8	601	8	644	31	93
GJ1_088.FIN2	GJ1	281	24	0.03	0.8091	0.0130	0.0977	0.0012	0.4753	0.0601	0.0007	602	7	601	7	604	25	99
GJ1_037.FIN2	GJ1	289	27	0.03	0.8127	0.0130	0.0976	0.0012	0.3565	0.0600	0.0007	604	7	601	7	608	25	99
GJ1_326.FIN2	GJ1	280	26	0.03	0.8176	0.0130	0.0977	0.0012	0.5171	0.0606	0.0007	606	8	601	7	622	26	97
GJ1_121.FIN2	GJ1	293	26	0.03	0.8133	0.0130	0.0976	0.0012	0.3175	0.0604	0.0007	605	7	601	7	617	23	97
GJ1_224.FIN2	GJ1	279	24	0.03	0.8128	0.0130	0.0975	0.0012	0.1157	0.0605	0.0008	604	7	600	7	622	26	96
GJ1_020.FIN2	GJ1	284	26	0.03	0.8142	0.0130	0.0975	0.0012	0.3332	0.0609	0.0008	605	8	600	7	630	27	95
GJ1_190.FIN2	GJ1	273	25	0.03	0.8165	0.0130	0.0975	0.0012	0.3559	0.0606	0.0007	606	7	600	7	624	26	96
GJ1_172.FIN2	GJ1	273	23	0.03	0.8061	0.0130	0.0975	0.0012	0.3925	0.0599	0.0007	600	7	600	7	596	27	101
GJ1_173.FIN2	GJ1	290	24	0.03	0.8130	0.0130	0.0974	0.0012	0.3095	0.0606	0.0008	604	8	599	7	620	27	97
GJ1_258.FIN2	GJ1	278	28	0.03	0.8214	0.0130	0.0974	0.0011	0.2326	0.0610	0.0007	610	7	599	7	641	26	93
GJ1_241.FIN2	GJ1	293	28	0.03	0.8120	0.0150	0.0974	0.0012	0.6686	0.0605	0.0008	604	9	599	7	624	29	96
GJ1_155.FIN2	GJ1	290	26	0.03	0.7973	0.0130	0.0973	0.0012	0.1561	0.0599	0.0008	595	7	598	7	595	30	101
GJ1_071.FIN2	GJ1	290	26	0.03	0.8065	0.0130	0.0972	0.0011	0.3027	0.0603	0.0007	601	7	598	7	610	26	98
GJ1_156.FIN2	GJ1	310	26	0.03	0.8084	0.0140	0.0971	0.0012	0.4379	0.0603	0.0007	601	8	598	7	618	27	97
GJ1_138.FIN2	GJ1	260	25	0.04	0.8104	0.0140	0.0969	0.0012	0.2629	0.0606	0.0008	602	8	596	7	620	29	96
GJ1_139.FIN2	GJ1	295	24	0.03	0.8127	0.0140	0.0969	0.0012	0.3440	0.0609	0.0008	604	8	596	7	637	28	94
GJ1_207.FIN2	GJ1	277	27	0.03	0.8082	0.0130	0.0967	0.0012	0.3616	0.0607	0.0007	601	7	595	7	625	24	95
GJ1_257.FIN2	GJ1	292	28	0.03	0.8044	0.0130	0.0963	0.0012	0.5747	0.0606	0.0007	599	8	593	7	625	24	95
average					0.8150		0.0978			0.0604		605		602		618		

[a]U and Pb concentrations and Th/U ratios are calculated relative to GJ-1 reference zircon

[b]Corrected for background and within-run Pb/U fractionation and normalised to reference zircon GJ-1 (ID-TIMS values/measured value); $^{207}Pb/^{235}U$ calculated using ($^{207}Pb/^{206}Pb$)/($^{238}U/^{206}Pb$ * 1/137.88)

[c]Rho is the error correlation defined as the quotient of the propagated errors of the $^{206}Pb/^{238}U$ and the $^{207}/^{235}U$ ratio

[d]Quadratic addition of within-run errors (2 SD) and daily reproducibility of GJ-1 (2 SD)

[e]Corrected for mass-bias by normalising to GJ-1 reference zircon (~0.6 per atomic mass unit) and common Pb using the model Pb composition of Stacey & Kramers (1975)

7.6 Electronic Appendix EA6 - U-Pb data for all samples collected from the Postberg Centre in the Saldanha Bay Volcanic Complex.

Table 23: EA6.1 - U-Pb data for sample MM1 (Postberg Centre Jacob's Bay Ignimbrite)

Electronic Appendix EA6, Table EA6.1 U-Pb data for sample MM1 (Postberg Centre Jacob's Bay Ignimbrite)

							RATIOS							AGES [Ma]						Conc.
Sample	Analysis	U [ppm][a]	Pb [ppm][a]	$^{206}Pb/^{204}Pb$	Th/U[a]	comment	$^{207}Pb/^{235}U$[b]	2 s[d]	$^{206}Pb/^{238}U$[b]	2 s[d]	rho[c]	$^{207}Pb/^{206}Pb$[e]	2 s[d]	$^{207}Pb/^{235}U$	2 s	$^{206}Pb/^{238}U$	2 s	$^{207}Pb/^{206}Pb$	2 s	%
MM1	A_004	186	16	1971	0.77		0.714	0.031	0.0877	0.0019	0.50	0.0591	0.0022	547	24	542	12	569	82	95
MM1	A_005	103	9	6446	0.97		0.708	0.036	0.0880	0.0020	0.44	0.0583	0.0027	544	28	544	12	543	100	100
MM1	A_006	165	14	11392	0.66		0.700	0.041	0.0873	0.0021	0.42	0.0582	0.0031	539	32	540	13	536	117	101
MM1	A_007	146	13	66193	0.52		0.701	0.048	0.0872	0.0029	0.49	0.0583	0.0035	539	37	539	18	541	131	100
MM1	A_008	373	33	3884	0.21		0.709	0.031	0.0877	0.0019	0.48	0.0586	0.0023	544	24	542	11	552	84	98
MM1	A_014	333	29	16184	0.19		0.707	0.025	0.0871	0.0018	0.60	0.0589	0.0016	543	19	538	11	563	61	96
MM1	A_015	580	51	266656	0.04		0.706	0.024	0.0882	0.0019	0.62	0.0581	0.0015	543	18	545	11	534	58	102
MM1	A_016	115	10	2334	0.80		0.697	0.033	0.0870	0.0019	0.46	0.0581	0.0025	537	26	538	12	535	93	101
MM1	A_017	192	17	8675	0.35		0.677	0.026	0.0860	0.0018	0.57	0.0571	0.0018	525	20	532	11	495	69	107
MM1	A_018	254	22	1730	0.67		0.696	0.026	0.0872	0.0019	0.58	0.0579	0.0017	537	20	539	11	527	66	102
MM1	A_021	111	10	50433	0.76		0.690	0.029	0.0866	0.0019	0.51	0.0578	0.0021	533	23	535	12	522	80	103
MM1	A_022	492	43	43407	0.04		0.703	0.024	0.0867	0.0018	0.61	0.0588	0.0016	540	19	536	11	560	59	96
MM1	A_023	130	11	36491	0.54		0.708	0.031	0.0877	0.0019	0.49	0.0586	0.0023	544	24	542	12	552	84	98
MM1	A_024	146	13	11676	0.36		0.690	0.028	0.0865	0.0019	0.54	0.0578	0.0020	533	21	535	11	523	74	102
MM1	A_025	160	14	2880	0.60		0.698	0.027	0.0871	0.0019	0.54	0.0581	0.0019	538	21	538	11	535	72	101
MM1	A_026	137	12	62597	0.51		0.693	0.029	0.0871	0.0019	0.52	0.0577	0.0020	535	22	539	12	518	77	104
MM1	A_027	220	19	100822	0.25		0.698	0.026	0.0873	0.0019	0.57	0.0580	0.0018	538	20	539	11	531	68	102
MM1	A_028	269	23	3922	0.55		0.690	0.025	0.0863	0.0018	0.58	0.0580	0.0017	533	19	533	11	530	65	101
MM1	A_029	876	76	399587	0.20		0.698	0.023	0.0868	0.0018	0.63	0.0583	0.0015	538	18	537	11	541	56	99
MM1	A_030	263	23	36174	0.40		0.696	0.029	0.0869	0.0018	0.50	0.0581	0.0021	536	23	537	11	534	80	101
~~MM1~~	~~A_031~~	~~418~~	~~36~~	~~425~~	~~0.48~~	~~residual cPb~~	~~0.770~~	~~0.043~~	~~0.0856~~	~~0.0018~~	~~0.38~~	~~0.0652~~	~~0.0033~~	~~580~~	~~32~~	~~530~~	~~11~~	~~781~~	~~108~~	~~68~~
MM1	A_032	69	6	1108	0.65		0.706	0.044	0.0865	0.0019	0.36	0.0593	0.0034	543	34	535	12	577	125	93
MM1	A_033	301	26	136826	0.31		0.687	0.025	0.0863	0.0018	0.58	0.0578	0.0017	531	19	533	11	521	65	102
MM1	A_034	88	8	472	0.41		0.701	0.033	0.0875	0.0019	0.47	0.0581	0.0024	539	26	541	12	532	92	102
MM1	A_035	151	13	1764	0.37		0.709	0.032	0.0887	0.0019	0.47	0.0580	0.0023	544	25	548	12	530	88	103

[a] U and Pb concentrations and Th/U ratios are calculated relative to GJ-1 reference zircon

[b] Corrected for background and within-run Pb/U fractionation and normalised to reference zircon GJ-1 (ID-TIMS values/measured value); $^{207}Pb/^{235}U$ calculated using ($^{207}Pb/^{206}Pb$)/($^{238}U/^{206}Pb$ * 1/137.88)

[c] Rho is the error correlation defined as the quotient of the propagated errors of the $^{206}Pb/^{238}U$ and the $^{207}/^{235}U$ ratio

[d] Quadratic addition of within-run errors (2 SD) and daily reproducibility of GJ-1 (2 SD)

[e] Corrected for mass-bias by normalising to GJ-1 reference zircon (~0.6 per atomic mass unit) and common Pb using the model Pb composition of Stacey & Kramers (1975)

Table 24: EA6.2 - U-Pb data for sample MM2 (Postberg Centre Jacob's Bay Ignimbrite)

Electronic Appendix EA6, Table EA6.2 U-Pb data for sample MM2 (Postberg Centre Jacob's Bay Ignimbrite)

							RATIOS							AGES [Ma]						Conc.
Sample	Analysis	U [ppm][a]	Pb [ppm][a]	$^{206}Pb/^{204}Pb$	Th/U[a]	comment	$^{207}Pb/^{235}U$[b]	2 s[d]	$^{206}Pb/^{238}U$[b]	2 s[d]	rho[c]	$^{207}Pb/^{206}Pb$[e]	2 s[d]	$^{207}Pb/^{235}U$	2 s	$^{206}Pb/^{238}U$	2 s	$^{207}Pb/^{206}Pb$	2 s	%
MM2	A_043	56	5	29748	0.85		0.719	0.035	0.0893	0.0020	0.45	0.0584	0.0026	550	27	551	12	544	96	101
MM2	A_044	145	13	1139	0.51		0.707	0.038	0.0879	0.0019	0.40	0.0584	0.0029	543	29	543	12	543	107	100
MM2	A_045	129	11	67626	0.35		0.705	0.028	0.0875	0.0019	0.54	0.0584	0.0019	542	21	541	11	546	73	99
MM2	A_046	88	8	1090	0.78		0.700	0.058	0.0867	0.0019	0.26	0.0586	0.0047	539	45	536	12	551	176	97
MM2	A_047	266	23	7472	0.30		0.703	0.025	0.0880	0.0018	0.58	0.0580	0.0017	541	19	544	11	528	64	103
MM2	A_048	122	11	4257	0.54		0.708	0.038	0.0885	0.0019	0.40	0.0580	0.0028	544	29	547	12	531	106	103
MM2	A_049	196	17	4204	0.94		0.711	0.039	0.0868	0.0018	0.39	0.0595	0.0030	546	30	536	11	584	110	92
MM2	A_050	149	13	2903	0.40		0.717	0.029	0.0890	0.0019	0.53	0.0584	0.0020	549	22	550	12	545	75	101
MM2	A_051	244	21	2967	0.31		0.695	0.032	0.0868	0.0019	0.47	0.0580	0.0024	536	25	537	12	531	90	101
MM2	A_052	140	12	73418	0.43		0.704	0.028	0.0876	0.0019	0.53	0.0583	0.0020	541	22	541	12	540	74	100
MM2	A_055	225	20	117230	0.38		0.697	0.025	0.0871	0.0018	0.59	0.0581	0.0017	537	19	538	11	533	64	101
MM2	A_056	262	23	841	0.29		0.703	0.077	0.0860	0.0020	0.21	0.0593	0.0064	540	59	532	12	577	233	92
MM2	A_057	264	23	3040	0.44		0.695	0.030	0.0869	0.0018	0.48	0.0580	0.0022	536	23	537	11	528	83	102
MM2	A_058	185	16	97593	0.68		0.708	0.028	0.0880	0.0019	0.54	0.0583	0.0019	543	21	544	12	542	73	100
MM2	A_059	97	8	50222	1.02		0.695	0.038	0.0862	0.0019	0.40	0.0584	0.0029	536	29	533	12	546	109	98
MM2	A_060	219	19	2056	0.56		0.702	0.046	0.0868	0.0018	0.32	0.0587	0.0037	540	36	536	11	555	136	97
MM2	A_061	67	6	833	0.74		0.695	0.038	0.0865	0.0019	0.41	0.0583	0.0029	536	29	535	12	541	110	99
MM2	A_062	297	26	156698	0.27		0.707	0.026	0.0881	0.0018	0.58	0.0582	0.0017	543	20	544	11	536	65	102
MM2	A_063	241	21	122814	0.45		0.694	0.040	0.0850	0.0018	0.36	0.0592	0.0032	535	31	526	11	576	118	91
MM2	A_064	252	21	8849	0.36		0.681	0.025	0.0846	0.0018	0.57	0.0584	0.0018	527	19	523	11	544	66	96
MM2	A_065	67	6	13307	0.83		0.701	0.034	0.0870	0.0019	0.46	0.0584	0.0025	539	26	538	12	546	95	98
MM2	A_066	80	7	41553	0.62		0.699	0.034	0.0872	0.0019	0.45	0.0582	0.0025	538	26	539	12	537	95	100
MM2	A_067	123	11	703	0.77		0.704	0.035	0.0879	0.0019	0.43	0.0581	0.0026	541	27	543	12	532	100	102
MM2	A_068	97	9	51177	0.76		0.700	0.035	0.0877	0.0019	0.43	0.0579	0.0026	539	27	542	12	525	99	103
MM2	A_069	75	6	37271	1.13		0.670	0.045	0.0835	0.0018	0.33	0.0582	0.0037	521	35	517	11	537	138	96

[a] U and Pb concentrations and Th/U ratios are calculated relative to GJ-1 reference zircon

[b] Corrected for background and within-run Pb/U fractionation and normalised to reference zircon GJ-1 (ID-TIMS values/measured value); $^{207}Pb/^{235}U$ calculated using ($^{207}Pb/^{206}Pb$)/($^{238}U/^{206}Pb$ * 1/137.88)

[c] Rho is the error correlation defined as the quotient of the propagated errors of the $^{206}Pb/^{238}U$ and the $^{207}/^{235}U$ ratio

[d] Quadratic addition of within-run errors (2 SD) and daily reproducibility of GJ-1 (2 SD)

[e] Corrected for mass-bias by normalising to GJ-1 reference zircon (~0.6 per atomic mass unit) and common Pb using the model Pb composition of Stacey & Kramers (1975)

Table 25: EA6.3 - U-Pb data for sample MM3 (Postberg Centre Jacob's Bay Ignimbrite)

Electronic Appendix EA6, Table EA6.3 U-Pb data for sample MM3 (Postberg Centre Jacob's Bay Ignimbrite)

							RATIOS							AGES [Ma]						Conc.
Sample	Analysis	U [ppm][a]	Pb [ppm][a]	$^{206}Pb/^{204}Pb$	Th/U[a]	comment	$^{207}Pb/^{235}U$[b]	2 s[d]	$^{206}Pb/^{238}U$[b]	2 s[d]	rho[c]	$^{207}Pb/^{206}Pb$[e]	2 s[d]	$^{207}Pb/^{235}U$	2 s	$^{206}Pb/^{238}U$	2 s	$^{207}Pb/^{206}Pb$	2 s	%
MM3	A_077	238	20	122017	0.58		0.685	0.024	0.0853	0.0018	0.60	0.0583	0.0017	530	19	528	11	540	62	98
MM3	A_078	73	6	38629	0.43		0.707	0.032	0.0878	0.0019	0.48	0.0584	0.0023	543	25	543	12	544	87	100
MM3	A_079	324	28	169417	0.40		0.684	0.023	0.0870	0.0018	0.61	0.0570	0.0015	529	18	538	11	492	60	109
MM3	A_080	168	15	1524	0.51		0.713	0.027	0.0879	0.0019	0.56	0.0588	0.0018	546	21	543	11	560	68	97
MM3	A_081	203	18	3445	0.31		0.702	0.026	0.0872	0.0018	0.57	0.0584	0.0018	540	20	539	11	545	67	99
MM3	A_082	155	13	1510	0.47		0.688	0.026	0.0860	0.0018	0.56	0.0580	0.0018	532	20	532	11	530	70	100
MM3	A_083	199	17	103712	0.40		0.698	0.026	0.0871	0.0018	0.57	0.0582	0.0018	538	20	538	11	535	67	101
MM3	A_084	308	27	1640	0.30		0.716	0.050	0.0865	0.0018	0.30	0.0600	0.0040	548	38	535	11	604	144	89
MM3	A_085	184	16	95712	0.40		0.694	0.031	0.0868	0.0018	0.48	0.0579	0.0022	535	24	537	11	527	85	102
MM3	A_086	197	17	1176	0.93		0.689	0.058	0.0847	0.0018	0.25	0.0590	0.0048	532	45	524	11	565	178	93
MM3	A_089	267	23	139606	0.15		0.699	0.025	0.0873	0.0018	0.59	0.0580	0.0017	538	19	540	11	531	63	102
MM3	A_090	830	72	495	0.30		0.705	0.027	0.0872	0.0018	0.55	0.0586	0.0019	542	21	539	11	553	70	97
MM3	A_091	337	30	182640	0.19		0.731	0.025	0.0904	0.0019	0.61	0.0587	0.0016	557	19	558	12	554	60	101
MM3	A_092	87	8	13702	0.56		0.701	0.040	0.0881	0.0019	0.39	0.0578	0.0030	540	30	544	12	521	114	104
MM3	A_093	97	9	1540	0.42		0.712	0.032	0.0880	0.0019	0.48	0.0587	0.0023	546	25	544	12	556	87	98
MM3	A_094	108	9	3356	0.60		0.684	0.029	0.0855	0.0019	0.52	0.0580	0.0021	529	22	529	12	531	79	100
MM3	A_095	165	14	86255	0.38		0.701	0.028	0.0874	0.0019	0.54	0.0581	0.0019	539	21	540	11	534	73	101
MM3	A_096	87	8	513	0.68		0.711	0.061	0.0881	0.0019	0.25	0.0585	0.0049	545	47	544	12	550	182	99
MM3	A_097	292	25	17336	0.28		0.700	0.025	0.0869	0.0018	0.58	0.0585	0.0017	539	20	537	11	547	65	98
MM3	A_098	182	16	15117	0.23		0.697	0.027	0.0871	0.0019	0.56	0.0580	0.0018	537	21	538	11	531	69	101
MM3	A_099	67	6	598	0.76		0.696	0.034	0.0866	0.0019	0.46	0.0583	0.0025	536	26	535	12	540	95	99
MM3	A_100	53	5	3069	0.94		0.704	0.036	0.0880	0.0020	0.44	0.0581	0.0027	541	28	544	12	532	101	102
MM3	A_101	229	20	3768	0.42		0.704	0.027	0.0878	0.0019	0.56	0.0582	0.0018	541	21	542	11	535	69	101
MM3	A_102	322	28	18205	0.39		0.699	0.025	0.0872	0.0018	0.59	0.0581	0.0017	538	19	539	11	535	64	101
MM3	A_103	245	21	1145	0.38		0.692	0.036	0.0860	0.0018	0.41	0.0583	0.0027	534	28	532	11	542	103	98

[a] U and Pb concentrations and Th/U ratios are calculated relative to GJ-1 reference zircon

[b] Corrected for background and within-run Pb/U fractionation and normalised to reference zircon GJ-1 (ID-TIMS values/measured value); $^{207}Pb/^{235}U$ calculated using ($^{207}Pb/^{206}Pb$)/($^{238}U/^{206}Pb$ * 1/137.88)

[c] Rho is the error correlation defined as the quotient of the propagated errors of the $^{206}Pb/^{238}U$ and the $^{207}/^{235}U$ ratio

[d] Quadratic addition of within-run errors (2 SD) and daily reproducibility of GJ-1 (2 SD)

[e] Corrected for mass-bias by normalising to GJ-1 reference zircon (~0.6 per atomic mass unit) and common Pb using the model Pb composition of Stacey & Kramers (1975)

Table 26: EA6.4 - U-Pb data for sample Pos 1 (Postberg Centre Tsaarsbank Ignimbrite)

Electronic Appendix EA6, Table EA6.4 U-Pb data for sample Pos 1 (Postberg Centre Tsaarsbank Ignimbrite)

					RATIOS							Ages (Ma)						Conc.
Sample	Analysis	U [ppm][a]	Pb [ppm][a]	Th/U[a]	$^{207}Pb/^{235}U$[b]	2 σ[d]	$^{206}Pb/^{238}U$[b]	2 σ[d]	rho[c]	$^{207}Pb/^{206}Pb$[e]	2 σ[d]	$^{207}Pb/^{235}U$	2 σ	$^{206}Pb/^{238}U$	2 σ	$^{207}Pb/^{206}Pb$	2 σ	%
POS-1	A_217.FIN2	330	322	0.28	1.1157	0.0170	0.1248	0.0015	0.2733	0.0649	0.0007	761	8	758	8	776	22	98
POS-1	A_235.FIN2	72	87	0.46	0.7190	0.0180	0.0879	0.0011	0.1438	0.0595	0.0014	548	11	543	7	571	51	95
POS-1	A_230.FIN2	165	106	0.26	0.7112	0.0130	0.0878	0.0011	0.2451	0.0586	0.0009	547	8	543	6	561	33	97
POS-1	A_215.FIN2	84	134	0.65	0.7070	0.0150	0.0874	0.0011	0.2618	0.0588	0.0010	542	9	540	7	560	39	96
POS-1	A_249.FIN2	166	119	0.27	0.7047	0.0130	0.0872	0.0011	0.2740	0.0585	0.0009	541	8	539	7	547	32	99
POS-1	A_228.FIN2	94	79	0.36	0.6900	0.0220	0.0871	0.0012	0.1931	0.0575	0.0017	532	13	538	7	516	60	104
POS-1	A_221.FIN2	271	166	0.25	0.7044	0.0130	0.0871	0.0011	0.2513	0.0587	0.0008	541	8	538	6	558	32	96
POS-1	A_219.FIN2	72	104	0.59	0.6970	0.0160	0.0870	0.0011	0.1556	0.0579	0.0012	536	9	538	7	520	44	103
POS-1	A_234.FIN2	111	138	0.51	0.6840	0.0150	0.0865	0.0011	0.3165	0.0574	0.0011	530	9	535	6	517	41	103
POS-1	A_237.FIN2	105	93	0.36	0.6970	0.0180	0.0864	0.0011	0.1280	0.0585	0.0013	537	11	535	7	538	50	99
POS-1	A_251.FIN2	127	244	0.75	0.6990	0.0140	0.0863	0.0010	0.2168	0.0589	0.0010	538	8	534	6	562	37	95
POS-1	A_227.FIN2	91	150	0.69	0.6920	0.0140	0.0862	0.0011	0.1661	0.0580	0.0010	534	8	533	6	526	38	101
POS-1	A_220.FIN2	107	163	0.64	0.6930	0.0130	0.0861	0.0011	0.1834	0.0585	0.0010	536	8	532	6	550	37	97
POS-1	A_263.FIN2	143	133	0.39	0.6820	0.0140	0.0857	0.0011	0.3477	0.0579	0.0009	529	8	530	7	528	35	100
POS-1	A_252.FIN2	87	97	0.43	0.6850	0.0170	0.0856	0.0011	0.1399	0.0579	0.0013	529	10	530	6	535	48	99
POS-1	A_238.FIN2	131	201	0.61	0.6800	0.0150	0.0844	0.0010	0.2266	0.0583	0.0010	528	9	522	6	547	40	95
POS-1	A_256.FIN2	77	110	0.57	0.6910	0.0160	0.0871	0.0011	0.1588	0.0574	0.0012	534	10	538	7	507	44	106
POS-1	A_218.FIN2	101	171	0.63	0.8440	0.0160	0.1003	0.0014	0.2788	0.0616	0.0010	621	9	616	8	654	36	94
POS-1	A_246.FIN2	80	123	0.59	0.7030	0.0150	0.0862	0.0011	0.0373	0.0592	0.0012	540	9	533	6	568	44	94
POS-1	A_255.FIN2	229	104	0.18	0.7014	0.0130	0.0857	0.0011	0.4315	0.0594	0.0009	539	8	530	7	582	32	91
POS-1	A_245.FIN2	199	130	0.24	0.7117	0.0120	0.0865	0.0011	0.1377	0.0596	0.0009	545	7	535	6	590	32	91
POS-1	A_243.FIN2	136	215	0.61	0.7276	0.0130	0.0876	0.0011	0.2214	0.0598	0.0009	555	8	541	7	600	34	90
POS-1	A_259.FIN2	69	122	0.69	0.7340	0.0160	0.0875	0.0011	0.0617	0.0604	0.0012	558	10	541	7	611	45	89
POS-1	A_216.FIN2	84	79	0.35	0.6820	0.0150	0.0819	0.0011	0.2211	0.0602	0.0012	528	9	508	7	626	44	81
POS-1	A_253.FIN2	115	114	0.37	0.7400	0.0160	0.0863	0.0011	0.2758	0.0620	0.0011	562	9	534	7	668	37	80
POS-1	A_260.FIN2	75	186	0.96	0.7370	0.0220	0.0863	0.0012	0.4781	0.0626	0.0017	559	13	534	7	685	53	78
POS-1	A_226.FIN2	148	119	0.33	0.7290	0.0170	0.0849	0.0011	0.1520	0.0622	0.0012	557	10	525	7	685	44	77
POS-1	A_247.FIN2	74	80	0.36	0.7720	0.0230	0.0886	0.0012	0.0509	0.0629	0.0018	580	13	547	7	714	56	77
POS-1	A_236.FIN2	225	101	0.17	0.6790	0.0140	0.0798	0.0010	0.0076	0.0616	0.0010	526	8	495	6	648	36	76
POS-1	A_232.FIN2	214	547	0.90	0.5917	0.0110	0.0651	0.0008	0.2091	0.0583	0.0010	472	7	407	5	539	35	75
POS-1	A_250.FIN2	278	82	0.11	0.6860	0.0160	0.0805	0.0012	0.5316	0.0618	0.0011	530	9	499	7	668	38	75
POS-1	A_233.FIN2	215	110	0.21	0.7010	0.0140	0.0822	0.0011	0.2981	0.0621	0.0011	539	8	509	7	684	35	74
POS-1	A_239.FIN2	260	311	0.42	0.7910	0.0250	0.0867	0.0011	0.4796	0.0658	0.0018	589	14	536	6	786	56	68
POS-1	A_231.FIN2	141	86	0.19	0.7960	0.0190	0.0865	0.0011	0.2459	0.0669	0.0014	596	11	535	7	822	44	65
POS-1	A_262.FIN2	105	86	0.26	0.7650	0.0190	0.0837	0.0012	0.0005	0.0663	0.0017	578	11	519	7	802	54	65
POS-1	A_265.FIN2	161	339	0.83	0.7330	0.0140	0.0811	0.0010	0.2328	0.0656	0.0010	559	8	503	6	789	33	64
POS-1	A_229.FIN2	111	50	0.17	0.6780	0.0180	0.0764	0.0011	0.3406	0.0645	0.0013	525	10	475	6	747	43	64
POS-1	A_242.FIN2	118	78	0.22	0.6900	0.0140	0.0759	0.0010	0.1777	0.0657	0.0012	532	8	472	6	788	38	60
POS-1	A_248.FIN2	73	194	0.91	0.7970	0.0220	0.0818	0.0011	0.0801	0.0704	0.0018	593	13	507	6	927	55	55
POS-1	A_264.FIN2	276	160	0.10	0.9100	0.0390	0.0843	0.0012	0.1165	0.0782	0.0034	649	14	521	7	1124	56	46
POS-1	A_254.FIN2	71	115	0.52	0.7830	0.0280	0.0761	0.0011	0.0739	0.0748	0.0025	586	16	473	7	1051	70	45
POS-1	A_261.FIN2	121	195	0.51	0.8600	0.0170	0.0804	0.0010	0.2672	0.0776	0.0013	629	9	499	6	1134	34	44
POS-1	A_222.FIN2	127	220	0.34	1.1440	0.0400	0.0773	0.0019	0.0098	0.1062	0.0034	770	15	480	11	1738	50	28
POS-1	A_244.FIN2	35	109	0.45	2.1500	0.1700	0.1012	0.0021	0.7844	0.1510	0.0099	1156	59	621	12	2380	120	26

[a]U and Pb concentrations and Th/U ratios are calculated relative to GJ-1 reference zircon

[b]Corrected for background and within-run Pb/U fractionation and normalised to reference zircon GJ-1 (ID-TIMS values/measured value); $^{207}Pb/^{235}U$ calculated using $(^{207}Pb/^{206}Pb)/(^{238}U/^{206}Pb * 1/137.88)$

[c]Rho is the error correlation defined as the quotient of the propagated errors of the $^{206}Pb/^{238}U$ and the $^{207}/^{235}U$ ratio

[d]Quadratic addition of within-run errors (2 SD) and daily reproducibility of GJ-1 (2 SD)

[e]Corrected for mass-bias by normalising to GJ-1 reference zircon (~0.6 per atomic mass unit) and common Pb using the model Pb composition of Stacey & Kramers (1975)

Table 27: EA6.5 - U-Pb data for sample Pos 2 (Postberg Centre Tsaarsbank Ignimbrite)

Electronic Appendix EA6, Table EA6.5 U-Pb data for sample Pos 2 (Postberg Centre Tsaarsbank Ignimbrite)

						RATIOS							Ages (Ma)						Conc.
Analysis	Sample	U [ppm][a]	Pb [ppm][a]	Th/U[a]	comment	$^{207}Pb/^{235}U$[b]	2 σ[d]	$^{206}Pb/^{238}U$[b]	2 σ[d]	rho[c]	$^{207}Pb/^{206}Pb$[e]	2 σ[d]	$^{207}Pb/^{235}U$	2 σ	$^{206}Pb/^{238}U$	2 σ	$^{207}Pb/^{206}Pb$	2 σ	%
POS-2	A_270.FIN2	112	270	0.47		2.1610	0.0370	0.1967	0.0024	0.2113	0.0796	0.0011	1168	12	1157	13	1191	27	97
POS-2	A_271.FIN2	122	218	0.34		2.1500	0.0340	0.1963	0.0024	0.3315	0.0792	0.0009	1165	11	1156	13	1177	22	98
POS-2	A_324.FIN2	62	238	0.74		2.0360	0.0390	0.1869	0.0024	0.3007	0.0788	0.0012	1128	13	1105	13	1163	31	95
POS-2	A_293.FIN2	143	163	0.47		0.7230	0.0150	0.0901	0.0011	0.3723	0.0583	0.0009	553	9	556	7	537	35	104
POS-2	A_337.FIN2	194	116	0.27		0.7117	0.0120	0.0880	0.0010	0.0611	0.0590	0.0008	546	7	544	6	566	30	96
POS-2	A_285.FIN2	199	78	0.17		0.7063	0.0130	0.0879	0.0011	0.2498	0.0583	0.0008	542	8	543	6	535	32	102
POS-2	A_307.FIN2	160	96	0.25		0.7160	0.0140	0.0878	0.0011	0.0738	0.0587	0.0009	548	8	543	6	556	36	98
POS-2	A_266.FIN2	242	116	0.18		0.7062	0.0130	0.0876	0.0011	0.3517	0.0586	0.0009	542	8	541	7	558	31	97
POS-2	A_300.FIN2	146	366	1.04		0.7060	0.0140	0.0876	0.0011	0.1587	0.0583	0.0010	542	8	541	6	546	36	99
POS-2	A_277.FIN2	259	568	0.92		0.7107	0.0120	0.0876	0.0010	0.2109	0.0589	0.0008	545	7	541	6	566	29	96
POS-2	A_305.FIN2	42	69	0.62		0.7220	0.0320	0.0864	0.0012	0.6390	0.0601	0.0024	544	17	534	7	551	81	97
POS-2	A_303.FIN2	71	145	0.85		0.7000	0.0160	0.0862	0.0011	0.0526	0.0588	0.0012	538	10	533	7	551	47	97
POS-2	A_313.FIN2	117	89	0.32		0.6990	0.0210	0.0883	0.0013	0.2358	0.0570	0.0015	541	12	546	8	494	56	110
POS-2	A_283.FIN2	143	114	0.34		0.6970	0.0140	0.0874	0.0011	0.2414	0.0577	0.0010	537	8	540	6	509	37	106
POS-2	A_311.FIN2	111	131	0.47		0.7400	0.0160	0.0896	0.0011	0.0066	0.0596	0.0012	562	9	553	7	587	43	94
POS-2	A_334.FIN2	113	90	0.28		0.7250	0.0150	0.0886	0.0011	0.0636	0.0594	0.0010	554	9	547	7	581	37	94
POS-2	A_278.FIN2	88	107	0.50		0.7410	0.0180	0.0896	0.0012	0.0620	0.0598	0.0013	562	10	553	7	589	48	94
POS-2	A_295.FIN2	247	107	0.11		1.4160	0.0320	0.1459	0.0027	0.8808	0.0705	0.0008	896	14	878	15	943	22	93
POS-2	A_267.FIN2	122	100	0.34		0.7020	0.0140	0.0860	0.0010	0.1045	0.0588	0.0010	541	9	532	6	572	40	93
POS-2	A_331.FIN2	105	84	0.32		0.7360	0.0160	0.0886	0.0011	0.1021	0.0600	0.0012	559	10	547	7	589	44	93
POS-2	A_284.FIN2	186	120	0.25		0.7390	0.0150	0.0897	0.0011	0.2590	0.0599	0.0010	561	9	553	7	596	34	93
POS-2	A_318.FIN2	211	238	0.49		0.7027	0.0120	0.0858	0.0011	0.1950	0.0592	0.0008	541	7	531	6	574	29	92
POS-2	A_336.FIN2	98	122	0.52		0.7270	0.0170	0.0877	0.0011	0.0680	0.0599	0.0013	553	10	542	6	590	46	92
POS-2	A_312.FIN2	104	150	0.59		0.7080	0.0140	0.0866	0.0011	0.2152	0.0593	0.0010	544	8	535	6	584	37	92
POS-2	A_306.FIN2	118	103	0.38		0.6930	0.0140	0.0839	0.0010	0.1090	0.0591	0.0010	534	8	520	6	575	36	90
POS-2	A_289.FIN2	222	73	0.13		0.7005	0.0120	0.0851	0.0011	0.2979	0.0597	0.0009	540	8	527	7	589	31	89
POS-2	A_286.FIN2	353	129	0.14		0.7079	0.0120	0.0854	0.0010	0.3460	0.0602	0.0008	544	7	528	6	604	27	87
POS-2	A_321.FIN2	105	229	0.87		0.7180	0.0180	0.0860	0.0012	0.4674	0.0607	0.0012	549	10	532	7	621	41	86
POS-2	A_282.FIN2	173	213	0.53		0.7110	0.0140	0.0851	0.0010	0.0682	0.0605	0.0010	545	8	526	6	619	34	85
POS-2	A_315.FIN2	122	156	0.51		0.7440	0.0160	0.0874	0.0012	0.3576	0.0619	0.0011	564	9	540	7	657	38	82
POS-2	A_287.FIN2	243	169	0.28		0.7381	0.0130	0.0867	0.0010	0.2760	0.0615	0.0008	561	8	536	6	656	29	82
POS-2	A_330.FIN2	273	126	0.18		0.7118	0.0120	0.0840	0.0011	0.3763	0.0612	0.0008	545	7	520	6	646	29	80
POS-2	A_304.FIN2	183	215	0.45		0.7580	0.0170	0.0887	0.0011	0.3758	0.0624	0.0012	574	10	548	7	692	39	79
POS-2	A_314.FIN2	143	81	0.19		0.7620	0.0170	0.0876	0.0011	0.0917	0.0625	0.0012	575	10	541	7	685	39	79
POS-2	A_320.FIN2	117	222	0.77		0.7380	0.0160	0.0849	0.0011	0.1672	0.0629	0.0012	561	9	525	6	702	38	75
POS-2	A_338.FIN2	72	66	0.39		0.7640	0.0240	0.0870	0.0015	0.4101	0.0635	0.0017	574	14	537	9	721	59	75
POS-2	A_298.FIN2	118	72	0.20		0.7910	0.0160	0.0889	0.0011	0.0073	0.0643	0.0012	592	9	549	7	751	41	73
POS-2	A_341.FIN2	1045	144	0.02		0.6970	0.0110	0.0805	0.0011	0.6621	0.0631	0.0006	537	6	499	7	711	21	70
POS-2	A_316.FIN2	115	209	0.62		0.9020	0.0270	0.0947	0.0014	0.1480	0.0694	0.0019	654	13	583	8	878	53	66
POS-2	A_268.FIN2	40	90	0.89		0.8330	0.0390	0.0871	0.0013	0.3704	0.0683	0.0029	613	22	538	8	866	91	62
POS-2	A_294.FIN2	50	22	0.13		0.7920	0.0240	0.0852	0.0013	0.0884	0.0672	0.0020	594	14	527	8	864	63	61
POS-2	A_296.FIN2	144	97	0.21		0.8040	0.0210	0.0841	0.0011	0.0773	0.0690	0.0015	597	12	521	7	884	45	59
POS-2	A_339.FIN2	92	93	0.45		0.7830	0.0190	0.0827	0.0011	0.1831	0.0683	0.0015	588	11	512	7	876	45	58
POS-2	A_340.FIN2	76	71	0.32		0.9240	0.0360	0.0918	0.0013	0.1548	0.0731	0.0026	659	19	566	8	978	66	58
POS-2	A_319.FIN2	192	126	0.17		0.8450	0.0210	0.0851	0.0011	0.4766	0.0718	0.0014	620	11	526	7	970	39	54
POS-2	A_279.FIN2	90	191	0.77		0.9020	0.0210	0.0888	0.0012	0.3044	0.0733	0.0015	651	11	549	7	1019	41	54
POS-2	A_328.FIN2	318	124	0.04		0.8820	0.0150	0.0863	0.0011	0.2093	0.0732	0.0011	642	8	534	7	1022	32	52
POS-2	A_317.FIN2	42	49	0.36		0.9700	0.0550	0.0885	0.0014	0.0388	0.0790	0.0043	671	25	547	8	1053	89	52
POS-2	A_299.FIN2	63	63	0.33		0.8270	0.0250	0.0817	0.0012	0.5654	0.0739	0.0019	612	14	506	7	1026	50	49
POS-2	A_273.FIN2	45	106	0.85		0.9850	0.0380	0.0880	0.0012	0.3143	0.0796	0.0028	692	19	544	7	1176	73	46
POS-2	A_288.FIN2	212	177	0.14		1.0150	0.0410	0.0875	0.0012	0.2579	0.0842	0.0030	708	20	541	7	1267	67	43
POS-2	A_280.FIN2	175	401	0.79		1.0520	0.0290	0.0896	0.0012	0.3921	0.0846	0.0019	729	14	553	7	1298	45	43
POS-2	A_335.FIN2	119	154	0.31		1.0690	0.0270	0.0872	0.0011	0.0492	0.0886	0.0019	736	13	539	7	1382	42	39
POS-2	A_323.FIN2	82	100	0.23		1.1150	0.0270	0.0890	0.0011	0.3655	0.0904	0.0019	760	13	550	7	1431	42	38
POS-2	A_281.FIN2	65	124	0.40		1.4440	0.0490	0.0998	0.0015	0.1086	0.1040	0.0029	902	20	613	9	1671	50	37
POS-2	A_322.FIN2	99	162	0.35		1.1930	0.0430	0.0855	0.0012	0.1017	0.1009	0.0035	795	19	529	7	1606	52	33
POS-2	A_332.FIN2	143	159	0.04		1.2990	0.0350	0.0889	0.0012	0.0045	0.1051	0.0027	841	14	549	7	1704	44	32
POS-2	A_329.FIN2	441	404	0.19		0.7450	0.0210	0.0579	0.0008	0.0738	0.0826	0.0022	563	12	363	5	1235	52	29
POS-2	A_297.FIN2	166	718	0.19		2.9600	0.1500	0.1074	0.0019	0.8215	0.1971	0.0073	1386	37	657	11	2782	61	24
POS-2	A_302.FIN2	223	781	0.53		1.9910	0.0430	0.0897	0.0011	0.2915	0.1611	0.0029	1111	15	554	7	2470	30	22
POS-2	A_333.FIN2	184	876	0.16		2.6700	0.1800	0.0840	0.0012	0.5600	0.2200	0.0130	1280	54	520	7	2850	120	18

[a]U and Pb concentrations and Th/U ratios are calculated relative to GJ-1 reference zircon

[b]Corrected for background and within-run Pb/U fractionation and normalised to reference zircon GJ-1 (ID-TIMS values/measured value); $^{207}Pb/^{235}U$ calculated using $(^{207}Pb/^{206}Pb)/(^{238}U/^{206}Pb * 1/137.88)$

[c]Rho is the error correlation defined as the quotient of the propagated errors of the $^{206}Pb/^{238}U$ and the $^{207}/^{235}U$ ratio

[d]Quadratic addition of within-run errors (2 SD) and daily reproducibility of GJ-1 (2 SD)

[e]Corrected for mass-bias by normalising to GJ-1 reference zircon (~0.6 per atomic mass unit) and common Pb using the model Pb composition of Stacey & Kramers (1975)

7.7 Electronic Appendix EA7 - Rb, Sr, Sm, Nd tracer-isotope data for samples collected from the Postberg Centre in the Saldanha Bay Volcanic Complex.

Table 28: EA7.1 - Tracer-isotope data for collected samples from the Postberg Centre (Jacobs Bay Ignimbrite)

Electronic Appendix EA7, Table EA7.1 Tracer-isotope data for collected smaples from the Postberg Centre (Jacobs Bay Ignimbrite)

Sample	Chem#	Sm (ppm)	Nd (ppm)	$^{147}Sm/^{144}Nd$	$^{143}Nd/^{144}Nd$	s.e. 2s(min)	n	ε(Nd)	Chem#	Rb (ppm)	Sr (ppm)	$^{87}Rb/^{86}Sr$	$^{87}Sr/^{86}Sr$	s.e. 2s(min)	n
MM1	1236	10.03565	49.68734	0.122095051	0.512240291	4.02179E-06	79	-7.60214	1268	225.6699	89.38232	7.473861979	0.7614488	0.00001348	76
MM2	1237	10.20796	52.02603	0.118608237	0.512224233	3.40336E-06	79	-7.91541	1269	241.7544	94.94497	7.532604473	0.7548259	0.00000992	76
MM3	1238	10.57333	53.29033	0.119939127	0.51223393	4.03136E-06	76	-7.72623	1270	227.8422	102.0587	6.602734739	0.7523044	0.00001082	75

Departamento de Geología, Centro de Investigación Científica y de Educación Superior de Ensenada (CICESE) in the state of Baja California (Mexico)

CHUR after Bouvier et al. (2008)

Table 29: EA7.2 - Tracer-isotope data, calculated at 538 Ma, for collected samples from the Postberg Centre (Jacobs Bay Ignimbrite)

Electronic Appendix EA7, Table EA7.2 Tracer-isotope data, calculated at 538 Ma, for collected smaples from the Postberg Centre (Jacobs Bay Ignimbrite)

Sample	$^{87}Sr/^{86}Sr_0$	Rb (ppm)	Sr (ppm)	$^{87}Rb/^{86}Sr$ (calc.)	$^{87}Sr/^{86}Sr_t$	εNdt	tDM (Ga)
MM1	0.704132	225.6698582	89.38231984	7.473861979	0.7614488	-7.602142043	1.430
MM2	0.697057	241.7544494	94.94496574	7.532604473	0.7548259	-7.915406817	1.405
MM3	0.701667	227.8422425	102.0587028	6.602734739	0.7523044	-7.726233527	1.409

Sample	$^{143}Nd/^{144}Nd_0$	Sm (ppm)	Nd (ppm)	$^{147}Sm/^{144}Nd$ (calc.)	$^{143}Nd/^{144}Nd_t$	εNd_i	t2DM (Ga)
MM1	0.51181	10.03565461	49.68734128	0.122095051	0.512240291	-2.63	1.411
MM2	0.511806	10.20796195	52.02602644	0.118608237	0.512224233	-2.71	1.417
MM3	0.511811	10.57333197	53.29033429	0.119939127	0.51223393	-2.61	1.409